NASA TECHNICAL TRANSLATION

NASA TT F-457

NASA TT F-457

THEORY OF STELLAR SPECTRA

by V. V. Sobolev

Izdatel'stvo "Nauka",
Moscow, 1966

NATIONAL AERONAUTICS AND SPACE ADMINISTRATION • WASHINGTON, D. C. • JUNE 1967

THEORY OF STELLAR SPECTRA

By V. V. Sobolev

Translation of "Teoriya zvezdnykh spektrov."
Izdatel'stvo "Nauka," Moscow, 1966.

PREFACE

/5*

The only source of our information on stars is their radiation. From stellar spectra we judge the structure of stellar atmospheres, their chemical composition, and physical processes taking place there. Spectrograms are interpreted on the basis of the theory of stellar spectra, wherein lies its enormous value for astrophysics.

Until recently astronomers could observe stellar radiation only in a very small range of frequencies making up the visible region of the spectrum. However, about 20 years ago radio astronomy came into being which permits investigating the radiation of celestial bodies in a completely different spectral region. Quite recently, in connection with the launching of satellites and rockets, there arose the theoretical possibility of obtaining stellar spectra in any frequency range. So far, highly useful spectrograms of stars and the sun have been obtained in the so-called rocket ultraviolet. It is obvious that this broadening of observational data will even further increase the significance of the theory of stellar spectra. At the same time it is necessary to improve and extend this theory.

The surface layers of stars, out of which their spectra arise, represent strongly ionized gases, i.e., plasma. Plasma studies are also being carried out in physics laboratories, having increased in intensity of late. Methods used by physicists in studying plasmas are in many respects similar to methods used by astrophysicists in studying stellar atmospheres. Therefore, the theory of stellar spectra is of interest not only to astrophysicists but also to physicists.

/6

An excellent example of the broad interest in the theory of stellar spectra is the summer seminary on problems of this theory, organized by the Astronomical Council of the Academy of Sciences of the USSR and the Leningrad University and held in Leningrad in June 1964. About 150 young astrophysicists and physicists of the Soviet Union participated in the sessions. This book was written on the basis of the lectures given at that time.

The first part of the book examines atomic processes associated with the formation of spectra, with special emphasis on calculation of the energy levels of the atom and the probability of transitions between these levels. The second part deals with the theory of radiation transfer, which forms an important aspect of the theory of stellar spectra. The next two parts discuss the most essential problems in the formation of spectra of different types of stars and nebulae. The last part, devoted to ultraviolet spectra of celestial bodies, mainly gives a review of observational data and their qualitative interpretation (since, as yet, no quantitative theory of these spectra has been established).

The diversity of the problems of the modern theory of stellar spectra makes

---

* Numbers given in the margin indicate pagination in the original foreign text.

it impossible to present them with sufficient completeness in a single monograph. The authors of this book have endeavored to acquaint the reader with the most important of these problems.

Editorial Board.

TABLE OF CONTENTS

	Page
Preface	iii
PART I. PHYSICAL PROCESSES CONNECTED WITH THE FORMATION OF SPECTRA	1
Plasma Spectroscopy (S.E.Frish)	1
Calculations of Atomic Energy Levels (A.P.Yutsis and Ya.I.Vizbarayte)	23
Theory of Atomic Transitions (G.F.Drukarev)	48
PART II. THEORY OF RADIATIVE TRANSFER	64
Certain Nonlinear Problems of the Theory of Radiative Transfer (V.A.Ambartsumyan)	64
Radiative Diffusion in Gases (V.V.Sobolev)	75
Determination of the Populations of Excited Levels in an Optically Thick Gas Layer (V.V.Ivanov)	92
Nonstationary Radiation Field (I.N.Minin)	116
Randomized Problem of Diffuse Reflection (R.V.Ambartsumyan)	135
PART III. SPECTRA OF FIXED STARS	140
Models of Stellar Atmospheres (V.V.Sobolev)	140
Continuous Spectra of Hot White Dwarfs (A.K.Kolesov)	147
Model Atmospheres of Main-Sequence Stars of Class M (V.G.Buslavskiy)	152
Determination of the Chemical Composition of Stellar Atmospheres (A.A.Boyarchuk)	160
PART IV. SPECTRA OF NONSTATIONARY STARS AND INTERSTELLAR MATTER	170
Spectra of Nonstationary (Variable) Stars (V.G.Gorbatskiy)	170
Analysis of the Emission Spectra of Nonstationary Stars (A.A.Boyarchuk)	194
Spectra of Interstellar Matter (S.A.Kaplan)	203
Radio Observations of Planetary Nebulae (Yu.N.Pariyskiy)	216
PART V. SPECTRA OF CELESTIAL BODIES IN THE FAR ULTRAVIOLET REGION	220
Spectra of Celestial Bodies in the Far Ultraviolet Region (G.A.Gurzadyan)	220

PART I. PHYSICAL PROCESSES CONNECTED WITH THE FORMATION OF SPECTRA

/7

A series of lectures by different authors, taken from a seminary on the problems of the theory of stellar spectra in the field of radio astronomy including information obtainable by extraterrestrial spectroscopy, is presented. The monograph is divided into five parts, dealing with the basic physical principles of atomic processes in the formation of spectra; plasma spectroscopy; radiation transfer; formation of spectra of various types of stars and nebulae; and observational data processing relative to the ultraviolet spectra of celestial bodies. Recent theories on the evolution of the cosmos, composition of interstellar matter, atomic transition, plasma physics, and mathematics of radiative transfer are compared with older concepts and evaluated.

PLASMA SPECTROSCOPY

/9

S.E.Frish

1. Introduction

Plasma spectroscopy deals with the study of the radiation of plasma, i.e., strongly ionized quasi-neutral gases. Such a study can follow two different directions: a) explanation of the processes occurring in plasma, on the basis of an experimental study of the spectrum emitted by the plasma; b) theoretical calculation of the plasma spectrum, based on its characteristics obtained by non-optical methods. In this lecture we will deal with both directions but will not specifically demarcate them.

Generally speaking, plasma is a highly complex object, inhomogeneous in space, changing in time, and composed of several components (mixture of gases). The physicist has the advantage over the astronomer in that he is able to create the objects of observation; in so doing he can select his conditions such that the object has the simplest possible form. The study of plasma, of course, begins with its most elementary aspects. Therefore, let us examine the simplest case: a spatially homogeneous low-pressure plasma in a pure atomic gas.

The emission and absorption of a specific spectrum line of frequency ν_{ki} has to do with atomic quantum transitions between two stationary states k and i (Fig.1). It is known that, according to Einstein, three types of transitions must be considered: a) spontaneous radiative transitions, b) induced radiative transitions, c) absorptive transitions. The number of events of these transitions in unit time per unit volume is equal to

a) $\Delta N_{ki} = N_k A_{kl},$

b) $\Delta N'_{ki} = N_k B_{ki} \rho(\nu_{kl}),$ (1)

c) $\Delta N_{lk} = N_i B_{ik} \rho(\nu_{kl}).$

Here, N_k and N_i are the concentrations of atoms in the k-th and i-th states, while A_{k1}, B_{k1}, and B_{1k} are the Einstein coefficients and $\rho(\nu_{k1})$ is the radiation density at frequency ν_{k1}. Between the three Einstein coefficients there exists a correlation, so that they can be reduced to a single coefficient; below we will use the coefficient A_{k1} (probability of transition). /10

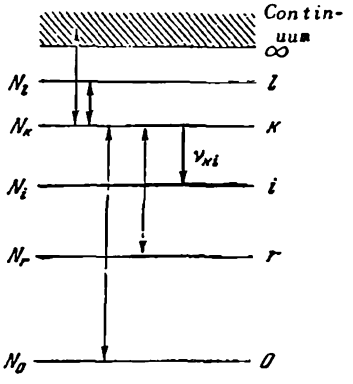

Fig.1

The radiant energy at frequency ν_{k1} in unit time from unit volume is equal to

$$W_0 = N_k A_{ki} h\nu_{ki} + N_k B_{ki} \rho(\nu_{ki}) h\nu_{kl}. \quad (2)$$

The second term in this formula corresponds to induced transitions. If this term can be neglected [case of low radiation density $\rho(\nu_{k1})$], then

$$W_0 = N_k A_{kl} h\nu_{ki}. \quad (2a)$$

The quantity W_0 determines the primary ("true") brightness of the line referred to unit volume of the radiating plasma. The actually observed line brilliance differs from the "true" brightness since the plasma has a certain thickness l and since the light from each volume element of plasma is partially absorbed before it escapes from its limits (phenomenon of self-absorption of light, or resorption). Leaving aside for the present the phenomenon of resorption, let us examine the power of the primary radiation W_0. As shown by eq.(2), for determining W_0 the concentration of atoms N_k must be known. The latter, generally speaking, can be found from the kinetic equation

$$\frac{dN_k}{dt} = C(t) + C'(t), \quad (3)$$

where C(t) is the rate of populating of the level k, while C'(t) is the rate of its disintegration. For a stationary plasma $\frac{dN_k}{dt} = 0$ and from eq.(3), we obtain /11

$$C(t) + C'(t) = 0. \quad (4)$$

The principal populating processes in plasma are: a) electron collisions of the first kind, b) collisions of the second kind with excited atoms, c) absorption of photons, d) successive transitions from higher levels (spontaneous, induced, or occurring under the effect of collisions of the second kind with

electrons and atoms), e) recombination processes.

The principal disintegrating processes are: a) spontaneous emission, b) induced emission, c) collisions of the second kind with atoms and electrons, d) collisions of the first kind with electrons lifting the atom to higher energy states or ionizing it, e) quenching collisions with the walls of a vessel in which the plasma is enclosed.

We will disregard collisions in neutral atoms and ions (except collisions of the second kind) since they play a role only at large relative velocities of the colliding particles.

If the number of populating processes is denoted by ΔN_{ik} and the number of disintegrating processes by $\Delta N'_{ki}$, then the condition of a stationary state [eq.(4)] for the k-th level is written as

$$\sum_i \Delta N_{ik} + \sum_l \Delta N'_{kl} = 0. \tag{4a}$$

Summation here is carried out for all types of processes. Condition (4a) must be supplemented by the condition of constancy of the total number N of particles per unit volume:

$$N_0 + \sum_k N_k + \sum_i N_i^+ = N, \tag{5}$$

where N_k and N_i^+, respectively, are the concentration of excited atoms and ions.

Since the number of excited states of atoms is infinite, conditions (4a) and (5) have an infinite system of equations with an infinite number of unknowns. The parameters entering these equations will be the transition probabilities A_{ki} between levels and the effective cross sections for collision Q_{ik} as well as quantities that characterize the state of the plasma: concentration /12 of electrons N_e and their velocity distribution function. Since such a system is unsolvable, we must introduce some simplifying assumptions. Furthermore, to solve the problem, it is obvious that we must know all transition probabilities and all effective cross sections. Let us first discuss the experimental methods of determining these quantities.

2. Experimental Methods of Determining Transition Probabilities and Effective Cross Sections

The basic experimental methods of determining the transition probabilities are: a) emission method, b) light absorption method, c) anomalous dispersion method (Rozhdestvenskiy's "hook" method). Since these methods are adequately elucidated in the literature (Ref.1, 2, 3) we will not discuss them in further detail. Let us point out only that not one of these methods gives the transition probability A_{ki} per se. The emission method yields the quantity $N_k A_{ki}$, where N_k is the concentration of atoms at the upper (radiation) level while the methods of absorption and anomalous dispersion give $N_i A_{ki}$, where N_i is the concentration at the lower (absorption) level. Thus, in all cases we are dealing with the

experimental determination of the product of the probability A_{ki} and the particle concentration. Hence, we can obtain only the relative values of A_{ki}. The possibility of finding the relative value of A_{ki} for groups of lines with a common upper or common lower level is obvious. However, it is easy to see that a combination of both methods, emission and absorption, permits finding also the relative values of A_{ki} and A_{ir} for two lines having in common only an intermediate level i (Fig.2). Actually, $N_i A_{ir}$ is determined by the emission method for a line of frequency ν_{ir} while $N_i A_{ki}$ is determined by the absorption method for the line of ν_{ki}. From these two relations we find A_{ki}/A_{ir}.

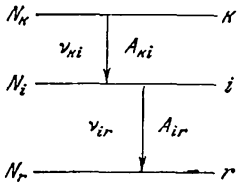

Fig.2

To find the absolute value of the transition probability A_{ki} we must know the absolute values /13 of the concentration of atoms in one of the states, k or i. For lines having the character of the lower normal state (i = 0, resonance lines, lines of the principal series), the concentration of normal atoms N_0 can be found from the temperature and pressure (vapor pressure). The absolute values of the transition probabilities for resonance lines of alkali metals were determined in this manner by D.S.Rozhdestvenskiy, and later by his students and associates, for numerous lines of the principal series of several elements. However, in most cases the pressure of the saturating metal vapors is known with insufficient accuracy, and therefore the absolute values have an appreciable error attached. For this reason, different methods of determining N_0 have recently been developed. Such methods include: a) the atomic beam method in which N_0 is determined by weighing the deposit formed on a plate on which the atomic beam impinges, b) a method based on a combination of one of the aforementioned methods of determining the product $N_0 A_{k0}$ with a method that permits measuring some other combination of the quantities N_0 and A_{k0}. As such a method we should mention that by N.P.Penkin, L.N.Shabanova, and Yu.N.Ostrovskiy (Ref.4, 5) based on a combination of the anomalous dispersion and total absorption methods. The underlying principle of this method is as follows: The value of the so-called "total" absorption A_λ, which is determined from the absorption of light of a given frequency ν_{ki} at very large optical densities (of the order of several thousands), is used together with the value $N_i A_{ki}$ obtained by the anomalous dispersion method. It follows from the theory that

$$A_\lambda = \frac{C}{\nu_{ik}^3} \sqrt{\frac{g_k}{g_i} N_i A_{ki} \gamma_{ki} l}.$$

Here, γ_{ki} is the attenuation factor equal to $1/\tau_k + 1/\tau_i + \gamma_c$, where τ_k and τ_i are the natural lifetimes of levels k and i, and γ_c is the attenuation factor /14 caused by collisions between atoms; l is the thickness of the absorbing layer; g_k and g_i are the statistical weights of the levels; C is a constant expressed by universal constants. Knowing the values of $N_i A_{ki}$, the measured value of total absorption A_λ can be used for finding γ_{ki}. For the resonance lines, we have $1/\tau_i = 0$ and $1/\tau_k = A_{k0}$; at low density of the gas, $\gamma_c = 0$.

The absolute value of A_{k0} is found in the same manner. The absolute values of the transition probabilities for the resonance lines of MgI, CaI, SrI, BaI,

and of a number of other atoms were measured by this method. The probabilities of intense dipole transitions are values of the order of 10^8 sec^{-1}.

For excited states, the concentrations of atoms N_i, with respect to N_0 and in the presence of thermodynamic equilibrium, can be obtained from the Boltzmann formula:

$$N_i = N_0 \frac{g_i}{g_0} e^{-W_i/kT}, \tag{6}$$

where W_i is the energy of the i-th state with respect to the normal state, k is the Boltzmann constant, and T is absolute temperature. In the absence of thermodynamic equilibrium, it is quite difficult to determine the concentrations of excited atoms.

It follows from the above statements that the accuracies of determining the relative and absolute values of transition probabilities differ greatly, with the former in most cases being determined much more accurately than the latter. In using the anomalous dispersion method, the error of relative measurement is usually about 5% and, at best, can be reduced to 1 - 2%. The emission and absorption methods give an error of the order of 10 - 15%. The absolute values of A_{ki} (with a few exceptions) are measured with less accuracy.

Methods for a theoretical calculation of the transition probabilities A_{ki} have been developed recently (Ref.6). When applied to a one-electron approximation, such calculations are rather reliable. For complex atoms, accurate calculations are more difficult to make.

Numerous experimental studies were made to determine the effective cross /15 sections of atomic excitation by electron collision. Usually, these investigations are based on the electron beam method. A beam of electrons of determined velocity v is injected into an enclosure filled with the monatomic vapor (gas) to be studied, at such a low pressure that collision can be considered as being of the single type. In that case, in unit time and per unit volume the number of direct ($0 \rightarrow k$) exciting collisions will be equal to

$$\Delta N_{0k}^{(e)} = N_0 n_e(v) Q_{0k}(v). \tag{7}$$

Here, $Q_{0k}(v)$ represents the effective cross section of direct excitation of the k-th level by electrons of velocity v; $n_e(v)$ denotes the number of electrons passing through unit beam cross section in unit time.

Assuming that population of the k-th level, in addition to direct collisions, takes place as the result of spontaneous transitions from higher levels (successive transitions) and that its disintegration is due only to spontaneous transitions to lower levels, we can write the steady-state condition in the form (see Fig.1)

$$N_0 n_e(v) Q_{0k}(v) + \sum_{l=k+1}^{\infty} N_l A_{lk} = N_k \sum_{r=0}^{k-1} A_{kr}. \tag{8}$$

Determining N_k from this, we obtain the following expression for the radiation power of a unit volume W_0 at a frequency ν_{ki}:

$$W_0 = N_k A_k h\nu_{kl} =$$

$$= N_0 n_e(v) \frac{A_{kl}}{\sum_{r=0}^{k-1} A_{kr}} \left\{ Q_{0k}(v) + \frac{\sum_{l=k+1}^{\infty} N_l A_{lk}}{N_0 n_e(v)} \right\} h\nu_{kl}. \qquad (9)$$

The quantity W_0 is measured directly; N_0 and $n_e(v)$ can also be obtained from the experimental conditions. However, eq.(9) indicates that, to find $Q_{0k}(v)$, it is also necessary to know all transition probabilities A_{ki}, A_{kr}, A_{lk} as well as the concentration of atoms N_l in all excited states higher than the k-th excited state.

To simplify eq.(9), let us note that, under the assumptions made, the concentration N_l at any l-th level is proportional to $N_0 \cdot n_e(v)$. Then, /16

$$N_l = C_l N_0 n_e(v).$$

Let us introduce the further designation

$$\overline{Q_{0k}(v)} = Q_{0k}(v) + \sum_{l=k+1}^{\infty} C_l A_{lk}. \qquad (10)$$

After this, eq.(9) becomes

$$W_0 = N_0 n_e(v) \frac{A_{kl}}{\sum_{r=0}^{k-1} A_{kr}} \cdot \overline{Q_{0k}(v)} \cdot h\nu_{kl}. \qquad (9a)$$

The quantity $\overline{Q_{0k}(v)}$ is called the effective cross section for direct excitation of the line. Finally, we write: $\overline{Q_{0k}(v)} = \overline{Q_{0k\,max}} \cdot f(v)$, where $\overline{Q_{0k\,max}}$ is the value of $\overline{Q_{0k}(v)}$ at the maximum (at the highest maximum, if there are several). The function f(v) is called the optical function of line excitation. It represents the dependence of the spectral line brightness W_0 on the velocity of the exciting electrons v.

A comparison of eqs.(9) and (9a) shows that the quantities $Q_{0k}(v)$ and $\overline{Q_{0k}(v)}$ do not coincide; the latter takes into account not only the direct excitation of the level by electron collision but also its population due to successive transitions. Original experiments led to the result that the dependence $\overline{Q_{0k}(v)}$ on v is depicted by a smooth curve with one, more or less sloping, maximum. This led to the conclusion that the role of successive transitions is negligible, since the appearance of each new successive transition should have produced a discontinuity on the curve or led to the appearance of a secondary maximum. It was subsequently learned that the smooth slope of the curves was

due to an experimental error: The exciting electron beam was insufficiently homogeneous relative to the velocities. Figure 3 shows the dependence of the optical function of excitation f on the energy eV of the exciting electrons for the green line of mercury (HgI, λ 5461 A) obtained from measurements with a highly monoenergetic electron beam (Ref.3). Under these conditions, the presence of several maxima is quite distinct on the curve. An analysis of the slope of this curve shows that most maxima are due to successive transitions. /17

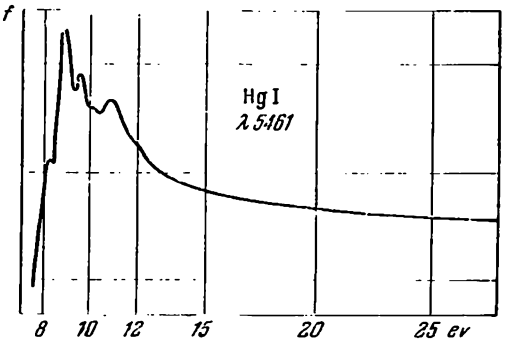

Fig.3

Generally speaking, it is impossible to neglect successive transitions. The cross sections $\overline{Q_{0k}(v)}$ found on the basis of eq.(9a) from experimentally measured W_0, N_0, and $n_e(v)$ are not the effective cross sections for level excitation. To find the latter, measurements for all lines participating in the cascade must be made. This will yield a system of equations of the type of eq.(9), whose solution permits finding the effective cross sections for level excitation $Q_{0k}(v)$. Such determinations have been made in individual cases, but only approximately. For the most part, we are familiar only with effective line excitation cross sections. These are represented by values of the order of 10^{-18} to 10^{-20} cm^2.

It should be mentioned that, to analyze phenomena occurring in plasma, we can limit ourselves mostly to defining the effective cross sections for line excitation. These quantities have even some advantage over the effective level excitation cross sections, since they automatically account for the role of successive transitions.

Along with the cross sections for direct excitation $0 \rightarrow k$ we often have to know the effective cross section for stepwise or "step" excitation $r \rightarrow k$, i.e., excitation from some intermediate level. This cross section cannot be obtained from experiments with an electron beam since, at the low pressures and low densities of the electron beam at which these experiments are carried out, the number of step excitations is too small to be noted. The value of the cross sections for step excitation, as will be shown below, can be found from observations of plasma radiation; it is by 2 - 3 orders of magnitude greater than the value of the direct excitation cross section. /18

A theoretical calculation of the effective excitation cross section is quite difficult and so far has not yielded reliable results.

3. Plasma and its Characteristics

By plasma we mean an ionized quasi-neutral gas, i.e., an ionized gas in

which, within each element of volume containing a sufficient number of particles, the overall electric charge is equal to zero. Below, we will examine only such plasmas in which only electrons and singly charged positive ions participate as charged particles. Then, by virtue of the quasi-neutrality of the plasma, the concentrations of electrons and ions will be equal: $N_e = N^+$. We will also consider that the concentration of electrons and excited atoms is low in comparison with the concentration of atoms in the normal state:

$$N_e \ll N_0; \quad N_k \ll N_0.$$

For the characteristic of the plasma, it is necessary to know the concentration of electrons N_e and the law of their velocity distribution. Let us express the latter by means of the distribution function $F(v)$. Then, the number of electrons dN_e whose velocities are within a given velocity range v, $v + dv$, will be equal to $dN_e = N_e F(v)dv$.

In the case of thermodynamic equilibrium of the plasma, the function $F(v)$ represents a Maxwellian distribution function with a temperature equal to the gas temperature. For the positive column of gas discharge, as shown by Langmuir in the 1920s, $F(v)$ can also be expressed, in satisfactory approximation, by /19 the Maxwellian function but with a temperature other than the gas temperature T. This temperature, known as the electron temperature T_e, for low-pressure plasmas at low discharge current density is much higher than the gas temperature: $T_e \gg T$ (for example, at $T = 300^\circ K$ the electron temperature may reach tens of thousands of degrees). With a rise in pressure and an increase in the discharge current density, T_e approaches T. The electron temperature is generally measured by the method of probe characteristics (Ref.7, 8). In the positive discharge column, the velocities of the migratory motion of the electrons are small in comparison with the velocities of their random motion and therefore do not play a role in the ionization and excitation processes of atoms.

In the discharge zones adjacent to the electrode - for example, in a hollow cathode - the electron velocity distribution differs markedly from Maxwellian. It was recently found that deviations from the Maxwellian law exist also in the positive gas discharge column. Yu.M.Kagan and coworkers (Ref.9) developed an experimental method of investigating the velocity (energy) distribution of electrons. In the positive discharge column these deviations occur mainly in the zone of high velocities, where there are fewer fast electrons than there should be according to the Maxwellian law. These deviations have practically no effect on the volt-ampere characteristics of the probe and thus remain unnoticed when investigating plasma properties by conventional gas methods. However, these deviations are highly essential in analyzing phenomena in plasmas. In fact, for the most part the excitation and ionization potentials of atoms are such that they fall within an electron velocity zone that is appreciably greater than that for which the Maxwellian curve has a maximum. In Fig.4 the solid curve 1 gives the Maxwellian distribution function of electron energies eV, while the broken curve corresponds to the actual electron distribution. Curve 2 shows the cross section for spectral line excitation $\overline{Q_{0k}}$, which is also expressed as a function of the electron energy eV. As the diagram shows, excitation is produced only by electrons of energies where the deviations from the /20 Maxwellian law are excessive.

These deviations from the Maxwellian distribution of electron velocities explain many cases of discrepancy between experimentally observed spectral line brightnesses and their values calculated on the basis of data obtained by the probe method.

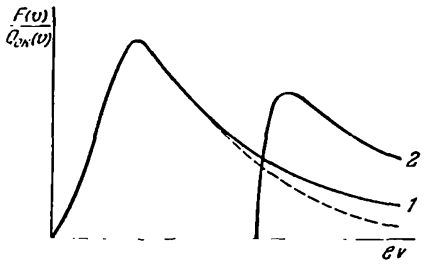

Fig.4

The second plasma characteristic, namely, the electron concentration N_e, is also experimentally determined by the probe method. In the region of low discharge current density j, a rather good proportionality exists between N_e and j. At greater current density, N_e increases more rapidly than j.

At relatively large N_e (greater than 10^{14} cm^{-3}), this quantity can be measured from the absorption of short radio waves and from the broadening of the spectral lines. Under these conditions, the electron temperature can be found from the brightness distribution in the continuous emission spectrum.

4. Plasma Radiation

The primary brightness of a spectral line, referred to unit length of radiating plasma, is expressed by a formula coinciding with eq.(2a):

$$I_0 = N_k A_{ki} h\nu_{ki}. \tag{2a}$$

The true radiation brightness, as stated before, differs from this quantity, first because the plasma has a finite length l and, second because partial absorption of light occurs within the plasma itself.

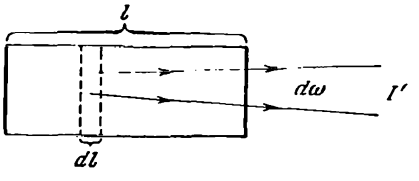

Fig.5

For simplicity, let us examine a homogeneous radiating column of length l (Fig.5). Then, the brightness of the line from the entire length of the column, for a frequency ν, will be equal to (Ref.1) /21

$$I' = \frac{I_0}{\varkappa_\nu}(1 - e^{-\varkappa_\nu l}), \tag{11}$$

where $\varkappa_\nu$ is the absorption coefficient. The quantity $\varkappa_\nu l$ is called the optical density of the plasma. Equation (11) shows that, at small optical densities $\varkappa_\nu l$, the brightness I′ increases in proportion to l and, at large $\varkappa_\nu l$, tends to a constant value $I_0/\varkappa_\nu$ (Fig.6).

Thus, at high optical densities an increase in the length of the radiating column l does not lead to an increase in line brightness I.

For a line of finite width, eq.(11) must be integrated over the line pro-

file. Ladenburg and Levi performed such calculations for a Doppler profile; they arrived at the following result:

$$I' = I_0 l S(\varkappa_0 l), \tag{12}$$

where $S(\varkappa_0 l)$ is the Ladenburg function (Ref.3) and $\varkappa_0$ is the absorption coefficient for the center of the line. The Ladenburg function has been tabulated. The value of $\varkappa_0$ can be determined experimentally from the integral line absorption, which is determined by the quantity $\int_0^\infty \varkappa_\nu d\nu$. For the Doppler profile /22

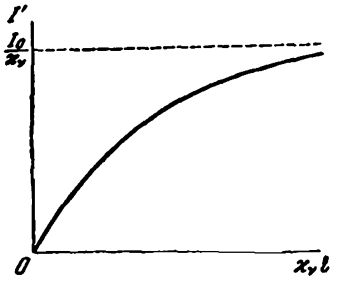

Fig.6

$$\int_0^\infty \varkappa_\nu d\nu = \frac{1}{2}\sqrt{\frac{\pi}{\ln 2}} \cdot \varkappa_0 \Delta\nu_D, \tag{13}$$

where $\Delta\nu_0$ is the Doppler width of the line. At small $\varkappa_0 l$, the Ladenburg function $S(\varkappa_0 l)$ is equal to unity and eq.(12) gives the same result as eq.(11): $I' = I_0 l$.

Let us now examine separately plasma in thermodynamic equilibrium and not in equilibrium.

a) Plasma in Thermodynamic Equilibrium

In a thermodynamic-equilibrium plasma, the velocity distribution is determined by the Maxwell law with the general temperature T for particles of all sorts (atoms, ions, electrons). The same temperature T enters the Boltzmann equation yielding the particle distribution by energy levels, and the Saha equation permitting calculation of the degree of ionization.

In the case of low optical density ($\varkappa_\nu l \ll 1$), resorption plays no noticeable role, and the line brightness referred to unit luminous column is equal to

$$I_0 = N_0 \frac{g_k}{g_l} e^{-W_k/kT} A_{kl} h\nu_{kl}. \tag{14}$$

The brightness ratio of the two lines equals

$$\frac{I_{01}}{I_{02}} = \frac{g_k}{g_l} \cdot \frac{A_{kl}}{A_{ll}} \cdot \frac{\nu_{kl}}{\nu_{ll}} e^{-\frac{W_k - W_l}{kT}}. \tag{15}$$

At high temperatures, when the role of ionization cannot be neglected, eq.(14) must be replaced by

$$I_0 = N_0 (1 - x_l) \frac{g_k}{g_l} e^{-W_k/kT} A_{kl} h\nu_{kl}, \tag{14a}$$

where the degree of ionization x_l is calculated from the Saha equation. A low-

density plasma, radiating according to the above laws, is called a Boltzmann radiator. The line brightness, in this case, depends on the temperature T, /23
the excitation temperature W_k, and the transition probability A_{ki} but does not depend on the effective excitation cross section $\overline{Q_{0k}}$. With increasing temperature T, the brightness of the given line at first increases as $e^{-W_k/kT}$ and then, owing to an increase in the degree of ionization x_j [eq.(14a)], begins to slow down; finally, passing through a maximum, it starts to drop as $x_j \to 1$.

One and the same plasma can be a Boltzmann radiator with respect to some lines (small $\varkappa_{0i}l$) and, at the same time, be no Boltzmann radiator with respect to other lines (large $\varkappa_{0i}l$).

At high optical densities, resorption must be taken into consideration. As a result of resorption, the line brightness I increases with increasing length of the luminous column l, as already stated, more slowly than in proportion to l.

At very high optical densities, induced emission begins to play a significant role along with absorption. This leads to the maximum brightness achievable by the spectral line as $\varkappa_\nu l \to \infty$, coinciding with the brightness of an ideal black body for the same frequency and at the same temperature T. The latter, as is known, is expressed by Planck's formula which, besides the universal constants, contains only frequency and temperature. The constants characterizing the atom (transition probabilities, excitation potentials, etc.) generally cease to play a role. Such a radiator is known as Planckian radiator.

b) Nonequilibrium Plasma

The theory of radiation of a nonequilibrium low-density plasma was first developed by V.A.Fabrikant (Ref.10). He studied the simplest case where the only process of level excitation was direct electronic excitation and the only process of disintegration was spontaneous transition. We will somewhat generalize these premises, having included successive transitions among the processes leading to population of the levels. Then, the line brightness can be expressed by a formula analogous to eq.(9a), except that the product $\overline{n_e(v)Q_{0k}(v)}$ must be replaced by $\int_{v_k}^{\infty} N_e F(v) v \overline{Q_{0k}(v)} dv$, since excitation is accomplished not by elec- /24
trons flying within the beam but by electrons in random motion within the volume of the plasma itself. Here, N_e is the number of electrons per unit volume of plasma electron concentration, $F(v)$ is their velocity distribution function, and v_k is the velocity corresponding to the excitation threshold of the k-th level. Thus, we obtain

$$I_0 = N_0 N_e \frac{A_{ki} h\nu_{ki}}{\sum_{r=0}^{k-1} A_{kr}} \int_{v_k}^{\infty} F(v) v \overline{Q_{0i}(v)} dv. \qquad (16)$$

As indicated above, the cross section $\overline{Q_{0k}(v)}$ takes into account the role of successive transitions.

Let us assume that the electron velocities have an equilibrium distribution, so that F(v) is a Maxwellian function. The dependence $\overline{Q_{0k}}$ on the velocity v, in most cases, is expressed by curves such as curve 2 in Fig.4. Fabrikant proposed a comparatively simple algebraic approximation for an analytic writing of the dependence $\overline{Q_{0k}}$ on v. However, we will proceed in an even simpler fashion and, using the mean value theorem, write

$$\int_{v_k}^{\infty} F(v)\, v\overline{Q_{0k}(v)}\, dv = (\overline{Q_{0k}})_{mean} \int_{v_k}^{\infty} F(v)\, v\, dv.$$

In most actual cases, the electron temperature is such that the maximum of the Maxwell function F(v) is located at velocities lower than v_k. Thanks to this, the function F(v) drops rapidly in the region where $\overline{Q_{0k}(v)} \neq 0$, and only those electrons whose velocities are close to v_k play a substantial role in the atomic excitation. The maximum of the curve $\overline{Q_{0k}(v)}$ usually lies at a velocity only slightly higher than v_k. Hence, it follows that $(\overline{Q_{0k}})_{mean}$ can be replaced by $(\overline{Q_{0k}})_{max}$. Then we have

$$\int_{v_k}^{\infty} F(v)\, v\overline{Q_{0k}(v)}\, dv = \overline{Q_{0k}}_{max} \cdot \int_{v_k}^{\infty} F(v)\, v\, dv. \tag{17}$$

When $\overline{Q_{0k}(v)}$ has a form greatly differing from that indicated, integration should be performed graphically. /25

For the Maxwell function F(v), the integral on the right-hand side of eq.(17) is selected. On changing from velocities v to electron energies eV, we obtain

$$\int_{v_k}^{\infty} F(v)\, v\, dv = C \cdot V_e^{-1/2}\left(V_k + \frac{2}{3}V_e\right) \cdot e^{-\frac{3}{2}\cdot\frac{V_k}{V_e}},$$

where C is a constant, V_k is the excitation potential of the k-th level, and V_e is the electron temperature expressed in potential units (on the basis of the equality $eV_e = \frac{3}{2} kT_e$). After this, the expression for the line brightness can be rewritten as

$$I_0 = CN_0N_e \frac{A_{ki}\nu_{ki}}{\sum_{r=0}^{k-1} A_{kr}} \cdot \overline{Q_{0k}}_{max}\, V_e^{-1/2}\left(V_k + \frac{2}{3}V_e\right) e^{-\frac{3}{2}\cdot\frac{V_k}{V_e}}. \tag{18}$$

The Planck constant here is included in C. Equation (18) indicates that

the line brightness depends both on the transition probabilities and on the effective cross section $\overline{Q_{0k\,max}}$ and the excitation potential V_k. For the resonance line, we have $\sum_{r=0}^{k-1} A_{kr} = A_{k0}$ and eq.(18) takes the following form:

$$I_0 = CN_0N_e\nu_{k0}\overline{Q_{0k\,max}}\ V_e^{-1/2}\left(V_k + \frac{2}{3}V_e\right)e^{-\frac{3}{2}\cdot\frac{V_k}{V_e}}. \qquad (18a)$$

Hence we see that the brightness of the resonance line does not depend on the transition probability A_{k0}.

Let us now examine the case where step excitation (transition r → k; see Fig.1) occurs together with direct excitation. Then, eq.(16) must be supplemented by a second term corresponding to this step process: /26

$$I_0 = N_0N_e\ \frac{A_{ki}h\nu_{ki}}{\sum_{r=0}^{k-1} A_{kr}} \int_{v_k}^{\infty} F(v)\,v\overline{Q_{0k}}(v)\,dv + \\ + N_rN_e\ \frac{A_{ki}h\nu_{ki}}{\sum_{r=0}^{k-1} A_{kr}} \int_{v_k'}^{\infty} F(v)\,v\overline{Q_{rk}}(v)\,dv,$$

where v_k' is the electron velocity sufficient to cause the transition r → k.

Considering that the same assumptions are made as above, we can integrate and obtain

$$I_0 = CN_e\ \frac{A_{ki}\nu_{ki}}{\sum_{r=0}^{k-1} A_{kr}}\ V_e^{-1/2}\left\{N_0\cdot\overline{Q_{0k\,max}}\left(V_k + \frac{2}{3}V_e\right)e^{-\frac{3}{2}\frac{V_k}{V_e}} + \right. \\ \left. + N_r\overline{Q_{rk\,max}}\left(V_k' + \frac{2}{3}V_e\right)e^{-\frac{3}{2}\frac{V_k'}{V_e'}}\right\}. \qquad (19)$$

Here, $\overline{Q_{rk\,max}}$ is the effective cross section at the maximum of step excitation and V_k' is the excitation potential corresponding to the transition r → k. Usually we have $N_r \ll N_0$, but since $V_k' < V_k$ the second term in parentheses may become important. Furthermore, as already noted, the effective cross section of step excitation is generally greater than the effective cross section of direct excitation.

Thanks to the presence of the exponential term $e^{-\frac{3}{2}\frac{V_k}{V_e}}$ in eqs.(18) and (19), the brightness of the lines strongly depends on the electron temperature V_e. However, it must be remembered that, if in a gas-discharge plasma the electron temperature V_e changes as a result of a variation in the gas pressure p or in the density of the discharge current j, then the electron concentration N_e will simultaneously change. Therefore, the dependence of line brightness on the discharge conditions, generally speaking, has a complex character. In the region

of low discharge current densities, the electron temperature rapidly decreases with increasing current density. However, there is a region where the electron temperature remains practically constant on any increase in current strength. /27 In that case, I_0 depends only on N_e. In direct excitation, according to eq.(18), this dependence is linear: $I_0 = aN_e$. In the presence of both direct and step excitation, eq.(19) must be used where it can be assumed that $N_r \sim N_e$; this leads to a quadratic character of the dependence I_0 on N_e so that $I_0 = aN_e + bN_e^2$. If $N_e \sim j$, we obtain such dependences also for the discharge current density j. Upon a variation in the gas pressure p (at constant j) the electron concentration N_e rises but the electron temperature drops. This may lead to the appearance of a maximum on the curve for the dependence of I_0 on p.

All above calculations were performed for the Maxwell distribution function F(v). However, as mentioned before, deviations from the Maxwell law occur not only in zones adjacent to the electrode but also in the positive column. In the positive column, these deviations are such that they lead to a deficiency of fast electrons, and thus may have a stronger effect on direct excitation than on step excitation. The relative role of step excitation is enhanced in the presence of deviations from Maxwellian electron velocity distribution.

Equations (18), (18a), and (19) pertain to the primary brightness I_0. To calculate the true brightness of a luminous plasma, allowance must be made for the phenomenon of resorption which may play an important role, especially for resonance lines.

5. Comparison of Calculations with Experiment

To illustrate the extent to which calculated and experimental data agree, we will present the results of certain recent studies on neon glow, made at the Physics Research Institute of the Leningrad State University. Luminescence was excited at low pressures ($\sim 10^{-2}$ mm Hg) in discharge tubes of special configuration which permitted measuring the magnitude of resorption along with the line brightness (Ref.1, 11). From the magnitude of resorption we obtained the /28 quantity $N_i A_{ki}$, where N_i is the concentration of atoms at the i-th (lower) level; furthermore, the magnitude of resorption and the observed line brightness I permits calculating its primary brightness I_0. From the latter the quantity $N_k A_{ki}$ is obtained, where N_k is the concentration at the k-th (upper) level.

Probes were inserted into the tube, which made it possible to measure both electron concentration and electron temperature.

A diagram of the neon levels is shown in Fig.7. The level $2p^6\ ^1S_0$ is the normal level; appreciably higher (approximately by 16.5 ev) lie four levels pertaining to the electronic $2p^5 3s$ configuration. Two of them ($^3P_0^o$ and $^3P_2^o$) are metastable, and two others ($^1P_1^o$ and $^3P_1^o$) are radiation levels. The two lines λ 743.8 and 735.9 A lying in the far ultraviolet of the spectrum correspond to transitions from the radiation levels to the normal level. Above the four $2p^5 3sX$ levels (by approximately 2 ev) are ten levels corresponding to the electronic configuration $2p^5 3p$. The transitions $2p^5 3pY \rightarrow 2p^5 3sX$ lead to emission

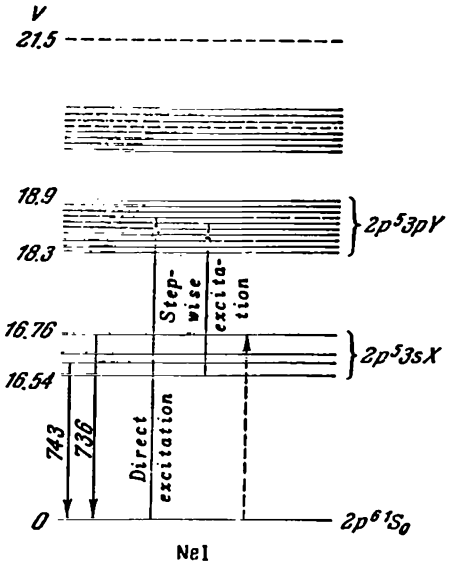
V
21.5
18.9
18.3
16.76
16.54
0
743
736
Direct excitation
Step-wise excita-tion
$2p^5 3pV$
$2p^5 3sX$
$2p^6 {}^1S_0$
NeI

Fig.7

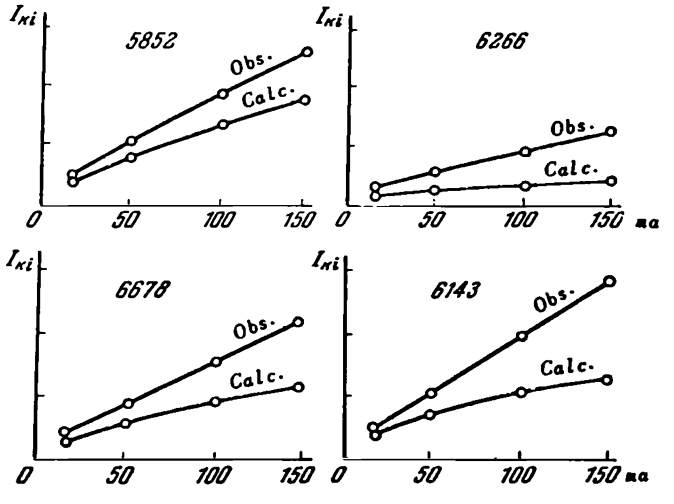
I_{Ni}
5852
Obs.
Calc.
6266
6678
6143
0
50
100
150
ma

Fig.8

of a group of bright neon lines lying in the red-orange region of the spectrum. The excitation of these lines was also investigated.

Evidently, both direct and step excitation of the $2p^5 3pY$ levels is possible (Fig.7). The original calculations were made on the assumption of the presence of only direct excitation, i.e., by means of a formula of the type of eq.(18). The effective cross sections $\overline{Q_{0k}}$ of direct excitations of all ten $2p^5 3pY$ levels were measured by the electron beam method (Ref.12). Their values for individual levels are within $1 \times 10^{-19} \sim 6 \times 10^{-19}$ cm^2. The concentration of normal atoms was determined from the gas pressure and temperature in the tube, and the electron concentration N_e and electron temperature T_e by the probe method. Measurements were taken for a pressure of 5×10^{-2} mm Hg and a discharge current strength of 18 to 150 ma, corresponding to discharge current densities of 3.7 to 31 ma/cm^2. Under these conditions, the electron velocity distribution should be close to Maxwellian, making application of the calculation formulas (18) and (19) valid.

Figure 8 shows the primary brightnesses of four neon lines: λ 5852, 6266, 6678, and 6143 Å as a function of the discharge current strength. The values /30 of I_{ki} obtained by measurements (observed) and those calculated on the assumption of the presence of only direct excitation (calculated) are given. As we see, for the weakest current (18 ma) the calculated and measured values of brightnesses coincide. To illustrate how well this works out, we are presenting the numerical data:

Wavelength λ, Å	Transition	Absolute Brightness in erg/cm^2 sec	
		Obs.	Calc.
5852	$3p^1S_0 \rightarrow 3s^1P_1^0$	313	360
6266	$3p^1P_1 \rightarrow 3s^3P_0^0$	41	44
6678	$3p^3P_2 \rightarrow 3s^1P_1^0$	58	69
6143	$3p^1D_2 \rightarrow 3s^3P_2^0$	104	88

With an increase in discharge current, there occurs an explicit divergence between the calculated and measured line brightnesses: The actual brightness is higher than the calculated value. This can be explained only by the presence of step excitation.

To calculate the portion of step excitation [second term in eq.(19)] it is necessary to know the concentration of excited atoms in the $2p^5 3sX$ states. These concentrations were determined by the resorption method. The results of such measurements are given in Fig.9. They can be used for calculating the step excitation, but we still need to know the effective cross sections for step excitation $2p^5 3s \rightarrow 2p^5 3p$. Since these cross sections $\overline{Q_{1k}}$ are not known, one can proceed in an inverse manner, calculating the values of $\overline{Q_{1k}}$ from the magnitude of divergence between the curves in Fig.8 and then defining the degree of convergence of these values calculated from measurements, for different discharge current strengths. The next table shows that there is full agreement.

The cross sections refer to the overall process of population from all four levels $2p^5 3sX$, since the experiment did not permit an observation of excitation, separately from the levels $2p^5 3s\,{}^1P_1^o$, ${}^3P_0^o$, ${}^3P_1^o$, ${}^3P_2^o$. /31

Level	$\overline{Q_{ik}} \times 10^{16}$ cm²			Mean
	50 ma	90 ma	150 ma	$\overline{Q_{ik}} \times 10^{16}$ cm²
$3p^1S_0$	8.4	10.6	9.0	9.3
$3p^1P_1$	5.5	5.2	5.6	5.4
$3p^3P_2$	8.0	9.1	7.8	8.3
$3p^1D_2$	9.9	10.9	9.2	10.0

This indicates that, at low pressure and relatively low density of the discharge current, the process of excitation of the $2p^5 3pY$ levels of neon is satisfactorily described by the analyzed scheme which accounts for both direct and step excitation. At a low discharge current density of ~3.7 ma/cm³ (electron concentration $N \sim 2 \times 10^9$ cm^{-3}) the role of the step process is negligible; at a discharge current density of ~30 ma/cm² ($N_e \sim 17 \times 10^9$ cm^{-3}) approximately half of all excitation events occur as a result of the step process. At even greater discharge current densities, the step process of excitation becomes the main process. /32

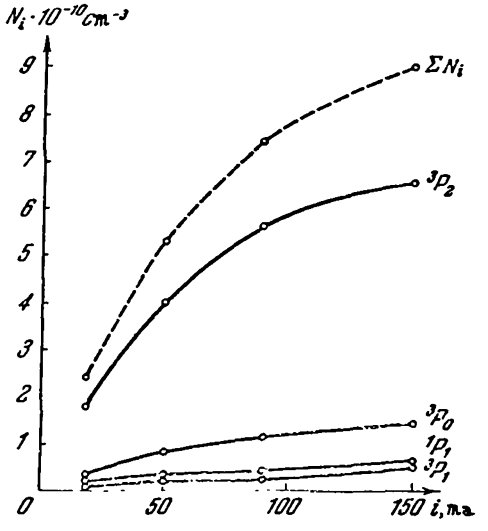

Fig.9

Let us now turn to the group of $2p^5 3sX$ levels (Fig.9). We note first of all that there is no substantial difference between the degree of population of the metastable and nonmetastable levels; for example, the population of the metastable level ${}^3P_0^o$ exceeds the population of the radiation level ${}^1P_1^o$ by less than a factor of 2. This is due to two causes: First, owing to resorption, the disintegration of the radiation levels proceeds much more slowly than would be the case at free release of radiation from the plasma volume ("radiative capture"); second, transitions occur between metastable and nonmetastable levels owing to collisions of the first and second kind with slow electrons. In narrow tubes at low pressures, disintegration of metastable atoms on the walls plays a major role.

The widely held opinion that, in a gas-discharge plasma, the metastable levels are populated much more heavily than nonmetastable levels is not valid even at low pressures and low current densities.

For radiation levels according to L.M.Biberman (Ref.13), in a cylindrical tube of radius R the effective lifetime is correlated with its radiation lifetime τ_k over the following relation:

$$\tau_{eff} = \varkappa_0 R \sqrt{\ln \varkappa_0 R}\,\tau_k, \tag{20}$$

where $\varkappa_0$ is the absorption coefficient at the line center;

$$\tau^k = \frac{1}{A^{k0}}.$$

If ΔN_{0k} is the number of excitation events of the k-th resonance level in unit time per unit volume, then the stationary-state condition yields

$$\Delta N_{0k} = N_k/\tau_{eff}.$$

Hence, on the basis of eq.(20) we obtain /33

$$N_k = \Delta N_{0k} \frac{\varkappa_0 R \sqrt{\ln \varkappa_0 R}}{A_{k0}}. \tag{21}$$

If excitation of the resonance level occurs only as a result of electron collision and if the electron velocities are distributed in accordance with the Maxwell law, then, according to our above statements, we can write

$$N_k = CN_0N_e \frac{\varkappa_0 R \sqrt{\ln \varkappa_0 R}}{A_{k0}} \overline{Q_{0k}} V_c^{-1/2} \left(V_k + \frac{2}{3} V_c\right) e^{-\frac{3}{2}\frac{V_k}{V_c}}. \tag{22}$$

We note that step excitation from resonance levels does not affect their degree of population. The fact is that, in a stationary state, each excitation event is canceled out by a population event owing to return radiative transition from higher levels.

The primary brightness of the resonance line I_0 can be found on the basis of the relation $I_{0k} = N_k A_{k0} h\nu_{k0}$. The actual brightness I'_{0k} is found from I_{0k} under consideration of resorption phenomena.

For both neon resonance lines, λ 743.8 and 735.9 Å, the effective cross sections $\overline{Q_{0k}}$ are unknown. Furthermore, measurement of the absolute brightnesses of these lines encounters substantial experimental difficulty since they lie in the far ultraviolet. Therefore, a check of the applicability of the investigated excitation scheme of the resonance lines was carried out, just as above, by comparing the values of the effective cross sections $\overline{Q_{0k}}$ calculated for different discharge current strengths.

For the concentrations of neon atoms N_k in the states $3s^1P_1^0$ and $3s^3P_1^0$ we used values determined from the resorption of lines lying in the visible orange-red portion of the spectrum (see Fig.9). On the basis of these values of N_k

and using eq.(22), we calculated the effective cross section Q_{0k} for four discharge current strengths: 18, 50, 90, and 150 ma. The gas pressure in all cases was 5×10^{-2} mm Hg.

The results of these calculations are given in the next table.

Levels	$\overline{Q_{0k}} \cdot 10^{16}$ cm²	
Current Strength, ma	$3s^3P_1^0$	$3s^3P_1$
18	3.2	2.0
50	2.4	1.8
90	2.7	1.9
150	2.8	3.1
Average	2.8	2.2

As we see, the agreement of the values of $\overline{Q_{0k}}$, on the basis of measurements made at different discharge current strengths, is completely satisfactory /34 (the discharge parameters, for example the electron concentration, vary in this case by a factor of almost 10). Thus, it can be considered that, at a low pressure (5×10^{-2} mm Hg) and at low discharge current density (4 - 30 ma/cm²), this simple excitation scheme of resonance levels is justified.

6. Role of Secondary Processes

The good agreement between calculated and observed concentrations (or line brightnesses) is observed only at low pressures. Upon an increase of pressure, even at low discharge current densities, deviations will occur: In most cases, the observed concentrations of excited atoms are appreciably less than calculated. Figure 10 shows the experimentally determined and calculated concentrations of excited neon atoms in the $2p^5 3s\,{}^1P_1^0$ and $^3P_2^0$ states at a discharge current strength of 90 ma and a pressure variation in the range of 5×10^{-2} to 3.5×10^{-1} mm Hg.

As we see, the experimental and calculated data differ appreciably: At $p = 3.5 \times 10^{-1}$ mm Hg, the observed concentration at the $^1P_1^0$ level is approximately one half of that calculated. Figure 11 shows the observed and calculated atom concentrations on the $2p^6 3p\,{}^1S_0$ and $^3P_2$ levels, at the same discharge current strength of 90 ma and in the same pressure range. Here again, /36 the observed values are lower than those calculated. The divergences at high discharge current strength and at high pressures are even more distinct, both in a direct-current discharge (Ref.14) and in a high-frequency discharge (Ref.15).

What are the reasons for these divergences? First of all, let us recall our previously mentioned deviation from the Maxwell law: There are fewer fast electrons in the plasma than at equilibrium distribution. However, this circumstance alone cannot explain all peculiarities of the experimental data. At

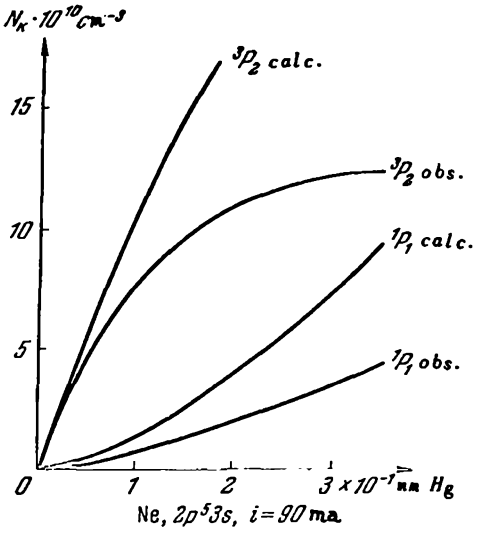
$N_к \cdot 10^{10}$ см$^{-3}$
$^3P_2$ calc.
$^3P_2$ obs.
$^1P_1$ calc.
$^1P_1$ obs.
15
10
5
0
1
2
3 x 10^{-1} мм Hg
Ne, $2p^53s$, $i = 90$ ma

Fig.10

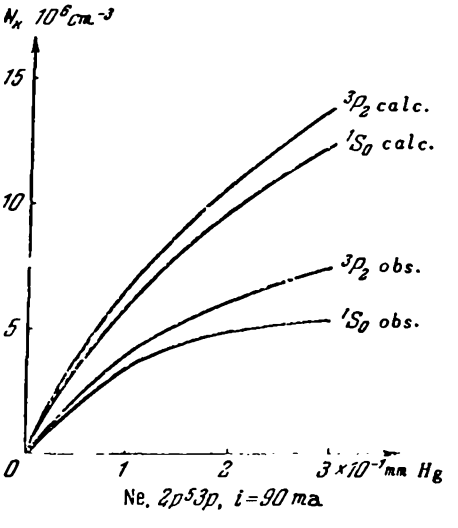
$N_к$ 10^6 см$^{-3}$
15
10
5
0
$^3P_2$ calc.
$^1S_0$ calc.
$^3P_2$ obs.
$^1S_0$ obs.
1
2
3 x 10^{-1} мм Hg
Ne. $2p^53p$, $i = 90$ ma

Fig.11

high current densities, the population of the $2p^5 3pY$ levels occurs almost entirely as a result of step excitation; the latter proceeds by slow electrons for which there should be no noticeable deviation from the Maxwell law (experimental values are taken in the calculation for the concentration of intermediate $2p^5 3sX$ states). Thus, we must acknowledge that there exists some other additional processes of level disintegration. One such process may be step ionization. Another possible process might be the formation of molecular ions of the type A_2^+ and their subsequent dissociation. Even more complex would be processes in a discharge in a mixture of gases where collisions of the second kind between excited and unexcited atoms become significant and where the probability of the occurrence and decay of molecule-ion formations is greater (Ref.16).

Summing up, one can say that the simple excitation scheme of plasma luminescence due to collisions with electrons, whose velocities have Maxwellian distribution, is valid only at very low pressures and at very low discharge current densities. Subsequently, deviations from Maxwellian electron velocity distribution become effective, and various secondary processes, most of which are little studied, begin to play an essential role.

At still higher pressures and densities of the discharge current, a simplification again takes place - the plasma begins to approach equilibrium in which the electron temperature tends to coincide with the temperature of the gas itself and the atoms are distributed, with respect to the excited levels, in accordance with the Boltzmann law.

REFERENCES /37

1. Mitchell, A. and Zemanskiy, M.: Resonance Radiation and Excited Atoms (Rezonansnoye izlucheniye i vozbuzhdennyye atomy). ONTI, 1937.
2. Rozhdestvenskiy, D.S.: Studies on the Anomalous Dispersion in Metal Vapors (Raboty po anomal'noy dispersii v parakh metallov). Izd. Akad. Nauk SSSR, 1951.
3. Frish, S.E.: Optical Spectra of Atoms (Opticheskiye spektry atomov). Fizmatgiz, 1963.
4. Ostrovskiy, Yu.N., Penkin, N.P., and Shabanova, L.N.: Dokl. Akad. Nauk SSSR, Vol.120, p.66, 1958; Izv. Akad. Nauk SSSR, Ser. Fiz., Vol.22, p.725, 1958.
5. Penkin, N.P.: Determination of Oscillator Forces in Atomic Spectra (Opredeleniye sil ostsillyatorov v spektrakh atomov). J. Quant. Spectrosc. Radiat. Transfer, Vol.4, p.41, 1964.
6. Sobel'man, I.I.: Introduction to the Theory of Atomic Spectra (Vvedeniye v teoriyu atomnykh spektrov). Fizmatgiz, 1960.
7. Kaptsov, N.A.: Electronics (Elektronika). Gostekhizdat, 1953.
8. Kagan, Yu.M. and Perel', V.I.: Usp. Fiz. Nauk, Vol.81, No.3, 1963.
9. Vorob'yeva, N.A., Kagan, Yu.M., and Milenin, R.M.: Zh. Tekhn. Fiz., Vol.33, p.571, 1963.
10. Fabrikant, V.A.: Tr. Vses. Elektrotekhn. Inst., No.41, 1941.
11. Frish, S.E. and Bochkova, O.P.: Vestn. Leningr. Univ., No.4, p.63, 1957.
12. Frish, S.E. and Revald, E.F.: Opt. i Spektroskopiya, Vol.15, p.726, 1963.
13. Biberman, L.M.: Zh. Eksp. Fiz., Vol.17, p.416, 1947; Dokl. Akad. Nauk SSSR,

Vol.19, p.507, 1948.
14. Kagan, Yu.M., Lyagushchenko, R.I., and Khokhayev, A.D.: Opt. i Spektroskopiya, Vol.14, p.598, 1963.
15. Bochkova, O.P., Razumovskaya, L.P., and Frish, S.E.: Opt. i Spektroskopiya, Vol.11, p.697, 1961.
16. Bogdanova, I.P., Bochkova, O.P., and Frish, S.E.: Dokl. Akad. Nauk SSSR, Vol.156, p.54, 1964.

CALCULATIONS OF ATOMIC ENERGY LEVELS /38

A.P.Yutsis and Ya.I.Vizbarayte

1. Introduction

Atomic spectra arise on transitions from one energy level to another. These levels are characterized by an aggregate of states, whose detection is one of the problems in studying many-electron atoms.

Problems associated with calculating many-electron atoms are amenable only to approximate solution. Therefore, the aggregates of the states characterizing the levels can be found only in first approximation. Refinement of the solution of the problem leads to a superposition of states which, in turn, results in a loss of clear representation when systematizing the levels. In view of this, one of the main problems is to find characteristics that will yield the best approximation to the true aggregates of states. At the present state of the art in the field of quantum atomic theory, this is achieved by selecting an appropriate method of vector addition of angular momenta, known as mode of coupling. One of the tasks of this paper is to examine the coupling modes giving the best approximation for phenomena most often encountered in atomic spectra.

Of exceptional importance in a study of spectra is the theoretical determination of the transition probability of an atom from one energy level to another, which is needed for estimating the intensity of individual spectral lines. This is especially important for spectra studied by astrophysicists since many of these cannot be observed under laboratory conditions.

The difference in the energy values for levels between which transition takes place is of importance in determining the transition probability. /39
Therefore, a theoretical determination of the energies of levels is highly essential in atomic theory. The bulk of this paper is devoted to this problem.

The energy of an atom depends on the state of the atom; therefore, its determination is based primarily on establishing the characteristic of the atom, mentioned above. The states of an atom are described by wave functions, used in calculations for the values of physical quantities in general and of energy in particular. For this reason, the accuracy of finding the energy is determined by the accuracy of constructing the wave functions of the states of the levels between which transition occurs, with the latter depending - as indicated above - on the suitability of mode of coupling selected. Thus, all these aspects of the problem make up a single problem that can be solved by the quantum theory of atomic spectra.

Besides selecting a specific coupling mode, the rapidity in finding an appropriate expression for energy greatly depends on the mathematical apparatus used. In first approximation, which is a rather adequate method of calculation, the wave function of the entire many-electron atom is constructed from single-electron wave functions.

At an early stage in the development of the quantum atomic theory, the wave function of the entire atom was built up in the form of determinants composed of one-electron wave functions. This had a decisive influence on the later mathematical apparatus by means of which calculations were carried out to the point where the energy can no longer be expressed by radial integrals. Subsequent calculation - for example, determination of radial one-electron wave functions - no longer depends on the apparatus by means of which the expression in terms of radial integrals is obtained. Thus, Hartree's self-consistent field method (Ref.1) and Fock's method (Ref.2) do not depend on the aforementioned mathematical apparatus since they constitute methods of solving another important part of the overall problem, namely, calculation of the atom.

The method of constructing wave functions as linear combinations of determinants stimulated progress in the theory of complex spectra. This method /40
forms the basis of the widely known book by Condon and Shortley (Ref.3) published in 1935 and of the noteworthy book by Hartree (Ref.4) published in 1957, as well as of numerous other books and journal articles.

At the beginning of the 1940s, a new and more convenient method was developed for calculating angular and spin variables in the search for expressions for physical quantities in terms of radial integrals. This is the so-called mathematical apparatus of irreducible tensorial operators, the foundation of which was laid by Racah in his works published in 1942, 1943, and 1949 (Ref.5, 6, 7). This method is based on constructing wave functions by direct coupling of angular momenta according to the so-called vector model. This method covers all systems of quantum particles. The theory of irreducible tensorial operators presented in Fano and Racah's book (Ref.8) and the theory of angular momenta given by others (Ref.9, 10) and in many other books [see, for example, Edmonds (Ref.11)] plays an important role in it. Both these problems constitute two aspects of the same problem - the theory of representations of three-dimensional rotation groups - since this theory is the starting point of the indicated method.

Recently, this new method has become so widespread that modern textbooks on the theory of atomic spectra are based on the mathematical apparatus of irreducible tensorial operators. This is characteristic for Sobel'man's new book (Ref.12) which encompasses a wide range of problems of quantum atomic theory, and Levinson and Nikitin's book (Ref.13) intended specifically for astrophysicists. The same can be said for books (Ref.14, 15) published in other countries.

In our report, after a brief account of the methods of constructing wave functions by means of the vector model, we will show the computational procedure for deriving energy expressions, under application of the mathematical apparatus of irreducible tensorial operators. The account will go as far as calculation of many-electron atoms containing two unfilled shells of equivalent electrons, with as complete as possible an information on the computational methods.

2. Characteristics of States and Wave Functions /41

Each electron of an atom is characterized by principal (n) and by orbital (l) quantum numbers. The quantum number l determines the eigenvalue of the

square of the orbital angular momentum, namely:

$$l^2\Psi(lm_l|r,\ \vartheta,\ \varphi) = l(l+1)\Psi(lm_l|r,\ \vartheta,\varphi) \tag{1}$$

(in a system of units where $\hbar = 1$). In addition to the orbital angular momentum the electron has a spin angular momentum for which we have the equation

$$s^2\Psi(sm_s|\sigma) = s(s+1)\Psi(sm_s|\sigma)\ \ (\sigma = \pm\tfrac{1}{2}). \tag{2}$$

In view of the sameness of s $\left(=\frac{1}{2}\right)$ for all electrons and many of their states, it is usually omitted in designations of atomic states.

In the wave function $\Psi(lm_l)$, the variables are usually separated

$$\Psi(lm_l) = \frac{P(nl|r)}{r} Y(lm_l|\vartheta,\varphi), \tag{3}$$

where $P(nl|r)$ is Hartree's radial wave function and $Y(lm_l|\vartheta,\varphi)$ is a spherical function normalized to unity.

The spin function is given a very simple form

$$\Psi(sm_s|\sigma) = \delta(m_s|\sigma). \tag{4}$$

In zero approximation, the states of one electron are characterized by a set of quantum numbers nlm_lm_s; the number of the states is equal to $(2s+1)(2l+1) = 2(2l+1)$. This set of states, treated as a level, is rather approximate since the interaction between magnetic moments related with the mechanical moments l and s causes it to split into two sets according to the coupling of moments

$$l + s = j\ (\text{or}\quad l + s = j = l \pm \tfrac{1}{2}). \tag{5}$$

The wave function in the momenta coupling (5) becomes, according to the vector model, as follows: /42

$$\Psi(lsjm) = \sum_{m_lm_s} \begin{bmatrix} l & s & j \\ m_l & m_s & m \end{bmatrix} \Psi(lm_l)\Psi(sm_s). \tag{6}$$

Here, the first multiplier under the summation sign is the coefficient of vector addition or the Clebsch-Gordan coefficient which most frequently is denoted as $(lsm_lm_s|lsjm)$. For these, separate tables have been compiled. The most common ones are algebraic formulas with a numerically given value of one of the momenta (Ref.3, 9).

The levels of a one-electron atom (or atom for which one electron is outside the filled shells) are characterized by the symbol ^2L_j, where L = S, P, D, F, G, H, ... = 0, 1, 2, 3, 4, 5 ... . In this case, L = l = s, p, d, f, g, h, ... = 0, 1, 2, 3, 4, 5, ... The level ^2L is called a doublet whose indi-

vidual components are characterized by values of $j = l \pm \frac{1}{2}$. Both levels make up a term, in this case a doublet term with the aforementioned number of possible states $2(2l + 1)$ which break down into two groups of $2j + 1\left(j = l \pm \frac{1}{2}\right)$ states for individual levels. In the particular case in which $L = S = 0$, j takes only one value $1/2$ ($j \geq 0$) and the term has only one component. This doublet is called undeveloped.

In the case of two electrons, the set of quantum numbers $n_1 l_1 n_2 l_2$ gives a so-called configuration (set of one-electron nl) consisting of $4(2l_1 + 1)(2l_2 + 1)$ possible states $n_1 l_1 n_2 l_2 m_{l1} m_{l1} m_{l2} m_{s2}$. In view of the interaction between electrons coupling takes place between the individual four (two orbital and two spin) angular momenta, which is mathematically represented by vector addition. The methods of this addition may differ. Let us give the most frequently encountered couplings:

LS-coupling:

$$\boldsymbol{l}_1 + \boldsymbol{l}_2 = \boldsymbol{L}, \quad \boldsymbol{s}_1 + \boldsymbol{s}_2 = \boldsymbol{S}, \quad \boldsymbol{L} + \boldsymbol{S} = \boldsymbol{J}; \tag{7}$$

Jl-coupling:

$$\boldsymbol{l}_1 + \boldsymbol{s}_1 = \boldsymbol{j}_1, \quad \boldsymbol{j}_1 + \boldsymbol{l}_2 = \boldsymbol{K}_1, \quad \boldsymbol{K}_1 + \boldsymbol{s}_2 = \boldsymbol{J}; \tag{8}$$

LS_0-coupling:

$$\boldsymbol{l}_1 + \boldsymbol{l}_2 = \boldsymbol{L}, \quad \boldsymbol{L} + \boldsymbol{s}_1 = \boldsymbol{K}_2, \quad \boldsymbol{K}_2 + \boldsymbol{s}_2 = \boldsymbol{J}; \tag{9}$$

JJ-coupling: /43

$$\boldsymbol{l}_1 + \boldsymbol{s}_1 = \boldsymbol{J}_1, \quad \boldsymbol{l}_2 + \boldsymbol{s}_2 = \boldsymbol{J}_2, \quad \boldsymbol{J}_1 + \boldsymbol{J}_2 = \boldsymbol{J}. \tag{10}$$

The first and fourth cases are traditional coupling modes which were used almost exclusively up to the 1940s. These, and only these, were used in Condon and Shortley's work (Ref.3). These two types of coupling are paired in that the first two pairs of momenta are added at first. Then their resultants, which are conveniently called intermediate, add up to the total momentum. The second and third types of coupling represent successive addition of the four momenta. The difference between them lies in the pair of momenta with which addition begins.

The Jl-coupling was proposed by Racah (Ref.16) in 1942 and the beginning of its use dates from that time. The LS_0-coupling was proposed by Gutman and Levinson (Ref.17). Independently of this, it was also established by Eriksson and Johansson (Ref.18) from experimental data, and is used for the characteristic of levels of specific spectra.

The first type of coupling, which is often termed Russell-Saunders coupling, is the most important in the spectra of astrophysical significance. Second place can be given to the Jl-coupling. Therefore, we will examine these two types, the first one in greater detail.

Various coupling modes give different divisions of the configuration

[aggregate of the states $4(2l_1 + 1)(2l_2 + 1)$] into individual groups of states representing the energy levels of a free atom. In the case of LS-coupling the groups of states can be divided by terms ^{2S+1}L, each of which contains $(2S + 1)(2L + 1)$ possible states characterized by the corresponding values of LSM_lM_s. Because the coupling of L and S forms a resultant J, the state systems of terms are distributed by components of the term characterized by the total quantum number J. Then the states are characterized by LSJM. The number of all states in the first and second cases is obtained in the following manner:

$$\sum_{LS}(2L+1)(2S+1)=\sum_{LSJ}(2j+1)=4(2l_1+1)(2l_2+1). \tag{11}$$

For example, in the configuration npn'f the following terms are possible: /44

$$^1D,\ ^3D,\ ^1F,\ ^3F,\ ^1G,\ ^3G, \tag{12}$$

yielding the following division by components of the terms:

$$^1D_2,\ ^3D_1,\ ^3D_2,\ ^3D_3,\ ^1F_3,\ ^3F_2,\ ^3F_3,\ ^3F_4,\ ^1G_4,\ ^3G_3,\ ^3G_4,\ ^3G_5. \tag{13}$$

Depending on parity, $l_1 + l_2$ configurations are called even and odd. In the case of odd configurations the index 0 is attached to the corresponding symbols denoting the terms. The example given above represents an even configuration $(1 + 3 = 4)$, therefore there is no additional index. If the configuration were, for example, npn'd, then the terms would be written as

$$^1P^0,\ ^3P^0,\ ^1D^0,\ ^3D^0,\ ^1F^0,\ ^3F^0, \tag{14}$$

since they originate from the odd $(1 + 2 = 3)$ configuration.

As we see, a two-electron energy spectrum consists of singlets and triplets. Because the components of the triplets are closely adjacent while singlets are more distant, it is often apparent from experimental data whether or not there is an LS-coupling suitable for the given configuration.

In the case of Jl-coupling, the set of states of the configuration breaks up into doublets which are denoted $J_1 l_2[K_1]$. The individual components of these doublets are characterized by the value $J = K_1 + \frac{1}{2}\left(s_2 = \frac{1}{2}\right)$, attached to the designation of the doublet as an index: $J_1 l_2[K_1]_J$. In the case of the configuration npn'f we will have doublets

$$\begin{gathered}\tfrac{1}{2}3\left[3\tfrac{1}{2}\right],\ \tfrac{1}{2}3\left[2\tfrac{1}{2}\right],\ \tfrac{3}{2}3\left[4\tfrac{1}{2}\right],\ \tfrac{3}{2}3\left[3\tfrac{1}{2}\right],\\ \tfrac{3}{2}3\left[2\tfrac{1}{2}\right],\ \tfrac{3}{2}3\left[1\tfrac{1}{2}\right].\end{gathered} \tag{15}$$

On dividing these doublets by components, we have

$$\tfrac{1}{2}3\left[3\,\tfrac{1}{2}\right]_4,\ \tfrac{1}{2}3\left[3\,\tfrac{1}{2}\right]_3,\ldots,\quad \tfrac{3}{2}3\left[1\,\tfrac{1}{2}\right]_2,\ \tfrac{3}{2}3\left[1\,\tfrac{1}{2}\right]_1. \tag{16}$$

The doublet structure (without distinguishing single levels) in the energy spectrum indicates the possibility of Jl-coupling. /45

In the case of LS_0-coupling the energy spectrum also consists of doublets which are designated $L[K_2]$; however, in this case all new doublets originating from the same L lie closely together.

Each addition of two momenta means the summing of two wave functions. In the case of the first two additions (7) we have the following relations:

$$\Psi(n_1l_1n_2l_2LM_L\,|\,\boldsymbol{r}_1,\boldsymbol{r}_2)=\sum_{m_{1l}m_{2l}}\begin{bmatrix}l_1 & l_2 & L\\ m_{1l}m_{2l}M_L\end{bmatrix}\times \\ \times\,\Psi(n_1l_1m_{1l}\,|\,\boldsymbol{r}_1)\,\Psi(n_2l_2m_{2l}\,|\,\boldsymbol{r}_2), \tag{17}$$

$$\Psi(s_1s_2SM_S\,|\,\sigma_1,\sigma_2)=\sum_{m_{1s}m_{2s}}\begin{bmatrix}s_1 & s_2 & S\\ m_{1s}m_{2s}M_S\end{bmatrix}\Psi(s_1m_{1s}|\sigma_1)\Psi(s_2m_{2s}|\sigma_2). \tag{18}$$

The third addition in (7) leads to a further summing of wave functions:

$$\Psi(n_1l_1n_2l_2LSJM\,|\,\boldsymbol{r}_1,\sigma_1,\boldsymbol{r}_2,\sigma_2)= \\ =\sum_{M_LM_S}\begin{bmatrix}L & S & J\\ M_LM_SM\end{bmatrix}\Psi(n_1l_1n_2l_2LM_L\,|\,\boldsymbol{r}_1,\boldsymbol{r}_2)\,\Psi(s_1s_2SM_S\,|\,\sigma_1,\sigma_2). \tag{19}$$

This function describing the states $^{2s+1}L_J$ does not satisfy the Pauli exclusion principle - is not antisymmetric relative to the interchange of the coordinates (or one-electron quantum numbers) of the electrons. This principle is satisfied by the function

$$\Psi(n_1n_2l_1l_2LSJM\,|\,x_1,x_2)=N_{LS}\,[\Psi(n_1l_1n_2l_2LSJM\,|\,x_1,x_2)+ \\ +(-1)^{l_1+l_2-L+s_1+s_2-S}\,\Psi(n_2l_2n_1l_1LSJM\,|\,x_1,x_2)]. \tag{20}$$

Here, $x_1=\boldsymbol{r}_1,\ \sigma_1$, and N_{LS} is the norming factor

$$N_{LS}=\begin{cases}\dfrac{1}{\sqrt{2}}, & \text{if}\quad n_1l_1\neq n_2l_2,\\ \dfrac{1}{2}, & \text{if}\quad n_1l_1=n_2l_2.\end{cases} \tag{21}$$

The antisymmetric nature of eq.(20) is obvious from the property of commutation of the coupling momenta which consists of the appearance of a coefficient equal to minus one in a power equal to the sum of the momenta being coupled /46

minus their resultant momentum.

The antisymmetric wave function in Jl-coupling is written as

$$\Psi(n_1 n_2 l_1 l_2 J_1 K_1 JM | x_1, x_2) = N_{Jl} [\Psi(n_1 l_1 n_2 l_2 J_1 K_1 JM | x_1, x_2) - \Psi(n_1 l_1 n_2 l_2 J_1 K_1 JM | x_2, x_1)], \quad (22)$$

$$N_{Jl} = \begin{cases} \frac{1}{\sqrt{2}}, & \text{if} \quad n_1 l_1 \neq n_2 l_2, \\ 0, & \text{if} \quad n_1 l_1 = n_2 l_2. \end{cases} \quad (23)$$

In this case, we have transposed the coordinates but not the quantum numbers, since transposition of the quantum numbers is associated with rather complex transformation which can be expressed by

$$\Psi(n_1 l_1 n_2 l_2 J_1 K_1 JM | x_1, x_2) = \sum_{J_1 K_1'} (l_1 s_1 (J_1) l_2 (K_1) s_2 J | l_2 s_2 (J_2) l_1 (K_1') s_1 J) \times \Psi(n_2 l_2 n_1 l_1 J_2 K_1' JM). \quad (24)$$

The function (22), just as functions in other couplings, can be obtained from eq.(20) by transformation

$$\Psi(n_1 n_2 l_1 l_2 J_1 K_1 JM | x_1, x_2) = \sum_{LS} (l_1 s_1 (J_1) l_2 (K_1) s_2 J | l_1 l_2 (L), s_1 s_2 (S), J) \times \Psi(n_1 n_2 l_1 l_2 LSJM | x_1, x_2), \quad (25)$$

where, as in eq.(24), the multiplier on the right-hand side in front of the wave function represents the transformation matrix.

Let us now examine the states of a shell of so-called equivalent electrons, which consists of a definite number of electrons with an identical nl. In this case, only LS- or jj-couplings are possible, the former being the more frequent type. Therefore, let us examine only the LS-coupling.

In the case of two equivalent electrons, the wave function is obtained directly from eq.(20), from where it follows that /47

$$\Psi(nl^2 LSJM | x_1, x_2) = \frac{1}{2} [1 + (-1)^{L+S}] \Psi(nlnlLSJM | x_1, x_2). \quad (26)$$

Hence we have the condition

$$L + S \text{ is an even number}, \quad (27)$$

whereas in the opposite case the wave function is equal to zero, which means exclusion (according to the Pauli principle) of such terms.

If the shell contains three equivalent electrons, the wave function is expressed in the following manner (for the two-electron terms we write L_0S_0):

$$\Psi(nl^3\alpha LSJM) = \sum_{L_0S_0} (l^3LS \| l^2(L_0S_0)\, l)\, \Psi(nl^2(L_0S_0)\, lLSJM). \tag{28}$$

The third multiplier on the right-hand side is termed the fractional parentage coefficient. This is superposed by the condition that the function of the three electrons be antisymmetric if the function of two electrons is antisymmetric. Summation of the momenta L and S to J on both sides of eq.(28) is identical, so that it is permissible to examine only one term from the sum. Then, in place of eq.(28) we have

$$\Psi(nl^3\alpha LSM_LM_S) = \\ = \sum_{L_0S_0} (l^3LS \| l^2(L_0S_0)\, l)\, \Psi(nl^2(L_0S_0)\, lLSM_LM_S). \tag{29}$$

The wave function on the right-hand side is the result of the following vector addition:

$$\Psi(nl^2(L_0S_0)\, lLSM_LM_S) = \sum_{M_{L_0}M_{S_0}m_l m_s} \begin{bmatrix} L_0 & l & L \\ M_{L_0} & m_l & M_L \end{bmatrix} \times \\ \times \begin{bmatrix} S_0 & s & S \\ M_{S_0} & m_s & M_S \end{bmatrix} \Psi(nl^2L_0S_0M_{L_0}M_{S_0})\, \Psi(lm_l). \tag{30}$$

In eqs.(28) and (29), the quantity α gives an additional characteristic of (identical) terms which in the case $l = 0.1$ is not obligatory; in the case of $l = 2$ we use the seniority number introduced by Racah (Ref.6) and denoting the number of electrons at which the corresponding term first appears. /48

A generalization of eq.(29) yields

$$\Psi(nl^N\alpha LSM_LM_S) = \sum_{L_0S_0} (l^NLS \| l^{N-1}(L_0S_0)\, l) \times \\ \times \Psi(nl^{N-1}(L_0S_0)\, lLSM_LM_S). \tag{31}$$

The fractional parentage coefficients for $l = 1$, 2 (the case $l = 0$ being trivial) are given by Racah (Ref.6) and also in other monographs (Ref.12 - 14).

If the shell is filled [having $2(2l + 1)$ electrons], only the single term ^1S is possible. This means that the total momenta are equal to zero. Such shells present no difficulties in theory, so that it is more important to study incomplete shells. If there are two of these in a given atom, the configuration is written as $n_1l_1^{N_1}n_2l_2^{N_2}$. With consideration of the characteristics of indi-

vidual shells we write $n_1 l_1^{N_1} n_2 l_2^{N_2} \alpha_1 L_1 S_1 \alpha_2 L_2 S_2$. The momenta L_1, S_1, L_2, S_2 can be coupled by the same types of coupling as in the case of two nonequivalent electrons ($N_1 = N_2 = 1$). Then, in eqs.(7) - (10) the quantities L_1, L_2, S_1, S_2 must be substituted for l_1, l_2, s_1, s_2 while everything else remains valid.

Antisymmetric wave functions of individual shells are derived on the basis of eq.(31), and then are correlated, in the same manner as for two electrons, with subsequent antisymmetrization with respect to electrons belonging to individual shells. In the case of LS-coupling a formula more complex than eq.(20) is obtained. As will be shown, properly chosen methods will avoid the use of rather complex formulas.

3. Derivation of an Expression for Energy; Cases of One- and Two-Electron Configurations

As is known, an operator is associated with any physical quantity in quantum mechanics. In the case of energy, this operator is the so-called Hamiltonian which is obtained from the energy equation over the coordinates $\mathbf{r}$ and /49 the momenta $\mathbf{p}$ by substituting $\mathbf{r} \rightarrow \mathbf{r}$, $\mathbf{p} \rightarrow i\nabla$ (∇ being the gradient operator). The Hamiltonian is denoted by H, and its matrix element, in abbreviated form, is written as

$$(KP \mid H \mid K'P') = \int \Psi^* (KP \mid X) H \Psi (K'P' \mid X) dX. \qquad (32)$$

Here, K denotes the configuration, P represents all other quantum numbers, and X all variables (spatial and spin) of these electrons. The integral symbolizes integration over all spatial variables and summation over all spin variables.

The energy matrix [eq.(32)] should be diagonal relative to KP for its diagonal elements to represent the values and the quantity with which the operator is associated. Good approximation is obtained by neglecting the matrix elements of eq.(32) for which $K \neq K'$ (one-configurational approximation) which can be done since these are small if they are not identically zero.

The entire set of quantum numbers P should be such that those matrix elements, for which $P \neq P'$, are small. Since P depends on the type of coupling, an important problem is the selection of a type of coupling for which the matrix (32) is diagonal relative to P with optimum exactness.

It should be mentioned that a method exists for diagonalizing the matrix (32), leading to a linear combination of wave functions with different P (and also of K in a multiconfigurational approximation); however, this would cancel the significance of the characteristic of the levels by means of sets of quantum numbers, discussed in the preceding Section. Therefore, an attempt must always be made to select such characteristics of the levels, and thus such types of coupling, that the matrix (32) will be as close as possible to diagonal.

The matrices for the operators of kinetic energy and energy of electrostatic interaction with the nuclear charge are diagonal relative to P and, furthermore, do not depend on P. Thus, they depend only on the configuration and are independent of the type of coupling or of the other characteristics. These opera-

tors, for the entire configuration, have the form

$$H^k = \sum_i H_i^k = \sum_i \left[-\frac{1}{2}\Delta_i - \frac{Z}{r_i} \right], \tag{33}$$

where Z is the nuclear charge and Δ_i is the Laplacian operator. Its matrix element is expressed by /50

$$\begin{aligned} \mathcal{E}^k = (n_1 l_1^{N_1} n_2 l_2^{N_2} \ldots | H^k | n_1 l_1^{N_1} n_2 l_2^{N_2} \ldots) = \\ = N_1 I(n_1 l_1) + N_2 I(n_2 l_2) + \ldots, \end{aligned} \tag{34}$$

where the radial integral

$$I(nl) = -\frac{1}{2}\int_0^\infty P(nl|r)\left[\frac{d^2}{dr^2} + \frac{2Z}{r} - \frac{l(l+1)}{r^2}\right] P(nl|r)\, dr \tag{35}$$

can be calculated by radial wave functions. Equations (33) and (35) are written in a system of units in which $\hbar = 1$, $e = 1$ (e being the absolute value of the electron charge) and which we will use in our entire discussion.

An important portion of the Hamiltonian consists of the operator of electrostatic interaction between electrons

$$H^e = \sum_{j>i} \frac{1}{r_{ij}}. \tag{36}$$

Its matrix is diagonal relative to the quantum numbers JM and, furthermore, does not depend on M. Therefore, P can be conveniently decomposed

$$P = QJM, \tag{37}$$

to yield the matrix elements relative to QJ. The operator Q gives rather extensive information on the investigated configuration, including the type of coupling, an additional characteristic in the presence of recurrent terms, etc.

Since the operator Q is absent in the case of one atomic electron we will begin our discussion with a two-electron configuration, which ensures accuracy of the solution to the problem. Let us examine in more detail the case of LS-coupling for which Q = LS and for which the matrix is independent of J at a given LS. We will use the well-known expansion

$$\frac{1}{r_{ij}} = \sum_k \frac{r_<^k}{r_>^{k+1}} (C_i^k \cdot C_j^k), \tag{38}$$

where C_i^k is the same spherical function as in eq.(3), except that it is not normed to unity but to $\left[\frac{4\pi}{2k+1}\right]^{1/2}$. The subscript denotes the number of the /51

coordinate and

$$(C_i^k \cdot C_j^k) = \sum_q (-1)^q C_{iq}^k C_{j,-q}^k = \sum_q (-1)^q C_{i,-q}^k C_{jq}^k \tag{39}$$

means the scalar product of these two spherical functions which have properties of irreducible tensors.

In place of H in eq.(32) let us use eq.(38) and in place of the wave function, eq.(20) without JM (in the absence of JM we must expand in functions of $M_l M_s$ in place of JM, by means of Clebsch-Gordan coefficients, and then use one term of the series). The use of eq.(39) from an earlier paper (Ref.9) will yield ($M_l M_s$ is omitted since the matrix element does not depend thereon)

$$\begin{aligned}\left(n_1 n_2 l_1 l_2 LS \left| \frac{1}{r_{12}} \right| n_1 n_2 l_1 l_2 LS\right) = \\ = 2N_{LS}^2 \sum_k \Big[(-1)^{l_1+l_2+L} (l_1 \| C^k \| l_1) (l_2 \| C^k \| l_2) \times \\ \times \begin{Bmatrix} l_1 l_2 L \\ l_2 l_1 k \end{Bmatrix} F_k (n_1 l_1, n_2 l_2) + (-1)^S (l_1 \| C^k \| l_2)^2 \times \\ \times \begin{Bmatrix} l_2 l_1 L \\ l_2 l_1 k \end{Bmatrix} G_k (n_1 l_1, n_2 l_2) \Big].\end{aligned} \tag{40}$$

Here,

$$\begin{Bmatrix} a b e \\ d c f \end{Bmatrix} \tag{41}$$

are the so-called 6j-coefficients. We must remember that the four sets of three parameters abe, acf, dbf, dce should constitute triads - the sums should be integers and one of the parameters cannot be greater than the sum of the other two. Furthermore, it is known from symmetry properties that the columns can be represented in any manner and two columns can be inverted [compare eq.(16.4) from (Ref.9)]. The values of these coefficients for all given parameters are taken from tables given elsewhere (Ref.19 or 20). Shortened tables of 6j-coefficients were given by us earlier (Ref.10). The corresponding algebraic ex- /52
pressions, for some numerically assigned parameters, are contained in other earlier papers (Ref.10, 11, 12).

The quantities $(l \| C^k \| l')$ are called reduced matrix elements of the operator C^k. For these, it should be noted that

$$(l \| C^k \| l') = (-1)^{l-l'} (l' \| C^k \| l). \tag{42}$$

Numerical values were given earlier (Ref.22). Some algebraic formulas, with one of the three parameters lkl' numerically assigned, are given in the accompanying table. These readily yield the corresponding values for all three numerically assigned parameters.

F_k and G_k are Slater radial integrals:

$$F_k (nl, n'l') = \int_0^\infty \int_0^\infty \frac{r_<^k}{r_>^{k+1}} P^2 (nl \mid r_1) P^2 (n'l' \mid r_2) \, dr_1 dr_2, \tag{43}$$

ALGEBRAIC FORMULAS FOR $(l' \| C_k \| l)$ WITH ONE OF THE PARAMETERS (k OR l') GIVEN NUMERICALLY

k	l'	$(l' \| C^k \| l)$	l'	k	$(-1)^{\frac{l'-l}{2}}(l' \| C^k \| l)$
0	l	$(2l+1)^{\frac{1}{2}}$	0	l	1
1	$l+1$	$(l+1)^{\frac{1}{2}}$	1	$l+1$	$\left[\frac{3(l+1)}{2l+3}\right]^{\frac{1}{2}}$
2	l	$-\left[\frac{l(l+1)(2l+1)}{(2l-1)(2l+3)}\right]^{\frac{1}{2}}$	2	l	$-\left[\frac{5l(l+1)}{(2l-1)(2l+3)}\right]^{\frac{1}{2}}$
2	$l+2$	$\left[\frac{3(l+1)(l+2)}{2(2l+3)}\right]^{\frac{1}{2}}$	2	$l+2$	$\left[\frac{3.5(l+1)(l+2)}{2(2l+3)(2l+5)}\right]^{\frac{1}{2}}$
3	$l+1$	$-\left[\frac{3l(l+1)(l+2)}{2(2l-1)(2l+5)}\right]^{\frac{1}{2}}$	3	$l+1$	$-\left[\frac{3.7l(l+1)(l+2)}{2(2l-1)(2l+3)(2l+5)}\right]^{\frac{1}{2}}$
3	$l+3$	$\left[\frac{5(l+1)(l+2)(l+3)}{2(2l+3)(2l+5)}\right]^{\frac{1}{2}}$	3	$l+3$	$\left[\frac{5.7(l+1)(l+2)(l+3)}{2(2l+3)(2l+5)(2l+7)}\right]^{\frac{1}{2}}$
4	l	$\frac{3}{2}\left[\frac{(l-1)l(l+1)(l+2)(2l+1)}{(2l-3)(2l-1)(2l+3)(2l+5)}\right]^{\frac{1}{2}}$	4	l	$\frac{9}{2}\left[\frac{(l-1)l(l+1)(l+2)}{(2l-3)(2l-1)(2l+3)(2l+5)}\right]^{\frac{1}{2}}$
4	$l+2$	$-\left[\frac{5l(l+1)(l+2)(l+3)}{2(2l-1)(2l+3)(2l+7)}\right]^{\frac{1}{2}}$	4	$l+2$	$-3\left[\frac{5l(l+1)(l+2)(l+3)}{2(2l-1)(2l+3)(2l+5)(2l+7)}\right]^{\frac{1}{2}}$
4	$l+4$	$\frac{1}{2}\left[\frac{5.7(l+1)(l+2)(l+3)(l+4)}{2(2l+3)(2l+5)(2l+7)}\right]^{\frac{1}{2}}$	4	$l+4$	$\frac{3}{2}\left[\frac{5.7(l+1)(l+2)(l+3)(l+4)}{2(2l+3)(2l+5)(2l+7)(2l+9)}\right]^{\frac{1}{2}}$

$$G_k(nl, n'l') = \int_0^\infty \int_0^\infty \frac{r_<^k}{r_>^{k+1}} P(nl|r_1) P(n'l'|r_1) P(nl|r_2) \times \times P(n'l'|r_2)\, dr_1\, dr_2. \quad (44)$$

These can be calculated by radial wave functions. Then eq.(40) can be written as

$$\left(n_0 n l_0 l LS \left| \frac{1}{r_{12}} \right| n_0 n l_0 l LS\right) = = \sum_k [a_k(l_0, l, L) F_k(n_0 l_0, nl) + b_k(l_0, l, L, S) G_k(n_0 l_0, nl)]. \quad (45)$$

Similar expressions, for other types of coupling, can be obtained directly or from the LS-coupling over suitable transformation. In these cases, a_k and b_k can depend also on J.

Many numerical values of the coefficients a_k and b_k for LS-coupling and for Jl-coupling are given in other reports (Ref.3, 22, 23). Algebraic formulas for a_k and b_k, at $l_0 = 1$ and at indeterminate l are given in (Ref.24), and at $l_0 = 2$ in (Ref.25) for LS, Jl, and LS_0 types of coupling.

The use of the property of 6j-coefficients (Sect.6.6) from (Ref.9) and also the equality (33.8) from (Ref.9) show that the operator /54

$$(l_1 \| C^k \| l_1)(l_2 \| C^k \| l_2) F_k(n_1 l_1, n_2 l_2)(u_1^k \cdot u_2^k) - - (l_1 \| C^k \| l_2)^2 G_k(n_1 l_1, n_2 l_2) \times \times \sum_r \begin{Bmatrix} l_1 l_2 k \\ l_2 l_1 r \end{Bmatrix} (-1)^r (2r+1) \left[\frac{1}{2}(u_1^r \cdot u_2^r) + 2(v_1^{r1} \cdot v_2^{r1}) \right], \quad (46)$$

summed with respect to k, gives eq.(40) when one term of the wave function [eq.(20)] with a normalizing factor equal to unity is used. In eq.(46), $v^{r1} = u^r s^1$ with the following determinations of u^r and s^1:

$$(l \| u^r \| l') = \delta(l, l') \quad (r = 0, 1, \ldots, 2l), \quad (47)$$

$$\left(\tfrac{1}{2} \| s^1 \| \tfrac{1}{2}\right) = \sqrt{\tfrac{3}{2}}. \quad (48)$$

As we see, the operator (46) permits obtaining the correct result without antisymmetrization of the wave functions; in other words, the requirement of the Pauli exclusion principle is taken into account by suitable modification of the operator.

In the case of two equivalent electrons, the integral G_k changes to F_k and the 6j-coefficients and reduced matrix elements of the operator C^k in both terms on the right-hand side of eq.(40) become identical, yielding

$$\left(nl^2 LS \left| \frac{1}{r_{12}} \right| nl^2 LS\right) = (-1)^L (l \| C^k \| l)^2 \begin{Bmatrix} l l L \\ l l k \end{Bmatrix} F_k(nl, nl), \quad (49)$$

provided condition (27) is satisfied. Otherwise the matrix element is equal to zero.

The next significant portion of energy is magnetic or spin interaction. Calculation of this energy component with a total operator is rather complex. In the case of two electrons, the matrix elements of the total operator for the configurations $n_0 l_0 n l$ at $l_0 = 0, 1, 2$, (l being indeterminate) were given previously (Ref.26; spin-spin interaction) and (Ref.27; spin-orbit interaction).

A good approximation is represented by the simplified spin-orbit interaction operator (spin-spin interaction is generally insignificant) having the form

/55

$$H^{s0} = \sum_i \xi_i (r_i) (l_i^1 \cdot s_i^1), \tag{50}$$

where ξ is a function of r given by the expression

$$\xi (r) = \frac{1}{2} \frac{1}{c^2} \frac{1}{r} \frac{dV}{dr} (V - \text{potential function}) \tag{51}$$

in atomic units (velocity of light c = 137). This function leads to the radial integral

$$\zeta (nl) = \int_0^\infty \xi (r) P^2 (nl|r) \, dr. \tag{52}$$

The operator (18), as any scalar operator, is diagonal relative to JM and does not depend on M. However, it does depend on J, which effects splitting of terms. In the case of one atomic electron, in accordance with eq.(33.8) from (Ref.9), we find

$$(nlsj \,|\, H^{s0} \,|\, nlsj) = \\ = (-1)^{l+s+j} \left[\frac{3}{2} l (l+1) (2l+1) \right]^{1/2} \begin{Bmatrix} l & s & j \\ s & l & 1 \end{Bmatrix} \zeta (nl). \tag{53}$$

Here we use the expression

$$(l \| l^1 \| l) = [l (l+1) (2l+1)]^{1/2}, \tag{54}$$

and also eq.(48) for the spin angular momentum. The 6j-coefficient in eq.(53) can be expressed by the formula

$$\begin{Bmatrix} a & b & e \\ b & a & 1 \end{Bmatrix} = (-1)^{a+b+e} \frac{c (e+1) - a (a+1) - b (b+1)}{2 [a (a+1) (2a+1) \, b (b+1) (2b+1)]^{1/2}}. \tag{55}$$

As an example, let us write the expression for the energy of a $2p$-electron:

$$\mathcal{E} (2pJ) = (2p^2 P_J \,|\, H^k + H^{s0} \,|\, 2p^2 P_J) = \\ = I (2p) + \frac{1}{2} \left[J (J+1) - \frac{11}{4} \right] \zeta (2p^2 P), \tag{56a}$$

$$\zeta (2p^2 P) = \zeta (2p). \tag{56b}$$

This shows that doublet splitting (or fine structure) is

$$\mathscr{E}\left(2p\,\frac{3}{2}\right)-\mathscr{E}\left(2p\,\frac{1}{2}\right)=\frac{3}{2}\zeta(2p^2P). \tag{57}$$

From experimental doublet splitting we can directly find the integral $\xi(2p)$. /56
Having the latter, we can determine the integral $I(2p)$ from the ionization energy by means of eq.(56).

In the case of a two-electron configuration, we use the wave function (20) and eqs.(33.8) - (33.10) from (Ref.9). This yields

$$\begin{aligned}(n_1n_2l_1l_2LSJ\,|\,H^{s0}\,|\,n_1n_2l_1l_2L'S'J)&=(-1)^{l_1+l_2+S+S'+J+1}\times\\ \times\left[\frac{3}{2}l_1(l_1+1)(2l_1+1)(2L+1)(2S+1)(2L'+1)(2S'+1)\right]^{1/2}&\times\\ \times\begin{Bmatrix}L&S&J\\S'&L'&1\end{Bmatrix}\begin{Bmatrix}l_1&L&l_2\\L'&l_1&1\end{Bmatrix}\begin{Bmatrix}s&S&s\\S'&s&1\end{Bmatrix}\zeta(n_1l_1)+(-1)^{l_1+l_2+L+L'+J+1}&\times\\ \times\left[\frac{3}{2}l_2(l_2+1)(2l_2+1)(2L+1)(2S+1)(2L'+1)(2S'+1)\right]^{1/2}&\times\\ \times\begin{Bmatrix}L&S&J\\S'&L'&1\end{Bmatrix}\begin{Bmatrix}l_2&L&l_1\\L'&l_2&1\end{Bmatrix}\begin{Bmatrix}s&S&s\\S'&s&1\end{Bmatrix}\zeta(n_2l_2).&\end{aligned} \tag{58}$$

If one is interested in diagonal matrix elements - and this is the case whenever the LS-coupling is suitable - the 6j-coefficients entering eq.(58) can be calculated from eq.(55).

As an example, let us write the expressions for the energy of configuration nsn'p. According to eqs.(34), (40), and (58), limiting ourselves to the diagonal matrix elements relative to LS, we obtain

$$\begin{aligned}\mathscr{E}(nsn'pLSJ)&=(nsn'pLSJ\,|\,H^k+H^s+H^{s0}\,|\,nsn'pLSJ)=\\ &=I(ns)+I(n'p)+F_0(ns,n'p)+\frac{1}{3}(-1)^S G_1(ns,n'p)+\\ &\quad+\delta(1,S)\frac{1}{4}[J(J+1)-4]\,\zeta(n'p).\end{aligned} \tag{59}$$

The coefficient of $\zeta(ns)$ is equal to zero since, in the 6j-coefficients, the triad conditions are not satisfied. The same is true of $\zeta(n'p)$ for the singlet term.

From eq.(59) we immediately find that

$$\mathscr{E}(nsn'p^3P_2)-\mathscr{E}(nsn'p^3P_1)=2\zeta(n'p^3P), \tag{60a}$$

$$\mathscr{E}(nsn'p^3P_1)-\mathscr{E}(nsn'p^3P_0)=\zeta(n'p^3P), \tag{60b}$$

$$\zeta(n'p^3P)=\frac{1}{2}\zeta(n'p). \tag{60c}$$

Here, eq.(60), just as eq.(57), expresses the well-known Lande rule.

On calculating the nondiagonal matrix element linking a triplet to a /57
singlet, a 6j-coefficient will appear in eq.(59), one parameter of which is

equal to zero. For such a 6j-coefficient, we have the formula

$$\begin{Bmatrix} a & b & c \\ d & c & 0 \end{Bmatrix} = (-1)^{a+b+c}\delta(a, c)\,\delta(b, d)\,[(2a+1)(2b+1)]^{-1/2}, \tag{61}$$

which will also be used later on. In this case the zero, according to symmetry properties, can be placed anywhere.

4. Case of One Shell of Equivalent Electrons

The expression for the kinetic and electrostatic energies relative to the nucleus is given by eq.(34). It remains to examine the electrostatic interaction between electrons and the spin-orbital interaction. We will discuss the mathematical apparatus suited to LS-coupling which is applicable for equivalent electrons. Let us introduce the operators

$$U^k = \sum_i u_i^k, \tag{62}$$

$$V^{k1} = \sum_i V_i^{k1} = \sum_i u_i^k s_i^1, \tag{63}$$

where u_i^k is determined from eq.(47), and s_i^1 from eq.(48).

According to eq.(23) (Ref.6) for one shell of l-electrons we have

$$\begin{aligned}(l^N\alpha LS\|X^{kk'}\|l^N\alpha'L'S') = N\sum_{\alpha_0L_0S_0}(l^N\alpha LS\|l^{N-1}\alpha_0L_0S_0l)\times\\ \times(L_0S_0lsLS\|x^{kk'}\|L_0S_0lsL'S')(l^{N-1}\alpha_0L_0S_0l\|l^N\alpha'L'S'),\end{aligned} \tag{64}$$

where $X^{kk'}$ can be $U^k(k'=0)$, $V^{k1}(k'=1)$ or any other operator composed of one-electron operators.

According to eq.(33.10) (Ref.9) we obtain /58

$$\begin{aligned}(L_0S_0lsLS\|u^k\|L_0S_0lsL'S') = (-1)^{L_0+l+L+k}\delta(S, S')\times\\ \times[(2L+1)(2L'+1)(2S+1)]^{1/2}\begin{Bmatrix} l & L & L_0 \\ L' & l & k \end{Bmatrix},\end{aligned} \tag{65}$$

$$\begin{aligned}(L_0S_0lsLS\|v^{k1}\|L_0S_0lsL'S') = (-1)^{L_0+S_0+l+s+L+S+k+1}\times\\ \times\left[\frac{3}{2}(2L+1)(2S+1)(2L'+1)(2S'+1)\right]^{1/2}\begin{Bmatrix} l & L & L_0 \\ L' & l & k \end{Bmatrix}\begin{Bmatrix} s & S & S_0 \\ S' & s & 1 \end{Bmatrix}.\end{aligned} \tag{66}$$

The reduced matrix elements of the operators U^k and V^{k1} for shells of p- and d-electrons are completely determined. Tables for U^2, V^{11}, and V^{21} are given elsewhere (Ref.6, 12 - 14). These make up a complete set of tables for p-electrons. The remaining cases of U^3, U^4, V^{31}, and V^{41} for the d-shell are given in (Ref.28). Some misprints are contained in all of these tables. The

corresponding corrections were given by Rudzikas (Ref.29).

As regards U^k, Rudzikas' tables (Ref.28) differ from the others in that they contain the factor $(2S + 1)^{1/2}$, meaning that the entire quantity

$$(l^N\alpha LS\|U^k\|l^N\alpha'L'S') = \\ = \delta(S, S')(2S+1)^{1/2} \times (l^N\alpha L\|U^k\|l^N\alpha'L'), \tag{67}$$

is tabulated there, whereas other authors (Ref.6, 12 - 14) give values of the reduced matrix element on the right-hand side of eq.(67) although the same designations are used as on the left-hand side of this equality. Generally, U^1 is not tabulated since its expression is very simple, namely:

$$(l^N\alpha LS\|U^1\|l^N\alpha'L'S') = \\ = \delta(\alpha LS, \alpha'L'S')\left[\frac{(2L+1)(2S+1)L(L+1)}{(2l+1)l(l+1)}\right]^{1/2}. \tag{68}$$

Other simple cases include:

$$(l^N\alpha LS\|U^0\|l^N\alpha'L'S') = N\delta(\alpha LS, \alpha'L'S')\left[\frac{(2L+1)(2S+1)}{2l+1}\right]^{1/2}, \tag{69}$$

$$(l^N\alpha LS\|V^{01}\|l^N\alpha'L'S') = \\ = \delta(\alpha LS, \alpha'L'S')\frac{[(2L+1)(2S+1)S(S+1)]^{1/2}}{(2l+1)^{1/2}}. \tag{70}$$

The following expression is highly useful: /59

$$(l^{4l+2-N}\alpha LS\|X^{kk'}\|l^{4l+2-N}\alpha'L'S') = \\ = -(-1)^{\frac{v-v'}{2}+k+k'}(l^N\alpha LS\|X^{kk'}\|l^N\alpha'L'S'), \tag{71}$$

provided that both ranks kk′ are not simultaneously equal to zero (v, v′ are seniority numbers contained in α, α', and in the case of p- and d-electrons α, α' = v, v′). In the opposite case, for the matrix elements we have

$$(l^{4l+2-N}\alpha LS|X^{00}|l^{4l+2-N}\alpha LS) = \\ = -(l^N\alpha LS|X^{00}|l^N\alpha LS) + (l^{4l+2}\alpha LS|X^{00}|l^{4l+2}\alpha LS). \tag{72}$$

On examining the electrostatic interaction of one shell of equivalent electrons we can prove on the basis of the expansion (38) that the coefficient of the radial integral $F_k(nl, nl)$ is a matrix element of the operator

$$\sum_{j>i}(C_i^k\cdot C_j^k) = \frac{1}{2}\left(\sum_i C_i^k\cdot\sum_j C_j^k\right) - \frac{1}{2}\sum_j(C_j^k\cdot C_j^k). \tag{73}$$

We use the relation

$$C_i^k \stackrel{*}{=} (l \| C^k \| l)\, U_i^k, \tag{74}$$

where the equal sign with the asterisk indicates that the equality holds when the matrix elements of both sides are taken. Then, eq.(73) can be represented as

$$\sum_{j>i=1}^{N} (C_i^k \cdot C_j^k) \stackrel{*}{=} \frac{1}{2} (l \| C^k \| l)^2 [(U_N^k \cdot U_N^k) - U_N^{kk0}]. \tag{75}$$

Here, U_N^k is determined by eq.(62), with the index indicating the number of electrons in the shell, and

$$U_N^{kk0} = \sum_{i=1}^{N} (u_i^k \cdot u_i^k). \tag{76}$$

Its matrix element is

$$(l^N \alpha LS | U^{kk0} | l^N \alpha' L' S') = N \delta (\alpha LS, \alpha' L' S') (2l+1)^{-1}. \tag{77}$$

For the coefficient f_k of the radial integral F_k we find the following expression (Ref.30): /60

$$f_k (l^N \alpha LS, l^N \alpha' LS) = \frac{1}{2} (l \| C^k \| l)^2 \Big\{ [(2L+1)(2S+1)]^{-1} \times \\ \times \sum_{\alpha'' L''} (-1)^{L-L''} (l^N \alpha LS \| U^k \| l^N \alpha'' L'' S) (l^N \alpha'' L'' S \| U^k \| l^N \alpha' LS) - \\ - N (2l+1)^{-1} \delta (\alpha, \alpha') \Big\}. \tag{78}$$

This formula is suitable for tables of U^k (Ref.28). When using the tables from (Ref.6, 12 - 14) the factor $(2S + 1)^{-1}$ must be omitted in eq.(78). By means of this formula, the expression for the energy of electrostatic interaction between electrons of one specific shell is conveniently determined. For this we need only the above-indicated tables for reduced matrix elements of the operator U^k. In the particular case when k = 0, the first indicated table, together with eq.(69), will yield

$$f_0 (l^N \alpha LS, l^N \alpha' LS) = \frac{N(N-1)}{2} \delta (\alpha, \alpha'). \tag{79}$$

If the shell is filled (N = 4l + 2), then for $f_k (k > 0)$ we obtain the formula (Ref.31)

$$f_k (l^{4l+2}\, {}^1S) = -(l \| C^k \| l)^2, \tag{80}$$

since the matrix elements of the operator U^k ($k \neq 0$) for a filled shell are equal to zero in accordance with eq.(71). Use of the table directly gives the values of f_k for the filled shell.

If the shell is almost filled (filled more than half, which means that N > > 2l + 1), the use of eq.(71) leads to the following relation:

$$f_k(l^{4l+2-N}\alpha LS,\ l^{4l+2-N}\alpha' LS) =$$
$$= \frac{1}{2}(l\|C^k\|l)^2\left\{(-1)^{\frac{v-v'}{2}}[(2L+1)(2S+1)]^{-1}\times\right.$$
$$\times\sum_{\alpha''L''}(-1)^{L-L''}(l^N\alpha LS\|U^k\|l^N\alpha''L''S)(l^N\alpha''L''S\|U^k\|l^N\alpha' LS)-$$
$$\left.-(4l+2-N)(2l+1)^{-1}\delta(\alpha,\alpha')\right\}. \qquad (81)$$

Consideration of eq.(78) further yields /61

$$f_k(l^{4l+2-N}\alpha LS,\ l^{4l+2-N}\alpha' LS) = (-1)^{\frac{v-v'}{2}} f_k(l^N\alpha LS,\ l^N\alpha' LS)-$$
$$-(2l+1-N)(2l+1)^{-1}(l\|C^k\|l)^2\delta(\alpha,\alpha'). \qquad (82)$$

Hence, eq.(80) also follows directly.

We see from eq.(82) that there is never any need to perform calculations for quasi-filled shells since the necessary expressions are obtained from corresponding results for partially filled shells.

To calculate the energy of the spin-orbit interaction of the shell of equivalent electrons, we note that according to eqs.(47) and (54)

$$l^1 \doteq [l(l+1)(2l+1)]^{\frac{1}{2}} u^1. \qquad (83)$$

Then, the operator (50) is represented by

$$H^{so} \doteq [l(l+1)(2l+1)]^{\frac{1}{2}} V^{110}\zeta(l), \qquad (84)$$

where $V^{11\,0}$ is an operator (63) fixed in the scalar product. The use of eq.(33.8) from an earlier paper (Ref.9) yields

$$(l^N\alpha LSJ\,|\,H^{so}\,|\,l^N\alpha' L'S'J) =$$
$$= (-1)^{L'+S+J}\begin{Bmatrix} LSJ \\ S'L'1 \end{Bmatrix}[l(l+1)(2l+1)]^{\frac{1}{2}}\times \qquad (85)$$
$$\times(l^N\alpha LS\|V^{11}\|l^N\alpha' L'S')\,\zeta(l).$$

The reduced matrix element on the right-hand side of this equality is tabulated in the aforementioned tables. When we are interested in the diagonal matrix elements (L = L′, S = S′), the 6j-coefficient on the right-hand side is calculated by eq.(55).

As an example, let us take $d^3\ {}^2P_J$. According to eq.(55) and Table XII (Ref.6) we obtain

$$(d^3\,{}^2P_J\,|\,H^{so}\,|\,d^3\,{}^2P_J) = \frac{1}{3}\left[J(J+1)-2\frac{3}{4}\right]\zeta(d). \qquad (86)$$

Hence, /62

$$\mathscr{E}\left(d^3\,{}^2P_{\frac{3}{2}}\right)-\mathscr{E}\left(d^3\,{}^2P_{\frac{1}{2}}\right)=\frac{3}{2}\zeta(d^2P), \tag{87a}$$

$$\zeta(d^2P)=\frac{2}{3}\zeta(d). \tag{87b}$$

If the shell is almost filled, then eq.(71) will yield

$$(l^{4l+2-N}\alpha LSJ\,|\,H^{s0}\,|\,l^{4l+2-N}\alpha'L'S'J)= \\ =-(-1)^{\frac{v-v'}{2}}(l^N\alpha LSJ\,|\,H^{s0}\,|\,l^N\alpha'L'S'J). \tag{88}$$

This shows that multiplets of quasi-filled shells are reversed in comparison with the corresponding multiplets of partially filled shells; in the case of a half-filled shell the simplified operator does not give term splitting as long as we limit ourselves to diagonal matrix elements ($v = v'$) since nondiagonal elements cannot be equal to zero. For example, for the p^3 configuration, eq.(85) and Table XI (Ref.6) yield ($v = 1$, $v' = 3$)

$$\left(p^3\,{}^2P_{\frac{3}{2}}\,|\,H^{s0}\,|\,p^3\,{}^4S_{\frac{3}{2}}\right)=-\zeta(l). \tag{89}$$

The matrix elements in the case of half-filled shells are responsible for term splitting which, however, usually is small. Nevertheless, it is of such an order that it cannot be neglected.

5. Case of Two Incomplete Shells

Let us discuss the configuration $l_1^{N_1}l_2^{N_2}$. Inside the shells, LS-coupling is suitable. For this reason, $\alpha_1L_1S_1\alpha_2L_2S_2$ will be in the characteristic. The quantum numbers L_1, S_1, L_2, S_2, as indicated in Section 2, can be correlated by any type of coupling. Let us examine the case of LS-coupling, since the energy equation for any other type of coupling can be obtained from this by proper transformation.

The electrostatic interaction inside the shells is expressed by the integrals $F_k(n_il_i,\ n_il_i)$ ($i = 1, 2$). In this case their coefficients are diagonal relative to $L_1S_1L_2S_2$ and, furthermore, the coefficient of $F_k(n_1l_1,\ n_1l_1)$ is /63 diagonal with respect to $\alpha_2\alpha_2'$ and vice versa. Anything else is done as described in the preceding Section.

The electrostatic interaction between the shells is determined by the operator

$$\sum_k\sum_{i=1}^{N_1}\sum_{j=N_1+1}^{N_1+N_2}(C_i^k\cdot C_j^k)\,\frac{r_<^k}{r_>^{k+1}}. \tag{90}$$

This matrix element, in antisymmetrization of the wave function relative to the electrons in different shells, is decomposed into direct and exchange parts.

The direct part is expressed by the integrals $F_k(n_1 l_1, n_2 l_2)$. Its coefficient is the matrix element of the operator

$$(l_1 \| C^k \| l_1)(l_2 \| C^k \| l_2)(U^k_{N_1} \cdot U^k_{N_2}). \tag{91}$$

This coefficient according to eq.(4.8) (Ref.30) is expressed as follows:

$$\begin{aligned} f_k(l_1^{N_1} l_2^{N_2} \alpha_1 L_1 S_1 \alpha_2 L_2 S_2, \alpha_1' L_1' S_1' \alpha_2' L_2' S_2', LS) = \\ = (l_1 \| C^k \| l_1)(l_2 \| C^k \| l_2)(-1)^{L_1'+L_2+L} \delta(S_1 S_2, S_1' S_2') \times \\ \times [(2S_1+1)(2S_2+1)]^{-\frac{1}{2}} \begin{Bmatrix} L_1 L_2 L \\ L_2' L_1' k \end{Bmatrix} \times \\ \times (l_1^{N_1} \alpha_1 L_1 S_1 \| U^k \| l_1^{N_1} \alpha_1' L_1' S_1)(l_2^{N_2} \alpha_2 L_2 S_2 \| U^k \| l_2^{N_2} \alpha_2' L_2' S_2). \end{aligned} \tag{92}$$

Here, we also need take into account what tables are used for U^k. In the case of the tables given in (Ref.6, 12 - 14), the factor $(2S_1 + 1)(2S_2 + 1)$ in the minus one-half degree must be disregarded. In the case of $k = 0$, eq.(69) yields

$$\begin{aligned} f_0(l_1^{N_1} l_2^{N_2}, \alpha_1 L_1 S_1 \alpha_2 L_2 S_2, \alpha_1' L_1' S_1' \alpha_2' L_2' S_2', LS) = \\ = N_1 N_2 \delta(\alpha_1 L_1 S_1 \alpha_2 L_2 S_2, \alpha_1' L_1' S_1' \alpha_2' L_2' S_2'). \end{aligned} \tag{93}$$

If the first of the shells is almost filled, application of eq.(71) will give

$$f_k(l_1^{4l_1+2-N_1} l_2^{N_2}) = -(-1)^{\frac{v_1 - v_1'}{2}} f_k(l_1^{N_1} l_2^{N_2}), \tag{94}$$

provided that $k > 0$. In the opposite case, eq.(93) must be used regardless of the degree of filling of the shells. /64

If both shells are almost filled, then

$$f_k(l_1^{4l_1+2-N_1} l_2^{4l_2+2-N_2}) = (-1)^{\frac{v_1 - v_1' + v_2 - v_2'}{2}} f_k(l_1^{N_1} l_2^{N_2}). \tag{95}$$

The quantum numbers are omitted in eqs.(94) and (95) since they are the same and arranged identically on both sides of these equalities. Here, it is obvious that $f_k(k > 0)$ is equal to zero provided that one of the shells is completely filled since, on the right-hand side, one of the shells will be empty, and direct interaction (classical type) with it is unthinkable.

To find the expression for the electrostatic energy of the exchange type (nonclassical), we use the operator (46) while all other operations remain as in the case of direct interaction. As mentioned in Section 2, this does away with antisymmetrization of the wave function in an explicit form. Thus, the coefficient g_k of the radial integral $G_k(n_1 l_1, n_2 l_2)$ will be the matrix element of the operator

$$- (l_1 \| C^k \| l_2)^2 \sum_r (-1)^r (2r+1) \begin{Bmatrix} l_1 l_2 k \\ l_2 l_1 r \end{Bmatrix} \left[\frac{1}{2} (U^r_{N_1} \cdot U^r_{N_2}) + 2 (V^{r_1}_{N_1} \cdot V^{r_1}_{N_2}) \right]. \tag{96}$$

Here, r changes from 0 to the least of the values of $2l_1$, $2l_2$. Then, for the coefficient g_k, the following expression [cf. eq.(4.12) in (Ref.30)] is valid:

$$\begin{aligned} g_k (l_1^{N_1} l_2^{N_2},\ \alpha_1 L_1 S_1 \alpha_2 L_2 S_2,\ \alpha_1' L_1' S_1' \alpha_2' L_2' S_2',\ LS) = &- (l_1 \| C^k \| l_2)^2 \times \\ \times \sum_r (-1)^r (2r+1) &\begin{Bmatrix} l_1 l_2 k \\ l_2 l_1 r \end{Bmatrix} \left[\frac{1}{2} (-1)^{L_1' + L_2 + L} \delta (S_1 S_2, S_1' S_2') \times \right. \\ &\left. \times [(2S_1+1)(2S_2+1)]^{-\frac{1}{2}} \begin{Bmatrix} L_1 L_2 L \\ L_2' L_1' r \end{Bmatrix} \times \right. \\ &\times (l_1^{N_1} \alpha_1 L_1 S_1 \| U^r \| l_1^{N_1} \alpha_1' L_1' S_1) (l_2^{N_2} \alpha_2 L_2 S_2 \| U^r \| l_2^{N_2} \alpha_2' L_2' S_2) + \\ &+ 2 (-1)^{L_1' + L_2 + L + S_1' + S_2 + S} \begin{Bmatrix} L_1 L_2 L \\ L_2' L_1' r \end{Bmatrix} \begin{Bmatrix} S_1 S_2 S \\ S_2' S_1' 1 \end{Bmatrix} \times \\ &\left. \times (l_1^{N_1} \alpha_1 L_1 S_1 \| V^{r1} \| l_1^{N_1} \alpha_1' L_1' S_1) (l_2^{N_2} \alpha_2 L_2 S_2 \| V^{r1} \| l_2^{N_2} \alpha_2' L_2' S_2') \right]. \end{aligned} \tag{97}$$

If the first of the shells is almost filled, eq.(71) will yield /65

$$\begin{aligned} g_k (l_1^{4l_1+2-N_1} l_2^{N_2}) = (-1)^{\frac{v_1 - v_1'}{2}} &g_k (l_1^{N_1} l_2^{N_2}) + (-1)^{\frac{v_1 - v_1'}{2}} \times \\ \times (l_1 \| C^k \| l_2)^2 &\sum_{r\ \text{even}} (2r+1) \begin{Bmatrix} l_1 l_2 k \\ l_2 l_1 r \end{Bmatrix} (-1)^{L_1' + L_2 + L} \times \\ \times \delta (S_1 S_2, S_1' S_2') &[(2S_1+1)(2S_2+1)]^{-\frac{1}{2}} \begin{Bmatrix} L_1 L_2 L \\ L_2' L_1' r \end{Bmatrix} \times \\ \times (l_1^{N_1} \alpha_1 L_1 S_1 \| U^r \| l_1^{N_1} \alpha_1' L_1' S_1) &(l_2^{N_2} \alpha_2 L_2 S_2 \| U^r \| l_2^{N_2} \alpha_2' L_2' S_2) - \\ - 4 (-1)^{\frac{v_1 - v_1'}{2}} (l_1 \| C^k \| l_2)^2 &\sum_{r\ \text{odd}} (2r+1) \begin{Bmatrix} l_1 l_2 k \\ l_2 l_1 r \end{Bmatrix} \times \\ \times (-1)^{L_1' + L_2 + L + S_1' + S_2 + S} &\begin{Bmatrix} L_1 L_2 L \\ L_2' L_1' r \end{Bmatrix} \begin{Bmatrix} S_1 S_2 S \\ S_2' S_1' 1 \end{Bmatrix} \times \\ \times (l_1^{N_1} \alpha_1 L_1 S_1 \| V^{r1} \| l_1^{N_1} \alpha_1' L_1' S_1') &(l_2^{N_2} \alpha_2 L_2 S_2 \| V^{r1} \| l_2^{N_2} \alpha_2' L_2' S_2') - \\ - N_2 (2l_2+1)^{-1} \delta (\alpha_1 L_1 S_1 \alpha_2 L_2 S_2,\ &\alpha_1' L_1' S_1' \alpha_2' L_2' S_2') \times \\ &\times (l_1 \| C^k \| l_2)^2. \end{aligned} \tag{98}$$

The last term arises from the summand at r = 0 since eq.(71) is then no longer valid and eq.(72) must be used [the case of r = 0 in eq.(93) should be included in the sum].

If both shells are almost filled, the following relation is valid:

$$g_k (l_1^{4l_1+2-N_1} l_2^{4l_2+2-N_2}) = (-1)^{\frac{v_1 - v_1' + v_2 - v_2'}{2}} g_k (l_1^{N_1} l_2^{N_2}) + \tag{99}$$

$$+2(l_1\|C^k\|l_2)^2\left(-2+\frac{N_1}{2l_1+1}+\frac{N_2}{2l_2+1}\right)\times$$
$$\times\delta(\alpha_1L_1S_1\alpha_2L_2S_2,\ \alpha_1'L_1'S_1'\alpha_2'L_2'S_2').$$

If the first shell is filled completely, then

$$g_k(l_1^{4l_1+2}l_2^{N_2})=-\frac{N_2}{2l_2+1}(l_1\|C^k\|l_2)\,\delta(\alpha_2L_2S_2,\ \alpha_2'L_2'S_2'). \tag{100}$$

This equality shows that the interaction of an unfilled shell with a filled shell does not depend on the state (direct interaction generally being equal to zero) of the unfilled shell at a given value of the number of electrons and /66
of the one-electron orbital quantum number.

If both shells are filled, then

$$g_k(l_1^{4l_1+2}l_2^{4l_2+2})=-2(l_1\|C^k\|l_2)^2. \tag{101}$$

The value of the last coefficient is obtained with the help of a table.

For the energy equation of the spin-orbit interaction [eq.(50)], we have $H^{SO}=H_{N_1}^{SO}+H_{N_2}^{SO}$ and the corresponding matrix element

$$\begin{aligned}
&(l_1^{N_1}l_2^{N_2}\alpha_1L_1S_1\alpha_2L_2S_2LSJ\,|\,H^{SO}\,|\,l_1^{N_1}l_2^{N_2}\alpha_1'L_1'S_1'\alpha_2'L_2'S_2'L'S'J)=\\
&=(-1)^{L'+S+J}\begin{Bmatrix}LSJ\\S'L'1\end{Bmatrix}[(2L+1)(2L'+1)(2S+1)(2S'+1)]^{\frac{1}{2}}\times\\
&\times(-1)^{L_1+L_2+L'+S_1+S_2+S'}\delta(\alpha_2L_2S_2,\ \alpha_2'L_2'S_2')[l_1(l_1+1)(2l_1+1)]^{\frac{1}{2}}\times\\
&\times\begin{Bmatrix}L_1LL_2\\L'L_1'1\end{Bmatrix}\begin{Bmatrix}S_1SS_2\\S'S_1'1\end{Bmatrix}(l_1^{N_1}\alpha_1L_1S_1\|V^{11}\|l_1^{N_1}\alpha_1'L_1'S_1')\,\zeta(l_1)+\\
&+(-1)^{L_1+L_2'+L+S_1+S_2'+S}\delta(\alpha_1L_1S_1,\ \alpha_1'L_1'S_1')[l_2(l_2+1)(2l_2+1)]^{\frac{1}{2}}\times\\
&\times\begin{Bmatrix}L_2LL_1\\L'L_2'1\end{Bmatrix}\begin{Bmatrix}S_2SS_1\\S'S_2'1\end{Bmatrix}(l_2^{N_2}\alpha_2L_2S_2\|V^{11}\|l_2^{N_2}\alpha_2'L_2'S_2')\,\zeta(l_2)].
\end{aligned} \tag{102}$$

When one or both shells are almost filled, eq.(71) is applied to the reduced matrix elements V^{11}, while everything else remains unchanged. If the shell is completely filled, V^{11} will be equal to zero and the corresponding term can be dropped.

In many spectra, two unfilled shells, one of which containing only one electron, are encountered. In that case the above formulas are simplified since, for $N_2=1$ ($\alpha_2\alpha_2'$ omitted and $L_2=l_2$, $S_2=s$), we have

$$(l_2\|U^k\|l_2)=(l_2\|U^k\|l_2)=1, \tag{103}$$

$$(l_2s_2\|V^{11}\|l_2s_2)=(l_2s_2\|v^{11}\|l_2s_2)=\sqrt{\frac{3}{2}}. \tag{104}$$

Here, the number of filled shells has no significance since the kinetic energy and the electrostatic energy relative to the nucleus are expressed by eq.(34), the direct electrostatic and spin-orbit interactions of any unfilled with any filled shell are equal to zero, and the exchange electrostatic interaction is determined by eq.(100). This is also independent of the number of unfilled shells. /67

The above mathematical apparatus is easily generalized for the case of any number of unfilled shells. It is only necessary to take into account the coupling order of L_iS_i(i = 1, 2, ...). Computational methods for such configurations are given elsewhere (Ref.30).

It should be pointed out that the above statements pertain to a method of calculation that might be called an approximation of the model of one-electron states (Ref.32). This is an approximation in which the wave function of the entire atom is constructed by means of one-electron wave functions, with all electrons of the shell of equivalent electrons being described by the same radial wave function. This approximation is rather good; however, in some respects further refinement is necessary. A brief description of methods of refining is given elsewhere (Ref.33).

Annotation to page 34. To obtain formulas, at $l' = l - k'$ and $k = l - k''$ symmetry properties of specular reflection (Ref.21)

$$(l-k'\|C^k\|l)=i(\bar{l}+k'\|C^k\|\bar{l}),\quad (l'\|C^{l-k''}\|l)=(-1)^{l''}(l'\|C^{\bar{l}+k''}\|\bar{l})$$

must be used; here, $\bar{l} = -l - 1$. In this formulation, for each negative factor under the square root an imaginary unit must be entered before the root, checking whether it is in the numerator or in the denominator and leaving their absolute values under the radical. Then, the imaginary units are canceled in the conventional manner.

REFERENCES

1. Hartree, D.R.: Proc. Cambridge Phil. Soc., Vol.24, pp.89, 111, 1928.
2. Fock, V.: Z. Physik, Vol.61, p.126, 1930; Tr. Gos. Optich. Inst., Vol.5, p.51, 1931.
3. Condon, E. and Shortley, G.: The Theory of Atomic Spectra. Izd. Inostr. Lit., 1949.
4. Hartree, D.: Calculations of Atomic Structures. Izd. Inostr. Lit., 1960.
5. Racah, G.: Phys. Rev., Vol.62, p.438, 1942.
6. Racah, G.: Phys. Rev., Vol.63, p.367, 1943.
7. Racah, G.: Phys. Rev., Vol.76, p.1352, 1949.
8. Fano, U. and Racah, G.: Irreducible Tensorial Sets. Academic Press, New York, 1959.
9. Yutsis, A.P., Levinson, I.B., and Vanagas, V.V.: Mathematical Apparatus of the Theory of Angular Momentum (Matematicheskiy apparat teorii momenta kolichestva dvizheniya). Izd. Polit. i Nauchn. Lit. LitSSR, Vil'nyus, 1960. /68

10. Yutsis, A.P. and Bandzaytis, A.A.: Theory of Angular Momentum in Quantum Mechanics (Teoriya momenta kolichestva dvizheniya v kvantovoy mekhanike). Izd. "Mintis", Vil'nyus, 1965.
11. Edmonds, A.R.: Angular Momentum in Quantum Mechanics. Princeton University Press, Princeton, 1957.
12. Sobel'man, I.I.: Introduction to the Theory of Atomic Spectra (Vvedeniye v teoriyu atomnykh spektrov). Fizmatgiz, 1963.
13. Levinson, I.B. and Nikitin, A.A.: Handbook of Theoretical Calculation of Line Intensities in Atomic Spectra (Rukovodstvo po teoreticheskomu vychisleniyu intensivnostey liniy v atomnykh spektrakh). Izd. Leningr. Gos. Univ., 1962.
14. Slater, J.C.: Quantum Theory of Atomic Structure, Vol.II. McGraw-Hill, New York, 1960.
15. Judd, B.R.: Operator Techniques in Atomic Spectroscopy. McGraw-Hill, New York, 1963.
16. Racah, G.: Phys. Rev., Vol.61, p.537, 1942.
17. Gutman, A.M. and Levinson, I.B.: Astron. Zh., Vol.37, p.86, 1960.
18. Eriksson, K.B.S. and Johansson, I.: Arkiv f. Fysik, Vol.19, p.235, 1961.
19. Rotenberg, M., Bivins, R., Metropolis, N., and Wooten, J.K.: The 3-j and 6-j Symbols. Crosby Lockwood, London, 1959.
20. Ishidzu, T.: Tables of the Racah Coefficients. Pan-Pacific Press, Tokyo, 1960.
21. Bandzaytis, A.A., Savukinas, A.Yu., and Yutsis, A.P.: Zh. Eksperim. i Teor. Fiz., Vol.46, p.385, 1964.
22. Vizbarayte, Ya.I. and Yutsis, A.P.: Tr. Akad. Nauk LitSSR, Ser.B, Vol.1(17), p.17, 1959.
23. Vizbarayte, Ya.I., Vosilyus, I.I., Savukinas, A.Yu., and Yutsis, A.P.: Tr. Akad. Nauk LitSSR, Vol.1(24), p.23, 1961.
24. Vizbarayte, Ya.I., Martishyus, V.I., Savukinas, A.Yu., and Yutsis, A.P.: Lit. Fiz. Sb., Vol.2, p.213, 1962.
25. Vizbarayte, Ya.I., Savukinas, A.Yu., and Yutsis, A.P.: Lit. Fiz. Sb., Vol.4, p.4, 1964.
26. Rudzikas, Z.B., Vizbarayte, Ya.I., and Yutsis, A.P.: Lit. Fiz. Sb., Vol.5, p.37, 1965.
27. Rudzikas, Z.B., Vizbarayte, Ya.I., Karaziya, R.I., and Yutsis, A.P.: Lit. Fiz. Sb., Vol.5, p.49, 1965.
28. Rudzikas, Z.B., Vizbarayte, Ya.I., Bandzaytis, A.A., and Yutsis, A.P.: Tr. Akad. Nauk LitSSR, Ser.B, Vol.4(31), p.3, 1962.
29. Rudzikas, Z.B., Karaziya, R.I., Vizbarayte, Ya.I., Bandzaytis, A.A., and Yutsis, A.P.: Lit. Fiz. Sb., Vol.5, p.31, 1965.
30. Yutsis, A.P., Vizbarayte, Ya.I., Karaziya, R.I., Savukinas, A.Yu., and Bandzaytis, A.A.: Lit. Fiz. Sb., Vol.4, p.197, 1964.
31. Yutsis, A.P., Vizbarayte, Ya.I., and Bandzaytis, A.A.: Lit. Fiz. Sb., Vol.2, p.121, 1962.
32. Fok, V.A., Veselov, M.G., and Petrishen', M.I.: Zh. Eksperim. i Teor. Fiz., Vol.10, p.723, 1940.
33. Yutsis, A.P.: Lit. Fiz. Sb., Vol.3, p.11, 1963, and also Magyar Fizikai Folyoirat, Vol.11, p.305, 1963.

THEORY OF ATOMIC TRANSITIONS /69

G.F.Drukarev

1.

Elementary processes of interaction of atoms, free electrons, and radiation play a fundamental role in the formation of the state of stellar matter, nebulae, etc. and determine the character of the spectrum emitted by stellar atmospheres. Therefore, information on the probabilities of the various processes is needed for constructing a theory of stars and for interpreting observed spectra.

It is necessary to differentiate between problems where it suffices to know the order of magnitude of the probability of a given process and problems where information requiring calculation of a high degree of accuracy is needed.

Numerous calculations of various degrees of accuracy performed up to now have revealed the following, quite important circumstance. An estimate calculation differs from an exact complex calculation by much more than by just the fact that one smooth curve (let us say the dependence of the effective scattering cross section of an electron on its energy) is replaced by another smooth curve of an identical type. The main difference lies in the fact that any increase in the accuracy of a calculation causes sharp maxima or minima to appear on the curves that depict the dependence of the probability of the given process on various parameters (energy of colliding particles, radiation frequency, etc.). In a rough estimate calculation, these features do not appear and the curves are smoothed.

This must be taken into account in defining the wanted degree of accuracy of data on the probability of various processes in a given astrophysical problem.

Briefly, we will discuss the means available to the modern theoretical /70
physicist for the calculation of transition probabilities.

For estimate calculations, simple approximation formulas giving the correct order of magnitude are in existence. They are not universal and are valid only in a certain specific range of values of various parameters entering into them. Highly accurate calculations generally require solving a set of complex integro-differential equations, performed on high-speed electronic computers. There are also general relations which tie in the probabilities of various processes. The best known relation is the so-called sum rule of oscillator strengths which relates the intensity of radiation in all possible transitions in a given atom from one specific initial state. Another example is the so-called unitarity relation which covers the effective cross section for elastic scattering and all possible processes of excitation upon collision of an electron of specific energy with an atom.

Let us also mention dispersion relations which incorporate integrals of effective energy cross sections (unlike the value of the cross section at a specific energy as in the unitarity relation).

The value of such general relations lies specifically in the fact that they permit checking the agreement of the magnitude of probabilities of various calculated processes with the approximation.

2.

Let us examine the expressions that define the meaning of the concept of transition probability.

Let us assume that in a certain volume Ω there are particles of two kinds (1) and (2) (actually, these can be complex systems). By virtue of the interaction of particles they pass from some initial state i to a final state f.

The number of transitions in unit time per unit volume is proportional to the particle concentrations n_1 and n_2 and can be represented as /71

$$N = n_1 n_2 w. \tag{1}$$

The quantity w denotes the transition probability, having the dimension $cm^3 sec^{-1}$ and being equal to $\frac{N}{n_1 n_2}$. At times, it is more convenient to refer the number of transitions not to unit concentration but to unit density of the flux, connected with the concentration by the relation

$$j = nv \tag{2}$$

(where v is the particle velocity).

The corresponding quantity is known as the effective cross section σ. If, for example, we are dealing with a flux of particles (1), then

$$\sigma = \frac{N}{j_1 n_2} = \frac{w}{v_1}. \tag{3}$$

As we see, the effective cross section has the dimension of area (cm^2), which justifies the name.

In the interaction of light with the system, the role of n is played by the number of photons. Here, it must be considered that, during the radiation of photons, the transition probability is not proportional to n but to n + 1.

3.

Let us formulate the problem of calculating the transition probability in quantum mechanics.

Let the systems (1) and (2) be characterized by the energy operators H_1 and H_2. In the absence of interaction, the systems are in stationary states $\psi_i(1)$ and $\varphi_i(2)$ with the energies E_i and ε_i respectively such that*

$$H_1\psi_i = E_i\psi_i,$$
$$H_2\varphi_i = \varepsilon_i\varphi_i.$$

It is still necessary to determine the normalization of the wave functions. Let us set

$$\int_\Omega |\psi|^2 d\tau = 1, \quad \int_\Omega |\varphi|^2 d\tau = 1, \tag{4}$$

where Ω is the normalization volume which we consider to be unity. (Ω is not contained in the final expressions, so that we can let Ω tend to ∞.) /72

Let us now assume that, at a certain instant of time (usually $t = -\infty$), the interaction $V(1, 2)$ is incorporated. Then the initial state stops being stationary, and transitions from φ_i, ψ_i to some other states become possible. Let us isolate some pair of final states ψ_f, φ_f and examine the transition $\psi_i\varphi_i \rightarrow \psi_f\varphi_f$.

In the processes of interest here, the final state of the composite system (1) + (2) belongs to a group of closely spaced energy levels (which merge into a continuous spectrum in the limiting case of an infinite normalization volume). Therefore, we are interested not so much in the transition probability to one of these levels as in the transition probability to a small energy interval ΔE close to some value of E. In addition, the final state may depend on some other variables besides energy (for example, the velocity direction of particles scattered after collision). Denoting these variables by Γ, let us deal with the differential transition probability in the interval $d\Gamma$.

For the differential transition probability with a time-independent interaction V, the expression

$$d\omega = \frac{2\pi}{\hbar}\left|\int \varphi_f^*\psi_f^* V\Psi_+ \, d\tau_1 \, d\tau_2\right|^2 \rho \, d\Gamma \tag{5}$$

is derived in quantum mechanics.

Here Ψ_+ is the eigenfunction of the operator $H = H_1 + H_2 + V$ corresponding to the eigenvalue of the energy

$$E = E_i + \varepsilon_i = E_f + \varepsilon_f \tag{6}$$

and tending to $\psi_i\varphi_i$ as $V \rightarrow 0$, while ρ is the number of states per unit energy interval close to E. Furthermore, Ψ_+ should exhibit a definite asymptotic

---

* For brevity we will designate $(x_1, y_1, z_1) \equiv (1)$, $(x_2, y_2, z_2) \equiv (2)$ while x, y, z are variables on which depend ψ and φ.

behavior with distance between the systems (1) and (2) (denoted by the symbol +). Below, we will discuss this behavior in greater detail.

4. /73

If the interaction V can be considered weak (for example, in the case of interaction of matter with light where the weakness V is related with a small value of the dimensionless parameter $\frac{e^2}{\hbar c} \sim \frac{1}{137}$, which determines the scale of electromagnetic effects), then we can simplify the expression for dw by substituting Ψ_+ by the quantity $\psi_1 \varphi_1$. Then,

$$dw = \frac{2\pi}{\hbar} \left| \int \psi_f^* \varphi_f^* V \psi_i \varphi_i \, d\tau_1 \, d\tau_2 \right|^2 \rho \, d\Gamma. \tag{7}$$

Let us introduce the notation

$$U = \int \varphi_f^*(1) \, V(1,2) \, \varphi_i(1) \, d\tau_1. \tag{8}$$

Then,

$$dw = \frac{2\pi}{\hbar} \left| \int \psi_f^* U \psi_i \, d\tau_2 \right|^2 \rho \, d\Gamma. \tag{9}$$

This expression coincides with the transition probability of the system in the first approximation of the theory of perturbations, under the effect of an external force field U.

In the case of interaction of charged particles with light, the role of φ_i is played by functions describing the state of the electromagnetic field.

The perturbation U has the form

$$U = -\frac{e}{mc} \sqrt{\frac{2\pi\hbar c^2}{\omega}} e \hat{p} e^{ikr} \quad \text{(emission of quanta)} \tag{10}$$

$$U = -\frac{e}{mc} \sqrt{\frac{2\pi\hbar c^2}{\omega}} e \hat{p} e^{-ikr} \quad \text{(absorption of quanta)} \tag{11}$$

Here, ω is the frequency of the field, e is the polarization vector, and $\hat{p}$ is the momentum operator acting on the wave function of a particle of charge e and mass m.

During absorption or emission of quanta, the energy of the field correspondingly decreases or increases by the magnitude $\hbar\omega$, i.e.,

$$\varepsilon_f - \varepsilon_i = \mp \hbar\omega. \tag{12}$$

According to eq.(6), this leads to the condition /74

$$E_f - E_i = \mp \hbar\omega. \tag{13}$$

Thus, the transition probability under the effect of the field is determined by the matrix element

$$M = \int \psi_f^* e\hat{p} e^{\pm ikr} \psi_i \, d\tau. \tag{14}$$

The functions ψ_i and ψ_f describe the state of the atom.

If ψ_i and ψ_f pertain to a discrete atomic spectrum, the corresponding transition will be emission or absorption of monochromatic quanta (spectral line). If ψ_f pertains to a continuous spectrum and ψ_i to a discrete spectrum, the process is photoionization (or photodissociation in the case where the initial state is a negative ion). The opposite process is recombination (or the formation of a negative ion). Finally, if both functions ψ_f and ψ_i pertain to a continuous spectrum, then bremsstrahlung or absorption occurs (sometimes this process is called free-free transition which is rather unfortunate since the electron undergoing transition is not free but is in the atomic field).

A review of the current state of the theory of these transitions and a summary of calculations are given elsewhere (Ref.1, 2).

5.

Let us examine the collision of an electron with an atom (Ref.3). In this case, it is conventional to characterize the process by the effective cross section $d\sigma$. The quantity $d\Gamma$ here is an element of the solid angle $d\varkappa = \sin\theta \, d\theta d\varphi$, into which the electron falls after collision.

The quantity ρ is equal to

$$\rho = \frac{mk_f}{(2\pi)^3\hbar^2}, \tag{15}$$

where k_f is associated with the momentum of the electron after collision over the relation

$$k_f = \frac{p_f}{\hbar}. \tag{16}$$

Furthermore, the wave function φ_f describing a free electron is equal (with consideration of normalization) to /75

$$\varphi_f = e^{ik_f r}. \tag{17}$$

Taking these relations into account, we have for the differential cross section

$$d\sigma = \frac{k_f}{k_i} |q_{if}(\theta)|^2 \, d\varkappa, \tag{18}$$

where

$$q_{if} = -\frac{m}{2\pi\hbar^2}\int e^{-ik_f r}\,\psi_f V\Psi_+\,d\tau. \tag{19}$$

The total cross section is

$$\sigma = \frac{k_f}{k_i}\int |q_{if}|^2\,d\varkappa.$$

The function ψ_f, just as above, is the atomic wave function.

If it coincides with the initial atomic function ψ_i, the collision is of the elastic scattering type. Otherwise inelastic scattering occurs, as a result of which the atom passes to an excited state (the case where one atomic electron is raised to an excited level is usually examined).

The function Ψ_+ in this case describes the state of the electron + atom system pertaining to a continuous spectrum. In an implicit form Ψ_+ contains information on the initial state of the atom (which can be both the ground state and the excited state).

The operator V is the Coulomb interaction energy of the electron bombarding the nucleus and atomic electrons:

$$V = -\frac{ze}{r} + \sum_i \frac{e}{|r - r_i|}.$$

If the atomic function ψ_f refers to a continuous spectrum, the process in question is of the ionization type. In this case, the expression $d\Gamma$ has a somewhat different form, namely,

$$d\Gamma = \eta^2 d\eta\; d\varkappa_\eta\, d\varkappa, \tag{20}$$

where the quantity η is the momentum of the electron emitted during ionization and $d\varkappa_\eta$ is the corresponding solid angle. /76

In studying the collision of an electron with an ion instead of with a neutral atom, the function $\psi_{i,f}$ must be represented by the wave function of the continuous spectrum of a Coulomb field and the Coulomb potential corresponding to an uncompensated charge must be subtracted from V.

The effective cross sections for various processes are connected by a certain relation, known as the unitarity relation

$$\frac{4\pi}{k_i}\operatorname{Im} q_{ii}(0) = \sum_f \sigma_{if}, \tag{21}$$

where $q_{ii(o)}$ is the amplitude of forward elastic scattering. The cross sections for all transitions, resolved by the law of conservation of energy, enter $\sum_f \sigma_{if}$.

The equation for the function Ψ_+ has the form

$$\left(-\frac{\hbar^2}{2m}\Delta + H_a + V\right)\Psi_+ = E\Psi_+, \tag{22}$$

where H_a is the atomic energy operator.

The energy E is equal to

$$E = \frac{\hbar^2 k_i^2}{2m} + E_i. \tag{23}$$

Here, $\frac{\hbar^2 k_i^2}{2m}$ is the energy of the bombarding electron and E_i the energy of the atom in the initial state.

Let us expand Ψ_+ in a system of atomic functions (with consideration of symmetry properties):

$$\Psi_+ = \sum_n \hat{A}\psi_n F_n \tag{24}$$

(where $\hat{A}$ is the symmetrization operator).

For example, for the simplest case of the collision of an electron with a hydrogen atom

$$\Psi_+ = \sum_n [\psi_n(1) F_n(2) \pm \psi_n(2) F_n(1)], \tag{25}$$

where the signs "-" and "+" in the brackets correspond to the triplet and singlet states of the system. /77

Owing to the relation between the magnitude of total spin of the system and the symmetry properties of the wave function, the amplitude q_{if} (and thus also the cross section) depends on the spin. The actually observed cross section pertains to a mixture of all possible mutual orientations of spin of both atom and electron, so that it represents an averaged quantity.

Thus, for the hydrogen atom

$$\langle\sigma\rangle = \frac{3}{4}\sigma_{\text{triplet}} + \frac{1}{4}\sigma_{\text{singlet}}. \tag{26}$$

We also note that successive consideration of the symmetry properties of the wave function is necessary to calculate, for example, such processes as transitions between singlet and triplet states of the helium atom and systems similar to it.

The aggregate of the coefficients (F_1, F_2, ...) represents the wave function of the electron in the atomic field. (We note that unlike the case under consideration, in discrete states of the "atom + electron" system a good approxi-

mation for Ψ is the expression

$$\Psi = \hat{A}\psi_n F_n,$$

so that the wave function of the electron reduces to one term.)

For F_n we obtain the set of equations

$$\Delta F_n + k_n^2 F_n = 2\sum_m \left(V_{nm}F_m + \int W_{nm}F_m\, d\tau\right),$$

where

$$k_n^2 = k_i^2 + \frac{2m}{\hbar^2}(E_n - E_i).$$

The quantities V_{nm} and the kernel of the exchange operator W_{nm} represent integrals containing atomic functions and the interaction energy V.

In particular, for the hydrogen atom, we have

$$V_{nm} = e^2\int \psi_n^*\left(\frac{1}{r} - \frac{1}{|r-r'|}\right)\psi_m\, dr',$$
$$W_{nm} = \pm e^2\psi_n^*(r)\left[\frac{1}{|r-r'|} + E_m - \frac{1}{2}k_n^2\right]\psi_m(r').$$

To determine F_n in single-valued form, it must be given the asymptotic /78 form. The asymptotic form of F_n is determined by properties which the function Ψ_+, entering the expression for the transition probability, must possess.

Namely,

$$F_n(r) \sim e^{ik_n r}\delta_{ni} + q_{in}\frac{e^{ik_n r}}{r}.$$

The term $e^{ik_n r}\delta_{ni}$ ensures the property of the function Ψ_+ that, as $V \to 0$, also $\Psi_+ \to \psi_i\varphi_i$.

As regards the divergent wave $\frac{e^{ik_n r}}{r}$, the presence of this expression (but not of the convergent waves $\frac{e^{-ik_n r}}{r}$ or their linear combination) is precisely the aforementioned asymptotic behavior which the function Ψ_+ must possess.

When $k_n^2 > 0$ the divergent wave $\frac{e^{ik_n r}}{r}$ describes electrons flying off after collision with an atom. The condition $k_n^2 > 0$ means that $\frac{\hbar^2 k_i^2}{2m} + E_i > E_n$, i.e., excitation of the level E_n is energetically possible. If $k_n^2 < 0$, there is not enough energy for excitation of the level E_n. In this case, k_n will be imaginary and thus $\frac{e^{ik_n r}}{r}$ will decrease exponentially as $r \to \infty$.

The amplitude q_{in} of the divergent wave agrees exactly with the quantity q_{in} determined by eq.(19).

Thus, if we have an exact solution of the system for F_n, the amplitude q_{in} can be found from the asymptotic behavior and there is no need for calculating q_{in} by means of eq.(19). However, in practice it is possible to obtain only a more or less successful approximate solution. The amplitude of the diverging wave q_{in}^{approx} in this case will not be equal to q_{in} determined from eq.(19) upon substituting the appropriate approximate expression for Ψ_+. The discrepancy between these quantities can serve as a criterion for the quality of the adopted approximation (and also as a check on the accuracy in numerical calculations). /79

The integral expression for amplitude [eq.(19)] also forms the base for investigating the overall structure and analytic properties of the amplitude q_{if}.

7.

Various approximations used in studying the system of equations for F_n can be classified according to which factors characterizing the collision process are taken into account and which are rejected.

Let us first examine slow electrons whose energy is insufficient for exciting the atom. Under these conditions, only one term is left in the asymptotic behavior for F_n

$$F_i \sim e^{ik_i r} + q_{ii}\frac{e^{ik_i r}}{r}. \qquad (27)$$

The remaining F_n decrease exponentially as $r \to \infty$. The roughest approximation is that in which all W_{in} and all nondiagonal V_{in} are neglected. In this approximation, the atom acts on the electron as some force center having an invariant rigid structure.

Consideration of the nondiagonal V_{in} corresponds to consideration of polarization of an atom by a bombarding electron. At large distances between atom and electron, the influence of this polarization reduces to the appearance of an additional interaction of the type of a charge-induced dipole $U \sim \frac{1}{r^4}$.

Consideration of the terms W_{in} corresponds to consideration of the identity of electrons, thanks to which the so-called exchange scattering in which the bombarding electron changes place with the atomic electron is indistinguishable from direct scattering and they both should be regarded as a single process.

Within the framework of the approximation disregarding polarization, one can sometimes resort to a further simplification, solving the equation for F_n by the method of successive approximations and setting $F_i = e^{ik_i r}$ on the right-hand side in first approximation.

The corresponding solutions are known as Born approximation (if $W_{in} = 0$) /80 and as Born-Oppenheimer approximation if exchange is taken into account.

If the energy of the bombarding electron is sufficient for excitation, let us say up to the k-th excited level, then if we disregard polarization the problem reduces to a set of k equations. The need for examining a set of k equations corresponds to the relation between cross sections of different processes [eq.(21)].

In eq.(21), the subscript for the initial state i may refer not only to the initial ground state of the atom but also to excited states, which corresponds to collision of an electron with an excited atom (the cross sections σ_{if} in this case describe so-called collisions of the second kind).

This yields a series of relations for different i and, in order that they be exactly satisfied, we must have an exact solution of the set of equations.

If transitions from the ground state to a given excited state play the principal role and all other transitions are unessential, we can leave only two equations in the system for F_n. The corresponding approximation is called a strong-coupling approximation of the two given states.

The approximation in which the effect of all inelastic processes on elastic scattering is disregarded is called the distorted wave method. The system of equations for F_n takes the form

$$\left.\begin{aligned} \Delta F_n + k_n^2 F_n &= V_{nn}F_n + \int W_{nn}F_n\,d\tau + \\ &\quad + V_{ni}F_i + \int W_{ni}F_i\,d\tau, \\ \Delta F_i + k_i^2 F_i &= V_{ii}F_i + \int W_{ii}F_i\,d\tau. \end{aligned}\right\} \tag{28}$$

Finally, the Born and Born-Oppenheimer approximations are the roughest. Both these approximations are based on the assumption that the interaction of an electron with an atom can be considered weak. At high energies, this is true beyond question.

In the Born method, we assume $\Psi_+ = \psi_i e^{ik_i r}$ and thus /81

$$q_{if} = -\frac{m}{2\pi\hbar^2}\int e^{i(k_i - k_f)r} V_{ii}\,d\tau. \tag{29}$$

In the Born-Oppenheimer method, exchange processes are taken into account:

$$q_{if} = -\frac{m}{2\pi\hbar^2}\int e^{-ik_f r}\left[V_{fi}e^{ik_i r} + \int W_{fi}e^{ik_i r'}\right]d\tau. \tag{30}$$

The extension of these approximations to the region of energies close to critical introduces a noticeable error but, in the case of the Born approximation, the order of magnitude is retained. In the Born-Oppenheimer method, conversely, a direct extension of the approximation to the near-critical region led

to errors by a factor of 20 - 30. However, it was shown (Ref.4) that, when neglecting certain terms which, at high energies, are small with respect to the principal term (and the retention of which would mean an increase in accuracy), an interpolation formula will be obtained that yields an intelligent approximate solution near the threshold.

8.

To solve equations in practice, the angular variables must be separated. For this, F_n is decomposed into partial waves:

$$F_n(r) = \sum_l \sqrt{4\pi(2l+1)}\, i^l \frac{f_{nl}(r)}{r} Y_{lm}(\theta, \varphi). \tag{31}$$

This decomposition corresponds to breaking up a beam of bombarding particles, in the classical theory of scattering, into an aggregate of individual trajectories characterized by specific impact parameters ρ. Actually, the angular momentum in the classical pattern is $mv\rho$ and in the quantum pattern, $l\hbar$. Equating both these expressions in accordance with the correspondence principle, it will be found that the impact parameter

$$\rho \sim l \frac{h}{mv} = l\lambda \tag{32}$$

corresponds to the quantum number l.

For f_{nl}, we obtain a system of the form /82

$$\frac{d^2 f_{nl}}{dr^2} + \left(k_n^2 - \frac{l(l+1)}{r^2}\right) f_{nl} = \sum_{n'l'} \left[V_{nn'll'} f_{n'l'} + \int_0^\infty W_{nn'll'} f_{n'l'}\, d\tau \right]. \tag{33}$$

The asymptotic behavior of f_{nl} has the form

$$f_{nl} \sim \frac{1}{k_n} \sin\left(k_n r - \frac{l_i \pi}{2}\right) \delta_{ni} + q_{nil_n l_i} \frac{e^{i\left(k_n r - \frac{l_n \pi}{2}\right)}}{r}. \tag{34}$$

The amplitude of q_{in} is expressed in terms of partial amplitudes as the series

$$q_{in} = \sum q_{inl_i l_n} Y_{l_i m_i}(\theta_i \varphi_i)\, Y_{l_n m_n}(\theta_n \varphi_n). \tag{35}$$

Equation (21) for partial amplitudes takes the form (in the simplest case when the initial state of the atom is the s-state):

$$\operatorname{Im} q_{ill} - k_l |q_{ill}|^2 = \sum_{n \neq 0} k_n |q_{inl}|^2. \tag{36}$$

9.

Elastic scattering of electrons. If scattering occurs below the excitation threshold, then $\mathrm{Im}\ q_l - k|q_l|^2 = 0$ (the subscript n is omitted here). Consequently, q_l can be represented as $q_l = \frac{1}{2ik}(e^{2i\delta_l} - 1)$ so that

$$\sigma_l = 4\pi \frac{(2l+1)}{k^2}\sin^2\delta_l;\ \sigma = \sum_l \sigma_l. \tag{37}$$

Furthermore, at sufficiently low velocities, we can limit ourselves to the s-wave alone ($l = 0$), since when $l = 1$

$$\rho \sim \frac{\hbar}{mv} = \lambda, \tag{38}$$

and if $\lambda \geq a_0$ (a_0 being the Bohr radius), the corresponding impact parameter will be practically outside the limits of action of the atomic field so that /83 the particles in a state with $l \neq 0$, for all practical purposes, are not scattered.

At a sufficiently low energy, when $\lambda \gg a_0$, the approximate relation

$$k\cot\delta = -\frac{1}{a} + \frac{1}{2}k^2 r_0 \tag{39}$$

holds (valid when polarization is disregarded; if polarization is taken into account the formula for k cot δ is somewhat more complex).

The quantity a is called the scattering length. It determines the magnitude of the cross section as $k \to 0$:

$$\sigma(0) = 4\pi a^2. \tag{40}$$

The quantity r_0 denotes the effective radius of the force field.

The scattering length depends on the intensity of the force field and on the sign of the potential energy. Interaction of an electron with an atom represents attraction so that the potential energy in this case is negative and is depicted by a potential well. (The depth of the well is greater, the higher the atomic number.) The dependence of the scattering length on the well depth is plotted in Fig.1. The quantity a becomes infinite when a bound state appears in the well. Near the point A (to the right of it) the following relation is valid:

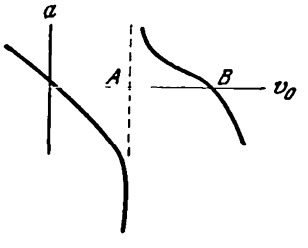

Fig.1

$$a \sim \frac{1}{\sqrt{\frac{2mW}{\hbar^2}}}, \tag{41}$$

where W is the depth of the level.

Near the point B the quantity a is small and the cross section will be abnormally small. This is the so-called Ramsauer effect.

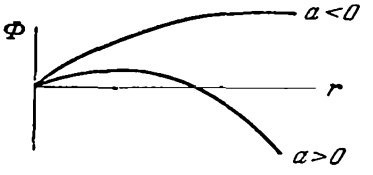

Fig.2

Let us examine the wave function at low energies. From eq.(34), at $l = 0$, it follows that the asymptotic behavior of f has the form /84

$$f \sim \frac{e^{i\delta}}{k} \sin(kr + \delta) \quad (r \to \infty).$$

From this it follows that the function $\Phi = e^{-i\delta} f$ will be real. Figure 2 shows the dependence $\Phi(r)$ for different scattering lengths a.

Since the same wave function enters the expression for the cross section of free-free transitions, one should expect a correlation to exist between the phenomena of elastic scattering and the behavior of the cross section for free-free transitions at low energy.

10.

Let us now study the energy dependence of the elastic scattering cross section.

The behavior of the cross section at low energies is shown in Figs.3 and 4, with Fig.3 corresponding to the normal shape of the cross section and Fig.4 showing the shape of the cross section in presence of the Ramsauer effect.

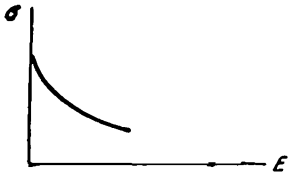

Fig.3

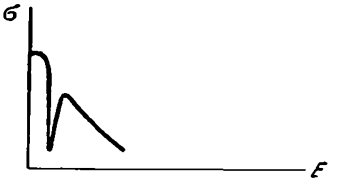

Fig.4

With an increase in energy of the electron colliding with the atom and its approach to the atomic excitation threshold there sometimes is a sharp resonance change of the scattering cross section (Fig.5). /85

Resonance near the threshold occurs when a bound state of the electron is possible in the field of the excited atom.

11.

Excitation of an atom by electron collision. In calculating the excitation cross section, the volume of computational work increases steeply. It becomes necessary to take into account a large number of partial waves, and considerations of the optimal l used in elastic scattering are inapplicable here. The structure of the system of equations also becomes quite complex. This is the reason for the fact that, until now, sufficiently accurate numerical calculations, with consideration of all basic factors, have been performed only for a few cases.

Fig.5

Most calculations are carried out with neglection of various factors.

Generally, approximate calculations yield an excitation function that is overestimated in comparison with the true function, and the "fine structure" is absent in it.

The general shape of the excitation functions is shown in Fig.6.

The position of the maximum of the excitation functions and its height depend both on the quantum characteristics (energy, moment) of the initial state and on the characteristics of the final state.

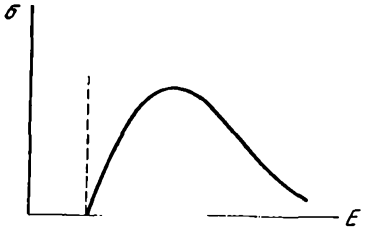

Fig.6

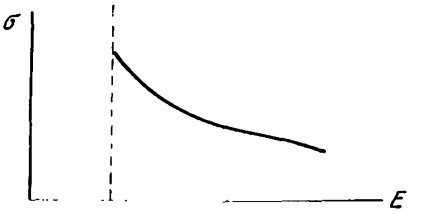

Fig.7

We note that, in the Born approximation with the use of some additional simplifications, the excitation cross section of optically resolved transitions can be expressed (Ref.3) by the oscillator strength of the corresponding transition [integral of the type of eq.(14)].

Resonance (of the type shown in Fig.5) near the excitation threshold of /86 the next level may also lie on the curve for the energy dependence of the excitation cross section of a given level. Two resonances in the excitation cross section of the $2\,^3S$ helium level were recently discovered.

The excitation cross section of ions, unlike that of atoms, remains finite at the threshold. The typical slope of the energy dependence is shown in Fig.7.

In excitation of multiply charged ions, a rather good approximation is the so-called Coulomb-Born approximation which structurally resembles the Born approximation but differs from it by the replacement of the wave functions of free motion [eq.(17)] by wave functions of a continuous Coulomb field spectrum.

In the Coulomb-Born approximation the excitation cross section of optically resolved transitions can also be expressed by the oscillator strength of the corresponding transition. However, in addition to the oscillator strengths, unlike the case of a neutral atom, a universal function as tabulated elsewhere (Ref.5), figures in the approximation formula for the cross section.

The greatest number of calculations of the excitation cross section for /87
various transitions has been performed for the simplest systems: H, He, He^+.

Calculations also are in existence for the excitation of complex atoms such as Na.

A review and detailed discussion of the results of the calculations are given in other reports (Ref.1, 3, 6, 7).

12.

Let us now discuss simple approximation formulas, yielding the magnitude of the effective cross section with an accuracy to within one order of magnitude.

The theoretical principle for obtaining such formulas lies in replacing the problem of the excitation of a given atomic state by a similar but much simpler problem of the probability of an electron transferring a given quantity of energy to an atom. The calculation of energy transfer can be greatly simplified by conceiving the collision between the knock-on and the atomic electrons as their being of the free type and by then approximately allowing for the field of the nucleus and the remaining atomic electrons.

A development of this concept, in different variants, is contained in a number of works (Ref.8, 9, 10, 11).

Let us give one of the simplest formulas of the cross section for excitation to the level n (Ref.8)

$$\left.\begin{aligned} \sigma &= N\frac{\pi e^4}{E}\left(\frac{1}{U_n}-\frac{1}{U_{n+1}}\right) \text{ at } U_{n+1}\leqslant E,\\ \sigma &= N\frac{\pi e^4}{E}\left(\frac{1}{U_n}-\frac{1}{E}\right) \text{ at } U_n\leqslant E\leqslant U_{n+1}. \end{aligned}\right\} \qquad (42)$$

Here U_n, U_{n+1} are the excitation energies of the n-th and (n + 1)-th levels respectively, E is the energy of the knock-on electron, and N the number of electrons in the shell.

In summation, it should be mentioned that there is a gap between the re-

quirements of astrophysicists and the trend of most extensive progress in specific calculations for electron-atom collisions. A close collaboration between astrophysicists and specialists in atomic collisions would help to narrow this gap.

REFERENCES /88

1. Atomic and Molecular Processes (Collection) [Atomnyye i molekulyarnyye protsessy (sbornik)]. Izd. "Mir", 1964.
2. Sobel'man, I.I.: Introduction to the Theory of Atomic Spectra (Vvedeniye v teoriyu atomnykh spektrov). Fizmatgiz, 1963.
3. Drukarev, G.F.: Theory of Electron-Atom Collisions (Teoriya stolknoveniy elektronov s atomami). Fizmatgiz, 1963.
4. Ochkur, V.I.: Zh. Eksperim. i Teor. Fiz., Vol.45, p.734, 1963.
5. Gaylitis, M.: Optika i Spektroskopiya, Vol.14, p.465, 1963.
6. Atomic Collisions (Collection of Articles) [Atomnyye stolknoveniya (sbornik statey)]. Izd. Akad. Nauk LatvSSR, 1963; Effective Electron-Atom Collision Cross Sections (Collection) [Effektivnyye secheniya stolknoveniy elektronov s atomami (sbornik)]. Izd. Akad. Nauk LatvSSR, 1965.
7. Atomic Collision Processes. McDowell Publ. Co., London, 1964.
8. Ochkur, V.I. and Petrun'kin, A.M.: Optika i Spektroskopiya, Vol.14, p.457, 1963.
9. Grizinsky, M.: Phys. Rev., Vol.115, p.374, 1959.
10. Stabler, R.: Phys. Rev., Vol.133A, p.1268, 1964.
11. Vriens, A.: Phys. Rev. Letters, Vol.9, p.295, 1964; Vol.10, p.170, 1964.

CERTAIN NONLINEAR PROBLEMS OF THE THEORY OF RADIATIVE TRANSFER /91

V.A.Ambartsumyan

1.

A relatively large portion of the classical problems of the theory of radiative transfer is set up and solved in linear approximation. In these problems the possible influence of the transferred radiation on the optical properties of the medium is disregarded. For example, let us treat the problem of diffuse transmission and reflection of light by a plane layer of a given optical thickness τ. We are fully aware that the optical thickness of any prescribed medium consisting, say, of plane-parallel layers generally depends on the density of radiation at its various depths. Therefore, it must also depend on the intensity of the light incident on the layer. Only under certain conditions may this dependence become unessential and be neglected. Thus, if we are dealing with a plane layer, with a finite number of atoms per square centimeter, and if we examine the problem of the diffusion of resonance radiation in this layer, this neglect is permissible if the radiation density is everywhere small, so that the percentage of excited atoms is also small. Under such conditions, the optical thickness can be considered as given. However, at high radiation densities one cannot disregard the effect of radiation on the optical properties of the medium, for example, on the volume absorption coefficient.

In essence, this state of affairs has always been acknowledged in theoretical astrophysics and attempts have always been made, in solving certain classical problems, to allow for the effect of radiation on the medium. This specifically is true for the problem of the transfer of ionizing radiation. Consideration of its effect on the medium is a characteristic feature of the classical theory of the H II regions. On the other hand, the rather inconsistent /92
allowance for nonlinear effects made many theoreticians be skeptical of attempts to apply the existing theories of absorption lines to spectral lines that correspond to transitions between excited states (lines of subordinate series). In any case, the area of nonlinear problems remains very little explored.

This naturally led to attempts to treat nonlinear problems by more systematic studies. A further incentive was created by the increased interest in experiments in which the luminous flux densities are high.

In such a systematic study of the problem, it is preferable to analyze relatively simple schemes that permit a clearer concept as to various characteristic nonlinear effects and a better analysis of complex cases arising in connection with experimental processes. Here, the phase relations will play a relatively minor role. In particular, this is the case for the examples dis-

cussed below.

In the study of nonlinear problems rather a wide range of different phenomena is involved and, to obtain definite results, it is preferable to place emphasis on specific processes and phenomena of a given type.

Let us start with the physical effects of clarifying or opacifying the medium, due to redistribution of atoms by energy levels. Strange as it may seem, at a specific arrangement of the energy levels of a given atom even small incident stationary fluxes may lead to appreciable lightening or dimming, as will be shown for a specific example.

Conversely, we will emphasize the nonlinear dependence of a diffusely reflected or diffusely transmitted flux on the magnitude of the stationary flux incident on the medium. We will give a typical example for which it is highly important to elicit this dependence.

2. /93

The effects associated with redistribution of atoms by states are substantial at high radiation densities, even in the simplest problem of the transfer of monochromatic radiation through a medium of finite thickness where this medium consists of atoms having only two energy levels and where a field of quanta is involved whose frequency corresponds to the transition between these states.

It is known that, in the linear theory for pure scattering, the diffuse transmission coefficient through a medium with a finite optical density τ in the one-dimensional problem (or, more accurately, in a one-dimensional approximation) has the following solution:

$$q = \frac{H}{F} = \frac{1}{1 + \frac{\tau}{2}}, \tag{1}$$

where H and F are the intensities of the transmitted and incident fluxes.

If the calculation takes into account the radiation-induced decrease of the volume scattering coefficient produced by transition of some atoms from the first state to the second (lightening), then we obtain

$$q = \frac{H}{F} = \frac{1 + \alpha F}{1 + \frac{\tau_0}{2} + \alpha F}, \tag{2}$$

where τ_0 already represents the limiting value of the optical thickness of the medium corresponding to the case where all atoms are in the lower state, and where the constant

$$\alpha = \frac{1}{a}\left(1 + \frac{g_2}{g_1}\right)$$

depends on the weights g_2 and g_1 of the state as well as on the factor

$$a = \frac{8\pi h\nu^3}{c^2}.$$

A comparison of eqs.(1) and (2) shows that the following cases are possible, depending upon the value of the incident flux F:

a) $\alpha F \ll 1$. In this case lightening is virtually absent and we can use the classical formula (1); /94
b) $1 \ll \alpha F \ll \tau_0/2$, where there is appreciable lightening;
c) $\alpha F \gg 1 + \tau_0/2$, where we approximately have: $H \approx F$, i.e., almost complete lightening of the medium.

Thus, everything depends on the value

$$\alpha F = \frac{F}{a}\left(1 + \frac{g_2}{g_1}\right). \tag{3}$$

The derivation of eq.(2) is based on the following simple considerations: It is obvious that eq.(1) is the correct solution of the problem for a given real optical depth τ (i.e., that which will hold at a given value of the flux F) not equal to τ_0. The entire matter reduces to the fact that, in the new formulation of the problem (nonlinear), τ is a quantity that should be derived from given values of F and τ_0. However, leaving τ undetermined for the moment, we can use the conventional linear theory for each τ to calculate the radiation field and hence the excitation of atoms n_2/n_1 as a function of the optical depth x (this function will also depend on F and on the total optical thickness τ as parameters)

$$\frac{n_2}{n_1} = p(x).$$

If k is the atomic absorption coefficient, we can write the equality

$$k(n_1 + n_2) = k\,\frac{1 + \frac{n_2}{n_1}}{1 - \frac{g_1}{g_2}\frac{n_2}{n_1}}\left(n_1 - \frac{g_1}{g_2}n_2\right) = \frac{1 + p(x)}{1 - \frac{g_1}{g_2}p(x)}\frac{dx}{ds},$$

where ds is an element of linear depth. Multiplying by ds and integrating with respect to the entire linear thickness of the layer, we obtain

$$\tau_0 = \int_0^{s_0} k(n_1 + n_2)\,ds = \int_0^{\tau} \frac{1 + p(x)}{1 - \frac{g_1}{g_2}p(x)}\,dx. \tag{4}$$

The right-hand side of this equation will thus be defined as some definite function τ. On inverting this function, we find τ as a function of τ_0 and F, /95 since p(x) depended on these quantities as parameters (depending also on x). On substituting the expression of τ relative to τ_0 and F into eq.(1), one easily obtains eq.(2).

This simple method of solving the nonlinear problem, which here requires no special skill, will be called by the somewhat awkward name "method of self-consistent optical depth". As shown in the following example, the method is useful also in certain more complex cases, which to some extent justifies the introduction of a special name.

3.

As is known, the little-studied problems of the theory of radiation transfer in a scattering and absorbing medium contain a group of problems pertaining to a type of multiple scattering in which a redistribution of energy between the frequencies of different lines occurs. In these problems, the radiation fields at different line frequencies mutually interact. Here, the already schematic presentation of a medium consisting of atoms with three energy levels produces considerable difficulties in the general case. Of course, the problem can be solved by making certain assumptions as to the smallness of some parameters entering the equation. For example, 32 years ago it became possible to develop the method of "separation of fields" for solving the problem of radiative equilibrium in hydrogen planetary nebulae. However, a study of other cases requires a systematic development of methods for solving nonlinear problems.

Let us first discuss the particular case where the transition $1 \to 2$ is forbidden and the state 2 is metastable. Here we can assume the radiation field to be stationary and also postulate that collisions are of no consequence.

In this case, owing to the absence of cyclic transitions $1 \to 2 \to 3 \to 1$ and vice versa, as many quanta ν_1 (corresponding to the transition $1 \to 3$) are emitted in each volume as are absorbed. The same is true for the frequency ν_2 (corresponding to the transition $2 \to 3$). Therefore, the problem essentially reduces to pure scattering, at each of the frequencies separately.

The distribution of atoms by levels is determined by the steady-state equations which in this case take on the simple form: /96

$$B_{1\to 3} n_1 \rho_1 = n_3 B_{3\to 1} (\sigma_1 + \rho_1), \tag{5}$$

$$B_{2\to 3} n_2 \rho_2 = n_3 B_{3\to 2} (\sigma_2 + \rho_2), \tag{6}$$

where

$$\sigma_i = \frac{8\pi h \nu_i^3}{c^3}.$$

Let us assume that we are dealing with low intensities:

$$\rho_1 \ll \sigma_1; \qquad \rho_2 \ll \sigma_2.$$

Then,

$$\frac{n_3}{n_1} = \frac{g_3}{g_1}\bar{\rho}_1, \qquad \frac{n_3}{n_2} = \frac{g_3}{g_2}\bar{\rho}_2, \tag{7}$$

where

$$\bar{\rho}_i = \frac{\rho_i}{\sigma_i}.$$

Now let us make the problem more specific. Let us assume that radiation fluxes F_1 and F_2, at frequencies ν_1 and ν_2, impinge on one side of a medium of finite thickness. We are seeking the diffusely transmitted fluxes H_1 and H_2, by examining the one-dimensional approximation.

Let us use the same method of self-consistent optical depths.

The given parameter is the number of atoms per square centimeter. Denoting by τ_1^0 and τ_2^0 the real optical thickness at the corresponding frequencies, we can obtain the quantity

$$\frac{1}{k_1}\tau_1^0 + \frac{1}{k_2}\tau_2^0 = N, \tag{8}$$

where k_1 and k_2 are the corresponding atomic absorption coefficients.

However, the quantities τ_1^0 and τ_2^0 are not known individually and must be determined from the problem as a function of the parameters F_1, F_2, and N.

Since, at each frequency, there is pure scattering, we can determine the radiation intensity at each frequency as a function of the corresponding optical depth x_i and of the parameters F_i and τ_i^0 and find the relations that characterize atomic excitation: /97

$$\frac{n_3}{n_1} = p_1(x_1), \quad \frac{n_3}{n_2} = p_2(x_2), \tag{9}$$

where, we repeat, p_1 and p_2 should depend also on the parameters F_1, τ_1^0 and F_2, τ_2^0, respectively.

From eq.(9) we have

$$n_1 p_1(x_1) = n_2 p_2(x_2), \tag{10}$$

or

$$k_1 n_1 p_1(x_1)\, ds = \frac{k_1}{k_2} k_2 p_2(x_2)\, ds, \tag{11}$$

where k_1 and k_2 are the corresponding atomic absorption coefficients.

Integrating eq.(11) with respect to the entire thickness of the layer, we obtain

$$\int_0^{\tau_1^0} p_1(x_1)\, dx_1 = \frac{k_1}{k_2}\int_0^{\tau_2^0} p_2(x_2)\, dx_2. \tag{12}$$

The left-hand side of this equality is some definite function of τ_1^0 and F_1 and the right-hand side, of τ_2^0 and F_2.

From the two equations (12) and (8) we can find τ_1^0 and τ_2^0 as a function of N, F_1, and F_2 from which the values of the fluxes H_i are obtained over the formula

$$H_i = \frac{F_i}{1 + \frac{1}{2}\tau_i^0}. \qquad (13)$$

As this calculation shows, for the flux H_1, for example, we obtain the expression

$$H_1 = \frac{F_1}{1 + \frac{k_1 N}{2\left(1 + \frac{g_2}{g_1}\frac{F_1}{F_2}\right)}}. \qquad (14)$$

Here, three different cases are of interest: /98

a) $F_1 \ll F_2$; then,

$$H_1 = \frac{F_1}{1 + \frac{1}{2}k_1 N}.$$

In other words, if the flux F_2 is larger than the flux F_1 in order of magnitude, then the flux H_1 is obtained - just as in the linear problem - on the assumption that all atoms are in the state 1.

b) $F_2 \ll F_1 \ll F_2 k_1 N$; then,

$$H_1 = \frac{g_2 F_1^2}{g_2 F_1 + \frac{1}{2} g_1 F_2 k_1 N}.$$

c) $F_1 \gg F_2 k_1 N$; in this case we have complete lightening of the medium at a frequency ν_1 and

$$H \approx F_1.$$

Thus, in our scheme the effect of lightening of the medium occurs at one of the frequencies, without the necessity of a very intense radiation flux. It is required only that the radiation flux at the other frequency be many times less than the radiation flux at the frequency at which we achieve lightening.

Thus, we have at our disposal a simple method of regulating the transparency of a given medium at each of two frequencies.

Under the above physical assumptions the other problem, i.e., that of diffuse reflection from a layer of infinitely large thickness, has a trivial solution: At both frequencies the reflected fluxes are equal to the incident fluxes because of the fact that, as already mentioned, pure scattering occurs at each frequency.

The situation becomes markedly more complex if we assume transmissions of $2 \rightarrow 1$. If we postulate that these transitions occur without radiation, i.e.,

that the energy is transmitted to the medium, and we can disregard reverse transitions of $1 \rightarrow 2$, it will be found that the corresponding problem on diffuse reflection is readily solved, except that this can no longer be done by the method of self-consistent optical depths but by the use of the invariance principle. Such a solution was found by one of my graduate students, a participant of the Erevan Seminar on the theory of radiation transfer. We will not give this solution here. /99

The question arises, however, how to apply the invariance principle to nonlinear problems. The cause of the nonlinearity is the fact that we no longer neglect the influence of radiation on the optical properties of the medium, on the values of the optical characteristics at each point of the medium. Furthermore, the operation of adding, let us say, some elementary layer to an already existing layer, performed when solving the problems on the basis of the invariance principle, proceeds on the assumption that the medium and the layer being added have everywhere the same optical characteristics (for example, a value of λ which is the ratio of the scattering coefficient to the extinction coefficient).

However, a more detailed study of the problem shows that the invariance principle can be used when the dependence of the optical characteristics on the radiation field is the same for all points of the medium.

4.

As a typical example, let us discuss the application of the invariance principle to the problem of diffuse transmission and reflection of light through a medium of finite thickness. Here we will again retain the one-dimensional approximation so as not to deal with angles of incidence and diffuse reflection, and also assume that pure scattering takes place.

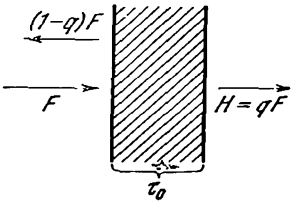

Fig.1

Let us recall how this problem is solved in the linear theory. The optical thickness of the layer τ_0 is given. It is assumed that the flux F is incident on one side of the layer (Fig.1); we must find the flux H that escapes from the opposite side. In view of the linearity of the problem it was assumed that the flux H is proportional to F so that it remains only to find the "coefficient of diffuse transmission" q entering into the formula $H = qF$. If we are dealing with a purely scattering medium, the diffusely reflected flux which, according to the law of conservation of energy, should be equal to $(1 - q)F$ is thus also determined. The unknown coefficient q should depend on τ_0 and the problem consists in finding the function $q(\tau_0)$. /100

A rather elegant method of finding the function $q(\tau_0)$ consists in obtaining the functional equation by examining the pattern of summation of two layers of optical thicknesses τ_1 and τ_2, which together make up one layer of optical thickness $\tau_1 + \tau_2$ (Fig.2).

As shown in Fig.2, we can examine the fluxes I_1 and I_2 obtained at the boundary between the two layers and proceeding in opposite directions. From the above-postulated properties of the scattering media we easily derive the equations

$$H = q(\tau_1 + \tau_2)F,$$
$$H = q(\tau_2)I_1,$$
$$I_1 = q(\tau_1)F + [1 - q(\tau_1)]I_2,$$
$$I_2 = [1 - q(\tau_2)]I_1.$$

In analyzing these equations as a system of four homogeneous equations with four unknowns H, F, I_1, and I_2, it can be stipulated that its determinant be equal to zero (condition of solvability). From here, we immediately obtain the functional equation for $q(\tau)$

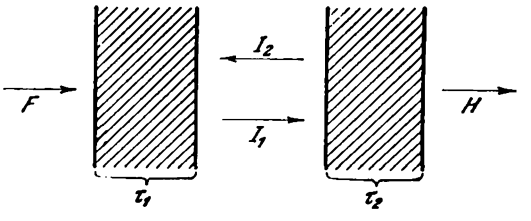

Fig.2

$$\frac{1}{q(\tau_1+\tau_2)} = \frac{1}{q(\tau_1)} + \frac{1}{q(\tau_2)} - 1, \qquad (15)$$

which is satisfied by the solution /101

$$q(\tau) = \frac{1}{1+a\tau}. \qquad (16)$$

The following complications and difficulties arise in the nonlinear case of the same problem.

First of all, in the diagram in Fig.1 it is no longer possible to set $H = q(\tau_0)F$; instead, it must be assumed that H is some function of F and of some parameter characterizing the thickness of the layer. For such a parameter, it is convenient to take the optical thickness at the limit when the intensities of all radiations are equal to zero. Let us designate this "limiting" optical thickness by σ_0. We should then have $H = \psi(F, \sigma_0)$. However, this is not all. In attempting to use the method of addition of layers we encounter the fact that two fluxes, F and I_2, enter one of the investigated layers. As a consequence of the nonlinearity of the phenomenon, the flux entering from the opposite side changes the optical properties of the medium and thus also that portion of the flux F which is subject to diffuse transmission. Therefore, we are forced to introduce a more general case and to study the result of the penetration of two fluxes, F_1 and F_2, into the medium. The pattern shown in Fig.3 is suitable for analysis. The quantity H_1 should depend on F_1, F_2, and σ_0. Likewise, H_2 should depend on these quantities. We obviously have

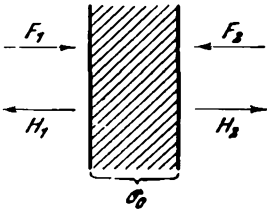

Fig.3

$$H_1 = \varphi(F_1, F_2; \sigma_0), \qquad (17)$$

$$H_2 = \varphi(F_2, F_1; \sigma_0), \tag{18}$$

and then proceed to finding this function.

In studying the addition scheme of two layers shown in Fig.4, we find between the six quantities H_1, H_2, H_3, F_1, F_2, and F_3, along with eqs.(17) and (18), another four dependences: /102

$$F_2 = \varphi(H_2, F_3; \sigma_2), \tag{19}$$
$$H_3 = \varphi(F_3, H_2; \sigma_2), \tag{20}$$
$$H_1 = \varphi(F_1, F_3; \sigma_1 + \sigma_2), \tag{21}$$
$$H_3 = \varphi(F_3, F_1; \sigma_1 + \sigma_2). \tag{22}$$

The next step is to reduce the problem to one functional equation.

Comparing eqs.(20) and (22), we have

$$\varphi(F_3, F_1; \sigma_1 + \sigma_2) = \varphi(F_3, H_2; \sigma_2).$$

Substituting into the right-hand side of this equality H_2 from eq.(18) will yield

$$\varphi(F_3, F_1; \sigma_1 + \sigma_2) = \varphi(F_3, \varphi(F_2, F_1; \sigma_1); \sigma_2). \tag{23}$$

On the other hand, substituting eq.(18) into eq.(19), we find

$$F_2 = \varphi(\varphi(F_2, F_1, \sigma_1), F_3; \sigma_2). \tag{24}$$

Let the solution of this equation, relative to F_2, be

$$F_2 = u(F_1, F_3; \sigma_1; \sigma_2). \tag{25}$$

The function u is wholly determined by assigning φ. On the basis of this, we can prove that by substituting eq.(25) into eq.(23) we obtain the equation

$$\varphi(F_3, F_1; \sigma_1 + \sigma_2) = \varphi(F_3, \varphi(u(F_1, F_3; \sigma_1, \sigma_2), F_1; \sigma_1); \sigma_2), \tag{26}$$

both sides of which are expressed by φ. Thus eq.(26), along with determining /103 the function u from eqs.(24) and (25), is some rather unique functional equation for the function φ.

Since it is quite difficult to solve directly the derived functional equation, we reduced it first to a differential equation, for which we assumed that σ_2 is a small quantity. Then, in place of eq.(19) we can write

$$F_2 = F_3 + \alpha(H_2, F_3)\sigma_2, \tag{27}$$

where $\alpha(H_2, F_3)$ is some function characterizing the medium. Likewise, instead of eq.(20) we have

$$H_3 = H_2 + \alpha(F_3, H_2)\,\sigma_2. \tag{28}$$

Eliminating now from the system of equations (17), (18), (21), (22), (27), and (28) the quantities H_1, H_2, H_3, and F_2 and, in so doing, discarding all terms of powers higher than σ_2, we obtain the following equation:

$$\frac{\partial\varphi(F_3, F_1; \sigma_1)}{\partial\sigma_1} = \frac{\partial\varphi(F_3, F_1; \sigma_1)}{\partial F_3}\alpha(\varphi(F_3, F_1; \sigma_1), F_3) + \alpha(F_3, \varphi(F_3, F_1; \sigma_1)). \tag{29}$$

A nonlinear differential equation for φ is obtained. For simplification we will use

$$H_3 = \varphi(F_3, F_1; \sigma_1) = z; \quad F_1 = x; \quad F_3 = y; \quad \sigma_1 = \sigma.$$

Then,

$$\frac{\partial z}{\partial\sigma} = \frac{\partial z}{\partial y}\alpha(z, y) + \alpha(y, z). \tag{30}$$

As $\sigma \to \infty$, our problem changes to one of finding the intensity of the flux z, diffusely reflected from an infinite layer when the flux y is incident upon it. Equation (30) then reduces to a more simple form:

$$\frac{\partial z}{\partial y}\alpha(z, y) + \alpha(y, z) = 0, \tag{31}$$

where z no longer depends on $x = F_1$.

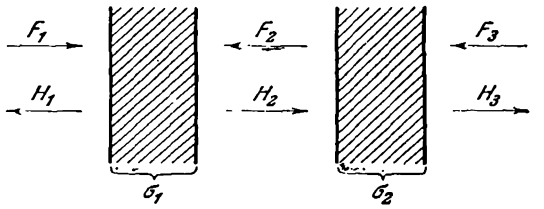

Fig.4

If we assume that isotropy occurs during an elementary event of scattering, then $\alpha(z, y)$ should have the following form: /104

$$\alpha(z, y) = -yk(z + y) + g(z + y). \tag{32}$$

For the initial condition $z = 0$, at $y = 0$, the solution of this equation has the simple form

$$yz = G(y + z), \tag{33}$$

where $G(\xi)$ is a function equal to

$$G(\xi) = \int_0^{\xi} \frac{g(x)}{k(x)}\,dx. \tag{34}$$

As a typical example, let us analyze the particular case when

$$\frac{g(x)}{k(x)} = \frac{\lambda}{2} \frac{a^2 \xi}{a^2 + \xi^2}.$$

This means that, of the energy absorbed in an elementary event, the portion

$$\lambda \frac{a^2}{a^2 + \xi^2}.$$

is scattered, i.e., upon an increase in the intensity of light the portion being scattered decreases. Then,

$$G(x) = \frac{\lambda}{4} a^2 \ln\left[1 + \frac{x^2}{a^2}\right],$$

and the solution has the form

$$yz = \frac{\lambda}{4} a^2 \ln\left[1 + \frac{(y+z)^2}{a^2}\right].$$

This solution indicates that, as $y \to \infty$, the albedo z/y approaches zero. By contrast, if $y \ll a$, we will have the usual formula for the linear case

$$\frac{z}{y} = \frac{2 - \lambda - \sqrt{1-\lambda}}{\lambda}.$$

We will not insist on other examples. Our purpose merely was to show that the invariance principle can be used successfully when solving at least certain problems of the nonlinear theory of radiative transfer. Of course, the application of the invariance principle to more complex problem than the simple scheme analyzed here will be of practical value.

RADIATIVE DIFFUSION IN GASES

/105

V.V.Sobolev

As is known, the theory of stellar spectra is one of the most important parts of theoretical astrophysics. This is because most of our information on stars is obtained from the radiation of their spectra.

The theory of stellar spectra is intimately connected with the problem of radiative diffusion in gases. We encounter this problem when studying other astrophysical objects: interstellar medium, planetary nebulae, shells of new stars, planetary atmospheres, etc. The solution of this problem is important also for a number of areas in physics (gas-discharge optics, plasma physics).

The theory of radiative diffusion in gases has progressed far. Both astrophysicists and physicists have participated in developing methods of this theory. It should also be recalled that some methods were elaborated from studies on the diffusion of particles (in particular, neutrons).

In this lecture we will study the theory of radiative diffusion at spectral line frequencies. We will limit ourselves to problems of greatest interest for the astrophysicist.

1. Elementary Scattering Event

Before discussing the theory of diffusion (or, in other words, multiple scattering) of radiation in gas, we must examine processes of radiative scattering in an element of volume.

Let σ_ν and ε_ν be the absorption and emission coefficients at a frequency ν, within a given line. The quantity $\sigma_\nu ds$ is the portion of the radiant energy absorbed over a path ds, while the quantity $\varepsilon_\nu d\nu dV d\omega dt$ is the quantity of /106 energy emitted by a volume dV in the time dt within the solid angle $d\omega$ in the frequency range from ν to $\nu + d\nu$.

The dependence of the absorption coefficient σ_ν on the frequency is due to many factors. The principal ones include the spread of the energy levels of atoms (or damping of radiation) and the Doppler effect due to thermal agitation of the atoms. As is known, when these factors act simultaneously, the absorption coefficient will be equal to

$$\sigma_\nu = nk_0 \frac{a}{\pi} \int_{-\infty}^{+\infty} \frac{e^{-y^2} dy}{(x+y)^2 + a^2}, \qquad (1)$$

where

$$x = \frac{\nu - \nu_0}{\Delta\nu_D}, \quad a = \frac{\Delta\nu_E}{\Delta\nu_D}. \qquad (2)$$

Here, $\Delta\nu_E$ and $\Delta\nu_D$ are the natural and Doppler line widths, k_0 is the atomic absorption coefficient at the center of the line for a = 0, and n is the number of absorbing atoms in 1 cm^3. When collisions are taken into account, the absorption coefficient is given by the same formula (1) but with a different value of a. When the Stark effect, produced by the presence of charged particles (ions and free electrons) near an atom, is taken into account, the expression for σ_ν becomes more complex. It should be mentioned that the theory of influence of the Stark effect on the form of the function σ_ν is highly developed at present.

The emission ε_ν is composed of two parts. The first part represents the coefficient of true emission which stems from the direct action of gas radiation sources (for example, collisions or recombinations). The second part is the result of absorption of energy in a line incident from all sides on the given volume and subsequent re-emission of the energy in the same line. This process we will call "radiative scattering in a spectral line". The probability of re-emission of a quantum in the line after absorption will be designated by λ. If $\lambda = 1$, we are dealing with pure radiative scattering.

Originally it had been assumed in the theory of spectral line radiative diffusion that, during an elementary scattering event, the radiation frequency remained constant (i.e., scattering was considered to be coherent). In this /107 case, the emission coefficient is equal to

$$\varepsilon_\nu = \lambda\sigma_\nu \int I_\nu \frac{d\omega}{4\pi} + \varepsilon_\nu^0, \tag{3}$$

where ε_ν^0 is the true emission coefficient, I_ν is the intensity of radiation incident on the given volume, and integration is carried out over all directions.

The theory of the formation of absorption lines in stellar spectra was based for a long time on the assumption of coherent scattering of radiation, i.e., on eq.(3). However, in 1929 Eddington (Ref.1) showed that this assumption might be erroneous. Further investigations established that, during an elementary scattering event, actually a redistribution of radiation by frequencies takes place, i.e., the radiative scattering is incoherent. In this case, eq.(3) is replaced by

$$\varepsilon_\nu = \lambda \int p(\nu, \nu')\, \sigma_{\nu'} d\nu' \int I_{\nu'} \frac{d\omega}{4\pi} + \varepsilon_\nu^0, \tag{4}$$

where $p(\nu, \nu')$ is the probability that, after absorption of a photon with frequency ν', a photon with frequency ν is emitted.

The form of the function $p(\nu, \nu')$ is determined by a number of factors. The spread of the energy levels of the atom leads to incoherence of radiative scattering. The question of the function $p(\nu, \nu')$ for this case was examined by Spitzer and Wooley (Ref.2, 3).

Incoherence of scattering in an element of volume is also due to the thermal agitation of atoms. The law of redistribution of radiation by frequencies due to the indicated factor was discovered for the resonance line by

Henyey and V.G.Levich (Ref.4, 5). Their formula includes the angle between the directions of the incident and scattered radiations. By integrating this formula with respect to the angle we obtain the following relation:

$$p(\nu, \nu')\,\sigma_{\nu'} = \frac{nk_0}{\pi\Delta\nu_D}\int_0^\infty e^{-(y+z)^2}\left[\tan^{-1}\frac{y+s}{a} + \tan^{-1}\frac{y-s}{a}\right]dy, \tag{5}$$

where /108

$$s = \frac{x+x'}{2}, \quad r = \frac{|x-x'|}{2}, \tag{6}$$

while σ_ν represents eq.(1). Equation (5) for the function $p(\nu, \nu')$ was also found by other methods (Ref.6, 7).

Still another reason for the frequency redistribution of radiation is the presence of extraneous particles near the atom. These particles cause a displacement of the energy levels of the atom, where the extent of such a shift may vary greatly during the stay of the atom in an excited state. Therefore, after absorption of a photon with frequency ν' the atom will emit a photon with a different frequency ν. It is obvious that the perturbing particle entrains the difference of energies of these photons. It can be assumed that, in this case, the probability of emitting a photon of frequency ν does not depend upon the frequency ν' of the absorbed photon. This process we will call complete frequency redistribution of radiation or fully incoherent scattering. It is easy to demonstrate that in the case of completely incoherent scattering the function $p(\nu, \nu')$ (which does not really depend on ν') has the form

$$p(\nu, \nu') = \frac{\sigma_\nu}{\int\sigma_{\nu'}d\nu'}. \tag{7}$$

The question of the influence of extraneous particles on the form of the function $p(\nu, \nu')$ has been studied briefly by Spitzer (Ref.8).

If the density of the gas is sufficiently high, complete frequency redistribution of radiation can be assumed in studies on the radiative diffusion in gases, i.e., we can use eq.(7). This assumption apparently holds in the case of stellar atmospheres. If the density of the gas is low, eq.(5) must be used for the function $p(\nu, \nu')$. In particular, this is the necessary procedure when studying diffusion of L_α-radiation in nebulae and the interstellar medium. The problem as to the extent to which replacement of eq.(5) by the vastly simpler formula (7) is permissible was investigated by Thomas and by Jefferies and White (Ref.9, 10). It follows from their results that such a substitution (at least for the central portions of the line) is roughly feasible.

Recently, Hummer (Ref.11) derived a rather general expression for the /109 function $p(\nu, \nu')$, from which the previously found formulas follow as a particular case. Hummer's article also contains a detailed bibliography on this subject matter.

2. Equation for Radiative Transfer

To solve the problem of radiative diffusion in gases, we should use the equation for radiative transfer which describes the rate of change of radiation intensity along the ray. The radiative transfer equation has the form

$$\frac{dI_\nu}{ds} = -\sigma_\nu I_\nu + \varepsilon_\nu. \tag{8}$$

In the case of coherent scattering of light eq.(3) must be substituted into eq.(8) to replace ε_ν. This yields

$$\frac{dI_\nu}{ds} = -\sigma_\nu I_\nu + \lambda\sigma_\nu \int I_\nu \frac{d\omega}{4\pi} + \varepsilon_\nu^0. \tag{9}$$

In the case of completely incoherent scattering of light, eq.(8), with the aid of eqs.(4) and (7), is replaced by

$$\frac{dI_\nu}{ds} = -\sigma_\nu I_\nu + \lambda\sigma_\nu \frac{\int \sigma_{\nu'}\, d\nu' \int I_{\nu'} \frac{d\omega}{4\pi}}{\int \sigma_{\nu'} d\nu'} + \varepsilon_\nu^0. \tag{10}$$

We see that eq.(9) determines the radiant intensity for each frequency separately, whereas the radiant intensities for all frequencies within the line enter eq.(10) together. Therefore, eq.(10) is appreciably more laborious for the solution than eq.(9). As explained earlier, diffusion of radiation in the spectral line should be described by eq.(10), which we will discuss later in the text.

Generally speaking, the quantities σ_ν, ε_ν^0, and λ entering eq.(10) can be arbitrary functions of the coordinates of a point. However, it is usually assumed in astrophysics that the medium consists of plane-parallel layers in which all these quantities depend only on one coordinate, namely, the depth of the /110 layer. This assumption is permissible specifically with respect to stellar atmospheres. In this case, eq.(10) takes the form

$$\cos\vartheta \frac{dI_\nu}{dr} = -\sigma_\nu I_\nu + \lambda\sigma_\nu \frac{\int \sigma_{\nu'}\, d\nu' \int I_{\nu'} \frac{d\omega}{4\pi}}{\int \sigma_{\nu'} d\nu'} + \varepsilon_\nu^0. \tag{11}$$

Here, the radiant intensity I_ν depends on the distance from the center of the star and on the angle ϑ between the direction of radiation and the normal to the atmospheric layers.

In each volume element of the stellar atmosphere, absorption and emission occur in the continuous spectrum (in particular at the frequencies of a given line) in addition to absorption and emission in the spectral line. The corresponding absorption and emission coefficients we will designate by $\varkappa$ and ε (within the line they can be considered independent of the frequency). With consideration of absorption and emission in the continuous spectrum the equation of radiative transfer, in place of eq.(11), will read

$$\cos\vartheta\frac{dI_\nu}{dr}=-(\sigma_\nu+\varkappa)I_\nu+\lambda\sigma_\nu\frac{\int\sigma_{\nu'}d\nu'\int I_{\nu'}\frac{d\omega}{4\pi}}{\int\sigma_{\nu'}d\nu'}+\varepsilon_\nu^0+\varepsilon. \tag{12}$$

Let us represent the emission coefficients ε_ν^0 and ε in the form

$$\varepsilon_\nu^0=\sigma_\nu B_0,\qquad \varepsilon=\varkappa B_*. \tag{13}$$

and introduce the notation

$$B=\lambda\frac{\int\sigma_{\nu'}d\nu'\int I_{\nu'}\frac{d\omega}{4\pi}}{\int\sigma_{\nu'}d\nu'}+B_0. \tag{14}$$

Usually, by B_* we mean the Planckian radiant intensity since, in stellar atmospheres, local thermodynamic equilibrium with respect to the continuous spectrum is assumed to exist. This does not hold for the quantity B_0.

Substitution of eqs.(13) and (14) into eq.(12) yields

$$\cos\vartheta\frac{dI_\nu}{dr}=-(\sigma_\nu+\varkappa)I_\nu+\sigma_\nu B+\varkappa B_*. \tag{15}$$

In eq.(15), not only the radiant intensity I_ν but also the quantity B is unknown since it is expressed by eq.(14) in terms of the quantity I_ν. Thus, we have two equations, (14) and (15), for determining two unknown functions I_ν and B. /111

Let us represent the absorption coefficient in the spectral line as

$$\sigma_\nu=\sigma_{\nu_0}\alpha(x), \tag{16}$$

where x is a dimensionless frequency determined by the first equation of the system (2). Let us also introduce the optical depth of the given position in the atmosphere for the central line frequency:

$$\tau=\int_r^\infty\sigma_{\nu_0}dr. \tag{17}$$

It is obvious that the radiant intensity I_ν will now be a function of τ, ϑ, and x and the quantity B a function of τ. Therefore, eqs.(14) and (15) can be rewritten as

$$B(\tau)=\frac{\lambda}{2}A\int\alpha(x)\,dx\int_0^\pi I(\tau,\vartheta,x)\sin\vartheta\,d\vartheta+B_0(\tau), \tag{18}$$

$$\cos\vartheta\frac{dI(\tau,\vartheta,x)}{d\tau}=[\alpha(x)+\beta]I(\tau,\vartheta,x)-\alpha(x)B(\tau)-\beta B_*(\tau). \tag{19}$$

In eq.(18) (as everywhere hereafter) integration with respect to x is carried out within the limits from $-\infty$ to $+\infty$, and the quantity A is determined by the

relation

$$A\int\alpha(x)\,dx=1. \tag{20}$$

In eq.(19) we mean by β the ratio of the absorption coefficient in a continuous spectrum to the absorption coefficient at the line center, i.e.,

$$\beta=\frac{\varkappa}{\sigma_{\nu_0}}. \tag{21}$$

Equations (18) and (19) must be supplemented by appropriate boundary conditions. However, these conditions are based on the fact that there is no /112 radiation incident on the atmosphere from without. If there is such radiation, its effect can be taken into account in the function $B_0(\tau)$.

From eqs.(18) and (19) we can obtain one equation for determining the function $B(\tau)$. For this we must solve eq.(19) relative to $I(\tau, \vartheta, x)$ and substitute the found expression into eq.(18). Having done this, we obtain

$$B(\tau)=\frac{\lambda}{2}A\int\alpha(x)\,dx\int_0^{\tau_0}[\alpha(x)B(\tau')+\beta B_*(\tau')]\times \\ \times \mathrm{Ei}\{[\alpha(x)+\beta]|\tau-\tau'|\}\,d\tau'+B_0(\tau), \tag{22}$$

where

$$\mathrm{Ei}\,\tau=\int_1^{\infty}e^{-\tau z}\frac{dz}{z} \tag{23}$$

and τ_0 is the optical thickness of the atmosphere at the line center. In the case of stellar atmospheres $\tau_0=\infty$; however, in the interest of generality we wrote eq.(22) for an arbitrary τ_0.

In the absence of absorption and emission in the continuous spectrum, i.e., when $\beta=0$, eq.(22) takes the form

$$B(\tau)=\frac{\lambda}{2}A\int_0^{\tau_0}B(\tau')\,d\tau'\int\alpha^2(x)\,\mathrm{Ei}\,[\alpha(x)|\tau-\tau'|]\,dx+B_0(\tau). \tag{24}$$

Thus, the problem of diffusion of radiation in the spectral line reduces to solving a system of equations (18) and (19) determining the functions $I(\tau, \vartheta, x)$ and $B(\tau)$, or to solving the integral equation (22) for the function $B(\tau)$. It is obvious that, after deriving the function $B(\tau)$ from eq.(22), the radiant intensity $I(\tau, \vartheta, x)$ is easily found from eq.(19).

The problem of diffusion of radiation in the spectral line was studied by astrophysicists as long ago as the 1930s. Originally, the radiative transfer equation was written with an arbitrary function $p(\nu, \nu')$ and expressions were sought for this function [see, for example Wooley's article (Ref.5)]. Then Houtgast (Ref.12) made the assumption of completely incoherent scattering and wrote the equation of radiative transfer in the form of eq.(12). This equa- /113 tion, with the purpose of determining the profiles of the absorption lines in stellar spectra, has been solved at numerous occasions. The problem was solved

by approximate methods in the investigations by Suemoto, Labs, Savedoff, Miyamoto (Ref.13 - 16) and others. Exact solutions of the problem were given by me (Ref.17), by Busbridge, by Ueno (Ref.18, 19), and by others.

The problem of diffusion of resonance radiation (specifically, radiation in the line L_α) is of great interest for the physics of gaseous nebulae. At first this problem was solved without consideration of the frequency change of the diffusing photon. In the works of the author (Ref.20) it was solved for the case of a nebula expanding with a velocity gradient on the assumption of complete radiation frequency redistribution [first with a rectangular contour of the absorption coefficient and then with an arbitrary form of the function $\alpha(x)$]. The integral equation describing diffusion of L_α-radiation in a fixed nebula with complete radiation frequency redistribution and with a Doppler contour of the absorption coefficient was first obtained by Zanstra (Ref.21). This equation, coinciding with eq.(24) for $\alpha(x) = e^{-x^2}$, was solved numerically by Koelbloed (Ref.22). In the papers by Unno, by the author, and by Osterbrock (Ref.6, 7, 23), the problem of diffusion of resonance radiation was solved for cases of complete and true radiation frequency redistribution, i.e., when the function $p(\nu, \nu')$ is given by eqs.(7) and (5), respectively. It turned out that similar results are obtained in both these cases. Field (Ref.24) studied the process of resonance radiation diffusion as a function of time.

In the physics literature, an integral equation of resonance radiation diffusion with complete frequency redistribution was first derived by L.M.Biberman and Holstein (Ref.25, 26). Later, similar equations were studied by many authors.

3. Approximate Solution

The aforementioned diffusion equations are usually solved either numerically or approximately. Let us now examine one of the approximate methods which does not yield a high accuracy but has the advantage of elucidating the essence of the matter (Ref.20, 27). /114

Let us denote by τ_0 the optical thickness of the investigated plane layer for the line center. The optical thickness of the layer for the dimensionless frequency x will be equal to $\tau_0\alpha(x)$. We will assume that $\tau_0 \gg 1$. The outer portions of the line, satisfying the inequality $\tau_0\alpha(x) \ll 1$, will be called the line wings. It is obvious that a photon, arising in the wing of the line, most likely will not undergo absorption in the layer and escape. On the other hand, a photon in the central portion of the line, satisfying the inequality $\tau_0\alpha(x) \gg \gg 1$, most likely is absorbed in the layer (if, of course, it does not arise near the layer boundary). If radiative diffusion occurs without a change in frequency, the photons in the line wings almost immediately will escape from the layer, whereas the photons in the central portions of the line escape from the layer only after a long process of diffusion, moving ever closer to the layer boundary. The matter is quite different for radiative diffusion with frequency redistribution. In this case, after each scattering event photons are formed in the line wings which encounter no obstruction of their escape from the layer, from any depth. Therefore, an appreciable portion of the photons formed at an

arbitrary site will be able to escape after diffusion through a comparatively small volume. Consequently, we can roughly state that the number of photons formed in some volume is equal to the number of photons escaping from this volume beyond the layer (and also, of course, to the number of photons experiencing true absorption).

These considerations readily yield an approximate solution of the integral diffusion equation. For simplicity we will pose $\beta = 0$, i.e., we will examine eq.(24) after having rewritten it as

$$B(\tau) = \int_0^{\tau_0} K(|\tau - \tau'|)\, B(\tau')\, d\tau' + B_0(\tau), \tag{25}$$

where we denote

$$K(\tau) = \frac{\lambda}{2} A \int \alpha^2(x)\, \mathrm{Ei}\,[\alpha(x)\,\tau]\, dx. \tag{26}$$

In eq.(25), we will remove from under the integral the value of the function $B(\tau')$ equal to $B(\tau)$. Then we approximately obtain /115

$$B(\tau)\left[1 - 2\int_0^{\infty} K(t)\, dt + \int_{\tau}^{\infty} K(t)\, dt + \int_{\tau_0-\tau}^{\infty} K(t)\, dt\right] = B_0(\tau). \tag{27}$$

However,

$$2\int_0^{\infty} K(t)\, dt = \lambda. \tag{28}$$

Therefore, from eq.(27) we have

$$B(\tau) = \frac{B_0(\tau)}{1 - \lambda + L(\tau) + L(\tau_0 - \tau)}, \tag{29}$$

where

$$L(\tau) = \int_{\tau}^{\infty} K(t)\, dt = \frac{\lambda A}{2} \int \alpha(x)\, \mathrm{Ei}_2\,[\alpha(x)\,\tau]\, dx, \tag{30}$$

and

$$\mathrm{Ei}_2\,\tau = \int_1^{\infty} e^{-\tau z} \frac{dz}{z^2}. \tag{31}$$

The quantity $L(\tau) + L(\tau_0 - \tau)$ represents the portion of photons escaping from the layer from a depth τ, while the quantity $1 - \lambda$ is the portion of photons undergoing true absorption. Therefore, eq.(29), in conformity with our earlier statements, means that the number of photons formed in the depth is equal to the number of photons that had escaped from the layer from this depth and perished during diffusion. Of course, eq.(29) can be used only when the function $B_0(\tau)$ changes at a moderate rate.

It is obvious that the ratio $\frac{B(\tau)}{B_0(\tau)}$ characterizes the average number of scatterings experienced by a photon formed at the optical depth τ. It follows from eq.(29) that this number is approximately equal to

$$N \approx \frac{1}{1-\lambda+L(\tau)+L(\tau_0-\tau)}. \tag{32}$$

Equation (32) is easily understood also on the basis of the physical meaning of the quantities entering it.

As an example, let us examine the case where the absorption coefficient /116 has a Doppler profile, i.e., $\alpha(x) = e^{-x^2}$. Here,

$$K(\tau) = \frac{\lambda}{\sqrt{\pi}} \int_0^\infty e^{-2x^2} \operatorname{Ei}(\tau e^{-x^2})\, dx \tag{33}$$

and

$$L(\tau) = \frac{\lambda}{\sqrt{\pi}} \int_0^\infty e^{-x^2} \operatorname{Ei}_2(\tau e^{-x^2})\, dx. \tag{34}$$

At $\tau \gg 1$, we have the following asymptotic formulas

$$K(\tau) = \frac{\lambda}{4\sqrt{\pi}\tau^2\sqrt{\ln\tau}} \tag{35}$$

and

$$L(\tau) = \frac{\lambda}{4\sqrt{\pi}\tau\sqrt{\ln\tau}}. \tag{36}$$

It should be emphasized here that the previous assumption of radiative diffusion in the spectral line without change in frequency leads to large errors in the determination of various physical quantities. We will give some examples:

1. Let pure radiative scattering (i.e., $\lambda = 1$) occur in a layer of large optical thickness. In this case, assuming constancy of the radiation frequency during diffusion for an average number of scatterings, we have

$$N \approx \tau_0^2. \tag{37}$$

However, eqs.(32) and (36) yield

$$N \approx \tau_0\sqrt{\ln\tau_0}. \tag{38}$$

2. If it is assumed that radiative diffusion occurs without a change in frequency, then - at $\lambda = 1$ - the entire energy of any frequency generated inside the layer should escape at the same frequency. Therefore, at an arbitrary optical thickness of the layer the profile of the emission line should be similar to the profile of the true emission coefficient (if we examine radiation fluxes escaping from the layer with a symmetric arrangement of the sources). However, at radiation frequency redistribution and at $\tau_0 \gg 1$, as explained above, /117 radiation will escape from the layer mainly in the wings of the line. Therefore, in reality the emission line will have a characteristic saddle-point profile. Here the line width will be greater the greater τ_0.

3. For the physics of planetary nebulae it is of interest to determine the force of the light pressure caused by radiation in the line L_α. This force acting on a unit volume is equal to

$$F = \frac{1}{c}\int \sigma_\nu H_\nu d\nu,$$

where H_ν is the radiant flux and c is the velocity of light. Let us examine the force F on the boundary of the nebula. On the assumption of coherent scattering, the radiant flux H_ν has a maximum at the line center and the force F proves to be rather large. However, if we take scattering to be incoherent, the flux H_ν at $\tau_0 \gg 1$ will have a minimum at the line center and the force F will be smaller. According to calculations by Zanstra (Ref.21), as soon as $\tau_0 \approx 10^4$, the force of the light pressure in the latter case will be approximately 300 times less than in the first case.

We see that the assumption of coherent scattering, in studies on radiative diffusion in the spectral line, is impermissible even as a first approximation.

4. Exact Solution

Contemporary methods of the theory of radiative transfer can be applied to the solution of equations of radiative diffusion in the spectral line (Ref.28 - 31). In part, this has already been done in a number of the aforementioned papers (Ref.17 - 19), in which the intensity of radiation escaping from the atmosphere was determined. Recently, however, methods have been developed that permit a much greater progress in the solution of these equations. In particular, these methods furnish exact solutions for a semi-infinite medium and asymptotic solutions for a medium of great optical thickness.

We have already examined the integral equation (25) whose kernel is determined by eq.(26). This equation is a particular case of equations with kernels depending on the modulus of the difference of the two arguments. Such /118
equations are often encountered in the theory of radiative diffusion and in other areas of mathematical physics. For this reason, they have recently been studied in much detail (Ref.32 - 34).

Let us examine the following integral equation with an arbitrary kernel depending on the modulus of the difference of the two arguments and with an arbitrary free term:

$$B(\tau) = \int_0^\infty K(|\tau - \tau'|)\, B(\tau')\, d\tau' + B_0(\tau). \qquad (39)$$

In the theory of radiative diffusion this equation determines the function of a source $B(\tau)$ in a semi-infinite medium, with the kernel $K(\tau)$ depending on the mechanism of radiative scattering, and the free term $B_0(\tau)$ characterizing the location and power of the energy sources.

Let $\Gamma(\tau, \tau')$ be the resolvent of eq.(39). Then, the solution of this equation for any function $B_0(\tau)$ is represented as

$$B(\tau) = B_0(\tau) + \int_0^\infty \Gamma(\tau, \tau') B_0(\tau') d\tau'. \tag{40}$$

From the known equation for the resolvent

$$\Gamma(\tau, \tau') = \int_0^\infty K(|\tau - \tau''|) \Gamma(\tau', \tau'') d\tau'' + K(|\tau - \tau'|) \tag{41}$$

we obtain also the following equation:

$$\frac{\partial \Gamma}{\partial \tau} + \frac{\partial \Gamma}{\partial \tau'} = \Phi(\tau) \Phi(\tau'), \tag{42}$$

where we denote $\Gamma(0, \tau) = \Phi(\tau)$. From eq.(42) we find (for $\tau' > \tau$):

$$\Gamma(\tau, \tau') = \Phi(\tau' - \tau) + \int_0^\tau \Phi(u) \Phi(u + \tau' - \tau) du. \tag{43}$$

Thus, the resolvent $\Gamma(\tau, \tau')$ depending on the two variables is expressed in terms of the function $\Phi(\tau)$, which depends only on one variable. To deter- /119 mine the function $\Phi(\tau)$ we can use the equation

$$\Phi(\tau) = \int_0^\infty K(|\tau - \tau'|) \Phi(\tau') d\tau' + K(\tau), \tag{44}$$

which follows from eq.(41). After finding the function $\Phi(\tau)$, eq.(43) is used for determining the resolvent $\Gamma(\tau, \tau')$ and then eq.(40) for defining the function $B(\tau)$ for any energy sources.

In addition to eq.(44), another equation can be obtained for determining the function $\Phi(\tau)$. In this case, we will consider that the kernel of the integral equation (39) is a superposition of exponents, i.e.,

$$K(\tau) = \int_a^b A(y) e^{-\tau y} dy. \tag{45}$$

Let us then introduce the auxiliary equation

$$B(\tau, y) = \int_0^\infty K(|\tau - \tau'|) B(\tau', y) d\tau' + e^{-\tau y}. \tag{46}$$

If $K(\tau)$ is represented by eq.(45) then a comparison of eqs.(44) and (46) will yield

$$\Phi(\tau) = \int_a^b A(y) B(\tau, y) dy. \tag{47}$$

Equation (46) is a particular case of eq.(39) for $B_0(\tau) = e^{-\tau y}$. Therefore, on the basis of eq.(40) we have

$$B(\tau, y) = e^{-\tau y} + \int_0^\infty \Gamma(\tau, \tau') e^{-\tau' y} d\tau'. \tag{48}$$

From this, incidentally, it follows that

$$B(0, y) = 1 + \int_0^\infty \Phi(\tau) e^{-\tau y} d\tau. \tag{49}$$

Using eqs.(42) and (49), we obtain from eq.(48)

$$\frac{\partial B(\tau, y)}{\partial \tau} = -yB(\tau, y) + B(0, y)\Phi(\tau), \tag{50}$$

or, after integration /120

$$B(\tau, y) = B(0, y)\left[e^{-\tau y} + \int_0^\tau e^{-(\tau-\tau')y}\Phi(\tau')\, d\tau'\right]. \tag{51}$$

Substituting eq.(51) into eq.(47) gives

$$\Phi(\tau) = M(\tau) + \int_0^\tau M(\tau - \tau')\Phi(\tau')\, d\tau', \tag{52}$$

where

$$M(\tau) = \int_a^b A(y) B(0, y) e^{-\tau y} dy. \tag{53}$$

Equation (52) is the sought equation for the function $\Phi(\tau)$. Applying the Laplace transform to this, we obtain

$$\int_0^\infty \Phi(\tau) e^{-s\tau} ds = \frac{1}{1 - \int_a^b A(y) B(0, y) \frac{dy}{y+s}} - 1. \tag{54}$$

Thus, the function $\Phi(\tau)$ can be found from eq.(54) by inversion of the Laplace transform. However, to do this we must know the function B(0, y).

To obtain the equation determining the function B(0, y) we substitute eq.(47) into eq.(49). This gives

$$B(0, y) = 1 + \int_a^b A(z)\, dz \int_0^\infty B(\tau, z) e^{-\tau y} d\tau. \tag{55}$$

However, eq.(50), with consideration of eq.(49), furnishes

$$\int_0^\infty B(\tau, z) e^{-\tau y} d\tau = \frac{B(0, y) B(0, z)}{y + z}. \tag{56}$$

Thus, to determine the function B(0, y) we obtain the following nonlinear integral equation:

$$B(0, y) = 1 + B(0, y)\int_a^b A(z)\,\frac{B(0, z)}{y+z}\,dz. \tag{57}$$

From eq.(57) we can also obtain the linear integral determining B(0, y): /121

$$B(0, y)\left[1 - 2\int_a^b A(z)\,\frac{z\,dz}{z^2 - y^2}\right] = 1 - \int_a^b A(z)\,\frac{B(0, z)}{z - y}\,dz. \tag{58}$$

Equation (57) is easily solved by numerical methods, and eq.(58) will yield the function B(0, y) in an explicit form.

It should be emphasized that the function B(0, y) not only plays an auxiliary role in determining the function $\Phi(\tau)$ but is also of great interest in itself since the intensities of radiation escaping from the medium are expressed in terms of it. The function B(0, y) [denoted by $\varphi(\eta)$] was first introduced into the theory of radiative transfer by V.A.Ambartsumyan (Ref.28) for the case of radiative diffusion without change in frequency. This function [designated by $H(\mu)$] was studied in detail by Chandrasekhar (Ref.29).

Later the function B(0, y) was also introduced into the theory of radiative diffusion with frequency redistribution (Ref.17). In particular, this function was used for determining the profile of the absorption line in the stellar spectrum.

Explicit expressions for the function B(0, y) were derived for various particular cases (Ref.29, 30, 35). By generalizing Cram's result given earlier (Ref.29), V.V.Ivanov (Ref.35) obtained

$$\ln B(0, y) = -\frac{1}{\pi}\int_0^\infty \ln T(iv)\,\frac{y\,dv}{y^2 + v^2}, \tag{59}$$

where

$$T(y) = 1 - 2\int_a^b A(z)\,\frac{z\,dz}{z^2 - y^2}. \tag{60}$$

The function $\Phi(\tau)$, as already stated, is found from eq.(54) by inversion of the Laplace transform. This can be done by the method of contour integration with consideration of eq.(58). At first the function $\Phi(\tau)$ was determined for the case of radiative diffusion without change in frequency (Ref.36). For the integral equation in question [eq.(39)] with a kernel of the form of eq.(45), /122 the function $\Phi(\tau)$ is given by the formula

$$\Phi(\tau) = \int_a^b \frac{A(y)\,e^{-\tau y}}{T^2(y) + \pi^2 A^2(y)}\,\frac{dy}{B(0, y)}. \tag{61}$$

Here, it is considered that the function T(y) has no poles in the complex plane. In the opposite case, appropriate residues must be added to eq.(61).

Equation (61) was derived by D.I.Nagirner (Ref.37). Earlier Busbridge (Ref.31) obtained similar expressions for solving eq.(39) in certain particular cases.

In applying this theory to specific problems, the kernel of the given integral equation must first be represented by eq.(45), i.e., the quantity A(y) must be defined. In the case of radiative diffusion without change in frequency, we have

$$K(\tau)=\frac{\lambda}{2}\operatorname{Ei}\tau=\frac{\lambda}{2}\int_1^\infty e^{-\tau y}\frac{dy}{y}. \tag{62}$$

Consequently, here $A(y)=\frac{\lambda}{2y}$, $a=1$, $b=\infty$.

In the case of radiative diffusion with frequency redistribution and a Doppler profile of the absorption coefficient, the kernel of the integral equation (39) is given by eq.(33) which can be rewritten as:

$$K(\tau)=\frac{\lambda}{\sqrt{\pi}}\int_0^\infty e^{-2x^2}dx\int_{e^{-x^2}}^\infty e^{-\tau y}\frac{dy}{y}. \tag{63}$$

Changing here the order of integration, we reduce $K(\tau)$ to the form of eq.(45), where

$$A(y)=\begin{cases}\dfrac{\lambda}{\sqrt{\pi y}}\displaystyle\int_{\sqrt{-\ln y}}^\infty e^{-2x^2}dx, & 0\leqslant y\leqslant 1,\\ \dfrac{\lambda}{2\sqrt{2y}}, & y\geqslant 1.\end{cases} \tag{64}$$

In like manner we find A(y) for other profiles of the absorption coefficient.

Substitution of the quantity A(y) into eqs.(59) and (61) yields the basic functions B(0, y) and $\Phi(\tau)$ for this problem. /123

In practical application, it is of interest that for certain radiation sources in the medium the function $B(\tau)$ is quite simply expressed by the function $\Phi(\tau)$. Let us assume, for example, that

$$B_0(\tau)=e^{-m\tau}. \tag{65}$$

Then, on the basis of eq.(51) we have

$$B(\tau, m)=B(0, m)\left[e^{-m\tau}+\int_0^\tau e^{-m(\tau-\tau')}\Phi(\tau')\,d\tau'\right], \tag{66}$$

where B(0, m) is expressed in terms of $\Phi(\tau)$ by eq.(49).

At uniform distribution of radiation sources in the medium we obtain from eq.(66)

$$B(\tau, 0) = B(0, 0)\left[1 + \int_0^{\tau} \Phi(\tau')\, d\tau'\right]. \tag{67}$$

The quantity B(0, 0) is readily determined from eqs.(57) and (58), which yield

$$B^2(0, 0) = \frac{1}{1 - 2\int_a^b A(y)\,\frac{dy}{y}} = \frac{1}{1 - 2\int_0^{\infty} K(\tau)\, d\tau}. \tag{68}$$

Taking also eq.(28) into consideration, eq.(67) is replaced by

$$B(\tau, 0) = \frac{1}{\sqrt{1-\lambda}}\left[1 + \int_0^{\tau} \Phi(\tau')\, d\tau'\right]. \tag{69}$$

As already stated, the intensity of radiation emitted by the medium can often be expressed directly by the function B(0, y). This is done, for example, when the function $B_0(\tau)$ is given by eq.(65).

From the radiative transfer equation follows that the intensity of radiation escaping from the medium at an angle ϑ to the normal with the dimensionless frequency x is equal to /124

$$I(0, \vartheta, x) = \alpha(x)\int_0^{\infty} B(\tau, m)\, e^{-\alpha(x)\sec\vartheta}\sec\vartheta\, d\tau. \tag{70}$$

A comparison of eqs.(70) and (56) yields

$$I(0, \vartheta, x) = B(0, m)\, B\left[0, \frac{\alpha(x)\sec\vartheta}{1 + m\frac{\cos\vartheta}{\alpha(x)}}\right]. \tag{71}$$

In the case of a uniform distribution of energy sources in the medium (i.e., for m = 0) eq.(71) gives

$$I(0, \vartheta, x) = B\left[0, \frac{\alpha(x)\sec\vartheta}{\sqrt{1-\lambda}}\right]. \tag{72}$$

On this note, we will end our account of the theory of radiative diffusion in a semi-infinite medium. We merely wish to mention that this theory is easily generalized to a plane layer of finite optical thickness (Ref.32). In this case, radiative diffusion is described by the integral equation (25). The resolvent of this equation $\Gamma(\tau, \tau', \tau_0)$, as in the case of $\tau_0 = \infty$, is expressed in terms of the function $\Phi(\tau, \tau_0) = \Gamma(0, \tau, \tau_0)$. Posing $B_0(\tau) = e^{-\tau y}$ in eq.(25), we obtain the auxiliary equation for $B(\tau, y, \tau_0)$. The intensities of the radiation escaping from a plane layer are expressed by the functions $B(0, y, \tau_0)$ and $B(\tau_0, y, \tau_0)$. To determine the functions $B(0, y, \tau_0)$, $B(\tau_0, y, \tau_0)$, and $\Phi(\tau, \tau_0)$ we derive equations similar to those in the case of $\tau_0 = \infty$. However, in difference to this case the indicated equations cannot be solved explicitly but must be

solved numerically.

Recently, the theory of radiative diffusion in a spectral line was greatly advanced in investigations by V.V.Ivanov (Ref.35, 38). In the first of these studies, radiative diffusion in a semi-infinite medium was investigated. In this paper are determined (in particular, in the form of tables and graphs) the function $B(0, y)$ and the profiles of the emission lines. In the second study, V.V.Ivanov investigated radiative diffusion in a plane layer of finite optical thickness. The most important result of this work was the derivation of asymptotic formulas for the functions $B(0, y, \tau_0)$ and $B(\tau_0, y, \tau_0)$ [designated by $X(x, \tau_0)$ and $Y(z, \tau_0)$] at large values of τ_0. /125

At present, the Leningrad University is in the process of tabulating functions encountered in the theory of radiative diffusion. This is done on electronic computers. V.V.Ivanov and V.T.Shcherbakov (Ref.39) have compiled function tables used to express the kernel of the integral equation of radiative diffusion (and similar functions). Tables of the functions $B(0, y)$ and $\Phi(\tau)$ describing the radiative diffusion in a semi-infinite medium will be published in the near future. Here it is proposed to take into account the presence of absorption and emission in a continuous spectrum, which will make it possible to determine not only the profiles of the emission lines but also the profiles of the absorption lines. Functions $B(0, y, \tau_0)$, $B(\tau_0, y, \tau_0)$, and $\Phi(\tau, \tau_0)$ describing the radiative diffusion in a plane layer of finite optical thickness will also be tabulated.

It can be expected that these tables will be useful both for astrophysical and for physical applications of the theory of radiative diffusion. One of our immediate problems is to apply these tables to interpreting the solar spectrum in the region of the "rocket" ultraviolet which contains numerous resonance lines.

REFERENCES

1. Eddington, A.S.: Monthly Notices Roy. Astron. Soc., Vol.89, p.620, 1929.
2. Spitzer, L.: Monthly Notices, Vol.96, p.794, 1936.
3. Wooley, R. v.d. R.: Monthly Notices, Vol.98, p.624, 1938.
4. Henyey, L.G.: Proc. Nat. Acad. Sci. U.S., Vol.26, p.50, 1941.
5. Levich, V.G.: Zh. Eksperim. i Teor. Fiz., Vol.10, No.11, 1940.
6. Unno, W.: Publ. Astron. Soc. Japan, Vol.3, p.158, 1951; Vol.4, p.100, 1952.
7. Sobolov, V.V.: Vestnik Leningr. Univ., No.5, 1955.
8. Spitzer, L.: Astrophys. J., Vol.99, p.1, 1944.
9. Thomas, R.N.: Astrophys. J., Vol.125, p.260, 1957.
10. Jefferies, J.T. and White, O.R.: Astrophys. J., Vol.132, p.767, 1960.
11. Hummer, D.G.: Monthly Notices, Vol.125, p.21, 1962.
12. Houtgast, J.: The Variations in the Profiles of Strong Fraunhofer Lines. Utrecht, 1942.
13. Suemoto, Z.: Publ. Astron. Soc. Japan, Vol.1, p.78, 1949.
14. Labs, D.: Z. Astrophys., Vol.28, p.150, 1951; Vol.34, p.173, 1954.
15. Savedoff, M.P.: Astrophys. J., Vol.115, p.509, 1952.
16. Miyamoto, S.: Publ. Astron. Soc. Japan, Vol.6, No.9, 1954; Vol.7, No.1, 1955.

17. Sobolev, V.V.: Astron. Zhurn., Vol.26, p.129, 1949; Vol.31, p.231, 1954. /126
18. Busbridge, I.W.: Monthly Notices, Vol.113, p.52, 1953.
19. Ueno, S.: Contr. Inst. Astrophys. Kyoto, No.64, 1956.
20. Sobolev, V.V.: Astron. Zhurn., Vol.21, p.143, 1944; Vol.34, p.694, 1957.
21. Zanstra, H.: Bull. Astron. Inst. Neth., Vol.11, p.1, 1949.
22. Koelbloed, D.: Bull. Astron. Inst. Neth., Vol.12, p.341, 1956.
23. Osterbrock, D.E.: Astrophys. J., Vol.135, p.195, 1962.
24. Field, G.B.: Astrophys. J., Vol.129, p.551, 1959.
25. Biberman, L.M.: Zh. Eksperim. i Teor. Fiz., Vol.17, p.416, 1947; Vol.19, p.584, 1949.
26. Holstein, T.: Phys. Rev., Vol.72, p.1212, 1947; Vol.83, p.1159, 1951.
27. Biberman, L.M.: Dokl. Akad. Nauk SSSR, Vol.59, p.659, 1948.
28. Ambartsumyan, V.A.: Nauchnyye Trudy, Vol.1, Yerevan, 1960.
29. Chandrasekhar, S.: Transfer of Radiant Energy. Izd. Inostr. Lit., 1953.
30. Sobolev, V.V.: Transfer of Radiant Energy in Stellar and Planetary Atmospheres (Perenos luchistoy energii v atmosferakh zvezd i planet). Gostekhizdat, 1956.
31. Busbridge, I.W.: The Mathematics of Radiative Transfer. Cambridge, 1960.
32. Sobolev, V.V.: Izv. Akad. Nauk ArmSSR, Ser. Fiz.-Mat. Nauk, Vol.11, p.39, 1958; Astron. Zh., Vol.36, p.573, 1959.
33. Kreyn, M.G.: UMN, Vol.13, No.5 (83), 1958.
34. Case, K.M.: Ann. Phys. (USA), Vol.2, p.384, 1957.
35. Ivanov, V.V.: Astron. Zh., Vol.39, p.1020, 1962.
36. Minin, I.N.: Dokl. Akad. Nauk SSSR, Vol.120, No.1, 1958.
37. Nagirner, D.I.: Astron. Zh., Vol.41, p.669, 1964.
38. Ivanov, V.V.: Astron. Zh., Vol.40, p.257, 1963.
39. Ivanov, V.V. and Shcherbakov, V.T.: Astrofizika, Vol.1, p.22, 1965.

DETERMINATION OF THE POPULATIONS OF EXCITED LEVELS IN AN OPTICALLY THICK GAS LAYER

/127

V.V.Ivanov

The opinion is widespread among astrophysicists that the work done by theoreticians on radiative transfer is quite remote from physics. Actually, this is not the case. The methods used in the transfer theory, and especially its results, have a very simple physical meaning. Of course, as in any theory laying claim not only to a qualitative description but also to a quantitative calculation, a specific mathematical apparatus has been developed. However, its development is not the goal but only the means of solving physical problems which would simply be impossible without it.

In the present article we will discuss in some detail one of the simplest problems of radiative transfer in a spectral line, with main emphasis on the physical aspect of the problem. The concepts and terminology used are the conventional and well known to any astrophysicist. Simultaneously with elucidating the physics of the solution process of this problem we will define the possible advantages of using the means of the modern theory of multiple scattering of light. We must forewarn that much of what we will state is not usually contained in papers on transfer theory. This is simply presumed to be known. However, the difficulties for many astrophysicists in attempting to familiarize themselves with works in this area, in the author's opinion, are largely due to an inadequate understanding of exactly the simplest points which we will discuss here. On the other hand, to clarify the current potentialities of the theory we should mention that the problem to be discussed here has not yet been conclusively solved despite its apparent simplicity. Until now, this problem is still a subject of detailed investigations. Certain very recent results will also be briefly discussed in this article.

1.

/128

Let us examine the following problem: Let there be a plane homogeneous layer of gas whose kinetic temperature T is the same at all points: T = const. It is assumed that the atoms of the gas have only two discrete levels, ground and excited, with populations n_1 and n_2, and further that the majority of the atoms are in the ground state so that $n_2 \ll n_1$. Then the total concentration of atoms will be $n = n_1 + n_2 \approx n_1$ and, by virtue of the assumption of homogeneity of the gas, n_1 = const. In addition to the atoms let there also be free electrons whose concentration n_e is the same everywhere in the gas: n_e = const; the electron temperature is equal to the kinetic temperature of the gas T and thus is also independent of the coordinates.

Let us consider two processes leading to the population of the excited level, namely upward transitions due to electron bombardment and photoexcitation, and two processes of emptying of the upper level, namely spontaneous transitions and collisions of the second kind. The problem is to calculate the population

of the excited level n_2 as a function of the distance from the boundary of the layer. It is assumed that no extraneous radiation is incident on the gas.

Before beginning the solution, it is useful to outline the expected result. It is obvious that electron collisions are the primary cause for the appearance of excited atoms. Photoexcitation is a secondary process since the radiation causing these transitions itself arises upon spontaneous transitions from the excited level, and if there were no electron collisions all atoms would simply be at the ground level. However, the thicker the gas layer, the higher the efficiency of the secondary mechanism of population, namely, photoexcitation. This can become many times - often even by several orders - higher than the efficiency of the primary mechanism which is electron collision. This can be explained quite simply. The quantum "generated" in the line, i.e., emitted by an atom upon transition from the upper level following excitation by an electron collision, leaves the medium or "dies" as a consequence of a collision of the second kind, generally not immediately but only after a number of absorption and re-emission events. /129 As a result, one excitation by an electron collision accounts for several photoexcitations, the number being greater the larger the average number of scatterings experienced by the quantum before escaping from the medium or "perishing" in a quenching collision. It is understandable that, other conditions being equal, the number of scatterings should increase with an increase of the layer thickness since the escape of quanta through the boundaries becomes more difficult in this case. An increase in the average number of scatterings will lead to an intensification of the role of photoexcitation in the populating of upper levels.

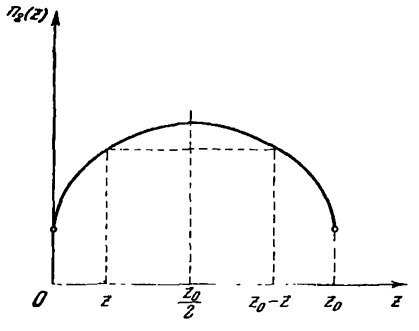

Fig.1

It is easy to understand that the concentration of excited atoms will depend on the depth in a manner similar to that shown schematically in Fig.1. Actually, by virtue of the symmetry of the problem, the conditions are completely identical at equal distances from the upper and lower boundaries. Therefore, the populations $n_2(z)$ and $n_2(z_0 - z)$ should be equal, i.e., the graph of $n_2(z)$ should be symmetric relative to $z = \frac{z_0}{2}$. Here z is the distance read off along the normal from the boundary and z_0 is the thickness of the entire layer. Furthermore, it is obvious that the concentration of excited atoms must be maximal in the middle of the layer $\left(\text{at } z = \frac{z_0}{2}\right)$ and decrease toward the boundaries. This is explained in the following manner: The processes emptying the upper level - spontaneous transitions and collisions of the second kind - everywhere act with the same efficiency since n_e = const and T_e = const. The efficiency /130 of excitation due to electron collisions is also everywhere identical. This is not so for the case of photoexcitation. The closer to the boundary, the greater will be the role of the radiation yield. This means the radiation density and

thus the efficiency of photoexcitation near the boundaries of the medium should be less. This decrease in the number of radiative excitations, which is in no way compensated, should cause a drop in the concentration of excited atoms toward the boundaries.

Let us now proceed to solution of the problem. As always in such cases where there is no thermodynamic equilibrium, to calculate the populations it is necessary to construct and solve steady-state equations. In our case the steady-state condition is written in the form

$$n_1 n_e b_{12} + n_1 B_{12} \rho_{12} = n_2 A_{21} + n_2 n_e a_{21}. \qquad (1)$$

Here A_{21}, B_{12} are Einstein coefficients, b_{12} and a_{21} are electronic and atomic coefficients of probability of electron collisions of the first and second kind, and ρ_{12} is the radiation density in a line corresponding to the transition $2 \rightarrow 1$. The first addend on the left-hand side gives the number of collision excitations and the second, the number of photoexcitations. Their sum should equal the total number of downward transitions which is composed of the number of spontaneous transitions ($n_2 A_{21}$) and the number of transitions due to collisions of the second kind ($n_2 n_e a_{21}$).

The steady-state equation would not be of much use if ρ_{12} were known. However, the radiation density in the line ρ_{12} is unknown. Since radiation in the line arises upon transitions from the upper level, the quantity ρ_{12} itself no longer depends on the concentration of excited atoms in a given volume element but at points of the medium, since the radiation contributing to ρ_{12} arises from everywhere. Therefore the steady-state equation (1) is not algebraic but constitutes an integral equation. This is the basic integral equation of the theory of multiple scattering of light. To give it the standard form in which it usually figures in works on the transfer theory, it is merely necessary to write the expression for the number of radiative excitations in an explicit form.

For simplicity, let us assume that the dependence of the absorption co- /131
efficient on the frequency is wholly determined by the Doppler effect caused by thermal agitation of the atoms. Then, the ratio of the absorption coefficient at a frequency x to the absorption coefficient at the line center, which we will designate by $\alpha(x)$, will be $\alpha(x) = e^{-x^2}$. Here, x is the distance from the line center in Doppler widths. This is a direct consequence of the fact that atoms in the ground state have a Maxwellian velocity distribution. We will assume that for the excited atoms the velocities also have a Maxwellian distribution. At first glance this may seem logical, but actually this is one of the essential assumptions that is not at all easy to prove. It is equivalent to the assumption of complete frequency redistribution upon scattering, i.e., the absence of any correlation between quantum frequencies before and after scattering. In fact, if line broadening is entirely determined by thermal agitation of the excited atoms with Maxwellian velocity distribution, then the line emitted by an element of volume should have a Doppler profile irrespective of the spectral distribution of the exciting radiation. This is precisely the assumption which constitutes the approximation of complete frequency redistribution.

In reality, the velocity distribution of excited atoms will differ from Maxwellian, for the following reason: Let us look at some volume element of a gas. For definitiveness, let it be taken somewhere near the boundary of the layer. As we will prove later, at a sufficiently great thickness of the layer, the radiation escaping from this layer has the spectral distribution schematically shown in Fig.2. We have an emission line with a deep dip in the center. It is clear that, when a given volume is irradiated by radiation of such a spectral distribution, the atoms with sufficiently large velocity components relative to the normal to the boundary will be excited more frequently than those that move parallel to the boundary. The reason lies in the strong dependence of the intensity of the exciting radiation on the frequency within the line. Therefore, the velocity distribution of excited atoms here proves to be dependent upon the spectral distribution of radiation incident on /132 the given volume, and may noticeably differ from Maxwellian. However, as already mentioned, we will neglect this circumstance and assume that the excited atoms have a Maxwellian velocity distribution. Later in the text, we will list papers in which an estimate of the error introduced by this approximation can be found. The overall conclusion permissible on the basis of the results obtained in the above papers amounts to the following: In calculating the line profile the approximation of complete frequency redistribution generally yields an accuracy quite sufficient for practical use.

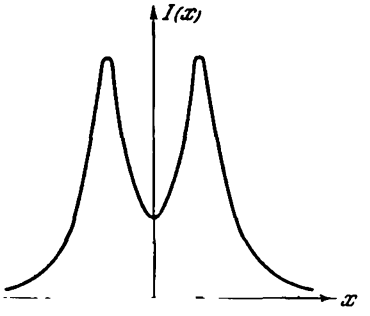

Fig.2

We can now obtain an explicit expression for the number of photoexcitations occurring per unit time in a 1-cm^2 volume of a thickness dz located at a depth z. Below, we will denote this volume by V. A similar volume of a thickness dz′ situated at a depth z′ will be designated by V′ (Fig.3). We will calculate the number of photoexcitations in V caused by radiation arriving from V′. In unit time, the volume V′ emits $A_{21}n_2(z')dz'$ quanta, of which $A_{21}n_2(x')dz' \times \times \frac{1}{\sqrt{\pi}} e^{-x^2} dx$ in the frequency range from x to x + dx (assumption of Maxwellian velocity distribution for the excited atoms!). We are interested in those quanta that reach the /133 volume V and are absorbed in it, thus causing photoexcitation. The distance between the volumes V and V′ is equal to $\frac{|z - z'|}{\cos \vartheta}$ where

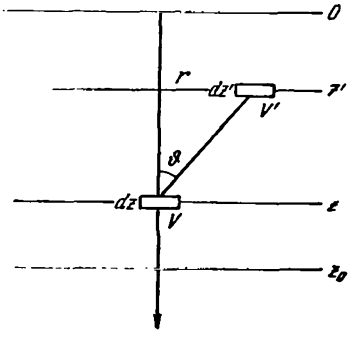

Fig.3

ϑ is an acute angle between the direction VV′ and the normal to the layer. The projection of the bases of the volume V onto VV′ is equal to cos ϑ. Therefore, the volume V is seen from V′ at a solid angle

$$\cos\vartheta:\ \frac{|z-z'|^2}{\cos^2\vartheta}=\frac{\cos^3\vartheta}{|z-z'|^2}.$$

In this solid angle, the volume V′ emits the following number of quanta with frequencies (x, x + dx):

$$A_{21}n_2(z')\,dz'\,\frac{1}{\sqrt{\pi}}e^{-x^2}\,dx\,\frac{\cos^3\vartheta}{4\pi|z-z'|^2}.$$

The next step is to determine how many of these quanta reach V. The absorption coefficient for radiation of a frequency x per unit volume is $k_0n_1e^{-x^2}$, where k_0 is the atomic absorption coefficient at the line center (assumption of Maxwellian velocity distribution for atoms in the ground state!). Therefore, the volume V, per unit time in the frequency range (x, x + dx), is struck by only

$$\frac{1}{4\pi}A_{21}n_2(z')dz'\,\frac{1}{\sqrt{\pi}}e^{-x^2}\exp\left\{-\frac{|z-z'|}{\cos\vartheta}\,k_0n_1e^{-x^2}\right\}dx\,\frac{\cos^3\vartheta}{|z-z'|^2}$$

quanta emitted by the volume V′. Since the thickness of the volume V measured along the direction VV′ is equal to $\frac{dz}{\cos\vartheta}$, a portion $\frac{k_0n_1dz}{\cos\vartheta}e^{-x^2}$ of all incident quanta will be absorbed. Thus, of the quanta emitted by the volume V′ at frequencies from x to x + dx, an amount

$$\frac{1}{4\pi}A_{21}n_2(z')dz'\,\frac{1}{\sqrt{\pi}}e^{-2x^2}dx\times$$
$$\times\exp\left\{-\frac{|z-z'|}{\cos\vartheta}\,k_0n_1e^{-x^2}\right\}\frac{\cos^2\vartheta}{|z-z'|^2}\,k_0n_1\,dz$$

is absorbed in the volume V. All told, the number of photoexcitations occurring in the volume V under the effect of the emission of V′, in unit time, will be /134

$$\frac{1}{4\pi}A_{21}n_2(z')\,dz'\,\frac{1}{\sqrt{\pi}}\int_{-\infty}^{\infty}e^{-2x^2}\exp\left\{-\frac{|z-z'|}{\cos\vartheta}\,k_0n_1e^{-x^2}\right\}dx\times$$
$$\times\frac{\cos^2\vartheta}{|z-z'|^2}\,k_0n_1\,dz.$$

To obtain the total number of photoexcitations in V it must be recalled that the emission of not just the volume V′ but of the entire layer contributes to the atomic excitation in V. Let us first integrate over the plane z′; we obtain

$$\frac{1}{4\pi}A_{21}n_2(z')\,dz'\cdot\frac{k_0n_1\,dz}{|z-z'|^2}\,\frac{1}{\sqrt{\pi}}\times$$
$$\times\int_0^{2\pi}d\varphi\int_0^{\infty}\int_{-\infty}^{\infty}e^{-2x^2}\exp\left\{-\frac{|z-z'|}{\cos\vartheta}\,k_0n_1e^{-x^2}\right\}dx\cdot\cos^2\vartheta\cdot r\,dr.$$

Considering that $r = |z - z'| \tan \vartheta$ (see Fig.3) and introducing the designation $\mu = \cos \vartheta$, we find in place of the last expression

$$\frac{1}{2} A_{21} n_2(z')\, dz' \cdot k_0 n_1\, dz \cdot \frac{1}{\sqrt{\pi}} \times$$

$$\times \int_0^1 \frac{d\mu}{\mu} \int_{-\infty}^{\infty} e^{-2x^2} \exp\left\{ - \frac{|z - z'|}{\mu} k_0 n_1 e^{-x^2} \right\} dx$$

or

$$A_{21} n_2(z')dz' \cdot \frac{1}{2} K(|z - z'| k_0 n_1) k_0 n_1 dz,$$

where we denote

$$K(l) = \frac{1}{\sqrt{\pi}} \int_{-\infty}^{\infty} e^{-2x^2} E_1(le^{-x^2})\, dx, \tag{2}$$

while $E_1(y)$ is the usual integral exponential function:

$$E_1(y) = \int_0^1 e^{-\frac{y}{\zeta}} \frac{d\zeta}{\zeta}.$$

To find the total number of photoexcitations per unit volume at a depth z, it remains to integrate the derived expression with respect to all depths z' /135 from 0 to z_0 and divide the result by the magnitude of the volume V equal to dz. In this manner, we find that

$$n_1 B_{12} \rho_{12} = \frac{1}{2} \int_0^{z_0} K(|z - z'| k_0 n_1) A_{21} n_2(z') k_0 n_1 dz'.$$

Substituting in this integral $k_0 n_1 z' = \tau'$ and designating $k_0 n_1 z = \tau$, $k_0 n_1 z_0 = \tau_0$, we finally have

$$n_1 B_{12} \rho_{12} = \frac{A_{21}}{2} \int_0^{\tau_0} K(|\tau - \tau'|)\, n_2(\tau')\, d\tau'. \tag{3}$$

The dimensionless variable τ has the following physical meaning: It is the distance measured in mean free paths of a quantum having the frequency of the line center. This quantity is known as the optical depth at the line center. The quantity τ_0 is the optical thickness of the entire layer. Equation (3) also yields the expression for the number of radiative excitations, whose derivation was our immediate goal.

With consideration of eq.(3), the steady-state equation (1) takes the form

$$A_{21} n_2(\tau) + a_{21} n_e n_2(\tau) = b_{12} n_e n_1 + A_{21} \cdot \frac{1}{2} \int_0^{\tau_0} K(|\tau - \tau'|)\, n_2(\tau')\, d\tau'. \tag{4}$$

To reduce it to a standard form, we divide both sides of the equation by $n_1(A_{21} + n_e a_{21})$. This yields

$$\frac{n_2(\tau)}{n_1} = \frac{n_e b_{12}}{A_{21} + n_e a_{21}} + \frac{A_{21}}{A_{21} + n_e a_{21}} \cdot \frac{1}{2} \int_0^{\tau_0} K(|\tau - \tau'|) \frac{n_2(\tau')}{n_1} d\tau'. \tag{5}$$

We designate

$$\lambda = \frac{A_{21}}{A_{21} + n_e a_{21}}. \tag{6}$$

This quantity has a simple physical meaning. The numerator contains the number of downward radiative transitions calculated per atom while the denominator contains the total number of transitions per unit time. Thus, the quantity λ constitutes the probability that a quantum absorbed by an atom will be re- /136 emitted by it. In the transfer theory, the quantity having this physical meaning is usually called albedo for single scattering, or the probability of survival of the quantum in scattering.

Having used the well-known relation between the probabilities of collisions of the first and second kinds,

$$b_{12} = \frac{g_2}{g_1} e^{-\frac{h\nu_{12}}{kT}} a_{21},$$

where g_1 and g_2 are the statistical weights of the levels, the first addend on the right-hand side of eq.(5) will become

$$\frac{n_e b_{12}}{A_{21} + n_e a_{21}} = \frac{g_2}{g_1} e^{-\frac{h\nu_{12}}{kT}} \frac{n_e a_{21}}{A_{21} + n_e a_{21}} = \frac{g_2}{g_1} e^{-\frac{h\nu_{12}}{kT}} (1 - \lambda). \tag{7}$$

Substituting eqs.(6) and (7) into eq.(5), we obtain

$$\frac{n_2(\tau)}{n_1} = \frac{g_2}{g_1} e^{-\frac{h\nu_{12}}{kT}} (1 - \lambda) + \frac{\lambda}{2} \int_0^{\tau_0} K(|\tau - \tau'|) \frac{n_2(\tau')}{n_1} d\tau' \tag{8}$$

or

$$\frac{g_1}{g_2} e^{\frac{h\nu_{12}}{kT}} \frac{n_2(\tau)}{n_1} = \frac{\lambda}{2} \int_0^{\tau_0} K(|\tau - \tau'|) \frac{g_1}{g_2} e^{\frac{h\nu_{12}}{kT}} \frac{n_2(\tau')}{n_1} d\tau' + 1 - \lambda. \tag{9}$$

Let us introduce the designation

$$S(\tau) = \frac{g_1}{g_2} e^{\frac{h\nu_{12}}{kT}} \frac{n_2(\tau)}{n_1}. \tag{10}$$

Then the steady-state equation (9) will have the final form

$$S(\tau) = \frac{\lambda}{2} \int_0^{\tau_0} K(|\tau - \tau'|) S(\tau') d\tau' + 1 - \lambda. \tag{11}$$

Thus, calculation of the degree of excitation in a plane-homogeneous and isothermal layer of gas reduces to solving eq.(11) for the function $S(\tau)$.

In the transfer theory, the quantity $S(\tau)$ is called the source function. Its physical meaning follows from eq.(10) which shows that the source function (with an accuracy to within a constant factor) simply represents the degree /137 of excitation. In the problem under consideration, n_1 is assumed to be independent of the coordinates. However, as soon as n_1 changes with the depth, the physical meaning of the source function remains the same. Its normalization, i.e., the value of the constant factor in eq.(10), is usually different, but this does not change the essence of the matter. With our selected normalization, the quantity $S(\tau)$, as follows from eq.(10), represents the ratio of the degree of excitation $\frac{n_2(\tau)}{n_1}$ at the given depth τ to the equilibrium degree obtained by the Boltzmann formula. Thus, the solution of the fundamental integral equation (11) gives the degree of excitation expressed in fractions of the Boltzmannian.

In eq.(11) the integral addend takes into account photoexcitations by the radiation of the gas itself, while the free term allows for excitations by the primary mechanism which, in this case, is electron collisions. In more complex cases, the power of the primary radiation sources may depend on the depth. Then the procedure reduces to solving the equation

$$S(\tau) = \frac{\lambda}{2}\int_0^{\tau_0} K(|\tau - \tau'|)\, S(\tau')\, d\tau' + S_0(\tau), \tag{12}$$

where the function $S_0(\tau)$ characterizes the power of the internal sources. It is considered to be known.

Equation (11) contains two parameters, τ_0 and λ. The first can take on any values from 0 to ∞, while the second is always included between 0 and 1. However, in astrophysical problems, one has to do mostly with the case where τ_0 is large and λ is close to unity. For example, in the case of scattering of L_α-quanta in the upper layers of the chromosphere the value of λ differs from unity by a value of the order of 10^{-5}. For emission of coronal ions in resonance lines, the values of $1 - \lambda$ are several orders of magnitudes smaller owing to the low electron concentration in the corona. The optical thickness of the layer τ_0 often reaches values of the order of 10^4 and more. Thus, most important for /138 application is the case where

$$\tau_0 \gg 1, \quad (1-\lambda)^{-1} \gg 1. \tag{13}$$

However, it must be stated that it is also the most difficult for investigation. The use of numerical methods for solving eq.(11) at such values of the parameters requires particular care and is inevitably associated with appreciable computational work which is virtually impossible to perform without the use of electronic computers. Anticipating somewhat, let us mention that noticeable progress has been made recently in investigating eq.(12) as to satisfaction of the inequalities (13); this permits an appreciable reduction in the volume of calculations and in some cases makes them unnecessary. However, before giving an account of these latest achievements, we would like to discuss some papers containing additional information on problems touched upon above.

Equation (11) was derived and numerically solved by L.M.Biberman (Ref.1, 2). The physical aspect of the above phenomena and certain problems analyzed at the start of the next Section are quite thoroughly discussed in the second of these articles which we will partially follow in our paper. We should also mention the recent article by A.Hearn (Ref.3) which contains more extensive numerical data. The most complete set of numerical data available at present is given in a paper by Avrett and Hummer (Ref.4) which we will cite frequently. That paper also contains a detailed discussion of numerical methods for solving eq.(12) and gives an extensive bibliography. The recent publications by A.Hearn and D.Hummer (Ref.5, 6) take up the problem of the accuracy obtained from an approximation of complete frequency redistribution [see also elsewhere (Ref.7, 4)]. Recently, this problem was investigated in detail by D.Hummer. The results of these investigations will be published in the Monthly Notices of the Royal Astronomical Society.

Radiative transfer in a spectral line with consideration of a frequency change in scattering is also thoroughly discussed in the monograph by V.V. Sobolev (Ref.8), containing results obtained up to 1956. The problem of scattering with frequency redistribution is solved in this book by methods of /139 the modern theory of multiple scattering of light. The article by V.V.Sobolev in this collection can serve as an introduction to these methods. We also could cite the works of R.Thomas (Ref.9, 10) and others (Ref.11, 3) on estimates of the characteristic values of the parameters t_0 and λ encountered in various astrophysical problems.

2.

Let us now discuss the character of the solution of the fundamental integral equation (11) and the simplifications that arise in various limiting cases. Since the values of the parameters τ_0 and λ will play an essential role in this discussion, we will quote them as additional arguments of the source function S which thus will now be denoted by $S(\tau, \tau_0, \lambda)$.

Let us begin with the simplest case where $\tau_0 = \infty$, i.e., where the medium can be considered semi-infinite. The criterion for judging whether this assumption can serve as a sufficiently good approximation will be given below. The source function for this semi-infinite medium will be designated by $S(\tau, \lambda)$. It satisfies the equation

$$S(\tau, \lambda) = \frac{\lambda}{2}\int_0^\infty K(|\tau - \tau'|)\, S(\tau', \lambda)\, d\tau' + 1 - \lambda, \qquad (14)$$

which we will discuss first. To make the discussion more graphic, Fig.4, borrowed from A.Hearn's study (Ref.3), shows the graph of $S(\tau, \lambda)$ for $\lambda = 0.99$ obtained by numerical solution of eq.(14). The diagram shows that, with an increase in depth, the source function approaches unity. This means that, at a sufficiently great depth, the population of the excited level differs little from the Boltzmann population. This result could be anticipated. Since the layer is isothermal, the only cause responsible for the deviation of the population of the excited level from equilibrium is the yield of quanta to the boundary. The farther we go from the boundary the smaller will be the role /140

of this process, and the degree of excitation should approach the Boltzmannian.

On the other hand, near the boundary the deviations rapidly increase and then become quite large. It turns out that at the boundary itself we have

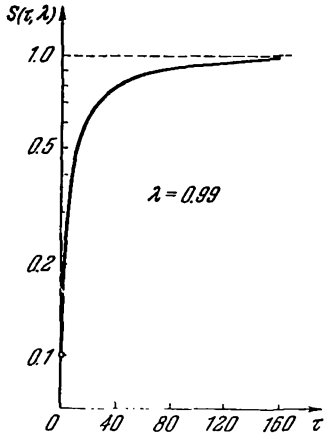

Fig.4

$$S(0, \lambda) = \sqrt{1 - \lambda} \tag{15}$$

[see below, eq.(25)]. Recalling the definition of λ, we obtain

$$S(0, \lambda) = \sqrt{\frac{n_e a_{21}}{A_{21} + n_e a_{21}}}. \tag{16}$$

At sufficiently low electron concentrations, $A_{21} \gg n_e a_{21}$. To this case, values of λ close to unity correspond. Here, secondary processes of photoexcitation serve as the main mechanism of populating the excited level. It follows from eq.(16) that, under this condition,

$$S(0, \lambda) = \sqrt{n_e}\left(\frac{a_{21}}{A_{21}}\right)^{1/2},$$

or, on the basis of eq.(10)

$$n_2(0) = \sqrt{n_e} n_1 \frac{g_2}{g_1} e^{-\frac{h\nu_{12}}{kT}} \left(\frac{a_{21}}{A_{21}}\right)^{1/2}. \tag{17}$$

Thus, we arrived at a conclusion which, at first glance, may seem somewhat unexpected: At low electron concentrations at the boundary of an isothermal semi-infinite layer of gas, the population of the excited level is proportional to the root of the electron concentration.

From eq.(15) it follows that, for $1 - \lambda \ll 1$, the population of the excited level near the boundary is substantially below the Boltzmann population. The difference may reach several orders of magnitude. This raises the logical /141 question as to the depth at which the assumption of a Boltzmann distribution can start serving as an intelligent approximation. The answer can be obtained from the following equations.

Let us examine an excited atom at a depth τ. The probability that a non-radiative downward transition will be accomplished is equal to $1 - \lambda$, with the probability λ of emission of a quantum. Some of the emitted quanta will escape from the medium without subsequent scattering. These can be defined as follows: The probability of emission of a quantum with a frequency x, x + dx in a solid angle $d\omega$ is

$$\frac{\lambda}{\sqrt{\pi}} e^{-x^2} dx \frac{d\omega}{4\pi}.$$

F-457

If the quantum is emitted in a direction making an angle ϑ with the outward normal $\left(0 \leq \vartheta < \frac{\pi}{2}\right)$ and then traverses the path $\frac{\tau}{\cos \vartheta}$ without scattering, it will escape from the medium. The probability that a quantum of frequency x undergoes no scattering at all along such a path is equal to

$$\exp\left\{-\frac{\tau}{\cos\vartheta}e^{-x^2}\right\}.$$

Thus, the probability that an excited atom at a depth τ emits, in the solid angle $d\omega$, a quantum with a frequency from x to x + dx which will escape from the medium without scattering at an angle ϑ to the normal is as follows:

$$\lambda \frac{1}{\sqrt{\pi}} e^{-x^2} \exp\left\{-\frac{\tau}{\cos\vartheta}\, e^{-x^2}\right\} dx \frac{d\omega}{4\pi}.$$

After integrating this expression with respect to a hemisphere and to all frequencies, we find the total probability of the escape of a quantum from the depth τ without scattering:

$$\lambda \frac{1}{\sqrt{\pi}} \int_{-\infty}^{\infty} e^{-x^2} dx \int_{2\pi} \exp\left\{-\frac{\tau}{\cos\vartheta}\, e^{-x^2}\right\} \frac{d\omega}{4\pi},$$

or

$$\frac{\lambda}{2} \frac{1}{\sqrt{\pi}} \int_{-\infty}^{\infty} e^{-x^2} dx \int_{0}^{\pi/2} \exp\left\{-\frac{\tau}{\cos\vartheta}\, e^{-x^2}\right\} \sin\vartheta\, d\vartheta.$$

Posing $\cos\vartheta = \zeta$, we obtain in place of the last expression /142

$$\frac{\lambda}{2} \frac{1}{\sqrt{\pi}} \int_{-\infty}^{\infty} e^{-x^2} E_2(\tau e^{-x^2})\, dx, \tag{18}$$

where $E_2(t)$ is an integral exponential function of the second order:

$$E_2(t) = \int_0^1 e^{-\frac{t}{\zeta}} d\zeta.$$

A comparison of eqs.(18) and (2) shows that our probability is equal to $\frac{\lambda}{2} L(\tau)$, where

$$L(\tau) \equiv \int_{\tau}^{\infty} K(\tau')\, d\tau' = \frac{1}{\sqrt{\pi}} \int_{-\infty}^{\infty} e^{-x^2} E_2(\tau e^{-x^2})\, dx. \tag{19}$$

As mentioned before, the escape of radiation through the boundary is responsible for the deviation of the population from the Boltzmannian type. Therefore, the magnitude of the deviation from equilibrium will be determined by the value of the parameter

$$u = \frac{\frac{\lambda}{2} L(\tau)}{1-\lambda}. \tag{20}$$

This represents the ratio of the probability of quantum emission immediately escaping from the medium to the probability of radiationless transition. When u is small, the escape of radiation plays a minor role and it can be roughly considered that the population of the excited level is of the Boltzmann type. However, at u = 1, the population is only by one-half smaller than equilibrium whereas, at $u = \frac{1}{3}$, the deviation amounts to only about 25%. On the other hand, when the value of u is large, the deviations may become appreciable. Later in the text, we will give the method by which these estimates were obtained.

We can already draw one important conclusion from the above statements. Let us denote by Λ the value of the optical depth τ to which there corresponds u = 1, i.e.,

$$\frac{1}{2} L(\Lambda) = 1 - \lambda, \tag{21}$$

where the factor λ on the left-hand side was replaced by unity, which is immaterial here since we are now dealing with ordinal estimates while λ is assumed as close to unity. The quantity Λ can be called the thermalization length. This length represents some optical distance characteristic for a medium with a given λ, namely a distance which a quantum is able to traverse before it "perishes" in scattering as a consequence of a collision of the second kind, having first transmitted its energy to the electronic gas [for more details, see elsewhere (Ref.4)]. /143

At large τ, the following asymptotic expression holds for $L(\tau)$:

$$L(\tau) = \frac{1}{2\sqrt{\pi\tau}\sqrt{\ln\tau}}. \tag{22}$$

With allowance for this expression, the determination of the thermalization length for the Doppler absorption coefficient and $1 - \lambda \ll 1$ takes the form

$$4\sqrt{\pi}(1-\lambda)\Lambda\sqrt{\ln\Lambda} = 1, \tag{23}$$

or, using the explicit expression for λ,

$$n_e \frac{a_{21}}{A_{21}} 4\sqrt{\pi}\Lambda\sqrt{\ln\Lambda} = 1.$$

We will encounter again the concept of thermalization length later in the text. The expediency of introducing this quantity is rather obvious, also in the problem which we will now analyze. We can say that a distance of the order of 2 - 3 thermalization lengths gives the thickness of that layer in the gas where deviations of the population from equilibrium are large. At greater

depths these deviations become small.

It is of interest to define the spectral distribution of the radiation emitted by a semi-infinite isothermal layer of gas. For the radiant intensity $I(0, \mu, x, \lambda)$ escaping from the medium with a given λ (i.e., with a given electron concentration), we have the following well-known expression:

$$I(0, \mu, x, \lambda) = \int_0^\infty e^{-\frac{\tau e^{-x^2}}{\mu}} S(\tau, \lambda) e^{-x^2} \frac{d\tau}{\mu}, \qquad (24)$$

where $\mu = \cos \vartheta$. Since, with our adopted normalization of the source function, this does not yield the absolute value of the population but only the ratio /144 of the population to the Boltzmann population, the radiant intensity $I(0, \mu, x, \lambda)$ is expressed in fractions of the equilibrium intensity, i.e., of the Planckian intensity. This latter must be taken in Wien's approximation since processes of induced emission are disregarded here and also can be disregarded since, from the very beginning, we had assumed that $n_2 \ll n_1$.

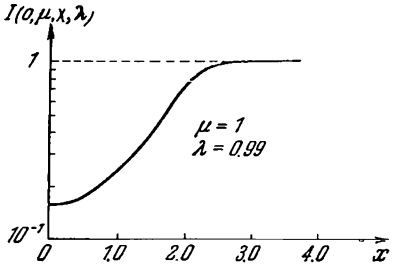

Fig.5

After all of our above statements there is no need to give a detailed explanation of the physical meaning of eq.(24). This formula expresses the fact that the escaping radiation is composed of quanta arriving from all depths and that, at the site of its emergence, the radiation is distributed by frequencies in proportion to e^{-x^2} and then weakens along the path toward the boundary $\left(\text{factor } \exp\left\{-\frac{\tau}{\mu} e^{-x^2}\right\}\right)$.

The intensity of radiation escaping along the normal ($\mu = 1$) from a medium with $\lambda = 0.99$ is plotted in Fig.5 as a function of the frequency. This diagram, just as the preceding one, has been taken from Hearn's paper (Ref.3). To obtain the intensity of the escaping radiation, Hearn carried out numerical integration by means of eq.(24). It is obvious from the plot that the isothermal semi-infinite layer of gas emits Planckian radiation, against whose background the absorption line can be distinguished. It is not difficult to understand the reason for the appearance of the line. If everywhere in the medium the population of the excited level were to be of the Boltzmann type, the source function $S(\tau, \lambda)$ would be identically equal to unity, in which case it would follow /145 from eq.(24) that $I(0, \mu, x, \lambda) \equiv 1$, i.e., the medium would emit Planckian radiation. However, there actually occurred a drop in the degree of excitation toward the boundary (see Fig.4). This is the real cause for the appearance of the absorption line.

So far our discussion has been mainly of a qualitative nature, and to illustrate the general assertions we used data obtained by numerical solution of the fundamental integral equation. Now, we will present results obtained with the use of analytical methods. In the case of a semi-infinite layer, these

permit solving the problem to the end.

The exact solution of eq.(14) has the form

$$S(\tau, \lambda) = \sqrt{1-\lambda}\left(1 + \int_0^{\tau} \Phi(\tau', \lambda)\, d\tau'\right), \tag{25}$$

where

$$\Phi(\tau, \lambda) = \frac{\lambda}{2}\int_0^{\infty} e^{-\frac{\tau}{z}} R(z, \lambda)\frac{G(z)dz}{zH(z,\lambda)}, \tag{26}$$

whence

$$R(z, \lambda) = \frac{1}{\left[1 - \lambda z^2 \int_0^{\infty} \frac{G(z')\,dz'}{z^2 - z'^2}\right]^2 + \frac{\lambda^2\pi^2}{4} z^2 G^2(z)}, \tag{27}$$

$$H(z, \lambda) = \exp\left\{-\frac{z}{\pi}\int_0^{\infty} \ln\left(1 - \lambda v^2 \int_0^{\infty} \frac{G(x)}{x^2 + v^2}\, dx\right)\frac{dv}{v^2 + z^2}\right\}. \tag{28}$$

Here,

$$G(z) = \frac{1}{\sqrt{2}}\left(1 - \frac{2}{\sqrt{\pi}}\int_0^{\sqrt{2\ln z}} e^{-t^2} dt\right) \tag{29}$$

for $z \geq 1$, and $G(z) = \frac{1}{\sqrt{2}}$ for $z < 1$.

The intensity of the outgoing radiation is expressed by $H(z, \lambda)$ in the following manner:

$$I(0, \mu, x, \lambda) = \sqrt{1-\lambda}\, H(\mu e^{x}, \lambda). \tag{30}$$

We note that the function $H(z, \lambda)$ given by eq.(28) is the solution of the integral equation /146

$$H(z, \lambda) = 1 + \frac{\lambda}{2} zH(z, \lambda)\int_0^{\infty} \frac{H(z', \lambda)}{z + z'} G(z')\, dz'. \tag{31}$$

The formulas give, in principle, the complete solution of the problem. However, their practical use is a rather difficult matter requiring numerous and laborious calculations. It is simpler to solve the initial equation (14) numerically than to use these formulas. Nevertheless, they are not only of a purely theoretical but also of a practical value. By means of these and similar formulas it has recently become possible to investigate simplifications that occur in the solution in various limiting cases. These simplifications are highly essential. In some cases they yield the answer immediately almost without any calculation, in others they greatly facilitate the use of numerical methods. We will give just one example.

As already mentioned, under conditions as they occur in astrophysics, collisions usually play a minor role owing to low density involved so that an absorption of a quantum is almost always followed by its re-emission. This is formally expressed by the inequality $1 - \lambda \ll 1$. In this limiting case, the

formulas are greatly simplified. It turns out that the source function $S(\tau, \lambda)$ depends, with a high degree of accuracy, not on the very quantities τ and λ but only on one argument, namely, on the quantity u determined by eq.(20). Therefore, we can write

$$S(\tau, \lambda) = 1 - F\left(\frac{\frac{\lambda}{2} L(\tau)}{1-\lambda}\right). \tag{32}$$

This relation shows that the following similitude principle is valid: The degree of excitation at a depth $\tau = \tau_1$ in a medium with $\lambda = \lambda_1$ is equal to the degree of excitation in a medium with $\lambda = \lambda_2$ at a depth $\tau = \tau_2$, where τ_1 and τ_2 are connected by the relation

$$\frac{L(\tau_1)}{1-\lambda_1} = \frac{L(\tau_2)}{1-\lambda_2}, \tag{33}$$

or, which comes to the same, /147

$$\frac{L(\tau_1)}{n_e^{(1)}} = \frac{L(\tau_2)}{n_e^{(2)}},$$

where $n_e^{(1)}$ and $n_e^{(2)}$ are the electron concentrations in the first and second media (their temperatures are considered to be identical). Strictly speaking, eq.(32) holds only for deep layers, but it does give good results even at $\tau < 1$ (the maximum error amounting to a few tens of percents).

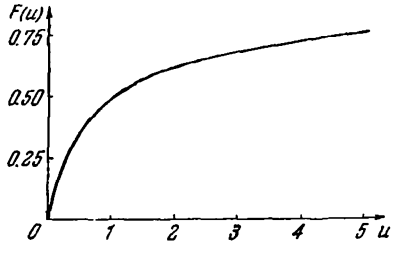

Fig.6

Because of the similitude principle, there is no need to solve eq.(14) each time. It can be solved just for one sufficiently small value of λ and the results can then be used for determining the function F(u). As soon as F(u) is found, eq.(13) becomes the solution for all λ close to unity. It is not particularly difficult to change from the variable u to τ since $L(\tau)$ has been tabulated (Ref.12); at large values of τ, the asymptotic expression (22) can be used.

The curve F(u) is given in Fig.6. The values of F(u) were obtained by the above-described method; here, the results of the numerical solution of eq.(14) for $\lambda = 1 - 10^{-10}$ (Ref.4) were used. As regards the values of F(u) at $u > 5$, the following expansion, valid for $u \gg 1$, provides an accuracy sufficient for practical application:

$$F(u) = 1 - \frac{2}{\pi\sqrt{u}} + \ldots. \tag{34}$$

This formula was found theoretically and confirmed by Avrett and Hummer's /148 numerical data obtained by direct solution of eq.(14).

The deviations from equilibrium are large at optical depths where $u \gg 1$.

It follows from eqs.(32) and (34) that, in this region,

$$S(\tau, \lambda) = \frac{2\sqrt{2}}{\pi}\sqrt{\frac{1-\lambda}{L(\tau)}}. \tag{35}$$

This formula holds for large values of τ. Thus, for $L(\tau)$ the asymptotic expression (22) can be used. Then, the last formula takes the form

$$S(\tau, \lambda) = \frac{4}{\pi^{3/2}}\sqrt{(1-\lambda)\tau\sqrt{\ln\tau}}, \tag{36}$$

or, with consideration of eqs.(10) and (6),

$$n_2(\tau) = \sqrt{n_e \cdot n_1}\frac{4}{\pi^{3/2}}\sqrt{\tau\sqrt{\ln\tau}}\frac{g_2}{g_1}e^{-\frac{h\nu_{12}}{kT}}\left(\frac{a_{21}}{A_{21}}\right)^{1/2}. \tag{37}$$

This simple expression, which is convenient for quick population estimates, yields excellent accuracy at small τ. A comparison with results obtained by direct numerical methods (Ref.4) shows that, for $\tau = 10$, the error is less than 5% and gradually decreases with an increase in τ; at $\tau = 10^3$, it amounts to fractions of a percent.

Although eq.(35), strictly speaking, holds only for large τ it also gives good results - as already mentioned - at small τ. Of course, in this case the values of $L(\tau)$ cannot be found from the asymptotic formula (22) but must be taken from tables (Ref.12). The order of the error produced by eq.(35) at small τ can be judged from the fact that, for $\tau = 0$, it follows that $S(0, \lambda) = 2/\sqrt{2}\pi^{-1}\sqrt{1-\lambda} = 0.900\sqrt{1-\lambda}$, whereas the exact value is equal to $\sqrt{1-\lambda}$. Thus, for $\tau = 0$, the error amounts to 10%. A comparison with the results of a numerical solution of eq.(14) (Ref.4) shows that for all τ the error does not exceed 30%.

We previously concluded that, at low electron concentrations, when $A_{21} \gg n_e a_{21}$, the population at the boundary of a semi-infinite layer is proportional to the root of the electron concentration. Now we see that this conclusion is valid for the entire region where the deviations of population from equilibrium are large (i.e., when the quantity u is noticeably larger than unity). /149

Let us turn to the region where deviations from equilibrium are small, as takes place for small u. Here, we can assume approximately that

$$F(u) = u. \tag{38}$$

This expression represents the first term of the series expansion of F(u) in the neighborhood of u = 0. Recalling the definition of the source function [eq.(10)] and of the parameter u [eq.(20)], we find from eq.(32) that, in this region,

$$n_2(\tau) = n_1 \frac{g_2}{g_1} e^{-\frac{h\nu_{12}}{kT}} \left(1 - \frac{A_{21}}{n_e a_{21}} \frac{1}{4\sqrt{\pi}\tau\sqrt{\ln\tau}}\right). \quad (39)$$

At depths where u is close to unity, for an estimate of the population we must use the formula

$$n_2(\tau) = n_1 \frac{g_2}{g_1} e^{-\frac{h\nu_{12}}{kT}} \left[1 - F\left(\frac{A_{21}}{n_e a_{21} 4\sqrt{\pi}\tau\sqrt{\ln\tau}}\right)\right], \quad (40)$$

recording the values of the function F from the graph (Fig.6). In precisely this manner we obtain the aforementioned (p.102) estimates of the deviations of population from equilibrium, when u = 1 and u = $\frac{1}{3}$.

We believe that these findings constitute a convincing argument for the vast possibilities afforded by the use of modern methods of the theory of multiple scattering of light. Without the help of analytical methods, it would hardly be possible to define all of the simplifications in the solution at $1 - \lambda \ll 1$, which we just discussed. This is substantiated by the following: Avrett and Hummer, having at their disposal quite extensive results of a numerical solution of the fundamental integral equation, subjected these to an "empirical" analysis. The only fact revealed was that at depths small in comparison with the thermalization length, i.e., where $u \gg 1$, the ratio $S(\tau, \lambda)/\sqrt{1-\lambda}$ does not depend on λ. This constitutes a particular corollary of eq.(35).

Methods by means of which the foregoing exact solution of the problem /150 was obtained, were developed by V.V.Sobolev (Ref.8, 13, 14). The application of these methods to solving the problem discussed in this Section is given in articles by the author (Ref.15, 16) and by D.I.Nagirner (Ref.17). A detailed investigation of the case $1 - \lambda \ll 1$ can be found in another paper (Ref.18), although a number of results given there were derived earlier, in particular in 1962 (Ref.15).

3.

If the optical thickness of the isothermal layer is finite, calculation of the population of the excited level reduces to determining the source function $S(\tau, \tau_0, \lambda)$ from the equation

$$S(\tau, \tau_0, \lambda) = \frac{\lambda}{2} \int_0^{\tau_0} K(|\tau - \tau'|) S(\tau', \tau_0, \lambda) d\tau' + 1 - \lambda. \quad (41)$$

As soon as the source function is found, the intensity of the escaping radiation expressed in fractions of Planckian radiation can be calculated by the formula

$$I(0, \mu, x, \tau_0, \lambda) = \int_0^{\tau_0} e^{-\frac{\tau e^{-x^2}}{\mu}} S(\tau, \tau_0, \lambda) e^{-x^2} \frac{d\tau}{\mu}. \quad (42)$$

So far, in solving eq.(41) and finding the line profiles from eq.(42),

numerical methods have been used almost exclusively. However, even here analytical methods can be of great help. It is true that many problems still remain unsolved in the investigation of eq.(41) for finite τ_0, but the few that are known permit the derivation of simple formulas in a number of cases.

Let us now discuss certain problems pertaining to the solution of eq.(41) and to calculation of the line profiles at large values of τ_0 and at values of λ close to unity, i.e., when the inequalities (13) are satisfied. This limiting case involves two important particular subcases. No doubt, it is understandable from our above statements that the character of the solution of eq.(41) must largely depend on the value of the parameter /151

$$u_0 = \frac{\frac{\lambda}{2} L(\tau_0)}{1-\lambda}. \tag{43}$$

The above-mentioned cases correspond to satisfaction of the inequalities $u_0 \ll 1$ and $u_0 \gg 1$.

If u_0 is small, the central portions of the layer will contain a region where the role of escape of radiation through the boundary is small in comparison with the role of collisions of the second kind. In this region, the population of the excited level is close to Boltzmannian, and the decline in concentration of the excited atoms toward the boundaries occurs approximately as if the medium were semi-infinite. Therefore, the condition $u_0 \ll 1$ serves as a criterion permitting to assume the medium as semi-infinite. In other words, the layer can be considered semi-infinite if its thickness is large with respect to the thermalization length.

In the opposite limiting case, when $u_0 \gg 1$, the situation is completely different. Here the role of true absorption, i.e., collisions of the second kind, is so minor that they can be disregarded. In this case, the concentration of excited atoms is entirely determined by the escape of radiation through the boundaries, with the concentration being much less than Boltzmannian at all depths. In the theory of transfer processes, this case is usually called the case of pure scattering. Here we can set $\lambda = 1$ in eq.(12). The source function determined by eq.(41) becomes simply proportional to $1 - \lambda$, and the factor λ in the integral term can be replaced by unity. Thus, in pure scattering the solution of the fundamental integral equation essentially depends only on one parameter, the optical thickness of the layer τ_0. In astrophysical problems such a situation is encountered frequently.

At present it is impossible to say very much as to the intermediate case where the quantity u_0 cannot be considered either very small or very large. We can expect that here some principle of similitude should exist such as that occurring for a semi-infinite medium; however, this problem has not been duly investigated.

The remaining part of this Section will be almost wholly devoted to /152 presenting results for the case where the thickness of the layer is small with respect to the thermalization length so that we can speak about pure scattering ($u_0 \gg 1$). Thus, we will limit the possible upper values of the electron concen-

tration. Actually, at $\tau_0 \gg 1$, the inequality $u_0 \gg 1$ means that

$$\frac{1}{4\sqrt{\pi}(1-\lambda)\tau_0\sqrt{\ln\tau_0}} \gg 1.$$

Making use of eq.(6) and considering that $1 - \lambda \ll 1$, i.e., $n_e a_{21} \ll A_{21}$, we obtain

$$n_e a_{21} \ll \frac{A_{21}}{4\sqrt{\pi}\tau_0\sqrt{\ln\tau_0}}. \qquad (44)$$

This inequality has a very simple physical meaning. It states that the time interval between two quenching collisions $\left(\frac{1}{n_e a_{21}}\right)$ should be much greater than the average time spent by a quantum in an absorbed state. This time is equal to the product of $\frac{1}{A_{21}}$ and the average number of scatterings (a value of the order of $\tau_0\sqrt{\ln\tau_0}$). Thus, in the solar corona and in the transition layer between the corona and the chromosphere the electron concentrations are comparatively low. Therefore, the condition (44) is satisfied for the majority of resonance lines of highly ionized atoms arising in these layers of the solar atmosphere, although the values of τ_0 for some of these lines are rather large.

In the case of pure scattering it is not difficult to calculate the total energy emitted in the line in all directions from a unit area of a homogeneous isothermal gas layer. Actually, if the condition (44) is satisfied, then all quanta appearing in the medium will escape through the boundaries. Therefore, the procedure reduces simply to calculating the total number of excitations by electron collision occurring in unit time in a column of unit cross section. However, if we want to define the spectral distribution of the escaping radiation, i.e., the line profile, as well as the manner in which this profile varies with a change in the angle of emergence of radiation, the process of radiative transfer must be studied. Furthermore, these problems are acquiring particu- /153
lar importance at present since, in the near future, profiles of numerous resonance lines of the emission of the corona and of the transition layer between corona and chromosphere will probably be obtained.

One of the possible ways of finding the line profiles, already mentioned above, is to determine the populations at all depths, i.e., to solve eq.(41). As soon as the source function is determined, the line profile is readily calculated from eq.(42). There exists also another way. The intensities of the escaping radiation can be determined without defining the source function, i.e., without determining the conditions within the medium, just from an examination of the conditions at the boundaries. Actually, both approaches are intimately correlated, but a discussion of this matter is outside the scope of our problem formulation. In the case of the homogeneous isothermal layer under discussion, the intensity of the escaping radiation expressed in fractions of the Planckian intensity can be represented by means of the second method in the form of

$$I(0, \mu, x, \tau_0, \lambda) = \\ = (1-\lambda) X(\infty, \tau_0, \lambda) [X(\mu e^{x^2}, \tau_0, \lambda) - Y(\mu e^{x^2}, \tau_0, \lambda)]. \quad (45)$$

Here, $X(z, \tau_0, \lambda)$ and $Y(z, \tau_0, \lambda)$ are some auxiliary functions satisfying the nonlinear integral equations:

$$\left.\begin{aligned} X(z, \tau_0, \lambda) &= 1 + \\ &+ \frac{\lambda}{2} z \int_0^\infty \frac{X(z', \tau_0, \lambda) X(z, \tau_0, \lambda) - Y(z', \tau_0, \lambda) Y(z, \tau_0, \lambda)}{z + z'} G(z') dz', \\ Y(z, \tau_0, \lambda) &= e^{-\frac{\tau_0}{z}} + \\ &+ \frac{\lambda}{2} z \int_0^\infty \frac{X(z, \tau_0, \lambda) Y(z', \tau_0, \lambda) - X(z', \tau_0, \lambda) Y(z, \tau_0, \lambda)}{z' - z} G(z') dz', \end{aligned}\right\} \quad (46)$$

where $G(z)$ is given by eq.(29). At $\tau_0 = \infty$, the function Y is identically equal to zero, and the function $X(z, \infty, \lambda)$ coincides with $H(z, \lambda)$ so that eq.(45), at $\tau_0 = \infty$, changes to eq.(30), and eq.(46) to eq.(31).

At first glance, it seems that the second method has no advantage over the first since, instead of solving one equation (41), we must now solve a system of two equations (46) which, furthermore, are nonlinear. However, this is not so. When using the first approach, we are forced to use numerical methods, whereas the second approach offers extensive possibilities for using analytical methods and investigating simplifications in various limiting cases. /154

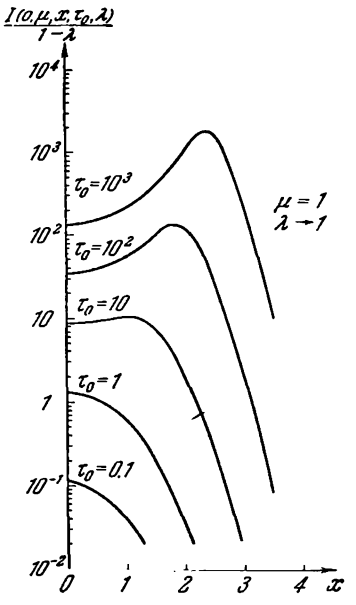

Fig.7

The problem of calculating the emission line profiles in pure scattering is a concise illustration of our above statements. First, we will present results obtained by numerical methods and then derive simple formulas that are convenient to use in everyday calculations. These formulas are derived by the use of analytical methods.

Figure 7 shows Hearn's (Ref.5) calculated profiles of lines emitted by a homogeneous isothermal gas layer for the case where the role of absorption can be neglected. The curves pertain to the event where radiation escapes along the normal, so that $\mu = 1$. The most characteristic feature of these curves is the gradual increase in line width with an increase in layer thickness and the appearance of a dip at the line center at large values of τ_0. We see from Fig.7 that the frequency x_{max} at which the intensity maximum is located satisfies the condition $\tau_0 e^{-x^2_{max}} = \text{const} = t_{max}$ with a high degree of accuracy, with the value of the constant

t_{max} not differing from unity in order of magnitude. An analysis of similar /155
curves, calculated for other angles of emergence of radiation, shows that as μ decreases the line becomes somewhat broader, and the position of the intensity maxima at large τ_0 satisfies the condition $\frac{\tau_0}{\mu} e^{-x^2_{max}} = t_{max}$. These results can be regarded as unique "experimental" data to which a theoretical explanation should be added.

An explanation can be obtained from investigating the functions $X(z, \tau_0, 1)$ and $Y(z, \tau_0, 1)$. It will be found that, if τ_0 and z simultaneously tend to infinity in such a manner that their ratio τ_0/z becomes constant, then at the limit we obtain

$$\left.\begin{aligned} \frac{X(z, \tau_0, 1)}{X(\infty, \tau_0, 1)} &= e^{-\frac{\tau_0}{2z}}\left[I_0\left(\frac{\tau_0}{2z}\right) + I_1\left(\frac{\tau_0}{2z}\right)\right], \\ \frac{Y(z, \tau_0, 1)}{X(\infty, \tau_0, 1)} &= e^{-\frac{\tau_0}{2z}}\left[I_0\left(\frac{\tau_0}{2z}\right) - I_1\left(\frac{\tau_0}{2z}\right)\right], \end{aligned}\right\} \tag{47}$$

where I_0, I_1 are Bessel functions of the imaginary argument. At finite τ_0, these equalities should be satisfied with a greater accuracy the larger τ_0 and z. Substituting eq.(47) into eq.(45), we obtain for the intensity of the escaping radiation the approximate expression:

$$I(0, \mu, x, \tau_0) = \\ = 2(1-\lambda) X^2(\infty, \tau_0, 1) e^{-\frac{\tau_0 e^{-x^2}}{2\mu}} I_1\left(\frac{\tau_0}{2\mu} e^{-x^2}\right). \tag{48}$$

This simple formula permits, in the most elementary manner, a calculation of the relative intensities at the line frequencies, i.e., its profile. At moderate values of the argument, the values of the Bessel function can be taken from tables; at $\frac{t}{2} = \frac{\tau_0}{2\mu} e^{-x^2} \gg 1$, the known asymptotic expansion can be used whose principal term has the form

$$I_1\left(\frac{t}{2}\right) = \frac{e^{\frac{t}{2}}}{\sqrt{\pi t}} + \cdots .$$

The line profiles calculated by eq.(48) are indistinguishable from those /156
shown in Fig.7. Here, we must emphasize that we are dealing with the relative frequency distribution of the energy since, to obtain the absolute values, we must have $X(\infty, \tau_0, 1)$.

It is interesting that, although eq.(48) was obtained for the case $\tau_0 \gg 1$ when the values of μ were not very close to zero, it does yield satisfactory results for all values of τ_0, beginning with the smallest. This is a simple coincidence: At $\tau_0 \ll 1$ and at a small value of the quantity

$$t = \frac{\tau_0 e^{-x^2}}{\mu}, \tag{49}$$

and since $I_1\left(\frac{t}{2}\right) = \frac{t}{4} + \ldots$ at small t, the intensity accidentally becomes proportional to e^{-x^2}. It is not surprising that the formula that yields correct results at small and large τ_0 also works well in the intermediate region.

Equation (48) represents a good approximation at large τ_0 and at $z \gg 1$. Furthermore, for radiation escaping in the central portions of the line at large angles to the normal (i.e., at small μ) the quantity $z = \mu e^{x^2}$ is small. Therefore, there are no grounds to expect that, at small μ, eq.(48) truly describes the shape of the central portions of the line.

It was "empirically" noted above that the frequency x_{max}, accounting for the intensity maximum, satisfies the condition $\frac{\tau_0}{\mu} e^{-x^2_{max}} = \text{const} = t_{max}$.

Actually, this equality is not exact but only asymptotic and is satisfied with a greater accuracy the larger τ_0. Now we can easily obtain the exact value of t_{max} as $\tau_0 \to \infty$. To determine the frequency of the intensity maximum we must differentiate eq.(48) with respect to x and equate the result to zero. Having done this, we arrive at the following equation for determining t_{max}:

$$I_1'\left(\frac{t_{max}}{2}\right) - I_1\left(\frac{t_{max}}{2}\right) = 0,$$

or, if we use the known properties of the Bessel functions,

$$I_0\left(\frac{t_{max}}{2}\right) - \left(1 + \frac{2}{t_{max}}\right) I_1\left(\frac{t_{max}}{2}\right) = 0.$$

The value of t_{max} is the root of this equation equal to 3.09, so that /157

$$\frac{\tau_0}{\mu} e^{-x^2_{max}} = 3.09. \qquad (50)$$

From this it follows that

$$|x_{max}| = \sqrt{\ln \frac{\tau_0}{\mu} - 1.13}. \qquad (51)$$

This is a rigorous asymptotic formula which is more exact the greater τ_0. It can be used in practice, beginning with $\tau_0 = 10$. It is obvious from the formula that when the line broadening is due to the Doppler effect, its width is a poor criterion for determining the optical thickness of the layer in which this line is formed. The depth of the central dip is appreciably more sensitive to a change in τ_0. This problem will not be discussed further here.

Detailed numerical data on the problem discussed in this Section can be found in the aforementioned papers by E.Avrett and D.Hummer (Ref.4) and by A.Hearn (Ref.3, 5). Rigorous methods for investigating the fundamental integral equation at finite τ_0 are presented in the book by V.V.Sobolev (Ref.8) and in his articles (Ref.13, 19). The X- and Y-functions satisfying eqs.(46) are studied in detail in several papers by the author (Ref.20, 21) which contain, in

particular, the derivation of formulas presented here without proof.

At present, the theory of radiative transfer in a spectral line is undergoing a period of vigorous development. This is due to two circumstances. First, in connection with the progress in astronomy beyond the atmosphere in recent years it has become possible to observe numerous resonance lines in the solar spectrum lying in the far ultraviolet. These lines arise in the corona and in the transition layer between corona and chromosphere, i.e., in regions transparent at continuous spectrum frequencies. However, at the frequencies of these very lines, the optical thickness of the layers responsible for their formation should be large in a number of cases. Therefore, the correct interpretation of the observational data, in particular of the line profiles, can be obtained only by investigating the process of radiative transfer. The second /158 fact giving impetus to the development of investigations on radiative transfer in the spectral line was the development of effective exact and approximate methods of solving the equation of radiative transfer. These methods have permitted the solution of numerous problems which could not be solved by previous methods.

Today, astrophysics is making increasing use of the theory of spectral line formation, developed more than 30 years ago on the basis of the false assumption of frequency constancy of the quantum in scattering. This theory is gradually being replaced by a new one based on an approximation of complete frequency redistribution. Recent achievements offer the hope that soon the new method will reach the level of simple calculation formulas, prepared tables, and graphs adapted for extensive use in astrophysics.

REFERENCES

1. Biberman, L.M.: Zh. Eksperim. i Teor. Fiz., Vol.17, p.416, 1947.
2. Biberman, L.M.: Zh. Eksperim. i Teor. Fiz., Vol.19, p.584, 1949.
3. Hearn, A.G.: Radiative Transfer of Doppler Broadened Resonance Lines. U.K. At. Energy Authority, Preprint CLM-P16, 1962; Proc. Phys. Soc. (London), Vol.81, p.648, 1963.
4. Avrett, E.H. and Hummer, D.G.: Monthly Notices, Vol.130, p.295, 1965.
5. Hearn, A.G.: Proc. Phys. Soc. (London), Vol.84, p.11, 1964.
6. Hummer, D.: J. Quant. Spectr. & Radiative Transfer, Vol.3, p.101, 1963.
7. Hummer, D.: Monthly Notices, Vol.125, p.21, 1962.
8. Sobolev, V.V.: Transfer of Radiant Energy in Stellar and Planetary Atmospheres (Perenos luchistoy energii v atmosferakh zvezd i planet). Gostekhizdat, 1956.
9. Thomas, R.N. and Zirker, J.B.: Astrophys. J., Vol.134, p.733, 1961.
10. Pecker, C. and Thomas, R.N.: Astrophys. J., Vol.137, p.967, 1963.
11. Kaplan, S.A. and Pikel'ner, S.B.: The Interstellar Medium (Mezhzvezdnaya sreda). Fizmatgiz, 1963.
12. Ivanov, V.V. and Shcherbakov, V.T.: Astrofizika, Vol.1, p.31, 1965.
13. Sobolev, V.V.: Izv. Akad. Nauk ArmSSR, Vol.11, p.39, 1958.
14. Sobolev, V.V.: Astron. Zh., Vol.36, p.573, 1959.
15. Ivanov, V.V.: Tr. Astron. Observ. Leningr. Gos. Univ., Vol.19, p.52, 1962.
16. Ivanov, V.V.: Astron. Zh., Vol.39, p.1020, 1962.

17. Nagirner, D.I.: Vestn. Leningr. Gos. Univ., No.1, p.142, 1964.
18. Ivanov, V.V.: Tr. Astron. Observ. Leningr. Gos. Univ., Vol.22, p.44, 1965.
19. Sobolev, V.V.: Dokl. Akad. Nauk SSSR, Vol.120, p.69, 1958.
20. Ivanov, V.V.: Astron. Zh., Vol.40, p.257, 1963.
21. Ivanov, V.V.: Astron. Zh., Vol.41, p.1097, 1964.

NONSTATIONARY RADIATION FIELD

/159

I.N.Minin

1. Introduction

The theory of nonstationary radiation fields treats problems of finding the time rate of change of quantities characterizing a radiation field in a medium capable of absorbing and emitting radiant energy. Here, the time rate of change of the intensity of sources and their location are considered as given.

If the duration of a noticeable change in the radiation field is large in comparison with the average residence time of a quantum in the medium, then we can consider that radiation equilibrium occurs at each instant of time. In other cases, when a marked change in the radiation field occurs during the mean residence time of a quantum in the medium, a special study of nonstationary processes of radiative diffusion is necessary. As examples of nonstationary radiation, we can mention the gradual increase in radiation of a medium when emission sources are instantaneously switched on or the de-excitation of a medium when the emission sources are instantaneously switched off.

The first steps in this theory were made by Milne (Ref.1) and Holstein (Ref.2) in studies on the diffusion of resonance radiation. A systematic examination of problems of the theory of nonstationary radiation fields was started by V.V.Sobolev (Ref.3 - 5) who used new methods and obtained exact solutions for a number of problems. Later, these investigations by V.V.Sobolev were expanded in many directions by S.A.Kaplan, I.A.Klimishin, and V.N.Sivers (Ref.6 - 8) and also by the author (Ref.9 - 11). The theory of nonstationary radiation fields has been examined in recently published articles, in which Bellman, Kalaba, Wing, and Ueno (Ref.12 - 14) use the generalized invariance principle to derive equations that determine functions characterizing radiation escaping from the medium. Some results of this trend in the theory of nonstationary diffusion of radiation are given in Wing's book (Ref.15). /160

At present the theory of nonstationary radiation fields has been reasonably well developed only for the case in which the optical properties of the medium do not change. For cases in which the optical properties of the medium do change, only a few special problems can be solved at present. Another possible case is that of the dependence of the optical properties of the medium on the radiation field, which is the most complex problem. In this respect, V.A. Ambartsumyan [see (Ref.16) and the present collection] has only recently been able to obtain some solutions for stationary radiation. Naturally, an investigation of nonstationary radiation is an even more complex problem.

In this paper, we will limit ourselves to a study of problems related to the diffusion of radiation in a medium whose optical properties do not change with time. Furthermore, we will consider that diffusion occurs without redistribution by frequencies.

2. Equation of Radiative Transfer

In the theory of nonstationary radiation fields, the residence time of a quantum in a given medium is of basic importance. Let us first examine the causes which lead to retardation of radiation and which determine the magnitude of the mean residence time of a quantum in the medium. A light quantum, upon scattering, remains in an absorbed state for a certain time. Designating the average length of this time interval by t_1, we can assume for a number of cases that the probability of emission of a quantum, absorbed at the instant $t = 0$, in the time interval from t to t + dt is equal to

$$e^{-\frac{t}{t_1}}\frac{dt}{t_1}. \tag{1}$$

Furthermore, the light quantum, for a certain time, will stay on a path between scatterings. If we take into account that the probability of absorption of the quantum along the path from s to s + ds is equal to $e^{-\alpha s}\alpha\, ds$, where α is the volume absorption coefficient, $s = ct$, c is the velocity of light, we find /161 for the probability of quantum absorption in the time interval from t to t + dt the following quantity:

$$e^{-\frac{t}{t_2}}\frac{dt}{t_2}, \tag{2}$$

where $t_2 = \frac{1}{\alpha c}$. The quantity t_2 represents the average time spent by the quantum on the path between two successive scatterings.

Let us assume for example that we are dealing with radiative transfer in a continuous spectrum and that the absorption coefficient is determined by the ionization of atoms. Then the law (1) is valid, in which the quantity t_1 is equal to

$$t_1 = -\frac{1}{n_e\sum_{i=1}^{\infty} C_i}, \tag{3}$$

where n_e is the number of electrons in 1 cm^3 and C_i is the coefficient of probability of recombination at the i-th atomic level. We note that, for hydrogen at temperatures of the order of 10,000°, we have $\sum_{i=1}^{\infty} C_i \approx 10^{-13}$ $cm^3 sec^{-1}$.

For radiative diffusion in the resonance line, we also have eq.(1) and $t_1 = \frac{1}{A_{21}}$, where A_{21} is the Einstein coefficient of probability of spontaneous transition from an upper level to a lower ($2 \rightarrow 1$). Usually, $A_{21} \approx 10^8$ sec^{-1} and thus $t_1 \approx 10^{-8}$ sec.

It is obvious that, to determine the average residence time of a light quantum in a given medium, the quantity $t_1 + t_2$ must be multiplied by the average

number of scatterings experienced by the quantum during diffusion in a given medium. Therefore, even if the value of $t_1 + t_2$ is small, the average residence time of the quantum in the medium may become appreciable at a sufficiently large number of scatterings.

To solve the problems of the theory of nonstationary diffusion of radiation we can use the transfer equation which takes into account the time rate of change of the radiation field characteristics. When deriving this equation we must bear in mind that the change in radiation intensity occurs both with a /162 change in distance along the ray and with the course of time. Let radiation of an intensity $I(s, t)$ be incident on an area element with area $d\sigma$, within the solid angle $d\omega$ and in the time interval from t to $t + dt$. We will assume that the direction of propagation of the incident radiation is perpendicular to the area under study. Then, the quantity of energy striking the indicated area will be equal to $I(s, t)\, d\sigma\, d\omega\, dt$. On another area element with the same area $d\sigma$ situated at a distance ds from the first, falls a quantity of energy equal to $I(s + ds, t + dt) d\sigma\, d\omega\, dt$. The difference in these amounts of energy is due both to absorption of energy in the volume $d\sigma\, ds$ and to emission of energy by this volume. Thus, we can write

$$I(s + ds, t + dt)\, d\sigma\, d\omega\, dt - I(s, t)\, d\sigma\, d\omega\, dt = \\ = -\alpha(s)\, ds\, I(s, t)\, d\sigma\, d\omega\, dt + \varepsilon(s, t)\, d\sigma\, d\omega\, ds\, dt,$$

where $\alpha(s)$ and $\varepsilon(s, t)$ are the volume absorption and emission coefficients, respectively. Since $ds = c\, dt$, the obtained correlation will yield the equation of radiative transfer

$$\frac{\partial I(s, t)}{\partial s} + \frac{1}{c}\frac{\partial I(s, t)}{\partial t} = -\alpha(s) I(s, t) + \varepsilon(s, t). \tag{4}$$

For simplicity, we will first assume that diffusion of radiation occurs in a one-dimensional medium. Denoting by $I_1(\tau, t)$ and $I_2(\tau, t)$ the intensity of radiation proceeding, at an optical depth τ at the instant of time t, toward increasing and decreasing depths respectively ($d\tau = \alpha\, ds$), in place of eq.(4) we have

$$\left.\begin{aligned} \frac{\partial I_1}{\partial \tau} + t_2 \frac{\partial I_1}{\partial t} &= -I_1 + B, \\ -\frac{\partial I_2}{\partial \tau} + t_2 \frac{\partial I_2}{\partial t} &= -I_2 + B, \end{aligned}\right\} \tag{5}$$

where $B = \frac{\varepsilon}{\alpha}$. Considering that the probability of emission of a quantum at some time interval after absorption is determined by the law (1) and that scattering is isotropic, we find

$$B(\tau, t) = \frac{\lambda}{2}\int_0^t [I_1(\tau, t') + I_2(\tau, t')] \cdot e^{-\frac{t-t'}{t_1}} \frac{dt'}{t_1}, \tag{6}$$

where λ is the probability of "survival" of the quantum in a single scattering

process.

/163

In the case of a constant absorption coefficient α, eqs.(5), with consideration of eq.(6), will yield a differential equation for determining the source function $B(\tau, t)$. With appropriate initial and boundary conditions, the solution of this equation completely determines the radiation of the medium. In particular, the use of eqs.(5) permits finding the intensities of radiation escaping from the medium.

Let us now examine a medium consisting of plane-parallel layers in which isotropic scattering of light occurs. For this case, the transfer equation (4) takes the form

$$\eta \frac{\partial I(\tau, \eta, t)}{\partial \tau} + t_2 \frac{\partial I(\tau, \eta, t)}{\partial t} = B(\tau, t) - I(\tau, \eta, t), \tag{7}$$

where $I(\tau, \eta, t)$ is the radiation intensity at the instant of time t at an optical depth τ, whose propagation direction, with the normal to the layers, makes an angle whose cosine is equal to η, and

$$B(\tau, t) = \frac{\lambda}{2} \int_{-1}^{+1} \left[\int_{0}^{t} I(\tau, \eta', t') e^{-\frac{t-t'}{t_1}} \frac{dt'}{t_1} \right] d\eta' + g(\tau, t), \tag{8}$$

with $g(\tau, t)\, d\tau$ being the quantity of energy emitted by sources located in an element of volume of 1 cm^2 cross section and an optical thickness $d\tau$ at an optical depth τ at a time t per second per unit solid angle.

Of course, the solution of eq.(7) is appreciably more difficult than the solution of the system of equations (5) and (6). On the other hand, it is known that a medium consisting of plane-parallel layers can be approximately replaced by a one-dimensional medium. Therefore, for simplicity we will discuss mainly radiative diffusion in a one-dimensional medium.

3. Probability of Escape of Quanta from a Medium

The direct solution of the transfer equation is not the only method in the theory of diffusion of radiation. At present there exist other methods whose effectiveness depends upon the circumstances.

To solve various problems of the theory of radiative transfer, V.V.Sobolev (Ref.17) proposed a probability method which he applied, in particular, to /164 the theory of nonstationary radiation fields (Ref.3 - 5). We will give some of the results obtained in this Section.

Let us introduce the quantity $p(\tau, t - t')\, dt$, which is the probability that a light quantum, absorbed at an optical depth τ at a time t', escapes from a one-dimensional medium through the boundary $\tau = 0$ in the time interval from t to $t + dt$. After obtainment of the indicated quantity, the intensity of radiation escaping from the medium is easily found by appropriate integration. Designating by $L(\tau, t')\, d\tau\, dt'$ the quantity of energy arriving directly from the

light source and absorbed in the optical thickness range from τ to $\tau + d\tau$ during the time interval from t' to $t' + dt'$, the intensities of radiation escaping from the medium can be written as

$$\left.\begin{aligned} I_2(0, t) &= \int_0^{\tau_0} d\tau \int_0^t L(\tau, t') p(\tau, t - t')\, dt', \\ I_1(\tau_0, t) &= \int_0^{\tau_0} d\tau \int_0^t L(\tau, t') p(\tau_0 - \tau, t - t')\, dt', \end{aligned}\right\} \tag{9}$$

where τ_0 is the optical thickness of the medium. The advantage of this method lies in the fact that, to solve any problem of the radiation of a given medium, only the one function $p(\tau, t)$ need be known.

To determine the probability of the escape of quanta from a given medium we can construct integral, differential, and functional equations. Here, we will present certain functional equations and their solutions.

Let us examine a one-dimensional semi-infinite medium with isotropic scattering and investigate the case where the average residence time of the quantum in an absorbed state appreciably exceeds the average residence time of the quantum along the path between two successive scatterings (i.e., $t_1 \gg t_2$). Wanted is the probability of escape of the quantum from the medium from an optical depth $\tau + \Delta\tau$, i.e., the quantity $p(\tau + \Delta\tau, u)$ where $u = \frac{t}{t_1}$. For this, let us represent the escape of a quantum from the depth $\tau + \Delta\tau$ as the escape of a quantum from the depth τ and its subsequent passage through an additional /165 layer of optical thickness $\Delta\tau$. The probability of escape of the quantum from the medium without scattering in the additional layer is equal to $p(\tau, u) \times (1 - \Delta\tau)$. To obtain the probability of escape of quanta from the medium, with scattering in the additional layer, the quantity $p(\tau, u')\Delta\tau$ must be multiplied by $p(0, u - u')du'$ and the product integrated with respect to u' from zero to u. The sum of the obtained probabilities represents the unknown quantity, i.e.,

$$p(\tau + \Delta\tau, u) = p(\tau, u)\cdot(1 - \Delta\tau) + \Delta\tau \int_0^u p(\tau, u')\cdot p(0, u - u')\, du',$$

from which, at $\Delta\tau \to 0$, it follows that

$$\frac{\partial p(\tau, u)}{\partial \tau} = -p(\tau, u) + \int_0^u p(\tau, u')\, p(0, u - u')\, du'. \tag{10}$$

Equation (10) does not completely determine the function $p(\tau, u)$ since, in deriving this expression, we disregarded the mechanism of scattering. Stipulating that the probability of quantum emission in the interval of dimensionless time from u to $u + du$, after its absorption, is equal to $e^{-u}du$, i.e., obeys the law (1), we obtain the following expression for $p(0, u)$:

$$p(0, u) = \frac{\lambda}{2} e^{-u} + \frac{\lambda}{2} \int_0^u e^{-u'} \rho(u - u')\, du', \tag{11}$$

where

$$\rho(u) = \int_0^\infty e^{-\tau} p(\tau, u)\, d\tau. \tag{12}$$

The quantity $\rho(u)du$ defines the probability that the quantum, after striking the medium, is reflected from it in the time interval from u to u + du. Equations (10) and (11) permit deriving both $p(\tau, u)$ and $\rho(u)$.

In determining the indicated quantities, the operational method based on the Laplace transform is applied. This method is widely employed in the theory of diffusion and thermal conductivity, and recently also in the theory of radiative transfer. Numerous handbooks and manuals are in existence which make /166 it comparatively easy to solve various problems by the operational method. The most complete is the three-volume handbook compiled by Doetsch (Ref.18). The same author has written a small book (Ref.19) which, in a concise form, gives the basic rules of operational calculus, knowledge of which in most cases is sufficient. The book includes tables for Laplace transformations, which facilitate the use of the operational method. We should also mention the extensive tables compiled by V.A.Ditkin and P.I.Kuznetsov (Ref.20).

Let us multiply both sides of eq.(10) by $e^{-\tau} d\tau$ and integrate from 0 to ∞. This yields

$$-p(0, u) + \rho(u) = -\rho(u) + \int_0^u \rho(u')\, p(0, u - u')\, du'. \tag{13}$$

Let us next use the Laplace transform. Multiplying both sides of eq.(13) by $e^{-su} du$, integrating with respect to u from 0 to ∞, and using the rules of operational calculus (Ref.19, p.26), we find

$$-\bar{p}(0, s) + \bar{\rho}(s) = -\bar{\rho}(s) + \bar{\rho}(s) \cdot \bar{p}(0, s), \tag{14}$$

where

$$\bar{p}(0, s) = \int_0^\infty e^{-su} p(0, u)\, du, \quad \bar{\rho}(s) = \int_0^\infty e^{-su} \rho(u)\, du. \tag{15}$$

Thus, in eq.(14) the functions $\bar{p}(0, s)$ and $\bar{\rho}(s)$ are Laplace-transformed from the functions $p(0, u)$ and $\rho(u)$ respectively, where s is the transformation parameter. In a like manner, we obtain from eq.(11)

$$\bar{p}(0, s) = \frac{\lambda}{2} \frac{1 + \bar{\rho}(s)}{1 + s}. \tag{16}$$

Substituting $p(0, s)$ from eq.(16) into eq.(14) and solving the obtained equation for $\bar{\rho}(s)$ we have

$$\bar{\rho}(s) = \frac{2}{\lambda}(s + 1) - 1 - \frac{2}{\lambda} \sqrt{(s + 1)^2 - \lambda(s + 1)}. \tag{17}$$

Now, to find $\rho(u)$ from the known function $\bar{\rho}(s)$ we must invert the Laplace transformation (Ref.19, p.111). Considering that the points $s = -1$ and $s = -(1 - \lambda)$ are branch points of the function $\bar{\rho}(s)$, we find /167

$$\rho(u) = \frac{2}{\pi}\lambda\int_0^1 e^{-(1-\lambda y)u}\sqrt{y(1-y)}\,dy. \tag{18}$$

Having the function $\rho(u)$, it is easy to determine the intensity of radiation escaping from the medium $I(u)$, when illuminated by external sources. If $I_0(u)$ is the intensity of radiation arriving from external sources at the boundary of the medium, then

$$I(u) = \int_{-\infty}^{u} I_0(u')\,\rho(u-u')\,du'. \tag{19}$$

For example, let the medium begin to be subjected to illumination by sources of constant intensity I_0, from the instant of time $u = 0$. Then, as is easily obtained from eq.(19),

$$I(u) = I_0 \cdot \int_0^u \rho(u)\,du. \tag{20}$$

If, during the time interval from $-\infty$ to 0, radiation of constant intensity I_0 strikes the boundary of the medium and if, as soon as $u = 0$, illumination of the medium stops, then eq.(19) will yield

$$I(u) = I_0\int_u^{\infty} \rho(u)\,du. \tag{21}$$

After determining the function $\rho(u)$ we can find $p(\tau, u)$ in the same manner. Having applied, to eq.(10), the Laplace transformation with respect to u, we obtain

$$\frac{d\bar{p}(\tau, s)}{d\tau} = -\bar{p}(\tau, s)\,[1 - \bar{p}(0, s)], \tag{22}$$

from which it follows that

$$\bar{p}(\tau, s) = \bar{p}(0, s)\,e^{-\tau[1-\bar{p}(0,\,s)]}. \tag{23}$$

From eqs.(16) and (17) we find /168

$$\bar{p}(0, s) = 1 - \sqrt{1 - \frac{\lambda}{1+s}}. \tag{24}$$

Therefore, substituting eq.(24) into eq.(23), we finally have

$$\bar{p}(\tau, s) = \left(1 - \sqrt{1 - \frac{\lambda}{1+s}}\right)e^{-\tau\sqrt{1-\frac{\lambda}{1+s}}}. \tag{25}$$

An inversion of eq.(25) has the form

$$p(\tau, u) =$$

$$= \frac{\lambda}{\pi}\int_0^1 e^{-(1-\lambda y)u}\left(\sin\tau\sqrt{\frac{1-y}{y}} + \sqrt{\frac{1-y}{y}}\cos\tau\sqrt{\frac{1-y}{y}}\right)dy. \qquad (26)$$

It is of interest to derive the asymptotic formulas which hold for $u \gg 1$. Here, let us examine $\rho(u)$, having first transformed eq.(18). A change of variable $y = 1 - z$ will yield

$$\rho(u) = \frac{2}{\pi}\lambda e^{-(1-\lambda)u}\int_0^1 e^{-\lambda z u}\sqrt{z(1-z)}\,dz. \qquad (27)$$

Assuming that $\lambda u \gg 1$, the value of the integral in eq.(27) will be determined by the integration range from $z = 0$ to $z \approx \frac{1}{\lambda u}$. In this case, the quantity $1 - z$ in the integrand function can be replaced by unity and the upper limit of integration can be taken as equal to infinity. Then we will have

$$\rho(u) \approx \frac{2}{\pi}\lambda e^{-(1-\lambda)u}\int_0^\infty e^{-\lambda z u}\sqrt{z}\,dz. \qquad (28)$$

The integral in eq.(28) is easily calculated and the asymptotic formula for $\rho(u)$ takes the form

$$\rho(u) \approx \frac{e^{-(1-\lambda)u}}{u\sqrt{\pi\lambda u}}. \qquad (29)$$

We note that eq.(29) can be derived also on the basis of eq.(17) and by using methods of the Laplace transformation theory (Ref.19, p.125).

The formulas derived above are valid for the case of $t_1 \gg t_2$. For /169
$t_2 \gg t_1$, the function $p(\tau, u)$ was derived by V.V.Sobolev (Ref.4) who also showed that $\rho(u)$ is determined for this case by eq.(18) with $u = \frac{t}{t_2}$.

4. Laplace Transformation of Functions Characterizing the Radiation Field

As shown in Section 3, the use of the Laplace transform is an effective method for solving problems of the theory of nonstationary diffusion of radiation. The author (Ref.9) has shown that the Laplace transform with respect to time of any function characterizing the radiation field can be obtained directly from solving the corresponding problem for conditions of stationary radiation. In this Section we will examine such a method and its application to the solution of a number of problems.

Let us take a homogeneous medium consisting of plane-parallel layers in which the quantities t_1 and t_2 are independent of coordinates and time. We will introduce the designations

$$u=\frac{t}{t_1+t_2}, \qquad \beta_1=\frac{t_1}{t_1+t_2}, \qquad \beta_2=\frac{t_2}{t_1+t_2}. \tag{30}$$

The radiation intensity $I(\tau, \eta, u)$ for this case is determined from eq.(7) which has been modified by the denotations (30). Let us apply to this equation the Laplace transform with respect to u, assuming that at the time u = 0 the medium is not radiating, i.e., that $I(\tau, \eta, 0) = 0$. As a result we obtain

$$\frac{\eta}{1+\beta_2 s}\frac{\partial \bar{I}(\tau, \eta, s)}{\partial \tau} = \\ = \frac{\lambda}{2(1+\beta_1 s)(1+\beta_2 s)}\int_{-1}^{+1}\bar{I}(\tau, \eta', s)\,d\eta' + \frac{\bar{g}(\tau, s)}{1+\beta_2 s} - \\ - \bar{I}(\tau, \eta, s), \tag{31}$$

where

$$\bar{I}(\tau, \eta, s)=\int_0^\infty e^{-su} I(\tau, \eta, u)\,du, \quad \bar{g}(\tau, s)=\int_0^\infty e^{-su} g(\tau, u)\,du. \tag{32}$$

On the other hand, for conditions of stationary radiation the equation of radiative transfer has the form /170

$$\eta\frac{\partial I(\tau, \eta)}{\partial \tau} = \frac{\lambda}{2}\int_{-1}^{+1} I(\tau, \eta')\,d\eta' + g(\tau) - I(\tau, \eta). \tag{33}$$

Let the solution of eq.(33) be known, i.e., the function $I(\tau, \eta)$ which, in addition to τ and η, depends also on the parameter λ and on $g(\tau)$. A comparison of eqs.(33) and (31) shows that, to find $\bar{I}(\tau, \eta, s)$, it is necessary in the solution of eq.(33) to replace λ by $\frac{\lambda}{(1+\beta_1 s)(1+\beta_2 s)}$, τ by $\tau(1+\beta_2 s)$, and $g(\tau)$ by $\frac{\bar{g}(\tau, s)}{1+\beta_2 s}$. Inverting $\bar{I}(\tau, \eta, s)$, we obtain the sought radiation intensity $I(\tau, \eta, u)$. Needless to say, if the indicated changes are made in any other function characterizing the stationary radiation field, this function is obtained in the same manner for conditions of nonstationary radiation.

Let us study, for example, the radiation of a one-dimensional semi-infinite medium with isotropic scattering. In the stationary case, for the probability of quantum escape $p(\tau)$ from an optical depth τ we have (Ref.5, p.177)

$$p(\tau) = (1-\sqrt{1-\lambda})\cdot e^{-\tau\sqrt{1-\lambda}}, \tag{34}$$

while, for the reflection factor (Ref.5, p.52) we obtain

$$\rho = \frac{2}{\lambda} - 1 - \frac{2}{\lambda}\sqrt{1-\lambda}. \tag{35}$$

Making the indicated substitutions of λ and τ in eqs.(34) and (35), we obtain the transformed functions $\bar{p}(\tau, s)$ and $\bar{\rho}(s)$. In particular, provided that $t_1 \gg t_2$, we easily find eqs.(25) and (17) from these general expressions for

$\bar{p}(\tau, s)$ and $\bar{\rho}(s)$ if we set $\beta_2 = 0$ therein. The inversion of the Laplace transform yields the functions $p(\tau, u)$ and $\rho(u)$ for any relation between the quantities t_1 and t_2. Inversion for the above general case was performed in investigations by the author (Ref.9, 10) in which the problem of the radiation of a one-dimensional infinite medium was also solved.

Let us now examine the problem of nonstationary radiation of a three-dimensional homogeneous infinite medium with uniformly distributed isotropic radiation sources. In the case of stationary radiation, let $4\pi B\, d\tau$ be the quantity of radiant energy emitted by a volume of 1 cm^2 cross section and an optical thickness $d\tau$ per unit time and let $4\pi g\, d\tau$ be the quantity of radiant energy emitted directly by the radiation sources located in a volume of 1 cm^2 cross section and an optical thickness $d\tau$ per unit time. Wanted is the source function B which in this case, as is readily understood, is independent of the coordinates or of the direction, for any indicatrix of light scattering in the medium. It is obvious that, for the existence of stationary radiation, the conditions $\lambda < 1$ must be satisfied. /171

In each scattering event, only the portion λ of the number of absorbed quanta "survives". Therefore, allowing for diffuse radiation we have

$$B = g(1 + \lambda + \lambda^2 + \ldots), \tag{36}$$

from which it follows that

$$B = \frac{g}{1-\lambda}. \tag{37}$$

As is obvious, the result (37) is also readily obtained from the equation of radiative transfer.

Let us now investigate the case of nonstationary radiation. Here, we must determine the quantity $\underline{B}(u)\, d\tau$ for the given quantity $g(u)\, d\tau$. Let us first determine the quantity $\bar{B}(s)\, d\tau$, using eq.(37) and replacing, according to the rule formulated above, λ by $\frac{\lambda}{(1+\beta_1 s)(1+\beta_2 s)}$, $d\tau$ by $d\tau(1+\beta_2 s)$, and g by $\frac{\bar{g}(s)}{1+\beta_2 s}$. Having made these changes, we obtain

$$\bar{B}(s) = \frac{\bar{g}(s)}{1 - \frac{\lambda}{(1+\beta_1 s)(1+\beta_2 s)}}. \tag{38}$$

At first, we will assume $g(u) = \delta(u)$ where $\delta(u)$ is the Dirac delta function. Physically, this corresponds to the instantaneous effect of sources of unit intensity at the instant of time $u = 0$. Since $\bar{\delta}(s) = 1$, then eq.(38), denoting for this case the source function by $B_\delta(u)$, is replaced by

$$\bar{B}_\delta(s) = 1 + \frac{\lambda}{(1+\beta_1 s)(1+\beta_2 s) - \lambda}. \tag{39}$$

Inverting eq.(39), we obtain (Ref.19, p.148) /172

$$B_\delta(u) = \delta(u) + \frac{\lambda}{\sqrt{1-4\beta_1\beta_2(1-\lambda)}}(e^{a_2 u} - e^{a_1 u}), \tag{40}$$

where

$$\left.\begin{aligned} a_1 &= -\frac{1}{2\beta_1\beta_2}[1 + \sqrt{1-4\beta_1\beta_2(1-\lambda)}], \\ a_2 &= -\frac{1}{2\beta_1\beta_2}[1 - \sqrt{1-4\beta_1\beta_2(1-\lambda)}]. \end{aligned}\right\} \tag{41}$$

At $\lambda = 1$, it follows from eq.(40) that

$$B_\delta(u) = \delta(u) + 1 - e^{-\frac{u}{\beta_1\beta_2}}. \tag{42}$$

Naturally, when $u \to \infty$ the quantity $B_\delta(u)$ for the given case approaches the value 1. Physically this means that, in the absence of true absorption, the radiant energy being emitted at the time $u = 0$ will be diffused in the medium for an infinitely long time.

If $\beta_1 = 0$, $\beta_2 = 1$ (or $\beta_2 = 0$, $\beta_1 = 1$, which gives the same result), eq.(40) will yield

$$B_\delta(u) = \delta(u) + \lambda e^{-(1-\lambda)u}. \tag{43}$$

It is easy to represent the solution of the problem for the arbitrary function $g(u)$ in terms of the function $B_\delta(u)$. In a manner similar to eq.(19), we can write

$$B(u) = \int_{-\infty}^{u} g(u')\, B_\delta(u-u')\, du'. \tag{44}$$

Thus, we have obtained the complete solution of the problem of nonstationary radiation of an infinite homogeneous medium with a uniform distribution of radiation sources.

In another paper by the author (Ref.11), the problem of nonstationary radiation of a semi-infinite medium with isotropic scattering was solved. A determination was made of the intensity of radiation escaping from a medium illuminated by parallel rays incident on the boundary of the medium, as well as illuminated by isotropic sources uniformly distributed in the medium.

The theory of a nonstationary radiation field can have diverse applications in physics and astrophysics. Investigation of the scattering of radiation in a resonance line under nonstationary conditions is an important case for physics. A comparison between theory and experiment yields valuable information on the optical properties of atoms and on the nature of the quantum diffusion process. This served as basis for corresponding theoretical studies (see Sect.1). /173

In astrophysics, the theory is being used for investigating radiation diffusion processes in various nonstationary objects: novae, solar prominences, etc. In subsequent Sections, we will discuss problems of nonstationary radiation of the outer layers of stars which arise in the study of novae and in the

theory of the reflection effect in binaries. We will assume the absorption coefficient as being frequency-independent. For conditions in the outer layers of the stars, $t_1 \gg t_2$ and obviously $\lambda = 1$.

5. Radiation of a Star after Shell Detachment

Let us first examine radiation of a one-dimensional semi-infinite medium after instantaneous disconnection of the radiation sources. The dimensionless time $u = \frac{t}{t_1}$ will be counted from the moment of disconnecting the sources. Let $R(\tau)\, d\tau$ be the quantity of energy enclosed between the optical depths τ and $\tau + d\tau$ at the instant of time $u = 0$. Then we have

$$I(u) = \int_0^\infty R(\tau)\, p(\tau, u)\, d\tau, \tag{45}$$

where I(u) is the intensity of radiation escaping from the medium. We note that the quantity $R(\tau)$ is connected with the source function $B(\tau)$ over the relation

$$R(\tau) = 2B(\tau). \tag{46}$$

Of particular interest is the case where, at the instant of disconnecting the light sources,

$$R(\tau) = a_0 + a_1\tau, \tag{47}$$

where a_0 and a_1 are some constants. Using eq.(45), we find /174

$$I(u) = a_0 A_0(u) + a_1 A_1(u), \tag{48}$$

where we denote

$$\left.\begin{aligned} A_0(u) &= \int_0^\infty p(\tau, u)\, d\tau, \\ A_1(u) &= \int_0^\infty \tau p(\tau, u)\, d\tau. \end{aligned}\right\} \tag{49}$$

From eq.(10) we easily obtain

$$-p(0, u) = -A_0(u) + \int_0^u A_0(u')\, p(0, u - u')\, du'. \tag{50}$$

Applying the Laplace transform to eq.(50), we find

$$\overline{A}_0(s) = \frac{\overline{p}(0, s)}{1 - \overline{p}(0, s)}. \tag{51}$$

Substituting into eq.(51) the expression for $\bar{p}(0, s)$ determined from eq.(24) for $\lambda = 1$, we have

$$\bar{A}_0(s) = \sqrt{1 + \frac{1}{s}} - 1, \tag{52}$$

which, after inversion of the Laplace transform, yields

$$A_0(u) = \frac{1}{\pi}\int_0^1 e^{-uy}\sqrt{\frac{1-y}{y}}\,dy. \tag{53}$$

The quantity $A_1(u)$ which is found in a like manner proves to be equal to

$$A_1(u) = 1 - A_0(u). \tag{54}$$

Finally, for the unknown intensity, under application of eqs.(48), (53), and (54), we obtain

$$I(u) = a_1 + \frac{a_0 - a_1}{\pi}\int_0^1 e^{-uy}\sqrt{\frac{1-y}{y}}\,dy. \tag{55}$$

Equation (55) can be used to solve the problem of the radiation of a star after detaching the shell. This problem arises in connection with the study of physical processes occurring during nova outbursts. Equation (55) constitutes the solution for a one-dimensional medium; however, it can be used also for an approximate solution of the indicated problem. /175

Let us denote by H the flux of radiation escaping from a star in a steady state and by I(u) the same quantity after detachment of the shell. In the steady state, the source function $B(\tau)$ is determined by the formula

$$B(\tau) = \frac{H}{2}(1 + \tau). \tag{56}$$

If the optical thickness of the detached layer is equal to τ_*, then $B(\tau)$ at the instant of detachment has the form

$$B(\tau) = \frac{H}{2}(1 + \tau_* + \tau), \tag{57}$$

where τ is the optical depth reckoned from the new boundary. After detachment of the shell luminescence will occur, as a result of which $B(\tau)$ will change from a value determined by eq.(57) to a value determined by eq.(56).

Taking eqs.(46) and (47) into account and using the value of $B(\tau)$ determined by eq.(56) for $u = 0$, we find $a_0 = a_1 = H$. Then eq.(55) yields the obvious result $I(u) = H$ corresponding to stationary radiation. When, at the initial instant, $B(\tau)$ corresponds to eq.(57), then eq.(55), at $a_0 = H(1 + \tau_*)$ and $a_1 = H$, will give the following value for I(u):

$$I(u) = H\left(1 + \frac{\tau_*}{\pi}\int_0^1 e^{-uy}\sqrt{\frac{1-y}{y}}\,dy\right). \qquad (58)$$

For large values of u, using the method indicated in Section 3, eq.(58) is replaced by

$$I(u) \approx H\left(1 + \frac{\tau_*}{\sqrt{\pi u}}\right). \qquad (59)$$

The results were obtained by V.V.Sobolev (Ref.4) who used the obtained solution in investigating the radiation of new stars. As is known (Ref.21, /176 Chapt.III), during a nova outburst detachment of the shell from the star occurs at the initial instant of time. It is of interest to estimate the quantity of energy emitted by the star during an arbitrary time interval. Since in the layer of detachment of the shell from the star we have $t_1 \approx 10^{-8}$ sec, then for all practical purposes we always have $u \gg 1$ or else eq.(59) can be used. Integrating eq.(59) from the start of the outburst up to the time u, we obtain for the quantity of energy emitted during the time between the indicated instants a value of the order of $H\tau_*\sqrt{u}$. For the energy emitted by the star from the instant of detachment of the shell to the instant of maximum brightness, calculations yield a value of the order of 10^{44} erg.

However, it follows from observations that the ejection of matter from a star, which occurs after detachment of the shell, leads to a loss of stellar mass comparable with the mass of the shell detached from the star at the start of the outburst. This circumstance should affect the radiation of the star close to the moment of maximum brightness. Therefore, it is of interest to study the problem of the radiation of a star under consideration of the ejection of matter from it after detachment of the shell. The next Section is devoted to this problem.

6. Radiation of a Star with Ejection of Matter

The formulated problem, strictly speaking, necessitates study of the radiation field in a medium whose optical properties change with time. However, we will limit ourselves here to an approximate solution, having replaced the continuous ejection of matter by detachment of the second shell at the instant of time u_1 after start of the nova outburst. The possibility of using the above approximation has to do with the fact that the intensity of ejection of matter from a star has a maximum some time after start of the outburst. Our problem consists in finding the luminosity of the star I(u) for $u \gg u_1$, provided that at the instant of time u_1 the second shell of optical thickness τ_*' is detached from the star.

If $B(\tau, u)$ is the source function at an optical depth τ at the time u after detachment of the first shell, then eqs.(45) and (46) for $u \gg u_1$ will yield /177

$$I(u) = 2\int_0^\infty B(\tau + \tau_*', u_1)\,p(\tau, u - u_1)\,d\tau. \qquad (60)$$

To determine the function $B(\tau, u)$ entering eq.(60), we proceed in the following manner: Let us first examine stationary radiation of a one-dimensional semi-infinite medium for an arbitrary λ. The source function $B(\tau)$ in this case is determined from the equation

$$B(\tau) = \frac{\lambda}{2}\int_0^\infty e^{-|\tau-\tau'|} B(\tau')\, d\tau' + g(\tau), \tag{61}$$

where the quantity $g(\tau)$ characterizes the rotation and intensity of the radiation sources. The solution of eq.(61) can be represented as

$$B(\tau) = \int_0^\infty \Gamma(\tau, \tau')\, g(\tau')\, d\tau' + g(\tau), \tag{62}$$

where $\Gamma(\tau, \tau')\, d\tau$ is the probability that a quantum emitted (absorbed) at optical depths τ' is subsequently emitted (absorbed) between the depths τ and $\tau + d\tau$ after any number of scatterings in the medium.

Under conditions of nonstationary radiation we must introduce $B(\tau, u)$ and $\Gamma(\tau, \tau', u)$. Let us examine the Laplace transform with respect to u of these functions $\overline{B}(\tau, s)$ and $\overline{\Gamma}(\tau, \tau', s)$, using the method given in Section 4. For this case we should substitute λ by $\frac{\lambda}{1+s}$ in the appropriate relations obtained for stationary radiation of the medium. Setting $g(\tau) = \frac{\lambda}{2} R(\tau)$ and carrying out the above substitution in eq.(62), we obtain

$$\overline{B}(\tau, s) = \frac{\lambda}{2(1+s)}\int_0^\infty \overline{\Gamma}(\tau, \tau', s)\, R(\tau')\, d\tau' + \frac{\lambda}{2(1+s)} R(\tau). \tag{63}$$

The function $\Gamma(\tau, \tau')$ has the form (Ref.22) /178

$$\Gamma(\tau, \tau') = (1 - \sqrt{1-\lambda})\, e^{-|\tau-\tau'|\sqrt{1-\lambda}} + \\ + \frac{(1-\sqrt{1-\lambda})^2}{2\sqrt{1-\lambda}} \left[e^{-|\tau-\tau'|\sqrt{1-\lambda}} - e^{-(\tau+\tau')\sqrt{1-\lambda}}\right]. \tag{64}$$

Substituting in eq.(64) λ by $\frac{\lambda}{1+s}$, we find

$$\overline{\Gamma}(\tau, \tau', s) = \left(1 - \sqrt{1 - \frac{\lambda}{1+s}}\right) e^{-|\tau-\tau'|\sqrt{1-\frac{\lambda}{1+s}}} + \\ + \frac{\left(1-\sqrt{1-\frac{\lambda}{1+s}}\right)^2}{2\sqrt{1-\frac{\lambda}{1+s}}} \left[e^{-|\tau-\tau'|\sqrt{1-\frac{\lambda}{1+s}}} - e^{-(\tau+\tau')\sqrt{1-\frac{\lambda}{1+s}}}\right]. \tag{65}$$

We note that the inversion in eq.(65) has been accomplished by the author in an earlier study (Ref.9).

After adopting for $R(\tau)$ the expression

$$R(\tau) = H(1 + \tau_* + \tau), \tag{66}$$

which corresponds to the conditions after detachment of the first shell, and substituting eqs.(65) and (66) into eq.(63), we have (for $\lambda = 1$)

$$\overline{B}(\tau, s) = \frac{H}{2s}(1 + \tau_\cdot + \tau) - \frac{H\tau_\cdot}{2s}\left(1 - \sqrt{\frac{s}{1+s}}\right)e^{-\tau\sqrt{\frac{s}{1+s}}}. \tag{67}$$

With consideration of eq.(25), we obtain from eq.(67)

$$B(\tau, u) = \frac{H}{2}[1 + \tau + \tau_\cdot \cdot \psi(\tau, u)], \tag{68}$$

where

$$\psi(\tau, u) = \int_u^\infty p(\tau, u')\,du'. \tag{69}$$

In particular, eq.(68) determines the temperature distribution in the outer layers of the star for the period after start of the outburst.

Substituting eq.(68) into eq.(60), we find

$$I(u) = H[1 + \tau_\cdot' A_0(u - u_1) + \tau_* b(u - u_1, u_1, \tau_\cdot')], \tag{70}$$

where /179

$$b(u, u_1, \tau_\cdot') = \int_0^\infty \psi(\tau + \tau_\cdot', u_1)\,p(\tau, u)\,d\tau, \tag{71}$$

while the function $A_0(u)$ is determined from eq.(53). Equation (70) also yields the exact solution of the problem in question.

Since we are interested in the values of $u - u_1 \gg 1$, we will hereafter use the asymptotic formula

$$A_0(u) \approx \frac{1}{\sqrt{\pi u}}. \tag{72}$$

To estimate the quantity $I(u)$ it must be considered that $0 < \psi(\tau, u) < 1$ if $0 < u < \infty$ and for any values of τ. Using eqs.(49), (70), and (72), we obtain

$$H\left[1 + \frac{\tau_\cdot'}{\sqrt{\pi(u - u_1)}}\right] < I(u) < H\left[1 + \frac{\tau_\cdot + \tau_\cdot'}{\sqrt{\pi(u - u_1)}}\right]. \tag{73}$$

We easily find from eq.(73) that the quantity of energy ΔE emitted during the time $\Delta u = u - u_1$ can be estimated from the inequalities

$$H\tau_\cdot'\sqrt{\Delta u} < \Delta E < H(\tau_\cdot + \tau_\cdot')\sqrt{\Delta u}. \tag{74}$$

Hence, if τ_* and τ'_* do not differ markedly, the quantity of energy emitted by a star after detachment of the second shell will be comparable to the quantity of energy emitted after detachment of the first shell. This fact must be taken into account when interpreting the observed curves of the outburst of novae during the premaximum period (Ref.21, Chapt.III). The formulas for the dependence of the stellar luminosity I(u) on the time u, obtained in the preceding and also in this Section, can be used for a theoretical plotting of the light curves of novae.

7. Reflection Effect in Close Binaries

In a close binary system when the cool star is illuminated by the hot star there occurs a rise in the temperature of the outer layers and, correspondingly, an increase in the brightness of the regions of the cool star facing the hot star. This leads to the phase effect (or reflection effect) observed in /180
eclipse systems. If there is axial rotation of the cool star relative to the direction to the hot star, then each area of the surface of the cool star will be subjected to periodic irradiation by the hot star. Since the process of radiation diffusion has some duration, the brightness distribution over the surface of the cool star will not be symmetric relative to the direction to the hot star. A calculation of this brightness distribution is of interest for studying eclipsing variables. It is obvious that the basic parameter entering the solution of this problem will be the value of the ratio of the mean residence time of the quanta in an absorbed state t_1 to the period of rotation of the cool star relative to the direction to the hot star.

We will not solve the formulated problem here but merely study the temperature change in the stellar atmosphere which produces additional extraneous illumination, for certain particular laws of the time rate of change of external illumination.

In this connection we cite the work by Swihart (Ref.23) who carried out a numerical solution of one such problem on an electronic computer. A semi-infinite atmosphere consisting of plane-parallel layers and illuminated by a flux of parallel rays, incident at some angle to the normal, was investigated. Illumination began from a certain instant of time by a constant flux and led to a gradual temperature rise in the atmosphere. A table giving the temperature fluctuations at various optical depths for various instants of time was one result of the calculations performed.

Using a one-dimensional semi-infinite medium as an atmospheric model, we will obtain analytic solutions. At the initial instant of time, let the intensity of the escaping radiation (coinciding with the flux for a one-dimensional medium) be equal to H. Then, for the source function $B(\tau)$ eq.(56) will be valid. At $u = 0$, the medium begins to be illuminated by external radiation whose intensity we will assume as equal to βH. In that case, the source function $B(\tau, u)$ can be represented as

$$B(\tau, u) = B(\tau) + \Delta B(\tau, u), \tag{75}$$

where the quantity $\Delta B(\tau, u)$ is due to radiation striking the medium from /181

without.

The author (Ref.9) showed that, if a medium is illuminated from without by radiation whose intensity is equal to $\delta(u)$ the following relation will be valid for the source function $B_\delta(\tau, u)$:

$$B_\delta(\tau, u) = p(\tau, u). \tag{76}$$

Hence, for $\Delta B(\tau, u)$ we find

$$\Delta B(\tau, u) = \beta H \int_0^u p(\tau, u')\, du'. \tag{77}$$

Equations (56), (75), and (77) furnish a solution for the formulated problems since the quantity $B(\tau, u)$ is proportional to the fourth power of the temperature (Ref.5, p.45).

It is also easy to solve the problem for the case where the medium cools off after "disconnecting" the external illumination at the instant of time $u = 0$. If irradiation occurs for an infinitely long time, we will have

$$\Delta B(\tau, u) = \beta H \int_{-\infty}^{0} B_\delta(\tau, u - u')\, du', \tag{78}$$

whence, using eq.(76), we obtain

$$\Delta B(\tau, u) = \beta H \int_u^{\infty} p(\tau, u')\, du'. \tag{79}$$

Let us now derive the asymptotic formula for $p(\tau, u)$ at $\lambda = 1$, which greatly facilitates the use of eqs.(77) and (79). Using the method presented at the end of Section 3, we easily derive, provided that $u \gg 1$, $u \gg \tau^2$,

$$p(\tau, u) \approx \frac{1+\tau}{2u\sqrt{\pi u}}. \tag{80}$$

Using eq.(80) in place of eq.(77), we obtain

$$\Delta B(\tau, u) \approx \beta H \left(1 - \frac{1+\tau}{\sqrt{\pi u}}\right), \tag{81}$$

while from eq.(79) we find /182

$$\Delta B(\tau, u) \approx \beta H \frac{1+\tau}{\sqrt{\pi u}}. \tag{82}$$

It follows from eqs.(81) and (82) that, for $\tau \approx 1$, an equilibrium state is established during an interval of dimensionless time $u \approx 10^3$, i.e., during the time $t \approx 10^3 \cdot t_1$. The parameters of the atmosphere are not given in Swihart's work (Ref.23). Therefore, we cannot compare the results of his work with the results obtained by calculation from our formulas. However, we can compare the equilibrium temperatures (for $u = \infty$). Close values are obtained for the equilibrium temperatures. We can assume that our simple solution of the problem is

sufficient for the purpose for which it is being used.

In conclusion, let us mention some other papers in which the theory of nonstationary radiation fields is applied to astrophysics. In a study on shock waves under space conditions, emerging from deep layers of the medium, S.A. Kaplan and I.A.Klimishin (Ref.24) determined the increment of radiation intensity before emergence of the wave. In this study, eq.(26) was used for the probability of escape of quanta from the medium $p(\tau, u)$. V.V.Sobolev (Ref.25) investigated nonstationary transfer of radiation within a star and obtained an estimate for the average time of energy output from any locus of the star.

REFERENCES

1. Milne, E.: J. London Math. Soc., Vol.1, p.40, 1926.
2. Holstein, T.: Phys. Rev., Vol.72, p.1213, 1947.
3. Sobolev, V.V.: Astron. Zh., Vol.29, No.4, p.406, 1952.
4. Sobolev, V.V.: Astron. Zh., Vol.29, No.5, p.517, 1952.
5. Sobolev, V.V.: Transfer of Radiant Energy in Stellar and Planetary Atmospheres (Perenos luchistoy energii v atmosferakh zvezd i planet). Gostekhizdat, 1956.
6. Kaplan, S.A., Klimishin, I.A., and Sivers, V.N.: Astron. Zh., Vol.37, No.1, p.9, 1960.
7. Kaplan, S.A. and Sivers, V.N.: Astron. Zh., Vol.37, No.5, p.824, 1960.
8. Kaplan, S.A.: Astron. Zh., Vol.39, No.4, p.702, 1962.
9. Minin, I.N.: Vestnik Leningr. Gos. Univ., No.13, p.137, 1959.
10. Minin, I.N.: Vestnik Leningr. Gos. Univ., No.19, p.124, 1962.
11. Minin, I.N.: Dokl. Akad. Nauk SSSR, Vol.154, No.5, p.1059, 1964.
12. Bellman, R., Kalaba, R., and Ueno, S.: Icarus, Vol.1, p.191, 1962. /183
13. Wing, M.: J. Math. and Mech., Vol.11, p.21, 1962.
14. Ueno, S.: J. Math. Analysis and Appl., Vol.4, No.1, p.1, 1962.
15. Wing, M.: An Introduction to Transport Theory. New York, 1962.
16. Ambartsumyan, V.A.: Dokl. Akad. Nauk ArmSSR, Vol.38, No.4, p.225, 1964.
17. Sobolev, V.V.: Astron. Zh., Vol.28, No.5, p.355, 1951.
18. Doetsch, G.: Handbook of Laplace Transformation (Handbuch der Laplace-Transformation). Vol.I, 1950; Vol.II, 1955; Vol.III, 1956.
19. Doetsch, G.: Handbook for Practical Application of the Laplace Transformation. Fizmatgiz, 1960.
20. Ditkin, V.A. and Kuznetsov, P.I.: Handbook on Operational Calculus (Spravochnik po operatsionnomu ischisleniyu). Gostekhizdat, 1951.
21. Gorbatskiy, V.G. and Minin, I.N.: Nonstationary Stars (Nestatsionarnyye zvezdy). Fizmatgiz, 1963.
22. Sobolev, V.V.: Izv. Akad. Nauk ArmSSR, Ser. Fiz.-Matem. Nauk, Vol.XI, No.5, p.39, 1958.
23. Swihart, T.: Astrophys. J., Vol.139, No.2, p.772, 1964.
24. Kaplan, S.A. and Klimishin, I.A.: Astron. Zh., Vol.37, No.2, p.281, 1960.
25. Sobolev, V.V.: Astron. Zh., Vol.37, No.3, p.387, 1960.

RANDOMIZED PROBLEM OF DIFFUSE REFLECTION /184

R.V.Ambartsumyan

The conventional theory of radiative transfer neglects the quantum nature of light so that its results are valid only in the limiting case of a large number of non-interacting quanta. In particular, it is important that the examined radiation beams be mutually incoherent since, in the conventional theory, the phenomenon of interference is disregarded. In the case of a small number of particles propagating in a medium, fluctuations begin to play a substantial role and the entire problem acquires a probabilistic character. In this case many different randomized solutions, depending on how randomization is introduced in an elementary scattering event of a particle, may generally correspond to a single macroscopic process (solution).

For example, let us examine the phenomenon of radiative transfer in the presence of both scattering and absorption. In the macroscopic theory, these two processes are introduced in the following manner: A quantity $I\,d\omega\,d\tau$ is absorbed from an elementary beam $I\,d\omega$ during passage through an optical thickness $d\tau$. Of this quantity, $\lambda I\,d\omega\,d\tau$ is scattered, and $(1-\lambda)\,I\,d\omega\,d\tau$ undergoes "true absorption".

When passing to the microscopic picture, it is natural to consider that λ is the probability of survival of a given quantum during an elementary scattering event, i.e., to consider that there are only two possibilities: survival or annihilation of the quantum. In many physical phenomena such a conception corresponds to the actual picture. However, one must never overlook another possibility, namely, that in which - during an elementary scattering event of a particle - n new particles will appear in its place with different probabilities p_n. In studying this more general case, it is natural to designate by λ the mathematical expectation $\Sigma np_n = \lambda$, and the difference between the cases $\lambda < 1$ and $\lambda > 1$ no longer is of such a fundamental character, although the numerical results, of course, are different.

1. Principal Equation of the Problem /185

For definitiveness, let us remain with the one-dimensional problem of diffuse reflection. A medium of optical depth τ in the given case acts as a particle multiplier in the sense that the reaction of the medium to the particle entering it from the left is diffuse reflection from the medium (also to the left) of a random quantity m of particles with probabilities P_m (see diagram below).

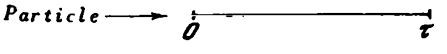

$\{p_n\}_{n=0}^{\infty}$. Our problem is to find these probabilities for a given distribution $\{p_n\}_{n=0}^{\infty}$. To render the problem well-defined, let us make the following assumptions relative to the behavior of the particles in the medium.

1. The mean free path of the particle inside the medium is distributed exponentially; it does not depend on the site of production of the particle, the direction of its flight, or the entire prehistory of the process.

2. The mean free path of the particle does not depend on the behavior of other particles during the lifetime of the given particle.

3. The number of new particles produced during an elementary scattering event does not depend on the site of occurrence of the scattering event, nor on the direction of flight of the scattered particle or on the entire prehistory of the process.

4. Each particle produced follows a direction of motion according to Bernoulli's scheme of independent trials with a probability 1/2.

Assumptions 1, 3, 4 mean that we are investigating a homogeneous and isotropic bar, and assumption 2 that we disregard the interaction of particles.

Let us denote

$$u(x) = \sum_{n=0}^{\infty} p_n x^n,$$

$$\varphi(x, \tau) = \sum_{n=0}^{\infty} P_n x^n.$$

For the function φ, let us derive a differential equation, using the so-called "invariance principle" (Ref.1). /186

To the main layer $[0, \tau]$ an additional layer of length $d\tau$ is added from the left. An event consisting of the medium reflecting a finite number of particles, is broken down into four nonoverlapping events:

a) No scattering events occur in the complementary layer.
b) The incident particle is scattered in the complementary layer, and the particles reflected from the main layer are not scattered in the complementary layer.
c) The incident particle is not scattered in the main layer but one particle of those reflected from the main layer is scattered therein.
d) Other possibilities.

As readily seen, the probability of the event d) has a magnitude of the order of $o(d\tau)$. Events a), b), c), and d) correspond to the addends on the right-hand side of the expansion:

$$\varphi(x, \tau + d\tau) = \sum_{k=0}^{\infty} P_k [1 - (k+1)\, d\tau]\, x^k +$$

$$+ d\tau \sum_{k=0}^{\infty} p_k \sum_{i=0}^{k} \frac{1}{2^k} C_k^i x^{k-i} \varphi^i(x, \tau) +$$
$$+ d\tau \sum_{n=0}^{\infty} nP_n x^{n-1} \sum_{k=0}^{\infty} p_k \sum_{i=0}^{k} \frac{1}{2^k} C_k^i x^{k-i} \varphi^i(x, \tau) + o(d\tau).$$

The limiting form of this relation is the equation

$$\frac{\partial \varphi(x, \tau)}{\partial \tau} = -\sum_{k=0}^{\infty} P_k (k+1) x^k +$$
$$+ \sum_{k=0}^{\infty} p_k \left[\frac{x + \varphi(x)}{2}\right]^k \cdot \left[1 + \sum_{n=0}^{\infty} nP_n x^{n-1}\right].$$

Introducing the function $U(x) = \sum_{k=0}^{\infty} \frac{p_k}{k+1} x^{k+1}$, the above-derived equation is written in the form

$$\frac{\partial \varphi(x, \tau)}{\partial \tau} = \frac{\partial}{\partial x}\left[-x\varphi(x, \tau) + 2U\left(\frac{x + \varphi(x)}{2}\right)\right]. \qquad (*)$$

The solution of this equation is not difficult since it can be reduced to a system of ordinary differential equations [see, for example, Stepanov (Ref.2)]. /187
We will discuss a few especially simple results, obtained for the limiting case of a finite bar ($\tau = \infty$).

The following reasoning is the usual method prompted by physical intuition in such cases: At an increase of τ to infinity, the quantity $\varphi(x, \tau)$ should tend to the limit $\varphi(x)$ so that $\frac{\partial \varphi(x, \tau)}{\partial \tau} \to 0$ as $\tau \to \infty$.

Passing to the limit as $\tau \to \infty$ in eq.(*), we obtain

$$\frac{\partial}{\partial x}\left[-x\varphi(x) + 2U\left(\frac{x + \varphi(x)}{2}\right)\right] = 0,$$

which, in turn, yields

$$-x\varphi(x) + 2U\left(\frac{x + \varphi(x)}{2}\right) = C. \qquad (1)$$

The selection of the constant of integration C on the basis of the condition $\varphi(1) = 1$ is not justified since one can a priori assume the existence of a positive probability P_∞ of reflection from the medium (in infinite time) of an infinite number of particles. This problem requires additional study.

2. Probability of the Reflection of an Infinite Number of Particles

Let us introduce the following auxiliary scheme: At the point x of a semi-

infinite medium let there appear a particle flying to the right (to the left) and let there be no other particles in the medium. We will designate by $\alpha(x)$ ($\beta(x)$) the probability of escape of an infinite number of secondary particles from the left end $x = 0$ of the medium. We note that

$$\alpha(0) = P_\infty.$$

It is easy to see that, if scattering of a particle flying to the right occurs at the point x, then the probability of escape from the left of an infinite /188 number of progeny of this particle will be equal to

$$1 - u\left[1 - \frac{\alpha(x) + \beta(x)}{2}\right].$$

Thus, for α and β we obtain the following system of equations:

$$\alpha(x) = \int_x^\infty e^{x-\xi}\left[1 - u\left(1 - \frac{\alpha(\xi) + \beta(\xi)}{2}\right)\right] d\xi, \tag{2}$$

$$\beta(x) = \int_0^x e^{\xi-x}\left[1 - u\left(1 - \frac{\alpha(\xi) + \beta(\xi)}{2}\right)\right] d\xi. \tag{3}$$

The system (2) - (3) has a trivial solution, and for eliciting P_∞ we must examine its nontrivial solutions.

Let us pose

$$Y(x) = \frac{\alpha(x) + \beta(x)}{2}. \tag{4}$$

Using eqs.(2) and (3) it is easy to check that

$$Y'(x) = \frac{\alpha(x) - \beta(x)}{2} \tag{4*}$$

and

$$Y''(x) = Y - 1 + u(1 - Y).$$

The order of the last equation is readily reduced. It proves to be equivalent to the equation

$$\frac{(Y')^2}{2} = \frac{Y^2}{2} - Y + U(1 - Y) + C'. \tag{5}$$

We can demonstrate that the functions $\alpha(x)$ and $\beta(x)$ have limits as $x \to \infty$, which we will denote by $\alpha(\infty)$ and $\beta(\infty)$. Then, $Y'(x) \to 0$ as $x \to \infty$ and, by virtue of eq.(4), $\alpha(\infty) = \beta(\infty) = Y(\infty)$. From eq.(2), by passing to the limit, we obtain the equation for

$$1 - Y(\infty) = u(1 - Y(\infty)), \tag{6}$$

which is easily solved by numerical methods. An important property is the /189 absence from this equation of positive solutions at $u'(1) = \lambda < 1$ and the presence of a unique positive solution at $\lambda > 1$.

This makes it possible to find the required value of the constant of integration C' in eq.(5), passing to the limit as $x \to \infty$:

$$C' = -\frac{Y^2(\infty)}{2} + Y(\infty) - U(1 - Y(\infty)).$$

Since $\beta(0) = 0$, then $Y(0) = \frac{\alpha(0)}{2}$ and also $Y'(0) = \frac{\alpha(0)}{2} = Y(0)$. Setting $x = 0$ in eq.(5) and substituting the value found for C', this will yield immediately the equation for $Y(0)$:

$$Y(0) = U(1 - Y(0)) + Y(\infty) - \frac{Y^2(\infty)}{2} - U(1 - Y(\infty)). \tag{7}$$

We can show that this equation always has a unique solution; therefore, at $\lambda \leq 1$ the value of $Y(0)$ proves to be equal to zero, together with $Y(\infty)$. At $\lambda > 1$ we have $Y(0) > 0$.

Thus, the system (6) - (7) readily gives $P_\infty = \frac{Y(0)}{2}$. As soon as P_∞ is known, we determine the constant in eq.(1), which takes the form

$$2U\left(\frac{x + \varphi(x)}{2}\right) - x\varphi(x) = 2U\left(\frac{2 - P_\infty}{2}\right) + P_\infty - 1. \tag{8}$$

Numerical results, i.e., the values of P_0, P_1, ..., from eq.(8) can be obtained by expanding the left-hand side in powers of the variable x.

Let us present the values of the first three probabilities for the case of $u(x) = e^{x-1}$:

$$P_0 = 2(1 - \ln 2) \approx 0.62,$$
$$P_1 = 4(1 - \ln 2) - 1 \approx 0.24,$$
$$P_2 = 2 - 4\ln^2 2 \approx 0.10.$$

In conclusion, we note that in the study of bars of infinite length /190 there arises the additional problem of calculating the critical length of the bar (for a given randomization) which can be determined as the lower bound of those values of τ for which $P_\infty > 0$. As demonstrated above, the critical length depends only on λ and can be calculated by the classical formula.

REFERENCES

1. Bellman, R., Kagiwata, H., Kalaba, R., and Prestrud, B.M.: Invariant Imbedding and Time-Dependent Transport Processes. Elsevier Publ. Co., New York, 1963.
2. Stepanov, N.N.: Course on Differential Equations (Kurs differentsial'nykh uravneniy). Gostekhizdat, 1953.

MODELS OF STELLAR ATMOSPHERES /193

V.V.Sobolev

An important aspect in theoretical astrophysics is the problem of calculating models of stellar atmospheres, i.e., finding the distribution of density, pressure, temperature, and other physical quantities in the atmosphere. On the basis of solution of this problem, the continuous and line spectra of a star are calculated.

When calculating the model of a stellar atmosphere, two quantities are assumed as given: the effective temperature of the star T_e and the acceleration due to gravity g in the stellar atmosphere. These quantities are determined by the following formulas

$$\sigma T_e^4 = \frac{L}{4\pi R^2}, \quad g = G\frac{M}{R^2}, \tag{1}$$

where M is the mass, R is the radius, L is the luminosity of the star, G is the gravitation constant, and σ is the Stefan constant. In addition to T_e and g the chemical composition of the stellar atmosphere is also assumed as given.

The calculation of models of stellar atmospheres is based on a number of assumptions. We will list the most essential.

1) The thickness of the atmosphere ΔR is assumed as very small with respect to the radius of the star R, as a consequence of which it can be considered that the atmospheric layers are plane-parallel. For most stars, the validity of this assumption does not cause doubt; for example, for the sun it is found that $\frac{\Delta R}{R} \approx 10^{-3}$.

2) It is assumed that the energy sources are located in the interior portion of the star and the energy is only transferred outward through the atmosphere. Here radiation is considered to be the basic mechanism of energy transfer. However, in some cases convective energy transfer must also be taken into consideration.

3) Thermodynamic equilibrium at a temperature T is assumed to be established at each point of the atmosphere. It is obvious that this assumption becomes /194 less accurate with decrease in depth.

4) It is assumed that mechanical equilibrium of the atmosphere exists or - more exactly - equilibrium of each volume element under the effect of three forces: gravity, gas pressure, and radiation pressure. This assumption does

not hold for variable stars only.

5) Constancy of the chemical composition in the atmosphere is assumed, but it is not precluded that the chemical composition changes substantially with depth.

6) When calculating models of stellar atmospheres, absorption of radiant energy is taken into account only in the continuous spectrum. Sometimes, also the effect of line absorption (so-called "blanketing effect") is taken into account.

Based on these assumptions, let us write the principal equations of the theory of stellar atmospheres.

Let $I_\nu(r, \vartheta)$ be the intensity of radiation proceeding at a distance r from the center of the star at an angle ϑ to the radius vector. For an atmosphere consisting of plane-parallel layers, the equation of radiative transfer has the form

$$\cos\vartheta \frac{dI_\nu}{dr} = -\alpha_\nu I_\nu + \varepsilon_\nu, \tag{2}$$

where α_ν and ε_ν are the absorption and emission coefficients, respectively.

Let us consider that the atmosphere contains no energy sources and sinks. Therefore, the quantity of energy emitted by a given volume element should be equal to the quantity of energy absorbed by this volume, i.e., we should have

$$\int_0^\infty \varepsilon_\nu d\nu = \frac{1}{2}\int_0^\infty \alpha_\nu d\nu \int_0^\pi I_\nu \sin\vartheta\, d\vartheta. \tag{3}$$

In place of eq.(3) we can use the following condition of constancy of the radiation flux in the atmosphere:

$$H = 2\pi \int_0^\infty d\nu \int_0^\pi I_\nu \cos\vartheta \sin\vartheta\, d\vartheta = \text{const} = \sigma T_e^4, \tag{4}$$

which follows from eqs.(2) and (3).

The assumption of local thermodynamic equilibrium in the atmosphere permits use of the Kirchhoff-Planck law: /195

$$\varepsilon_\nu = \alpha_\nu B_\nu(T), \tag{5}$$

where $B_\nu(T)$ is the Planck radiation intensity, i.e.,

$$B_\nu(T) = \frac{2h\nu^3}{c^2} \cdot \frac{1}{e^{\frac{h\nu}{kT}} - 1}. \tag{6}$$

The condition of mechanical equilibrium in the atmosphere yields

$$dp = -g\rho dr, \tag{7}$$

where p is the pressure and ρ the density. If we disregard light pressure (which, for most stars, plays no role), then the pressure p is expressed in terms of the density ρ and the temperature T by means of the equation of state of the gas:

$$p = \frac{k}{\mu m_H}\rho T, \tag{8}$$

where μ is the average molecular weight. Since the value of μ is calculated per particle (including the free electron), the Saha ionization formula must be used in determining μ.

To these equations we must add the expression for the absorption coefficient α_ν which depends on the physical conditions (i.e., on ρ and T) and on the chemical composition. It is readily obvious that these equations, together with the aforementioned expression for α_ν, permit determining the unknown values of ρ and T in relation to depth in the atmosphere.

Let us transform the above equations into another form. For this, let us introduce the optical depth

$$\tau_\nu = \int_r^\infty \alpha_\nu\, dr. \tag{9}$$

Then, the equation of radiative transfer (2), with consideration of eq.(5), takes the form

$$\cos\vartheta \frac{dI_\nu}{d\tau_\nu} = I_\nu - B_\nu(T). \tag{10}$$

Solving eq.(10) for I_ν and substituting the obtained expression of I_ν in terms of $B_\nu(T)$ into eqs.(3) and (4), we obtain /196

$$\int_0^\infty \alpha_\nu B_\nu(T)\, d\nu = \frac{1}{2}\int_0^\infty \alpha_\nu d\nu \int_0^\infty \mathrm{Ei}_1|\tau_\nu - \tau'_\nu| B_\nu(T')\, d\tau'_\nu, \tag{11}$$

$$2\pi\int_0^\infty d\nu\left[\int_{\tau_\nu}^\infty \mathrm{Ei}_2(\tau'_\nu - \tau_\nu) B_\nu(T')\, d\tau'_\nu - \right.$$

$$\left. - \int_0^{\tau_\nu} \mathrm{Ei}_2(\tau_\nu - \tau'_\nu) B_\nu(T')\, d\tau'_\nu\right] = \sigma T_e^4, \tag{12}$$

where

$$\mathrm{Ei}_1 x = \int_1^\infty e^{-xz}\frac{dz}{z}, \quad \mathrm{Ei}_2 x = \int_1^\infty e^{-xz}\frac{dz}{z^2}. \tag{13}$$

It is obvious that eq.(11), together with the condition $H = \sigma T_e^4$, is equivalent to eq.(12) since differentiation of eq.(12) with respect to r leads to eq.(11).

Substitution of eq.(8) into eq.(7) yields

$$\frac{d}{dr}\left(\frac{k}{\mu m_{\text{H}}}\rho T\right) = -g\rho. \tag{14}$$

Thus, to determine the two unknown functions ρ and T with respect to r, we have eqs.(14) and (12) [or eq.(11) with the condition $H = \sigma T_e^4$]. The values of α_ν and μ entering these equations depend only on ρ and T (for a given chemical composition).

After finding the values of ρ and T with respect to r it becomes easy to calculate the energy distribution in the continuous spectrum of the star. For this purpose, we used the following formula which determines the radiation flux escaping from the atmosphere at a frequency ν:

$$H_\nu = 2\pi \int_0^\infty B_\nu(T)\,\mathrm{Ei}_2\,\tau_\nu\, d\tau_\nu. \tag{15}$$

The system of equations (12) and (14) is quite difficult to solve. For this reason, so far as we know, the exact solution of this system has never been obtained. Still, it is of considerable interest to derive an exact solution /197 since approximate solutions are not very reliable. It is hoped that the use of electronic computers will permit obtaining numerical solutions of eqs.(12) and (14) with a high accuracy. At the same time, one can attempt to find exact analytic solutions of these equations for various particular expressions of the absorption coefficient.

Until now, eqs.(12) and (14) have been solved only approximately. This is done by reducing the problem to the case where the absorption coefficient no longer depends on the frequency. For this, we will denote α_ν by α and τ_ν by τ. We will also introduce the designation

$$\int_0^\infty B_\nu(T)\, d\nu = B(\tau). \tag{16}$$

Then eq.(11) takes the form

$$B(\tau) = \frac{1}{2}\int_0^\infty \mathrm{Ei}\,|\tau - \tau'|\, B(\tau')\, d\tau'. \tag{17}$$

Equation (17), known as the Milne equation, has been studied thoroughly. By means of the solution of this equation, taking into account that, at local thermodynamic equilibrium,

$$B(\tau) = \frac{\sigma}{\pi} T^4, \tag{18}$$

we obtain

$$T^4 = \frac{3}{4} T_e^4\,[\tau + q(\tau)], \tag{19}$$

where $q(\tau)$ is the Hopf function [monotonically increasing from $q(0) = 1/\sqrt{3}$

to $q(\infty) = 0.71$].

Let us also represent the absorption coefficient α as $\alpha = \varkappa\rho$ and take into account that

$$d\tau = -\varkappa\rho\, dr. \tag{20}$$

Then in place of eq.(7) we obtain /198

$$\frac{dp}{d\tau} = \frac{g}{\varkappa}. \tag{21}$$

Here, the quantity $\varkappa$ can be considered a function of T and ρ. Since the dependence of T on τ is given by eq.(19), then eq.(21) will furnish the quantity p as a function of τ. The transition from τ to r can be made by means of eq.(20).

Thus, in the case of frequency-independence of the absorption coefficient, calculation of the model of a stellar atmosphere can be performed exactly. As already mentioned, it is precisely to this case that the actual problem in which the absorption coefficient is a complex function of frequency, is approximately reduced. For this purpose, we replace the quantity α by the average absorption coefficient. Averaging of the absorption coefficient α_ν with respect to frequency can be done by various methods. In investigations on the calculation of stellar atmosphere models this averaging is done by one of the following formulas:

1) The Planck mean:

$$\alpha = \frac{\int_0^\infty \alpha_\nu B_\nu(T)\, d\nu}{\int_0^\infty B_\nu(T)\, d\nu}; \tag{22}$$

2) The Rosseland mean:

$$\frac{1}{\alpha} = \frac{\int_0^\infty \frac{1}{\alpha_\nu}\frac{\partial B_\nu(T)}{\partial T}\, d\nu}{\int_0^\infty \frac{\partial B_\nu(T)}{\partial T}\, d\nu}; \tag{23}$$

3) The Chandrasekhar mean:

$$\alpha = \int_0^\infty \alpha_\nu \frac{H_\nu^0}{H}\, d\nu, \tag{24}$$

where H_ν^0 is the radiation flux in an atmosphere in which the absorption coefficient does not depend on frequency.

The use of eqs.(19) - (21), with the mean absorption coefficient determined by one of these formulas, will furnish the approximate distribution of density and temperature in a real atmosphere. After this, the absorption /199

coefficient α_ν at any depth and thus the energy distribution in the continuous spectrum of the star, can be found by means of eq.(15).

The described approximate method of calculating stellar atmosphere models and continuous spectra of stars has been used repeatedly. Various authors have employed different formulas for determining the mean absorption coefficient (see Munch's article in the collection "Stellar Atmospheres", Izd. Inostr. Lit., 1963).

To estimate the error of the solution it is conventional to calculate, at different depths, the quantity

$$\delta = \frac{\Delta H}{H}, \tag{25}$$

where H is the radiation flux which should be constant in the atmosphere, and ΔH is the deviation of the flux from the value H in the approximate solution. If the quantity δ is small, the solution can be considered as satisfactory. However, it should be remembered that the quantity δ apparently is not a reliable criterion for the accuracy of the solution, i.e., even with a poor solution this quantity might be small. This again emphasizes the desirableness of obtaining an exact solution of eqs.(12) and (14).

It follows from the above statements that the most important quantity in the theory of stellar atmosphere is the absorption coefficient α_ν. This quantity is determined by all atoms in a given volume element, i.e., it represents a very complex function of frequency, density, temperature, and chemical composition. However, in stellar atmospheres the situation is simplified by the fact that hydrogen is the most widespread element. Therefore, absorption of radiant energy by hydrogen atoms plays the major role in the atmospheres of hot stars (in the case of very hot stars it is necessary to take also absorption by helium into consideration). Nevertheless, the role of hydrogen in the atmospheres of cool stars cannot be appreciable since, at low temperatures, hydrogen is almost completely in the ground state and absorbs only energy beyond /200 the boundary of the Lyman series (very little at low temperatures). Astrophysicists have long sought the source of absorption in the atmospheres of cool stars; finally, this source was found to be the negative ion of hydrogen, i.e., a hydrogen atom with an electron attached. The discovery of the negative ion of hydrogen as the main source of absorption in the atmospheres of cool stars (beginning with class F) and the calculation of the absorption coefficient α_ν due to this ion must be considered one of the most outstanding achievements of theoretical astrophysics.

The agreement between theoretical and observed energy distribution in the stellar spectrum is the criterion for correctness of the theory of stellar atmospheres. The calculated solar spectrum (on the assumption of a negative hydrogen ion as the main absorption source) proved to be in satisfactory agreement with the observed spectrum. Until recently, it was considered that, for hot stars, there was agreement between the calculated and observed spectra. However, this result pertains only to the visible spectrum region. Recent extraterrestrial observations showed that observation and theory do not agree in the far-ultraviolet region (at $\lambda < 2400$ Å) for stars of class B. The explanation for this divergence constitutes one of the important problems of the

theory of stellar spectra.

The following papers by V.G.Buslavskiy and A.K.Kolesov present results of calculating atmosphere models for various types of stars.

CONTINUOUS SPECTRA OF HOT WHITE DWARFS /201

A.K.Kolesov

The spectra of white dwarfs differ considerably from the spectra of main-sequence stars. These differences are due mainly to high densities in the atmospheres of white dwarfs. For example, broadening and overlapping of Balmer lines due to the Stark effect leads to a drop in radiation flux before the limit of the Balmer series. The influence of the lines on the appearance of the continuous spectrum increases with an increase in density. At high densities, the phenomenon of preionization of hydrogen atoms, i.e., the destruction of high quantum states under the effect of pressure, also becomes essential. Preionization causes a drop in ionization potential and, consequently, shows up in a shift of the Balmer jump toward lower frequencies.

Appearance of the continuous spectrum also depends to a large extent on the chemical composition of the stellar atmosphere. The characteristics of the spectra of a number of white dwarfs may be due to deviations of their chemical composition from normal. For example, the relative content of hydrogen in the atmospheres of these stars may be lower, and the content of helium higher, than in the atmospheres of main-sequence stars.

Observations of hot white dwarfs (Ref.1, 2) show that they are distinctly divided into two groups with respect to appearance of their spectra. One of these is made up by stars of the spectroscopic type DA, whose spectra contain hydrogen lines but no helium lines. The second group is made up by stars of types DO and DB with helium lines but without hydrogen lines in the spectra, He I lines being seen for the DB type stars and He II and He I lines for the DO type stars. Probably, the atmospheres of white dwarfs of type DA consist mainly of hydrogen, whereas the atmospheres of white dwarfs of types DO and DB consist of helium. Therefore, in what follows we will examine stars with hydrogen and helium atmospheres.

Models of hydrogen and helium atmospheres were calculated in papers /202 by the author (Ref.3, 4). The surface temperature T_0 and the acceleration due to gravity g were taken as the model parameters. The cases T_0 = 12,000, 15,000, and 20,000° (and, for helium atmospheres, also T_0 = 30,000°), log g = 6, 8, and 10 were examined. Taking into account the low accuracy of the observational data for continuous spectra of white dwarfs, we will limit the calculation to the first approximation and use the distribution of the temperature T with the optical depth τ in an approximation to a gray atmosphere:

$$T^4(\tau) = \sqrt{3}\,T_0^4[\tau + q(\tau)].$$

The distribution of pressure p with depth was found by numerical integration (using the Runge-Kutta method) of the equation of mechanical equilibrium

$$\frac{dp(\tau)}{d\tau} = \frac{g}{\bar{\varkappa}(p_e, T)}$$

for the boundary condition p(0) = 0. As the mean absorption coefficient $\bar{\varkappa}$, we used the Rosseland mean. The correlation of the electron pressure p_e with p and τ was found by the Saha ionization formula.

An idea of the physical conditions in the atmospheres of white dwarfs can be obtained from Tables 1 and 2. Table 1 gives the results of calculating a model of a hydrogen atmosphere with $T_0 = 20{,}000^\circ$, log g = 8, while Table 2 gives the results of calculating the model of a helium atmosphere with the same parameters. In these tables, the pressure p, the electron concentration n_e, the density ρ, and the geometric depth h are given as a function of the optical depth τ. The geometric depth is arbitrarily calculated from the same level in the stellar atmosphere, where $T = T_e$.

TABLE 1

/203

MODEL OF HYDROGEN ATMOSPHERE WITH $T_0 = 15{,}000^\circ$, log g = 8

τ	$p \cdot 10^{-5}$, $\frac{dyne}{cm^2}$	$n_e \cdot 10^{-17}$, cm^{-3}	$\rho \cdot 10^{7}$, $\frac{gm}{cm^3}$	$h \cdot 10^{-4}$, cm
0.1	0.92	0.200	0.364	—3.30
0.2	1.41	0.296	0.536	—2.20
0.4	2.24	0.448	0.799	—1.01
0.6	3.00	0.577	1.02	—0.17
0.8	3.72	0.694	1.21	0.48
1.0	4.43	0.802	1.39	1.03
2.0	7.86	1.28	2.18	2.91
3.0	11.2	1.68	2.86	4.23
4.0	14.4	2.04	3.45	5.25
5.0	17.5	2.37	4.00	6.08

TABLE 2

MODEL OF HELIUM ATMOSPHERE WITH $T_0 = 15{,}000^\circ$, log g = 8

τ	$p \cdot 10^{-7}$, $\frac{dyne}{cm^2}$	$n_e \cdot 10^{-17}$, cm^{-3}	$\rho \cdot 10^{8}$ $\frac{gm}{cm^3}$	$h \cdot 10^{-3}$, cm
0.1	1.03	0.378	3.08	—3.19
0.2	1.57	0.664	4.53	—1.75
0.4	2.16	1.26	5.85	—0.60
0.6	2.49	1.98	6.40	—0.07
0.8	2.72	2.76	6.70	0.28
1.0	2.88	3.61	6.82	0.52
2.0	3.24	8.28	6.53	1.07
3.0	3.43	13.4	6.02	1.36
4.0	3.56	18.2	5.51	1.59
5.0	3.65	22.4	5.11	1.76

Density inversion which is observed at large optical depths indicates that, at these depths, energy transfer by convection plays a role.

It is interesting to note that the continuous spectrum of white dwarfs is created in a rather thin layer of the atmosphere. A geometric distance of $\Delta h = 430$ m corresponds to the interval $\Delta\tau$ from $\tau = 0.1$ to $\tau = 1.0$ in the hydrogen atmosphere with $T_0 = 15{,}000^\circ$, log g = 8. In the case of the helium atmosphere with $T_0 = 15{,}000^\circ$, log g = 8, a value of $\Delta h = 36$ m corresponds to this interval $\Delta\tau$.

Using the results of calculation of model atmospheres, we found the energy distribution in the spectra of white dwarfs. The flux was calculated by the formula

$$H_\nu = \pi F_\nu = 2\pi \int_0^\infty B_\nu(\tau_\nu)\, \mathrm{Ei}_2(\tau_\nu)\, d\tau_\nu,$$

where B_ν is the Planck function, and /204 τ_ν is the monochromatic optical depth.

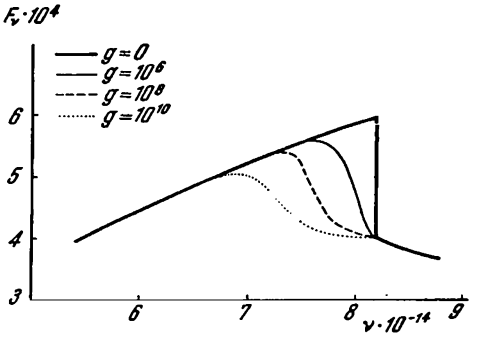

Fig.1

In the case of hydrogen atmospheres we took into account the effect of preionization. Absorption in the Balmer continuum was accounted for, beginning with the frequency

$$\nu_2 = \frac{\chi}{4h} - \frac{3e^2}{h}\sqrt[3]{\frac{4\pi n_i}{3}}\,\Gamma\left(\frac{2}{3}\right),$$

where χ is the ionization potential of the hydrogen atom, h is the Planck constant, e is the electron charge, n_i is the ion concentration, and Γ is the gamma-function. Preionization of hydrogen atoms produces an extensive change in the energy distribution of the spectrum before the Balmer series limit. The intensity of the continuous spectrum in this portion drops noticeably, and the magnitude of the Balmer jump decreases. At sufficiently large acceleration of

TABLE 3 /205

COLOR INDICES OF HYDROGEN WHITE DWARFS

T_0 / log g	12 000°			15 000°			20 000°		
	U−B	B−V	U−V	U−B	B−V	U−V	U−B	B−V	U−V
6	−0.73	−0.14	−0.87	−0.95	−0.16	−1.11	−1.09	−0.22	−1.32
8	−0.66	−0.13	−0.79	−0.94	−0.15	−1.09	−1.08	−0.22	−1.30
10	−0.71	−0.05	−0.76	−0.94	−0.11	−1.05	−1.08	−0.20	−1.28

TABLE 4

COLOR INDICES OF HELIUM WHITE DWARFS

T_0	log g	U − B	B − V	U − V
12 000°	8	−0.92	−0.17	−1.09
15 000°	8	−1.05	−0.21	−1.26
20 000°	8	−1.13	−0.26	−1.39
30 000°	6	−1.25	−0.31	−1.56
30 000°	10	−1.26	−0.32	−1.58

TABLE 5

INFLUENCE OF ABSORPTION LINES ON COLOR INDICES

Star	Spectrum	U − B Obs.	B − V Obs.	Δ(U − B)	Δ (B − V)	U − B Corr.	B − V Corr.
HZ 14	DA	−1.04	−0.15	+0.03	−0.04	−1.01	−0.19
L 1244−26	DA	−0.98	−0.15	+0.04	−0.04	−0.94	−0.19
He 3	DA	−0.90	−0.06	+0.07	−0.07	−0.83	−0.13
W 1346	DA	−0.87	−0.07	+0.07	−0.08	−0.80	−0.15
HZ 2	DA	−0.88	−0.05	+0.05	−0.06	−0.83	−0.11
L 930−80	DB	−0.99	−0.14	+0.03	−0.03	−0.96	−0.17
L 1573−31	DB	−0.97	−0.09	+0.02	−0.04	−0.95	−0.13

gravity g the Balmer jump virtually becomes invisible. The effect of preionization on the shape of the continuous spectrum for the case $T_0 = 12{,}000^\circ$ is shown in Fig.1.

Based on the energy distribution curves in the spectra and on the standard curves of spectral sensitivity of the apparatus used, we calculated, in the system U, B, V, the color indices U-B, B-V, and U-V. The results are shown in Tables 3 and 4.

Figure 2 represents the U-B, B-V diagram for white dwarfs. In this diagram, the theoretical ratios between the color indices U-B and B-V (for the case of log g = 8) are compared with the observed positions of DA, DO, and /206
DB type stars on the diagram. As a rule, white dwarfs are located to the right of the theoretical curve. This is explained by the influence of absorption lines. The Balmer lines in the spectra of hydrogen white dwarfs and the most intense helium lines (λλ 4472, 4026, etc.) in the spectra of helium white dwarfs are concentrated mainly in the transmittance zone of the filter B. The effect of the lines manifests itself in a decrease in U-B and an increase in B-V. For several white dwarfs for which observational data on the line profiles in the spectra are available, we calculated the corrections Δ (U-B) and Δ (B-V) for the influence of the absorption lines (Table 5). The corrected observational values of the color indices on the U-B, B-V diagram are close to the theoretical curves.

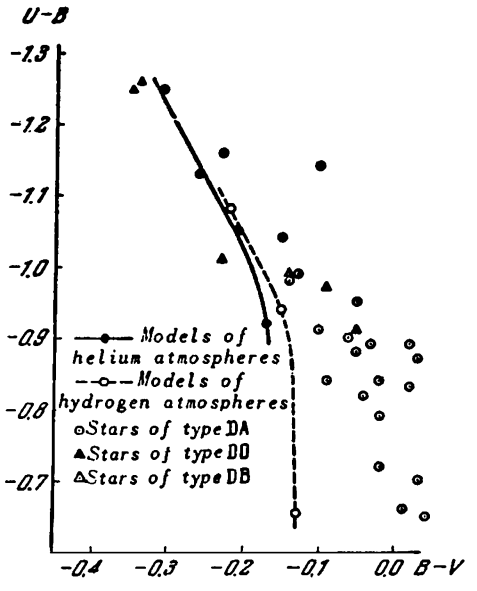

Fig.2

The color index U-V, at g ≈

≈ 10^8 $\frac{cm}{sec^2}$, depends weakly on g and is scarcely distorted by the effect of the absorption lines. Therefore, the quantity U-V can serve for determining the temperatures of white dwarfs. Their temperatures are found from Tables 3 and 4, by comparing the theoretical and observational values of U-V. It turns out that DA type stars occupy a wide temperature range. The hottest have a T_0 of about 20,000° whereas for the coolest, T_0 < 12,000°. White dwarfs of type DB are situated in the T_0 range from 10,000 to 15,000°. Stars of type DO have T_0 of the order of 30,000° and are the hottest of white dwarfs known.

/207

REFERENCES

1. Greenstein, J.L.: Handbook of Physics (Handbuch der Physik). Vol.51, p.161, 1958.
2. Greenstein, J.L.: Stellar Atmospheres. Chapt.19, Chicago, 1960. [Russian translation in Collection: "Stellar Atmospheres" ("Zvezdnyye atmosfery"), Chapter 19, Izd. Inostr. Lit., 1963.]
3. Kolesov, A.K.: Astron. Zh., Vol.41, p.240, 1964.
4. Kolesov, A.K.: Astron. Zh., Vol.41, p.485, 1964.

MODEL ATMOSPHERES OF MAIN-SEQUENCE STARS OF CLASS M /208

V.G.Buslavskiy

It is known from spectroscopic observations that practically the entire observed continuous spectrum of stars of late spectral classes is distorted by absorption bands of various molecular compounds. When constructing model atmospheres of late stars this circumstance should be taken into account; furthermore, the basic physical characteristics of many molecules important for astrophysics are either completely unknown or very unreliable. For example, for the molecule TiO, whose absorption bands are a very noticeable feature of stars of class M, the electron transition moments are completely unknown. This explains the fact that heretofore practically no model atmospheres of stars of late spectral classes have ever been calculated.

A model atmosphere of a main-sequence star of class M was calculated by Osterbrock (Ref.1) who assumed that the opacity of the atmosphere is determined only by absorption by negative hydrogen ions (absorption during free-free transitions was disregarded).

Several model atmospheres of red giants were calculated by Dumezil-Curien (Ref.2).

In the present paper, two model atmospheres of main-sequence stars of class M0 are constructed on the assumption that the atmosphere consists of hydrogen and metals. Assuming that these models approximately reflect the structure of real stars, we used them for investigating the absorption bands of TiO in spectra of main-sequence stars of class M.

1. Models of Stellar Atmospheres /209

Let us assume that the atmosphere of the star is in hydrostatic equilibrium, i.e., that at each point of the atmosphere the total pressure counterbalances the weight of the overlying layers. The equation of equilibrium has the form:

$$\frac{dp}{d\tau} = \frac{gp}{\alpha}, \tag{1}$$

where τ is the optical depth corresponding to the mean absorption coefficient α, p is the pressure at a depth τ, ρ is the density, and g is the acceleration due to gravity at the surface of the star.

It has been shown earlier (Ref.3), after an investigation of sources of opacity of a stellar atmosphere consisting of hydrogen and metals, that we have the following opacities created by absorption by negative hydrogen ions and metal atoms, namely,

$$\alpha_\nu = \alpha_\nu(H^-) + \alpha_\nu(M); \quad \alpha = \alpha(H^-) + \alpha(M), \tag{2}$$

where α_ν, $\alpha_\nu(H^-)$ and $\alpha_\nu(M)$ are the "total" absorption coefficient at a frequency ν of the continuous spectrum, the coefficient of absorption by ions H^-, and the coefficient of absorption by atoms of metals, while α, $\alpha(H^-)$, and $\alpha(M)$ are the corresponding mean absorption coefficients.

Usually, in investigating absorption by metal atoms these are replaced by some "average" metal, assuming the latter to be hydrogen-like. However [see Bates (Ref.4)] such a substitution leads to errors by a factor of 10 and sometimes of 100. Therefore, it is preferable to replace all metals by some real metal. We selected sodium as this metal. The following considerations were used as basis for this choice: It is known from observations that the continuous spectrum of late stars is practically "cut off" in the ultraviolet at $\lambda_0 \approx$ $\approx$ 3000 - 2000 Å. Therefore, it is obvious that metals can furnish only a small contribution to the "total" mean absorption coefficient, and their primary role is that of suppliers of free electrons in the stellar atmosphere. Since radiations at $\lambda < \lambda_0$ in the atmospheres of late stars have a low intensity, the free electrons are formed mainly upon ionization of metals with low ionization /210 potentials, i.e., alkaline and alkaline-earth atoms, one of which can be selected to represent the average. Thus, we will take

$$\alpha_\nu(M) \approx \alpha_\nu(Na), \ \alpha(M) \approx \alpha(Na). \tag{3}$$

Since the mean absorption coefficients are functions of the temperature, along with eq.(1) we should prescribe the temperature distribution in the stellar atmosphere. This has the form

$$T^4(\tau) = \sqrt{3}\, T_0^4 [\tau + q(\tau)], \tag{4}$$

where T_0 is the surface temperature of the star, and $q(\tau)$ is a slowly varying function whose values range between $q(0) = 0.58$ and $q(\infty) = 0.71$.

Let us integrate eq.(1) under the following conditions: medium consisting of hydrogen and metals, hydrogen-metals ratio equal to 10^4, $T_0 = 3000^\circ K$, and $g = 10^5$.

For a numerical integration of eq.(1), the boundary conditions must be known. The condition of $p = 0$ at $\tau = 0$ is not suitable since, at $\tau = 0$, the right-hand side of eq.(1) becomes infinite. We proceed in the following manner to select the boundary condition: In the surface layers $T \approx T_0$ and $\rho = \rho(p)$, $\alpha = \alpha(p)$. Then, integrating the equation

$$d\tau = -\frac{\alpha(p)\,dp}{g\rho(p)}, \tag{5}$$

we obtain

$$\tau = \frac{1}{g}\int_0^p \frac{\alpha(p')\,dp'}{\rho(p')} = \frac{1}{m_H g}\int_0^p \frac{\alpha(p')\,dp'}{n + n_2} = \frac{1}{m_H g}\int_0^p \frac{\alpha(p')\,dp'}{2n - n_1}, \tag{6}$$

where m_H is the mass of the hydrogen atom, n is the total number of hydrogen particles, i.e., atoms and molecules, n_1 is the number of neutral hydrogen atoms, and n_2 is the number of hydrogen molecules in 1 cm^3. Determining n_1 from the

dissociation formula

$$\frac{n_1^2}{n_2} = f_2(T_0), \tag{7}$$

where $f_2(T_0)$ is a known function of temperature taken for $T = T_0$, we obtain /211

$$\tau = \frac{kT_0}{2m_H g}\int_0^p \left(1 + \frac{1}{\sqrt{1+\frac{4p'}{kT_0 f_2(T_0)}}}\right)\frac{\alpha(p')}{p'}\,dp'. \tag{8}$$

We find from eq.(8) the boundary condition

$$p = 2.849\cdot 10^3 \quad \text{for} \quad \tau = 0.001. \tag{9}$$

Let us next integrate eq.(1) with the boundary condition (9) in the following manner: First we will neglect absorption by metal atoms and later take it into account. The results of the calculations are shown in Table 1, where the pressure calculated with and without consideration of absorption by metal atoms is designated, respectively, by p and p′. A comparison of p and p′ shows that absorption by metal atoms has little effect on the model atmosphere.

TABLE 1

τ	$T(\tau)$	$p'(\tau)$	$p(\tau)$	τ	$T(\tau)$	$p'(\tau)$	$p(\tau)$
0.001	3002	$2.849\cdot 10^3$	$2.849\cdot 10^3$	0.14	3215	$7.603\cdot 10^4$	$7.583\cdot 10^4$
0.002	3003	4.358	4.353	0.16	3241	8.175	8.153
0.003	3005	5.658	5.649	0.18	3267	8.687	8.663
0.004	3007	6.846	6.833	0.20	3293	9.135	9.110
0.005	3008	7.959	7.943	0.30	3402	$1.082\cdot 10^5$	$1.078\cdot 10^5$
0.006	3010	9.018	8.999	0.40	3498	1.201	1.197
0.007	3011	$1.004\cdot 10^4$	$1.001\cdot 10^4$	0.50	3584	1.293	1.289
0.008	3013	1.100	1.097	0.60	3662	1.369	1.365
0.009	3015	1.195	1.192	0.70	3734	1.437	1.432
0.01	3016	1.288	1.284	0.80	3802	1.498	1.493
0.02	3033	2.116	2.110	0.90	3866	1.554	1.549
0.03	3049	2.831	2.823	1.00	3927	1.607	1.602
0.04	3065	3.468	3.459	1.2	4039	1.711	1.707
0.05	3082	4.045	4.034	1.4	4143	1.813	1.809
0.06	3098	4.572	4.560	1.6	4239	1.914	1.910
0.07	3114	5.054	5.041	1.8	4328	2.013	2.009
0.08	3130	5.496	5.482	2.0	4413	2.111	2.107
0.09	3147	5.902	5.887	2.5	4604	2.266	2.261
0.10	3163	6.277	6.261	3.0	4776	2.365	2.360
0.12	3189	6.969	6.951				

2. Energy Distribution in the Stellar Spectrum /212

The energy distribution in the stellar spectrum is given by the formula [see, for example, Aller (Ref.5)]

$$H_\nu = 2\pi \int_0^\infty B_\nu(T)\, \mathrm{Ei}_2(\tau_\nu)\, d\tau_\nu, \tag{10}$$

where H_ν is the radiation flux escaping from the star at a frequency ν, $B_\nu(T)$ is the Planck function, $\mathrm{Ei}_2(\tau_\nu)$ is an integral exponential function of the second order, and τ_ν is the optical depth at the frequency of the continuous spectrum.

TABLE 2

λ (Å)	$T_* = 2000°$	
	H'_ν	H^*_ν
18 000	$0.256 \cdot 10^{-4}$	$0.676 \cdot 10^{-5}$
14 000	$0.892 \cdot 10^{-5}$	$0.520 \cdot 10^{-5}$
12 000	$0.427 \cdot 10^{-5}$	$0.390 \cdot 10^{-5}$
10 000	$0.206 \cdot 10^{-5}$	$0.236 \cdot 10^{-5}$
6 000	$0.172 \cdot 10^{-6}$	$0.166 \cdot 10^{-6}$
4 000	$0.134 \cdot 10^{-7}$	$0.300 \cdot 10^{-8}$

λ (Å)	$T_* = 2500°$	
	H'_ν	H^*_ν
18 000	$0.366 \cdot 10^{-4}$	$0.140 \cdot 10^{-4}$
14 000	$0.199 \cdot 10^{-4}$	$0.130 \cdot 10^{-4}$
12 000	$0.132 \cdot 10^{-4}$	$0.112 \cdot 10^{-4}$
10 000	$0.881 \cdot 10^{-5}$	$0.831 \cdot 10^{-5}$
6 000	$0.183 \cdot 10^{-5}$	$0.134 \cdot 10^{-5}$
4 000	$0.391 \cdot 10^{-6}$	$0.692 \cdot 10^{-7}$

λ (Å)	$T_* = 3000°$	
	H'_ν	H^*_ν
18 000	$0.468 \cdot 10^{-4}$	$0.232 \cdot 10^{-4}$
14 000	$0.381 \cdot 10^{-4}$	$0.241 \cdot 10^{-4}$
12 000	$0.289 \cdot 10^{-4}$	$0.228 \cdot 10^{-4}$
10 000	$0.225 \cdot 10^{-4}$	$0.189 \cdot 10^{-4}$
6 000	$0.802 \cdot 10^{-5}$	$0.542 \cdot 10^{-5}$
4 000	$0.235 \cdot 10^{-5}$	$0.561 \cdot 10^{-6}$

TABLE 3

λ (Å)	H_ν
4082	$0.159 \cdot 10^{-5}$
3500	$0.115 \cdot 10^{-5}$
3000	$0.717 \cdot 10^{-6}$
2500	$0.295 \cdot 10^{-6}$
2412	$0.268 \cdot 10^{-6}$

Since the temperature T is known as a function of τ, in order to find the dependence $T(\tau_\nu)$, we must determine the relation between τ and τ_ν. In the general case, this relation is obtained by the formula

$$\tau_\nu = \int_0^\tau \frac{\alpha_\nu}{\alpha} d\tau = \int_0^\tau \frac{\alpha_\nu(H^-) + \alpha_\nu(M)}{\alpha(H^-) + \alpha(M)} d\tau, \tag{11}$$

and calculation of the integral is carried out by means of the stellar atmosphere model constructed above. However, since $\alpha(H^-) \gg \alpha(M)$, we can consider in first approximation that absorption in the stellar atmosphere is due only to negative hydrogen ions. Then in place of eq.(11) we easily find

$$\tau_\nu = \int_{T_*}^{T} \frac{k_\nu(T)}{k(T)} B(T) \frac{d\tau}{dT} dT, \tag{12}$$

where k_ν is the absorption coefficient per ion H^-,

$$k(T) = \int_0^\infty k_\nu B_\nu(T)\, d\nu, \tag{13}$$

$$B(T) = \int_0^\infty B_\nu(T)\, d\nu = \frac{\sigma}{\pi} T^4, \tag{14}$$

and σ is the Stefan-Boltzmann constant.

The results of calculations on the /213 basis of eqs.(10) - (12) are given in Tables 2 and 3, in which the following designations are adopted: H'_ν are the radiation fluxes calculated on the assumption that absorption in the stellar atmosphere is determined only by negative hydrogen ions, H^*_ν are the corresponding Planck radiation fluxes, and H_ν is the radiation flux calculated on the assumption that absorption is determined both by

negative ions and by metals. The flux H_ν is calculated for $T_0 = 3000^\circ K$. At $\lambda > 4082$ Å, we have $H_\nu = H'_\nu$ owing to the inequality $\alpha(H^-) \gg \alpha(M)$.

3. Spectrophotometric Temperatures

The spectrophotometric or color temperature T_c of the examined portion of the spectrum is determined from the relation

$$\frac{d}{d\nu}\log H_\nu = \frac{d}{d\nu}\log\left(\frac{2\pi h\nu^3}{c^2}\cdot\frac{1}{\exp\left(\frac{h\nu}{kT_c}\right)-1}\right). \tag{15}$$

If, for calculating the integral in eq.(10), we use the Reiz formula (Ref.6) /214

$$H_\nu = 0.884\cdot\frac{2\pi h\nu^3}{c^2}\cdot\frac{1}{\exp\left(\frac{h\nu}{kT_1}\right)-1} + \\ + 0.116\cdot\frac{2\pi h\nu^3}{c^2}\cdot\frac{1}{\exp\left(\frac{h\nu}{kT_2}\right)-1}, \tag{16}$$

where $T_1 = T(\tau_\nu = 0.397)$ and $T_2 = T(\tau_\nu = 2.723)$, then eqs.(15) and (16) will yield approximately

$$\frac{1}{T_c} = \frac{1}{T_2} + \frac{\frac{1}{T_1}-\frac{1}{T_2}}{1+0.131\exp\left\{\frac{h\nu}{k}\left(\frac{1}{T_1}-\frac{1}{T_2}\right)\right\}}. \tag{17}$$

This relation also serves for determining T_c. In deriving eq.(17) we took advantage of the fact that, in eqs.(15) and (16) for the frequencies of the visible spectrum, we can neglect unity with respect to $\exp\left(\frac{h\nu}{kT}\right)$.

TABLE 4

λ (Å)	$T_0 = 2000^\circ$	$T_0 = 2500^\circ$	$T_0 = 3000^\circ$
	T_c	T_c	T_c
4000	2840	3830	4520
6000	2440	3180	3860
10000	2300	2990	3650

The results of calculations by means of eq.(17) are shown in Table 4. The values of T_1 and T_2 were obtained on the assumption that absorption in the stellar atmosphere is due only to negative hydrogen ions. The spectrophotometric temperature, corresponding to the spectrum region of about $\lambda = 4000$ Å and

calculated on the assumption that absorption in the atmosphere is due to negative hydrogen ions and metal atoms, proves to be equal to $T_c = 4270^\circ K$.

It is very difficult to obtain the color temperature of stars of late /215
classes from observations, since the continuous spectrum of these stars is so distorted by the bands of various molecular compounds that - for some spectral intervals - the concept of color temperature is generally meaningless. For main-sequence stars of spectral class M0 the color temperatures were determined by Seares and Joyner (Ref.7) and by Stebbins and Whitford (Ref.8). The first observers obtained $T_c = 3880^\circ K$ for the visible region of the spectrum, and the latter found $T_c = 3590^\circ K$ for a wavelength of $\lambda = 4220$ Å.

As we see, quite satisfactory agreement exists between our calculated and observed spectrophotometric temperatures.

4. Absorption Bands of TiO in Spectra of Class M Stars

Molecules of TiO have two systems of absorption bands in the visible spectrum region: The first, called the α-system, arises on electron transitions $X^3\Pi \rightarrow C^3\Pi$, where $X^3\Pi$ is the ground state of the molecule TiO and $C^3\Pi$ is the third excited state; the second, known as the γ-system, arises on electron transitions $X^3\Pi \rightarrow A^3\Delta$, where $A^3\Delta$ is the first excited state of the molecule.

Theoretically, the energy distribution within individual absorption bands of TiO has not yet been obtained; meanwhile, any investigation of the continuous spectrum of stars of the late class, which does not incorporate a study of molecular bands, would be incomplete. Therefore, we made a detailed study (Ref.9) of several problems associated with the presence of the absorption bands of TiO in the spectra of class M stars. For lack of space, we cannot further discuss these problems. Therefore, we present here only the basic results of that study (Ref.9) without the derivation.

To obtain the energy distribution within an individual band, the absorption coefficient within this band must be known. For the band (v', v'') of the α-system of TiO, which arises upon transition between the vibrational-rotational levels of the ground state characterized by the quantum number v'' and the vibrotor levels of the electron state $C^3\Pi$ characterized by the quantum number v', the absorption coefficient is equal to /216

$$k_{v'v''}(\beta) = \frac{8\pi^2\bar{\omega}_{v'v''}}{3hc\,(B_{v''} - B_{v'})} \frac{|q_{v'v''}|^2}{Z(T)} \exp\left(-\frac{E_{v''}}{0{,}695\,T}\right) \times \\ \times \pi n_0 |R_e|^2 \beta \exp\{-C(T)(1-\beta)\}, \qquad (18)$$

where $B_{v'}$, $B_{v''}$ are the vibrational constants of the levels v' and v'', $q_{v'v''}$ is the Franck-Condon factor, R_e is the electron transition moment $X^3\Pi \rightarrow C^3\Pi$, $Z(T)$ is the sum of states, $E_{v''}$ is the vibrational energy of the level v'', and n_0 is the number of TiO molecules in 1 cm^3,

$$\bar{\omega}_{v'v''} = E_4 + (E_{v'} - E_{v''}), \qquad (19)$$

E_4 is the energy of the electron state $C^3\Pi$,

$$\beta = \frac{\omega}{\bar{\omega}_{v'v''}}, \quad C(T) = \frac{\bar{\omega}_{v'v''} B_{v''}}{0.695 (B_{v''} - B_{v'}) T}, \tag{20}$$

$\omega = \frac{1}{\lambda}$ is the wave number of the investigated spectrum region. In the case of the γ-system, all quantities pertaining to the state $C^3\Pi$ in eq.(18) should be replaced by the corresponding quantities pertaining to the state $A^3\Delta$.

The quantity $n_0|R_e|^2$, which is unknown, enters eq.(18). In place of the quantity R_e we usually determine the oscillator strength for a given electron transition $f_e \sim |R_e|^2$. The quantity

$$p_e = \pi n_0 f_e \tag{21}$$

will be taken as a parameter figuring in the theory. At values of $p_e \leq 2.5 \times 10^7$, the contribution made by absorption in the TiO bands to the opacity of the atmosphere can be neglected in first approximation. In this case, to obtain the energy distribution within individual bands, the results of calculations of a model atmosphere consisting of hydrogen and metals can be used. Table 5 presents the energy distribution within the band (1, 0) of the γ-system of TiO,

TABLE 5

λ (Å)	β	m_β				m_β (obs.)
		$p_e = 10^7$	$p_e = 2.5 \cdot 10^7$	$p_e = 5 \cdot 10^7$	$p_e = 10^8$	
7052	0.943	0.72	0.72	0.72	0.72	0.67
7013	0.948	0.73	0.73	0.74	0.74	0.72
6983	0.952	0.75	0.75	0.76	0.76	0.76
6940	0.958	0.77	0.77	0.78	0.79	0.80
6916	0.962	0.78	0.78	0.79	0.81	0.80
6849	0.971	0.81	0.83	0.85	0.90	0.85
6807	0.977	0.84	0.88	0.93	1.03	0.97
6784	0.980	0.86	0.92	0.99	1.13	0.95
6748	0.986	0.91	1.00	1.16	1.31	1.02
6720	0.990	0.97	1.08	1.27	1.46	—
6685	0.995	1.05	1.20	1.45	1.85	1.05

obtained for different values of the parameter p_e. The values of m_β in Table 5 are equal to

$$m_\beta = -2.5 \log H_\nu - 11.5 \tag{22}$$

(the constant -11.5 is introduced to reduce the calculated values of m_β to the observed values). This same table presents the values of m_β in the band (1, 0) of the γ-system of TiO for main-sequence star of class M0 β And, obtained from van Hoff's observations (Ref.10). /217

Based on a comparison of the calculated and observed values of m_β, it can be assumed that, in the first approximation for the γ-system of TiO,

$$p_e \approx 2.5 \cdot 10^7.$$

REFERENCES

1. Osterbrock, D.: Astrophys. J., Vol.118, p.529, 1953.
2. Dumezil-Curien, P.: Ann. Astrophys., Vol.17, p.197, 1954.
3. Buslavskiy, V.G.: Vestn. Leningr. Univ., No.13, 1964.
4. Bates, D.R.: Monthly Notices, Vol.106, p.432, 1946.
5. Aller, L.: Astrophysics, Vol.I, Izd. Inostr. Lit., 1956.
6. Reiz, A.: Arkiv f. Math., Astr. och Fys., Vol.29, Part IV, 1943.
7. Seares, F. and Joyner, M.: Astrophys. J., Vol.98, p.261, 1943.
8. Stebbins, J. and Whitford, A.: Astrophys. J., Vol.102, p.318, 1945.
9. Buslavskiy, V.G.: Vestn. Leningr. Univ., No.7, 1965.
10. van Hoff, H.: Z. Astrophys., Vol.18, p.157, 1939.

DETERMINATION OF THE CHEMICAL COMPOSITION OF STELLAR ATMOSPHERES

/218

A.A.Boyarchuk

The article written by V.V.Sobolev (Ref.1, 2) reports on solutions of the equation of radiative transfer and on methods of calculating stellar atmosphere models. The present article makes use of the results of these calculations for determining the chemical composition of stellar atmospheres.

All our information on celestial bodies is based on analyses of the radiation arriving on earth from their surface. The monochromatic radiation flux in a continuous spectrum emitted by a star is equal to

$$H_\nu(0) = \int_0^\infty B_\nu(T(\tau))\,\mathrm{Ei}_2(\tau_\nu)\,d\tau_\nu, \tag{1}$$

where $B_\nu(T)$ is the Planck function, τ is the average optical depth used in calculating the model atmosphere, and τ_ν is the optical depth for radiation of frequency ν. Calculations of model stellar atmospheres yield the dependences $T(\tau)$ and $P_e(\tau)$. If the chemical composition of the atmosphere $\epsilon_i/\Sigma\epsilon_i$ is known, it is relatively easy, on the basis of these dependences, to find the relation between τ and τ_ν, i.e., $\tau_\nu = \tau_\nu(\tau, T, P_e, \epsilon_i/\Sigma\epsilon_i)$. Since, in the atmospheres of almost all stars, the main absorption source is hydrogen, only rather rough data on the chemical composition are needed here. It suffices to make certain that the relative hydrogen content in the atmosphere of an investigated star does not differ from that of the sun by more than a factor of 100. Thus, if we construct a model atmosphere, the quantity $H_\nu(0)$ can be calculated.

At the line frequencies, the flux of escaping radiation is equal to

$$H'_\nu(0) = \int_0^\infty B_\nu(T(\tau))\,\mathrm{Ei}_2(\tau'_\nu)\,d\tau'_\nu, \tag{2}$$

where τ'_ν is the optical depth for radiation at spectral line frequencies. /219
To calculate the integral on the right-hand side of eq.(2) we need know an additional function $\tau'_\nu(\tau)$. From a determination of the optical depth, we have

$$\tau'_\nu = \int_h^\infty (\alpha'_\nu + \alpha_\nu)\,dh, \tag{3}$$

where α'_ν and α_ν are the volume absorption coefficients at frequencies of the line and continuous spectrum respectively. The value of α'_ν depends on conditions in the stellar atmosphere and this dependence can be represented in explicit form:

$$\alpha'_\nu = k'_\nu \Phi(p_e, T) \frac{\varepsilon_i}{\Sigma\varepsilon_i} \frac{\rho(p_e, T, \varepsilon_i/\Sigma\varepsilon_i)}{m_H \bar{\mu}(\varepsilon_i/\Sigma\varepsilon_i)}. \tag{4}$$

Here k'_ν is the absorption coefficient at line frequencies distant by $\nu - \nu_{ik}$ from its center:

$$k'_\nu = \frac{e^2 \sigma_{ik} f_{ik}}{\pi^{1/2} m_e c} \cdot \int_{-\infty}^{+\infty} \frac{e^{\left(-\frac{\Delta\nu}{\Delta\nu_0}\right)^2} \frac{d\Delta\nu}{\Delta\nu_0}}{(\nu - \nu_{ik} - \Delta\nu)^2 + \delta_{ik}^2}, \tag{5}$$

where $\Delta\nu_0$ is the Doppler width, δ_{ik} is the attenuation constant, and f_{ik} is the oscillator strength.

The quantity $\Phi(p_e, T)$ is the portion of atoms encountered at the level i; $\varepsilon_i/\Sigma\varepsilon_i$ is the percentage of atoms of the investigated element among atoms of all elements, $\bar{\mu}(\varepsilon_i/\Sigma\varepsilon_i)$ is the mean molecular weight, and $\rho(P_e, T, \varepsilon_i/\Sigma\varepsilon_i)$ is the density of the atmosphere. We see that the quantity α'_ν ultimately depends on temperature, electron concentration, and chemical composition of the stellar atmosphere. It can be calculated on the basis of the previously calculated model atmosphere, i.e., on the basis of the dependences $P_e(\tau)$ and $T(\tau)$ for different values of $\varepsilon_i/\Sigma\varepsilon_i$, if the atomic constants δ_{ik} and f_{ik} are known.

Thus, at the spectral line frequencies the value of the escaping flux depends on the model atmosphere and on the chemical composition. This affords the theoretical possibility of determining the chemical composition on the basis of emission of the line spectrum of the star.

By means of the equalities (1) - (5) we can write the expression for /220
the residual line intensity, i.e., the intensity of radiation at spectral line frequencies expressed in intensity units of the continuous spectrum:

$$i(\nu - \nu_{ik}) = \frac{H'_\nu(0)}{H_\nu(0)} = \frac{\int_0^\infty B_\nu(T(\tau)) \operatorname{Ei}_2(\tau'_\nu) d\tau'_\nu}{\int_0^\infty B_\nu(T(\tau)) \operatorname{Ei}_2(\tau_\nu) d\tau_\nu} = \chi(\nu - \nu_{ik}, \varepsilon_i/\Sigma\varepsilon_i). \tag{6}$$

Equation (6) indicates that a comparison of the observed and calculated (for different values of $\varepsilon_i/\Sigma\varepsilon_i$) residual line intensities at a distance $\nu - \nu_{ik}$ from the line center will permit determining the quantity $\varepsilon_i/\Sigma\varepsilon_i$, i.e., the chemical composition of the atmosphere. However, residual intensities are rarely used in practice. The fact is that the line profile, its residual intensities, can be decisively influenced by rotation of the stars, inadequate resolving power of the spectrograph, and other factors. Therefore, it is more convenient to use the equivalent line width:

$$W = \int_{-\infty}^{+\infty} [1 - \chi(\nu - \nu_{ik}, \varepsilon_i/\Sigma\varepsilon_i)] d(\nu - \nu_{ik}) = W(\varepsilon_i/\Sigma\varepsilon_i). \tag{7}$$

This quantity does not depend on the resolution of the spectrograph, and its use for determining the chemical composition yields more reliable results than the use of residual intensities.

Thus, the problem of determining the chemical composition of the atmosphere reduces to the successive solution of eqs.(4), (3), (2), (1), (6), and (7) for a set of values of $\epsilon_i/\Sigma\epsilon_i$ and to a comparison of the results with observational data. The accuracy of determining the chemical composition by this method is rather high and is determined mainly by the accuracy of the observed equivalent line widths and by the quality of the theoretical model of the atmosphere.

However, determination of the chemical composition of the atmosphere by this method requires rather laborious calculations. Such calculations are justified only if rather accurate observational values of equivalent line widths are available. Despite the fact that, until now, numerous different model atmospheres have been calculated, they were used for analyzing the spectra of no more than a dozen stars. If no reliable observations are available or if information on the chemical composition, even if of a rather rough nature, is urgently needed it is possible to use the quite common method of the curve of growth. The relationship between the equivalent width and the number of atoms at a lower level is known as the growth curve. Such curves have been repeatedly calculated by different authors under various simplifying assumptions. A review of the subject is given, for example, by Aller (Ref.3). An essential shortcoming of using growth curves in determining the chemical composition is the assumption that all lines used arise under identical conditions. Such an assumption is not always true. Later in the text, we will discuss errors in the relative concentrations of elements which might be created by using this assumption. /221

Using the growth curve, the equivalent width will furnish the number of ions at a lower level. Furthermore, the number of atoms in some state of ionization must be determined. For this, we need know the excitation temperature.

Using the Boltzmann formula

$$\frac{n_i}{n_k} = \frac{g_i}{g_k} e^{-\frac{\varepsilon_i - \varepsilon_k}{kT}}, \tag{8}$$

we can write

$$\log \frac{n_i}{g_i} - \log \frac{n_k}{g_k} = \Theta(\varepsilon_k - \varepsilon_i), \quad \text{where } \Theta = \frac{5040}{T}. \tag{9}$$

Having determined from the growth curve the value of $\log (n_i/g_i)$ for different lines, it is easy to find the excitation temperature from eq.(9). However, in practice it is more convenient to determine this temperature by graphic means. As an example, Fig.1 shows determination of the excitation temperature in the atmosphere of the star α CMa with respect to FeI lines.

To determine the total concentration of atoms of the element in question, other states of ionization must also be taken into consideration. For this purpose we must know the temperature and the electron concentration. In principle, these quantities can be determined by simultaneous solution of the Saha /222

equation for different elements:

$$\frac{n^+}{n} n_e = \frac{u^+}{u} \frac{(2\pi mkT)^{3/2}}{h^3} e^{-\chi/kT}. \qquad (10)$$

However, this method does not provide the necessary accuracy, mainly because of the fact that elements whose lines are observed simultaneously in the spectra of normal stars have very close values of ionization potentials. We can assume that the ionization temperature is equal to the excitation temperature. However, numerous investigations have demonstrated that such assumptions are not very satisfactory (Ref.4). The following procedure gives good results: From the spectral class of the star, its effective temperature is determined. Then, on the basis of the equality

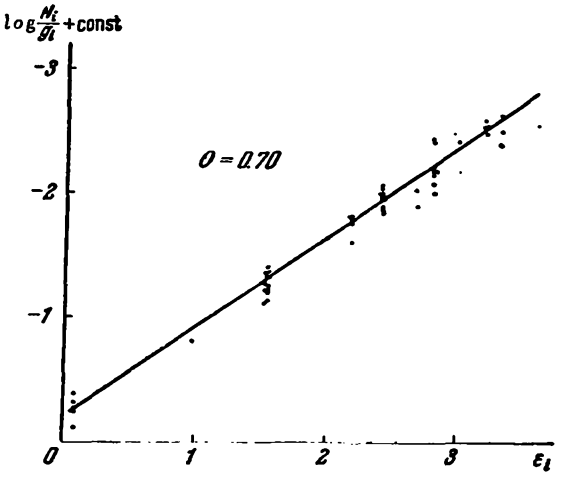

Fig.1

$$T^4 = \frac{T_{eff}^4}{2}\left(1 + \frac{3}{2}\tau\right) \qquad (11)$$

we find the temperature at the optical depth $\tau = 0.3$, at the effective level of formation of most lines, i.e., $T_{ion} = 0.92\ T_{eff}$. Knowing the ionization temperature, we can use the Saha formula to determine the electron pressure if lines of two atomic ionization states of the same element are observed in the spectrum. /223

To determine the electron concentration in stellar atmospheres one can also take advantage of the fact that the hydrogen line profiles and equivalent widths are highly sensitive to the Stark effect, i.e., strongly depend on the electron concentration.

The Inglis-Teller formula

$$\log n_e = 23.26 - 7.5 \log m \qquad (12)$$

relates the quantity m, the number of the last observed line of the Balmer series, with the electron concentration n_e. The dependence of the equivalent width of the hydrogen lines W_λ on the electron concentration is given by the Unsöld formula

$$n_e = \left(\frac{0.45}{R_c}\right)^{3/2} \cdot \frac{W_\lambda^{3/2}}{kN_2}, \qquad (13)$$

where R_c is the limiting depth of the line, k is some constant characterizing the Stark effect for the line in question (Ref.5), and N_2 is the number of

hydrogen atoms at the second level, which can be determined by the formula

$$N_2 = \frac{W_\lambda}{\pi^2 e^2 \lambda^2 f_{2i} m^{-1} c^{-2}}. \qquad (14)$$

Equation (14) holds only for an optically thin layer and, for most lines, gives a distinctly underestimated value of the quantity N_2. Therefore, in practice the quantity N_2 is calculated from the equivalent widths of all lines after which the largest value is taken. As an example, Fig.2 plots the quantity N_2 calculated by eq.(14) as a function of the number of the line for ν Cas (Ref.6).

The values of the electron concentration, determined by the above methods, usually coincide with an accuracy to within one order of magnitude (Ref.7). Since generally lines arriving at different depths are used, the differences in n_e /224 probably are produced by a change of n_e with depth.

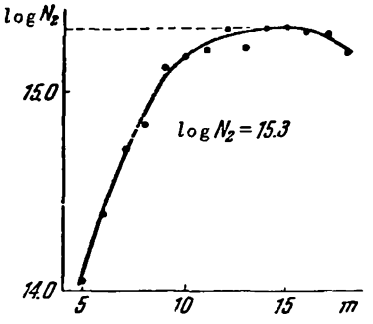

Fig.2

Despite the fact that the method of growth curves requires an additional determination of the quantities T_{ex}, T_{ion}, and n_e, it is much simpler than the method of model atmospheres and in many cases yields satisfactory accuracy.

In investigating the chemical composition of stellar atmospheres by the method of growth curves and by the method of model atmospheres, the values of the transition probabilities or oscillator strengths of the lines in question must be sufficiently well known.

We should mention that, unfortunately, far from all lines have known values of oscillator strength and not all of the known values of the oscillator strengths are of good accuracy. At the present state of the art in theoretical and experimental determinations of oscillator strengths, it must be admitted that, on the whole, the experimental values of oscillator strengths are best. However, for all practical purposes these values have not been determined for lines having a high excitation potential, or almost nc ion lines. For such lines it is often necessary to use theoretical values of oscillator strength. The best results are obtained by using the so-called "stellar" oscillator strengths.

These are determined in the following manner: Let us assume that we have a model atmosphere or a growth curve. From the equivalent widths with known values of the oscillator strength we first determine the concentration of atoms of the element in question. Then, we solve the opposite problem, namely, from the equivalent width with known atom concentration we determine the value of the oscillator strength by using the growth curve or the model atmosphere. The most complete list of "stellar" oscillator strengths has been published earlier /225 (Ref.8). That publication gives the values of oscillator strength for atomic and ionic lines of various elements in the spectral region of 3800 - 6700 Å. The problem of "stellar" oscillator strengths for FeII was studied by Bashek

(Ref.9).

Of the studies on the experimental values of oscillator strength we should mention Corliss' paper (Ref.10) which contains data on the lines of various atoms and ions. Numerous papers exist on the determination of experimental values of oscillator strength for a comparatively few lines of individual elements. An extensive bibliography of works containing oscillator strength data for lines observed in the spectra of hot stars was compiled by Kohl (Ref.11). A similar bibliography was assembled by Goldberg (Ref.12) for lines observed in the spectra of solar-type stars. The latter article contains a critical comparison of the oscillator strength data for lines of various elements, obtained by different authors. Recently, the State Optical Institute and Crimea Astrophysical Observatory of the USSR Academy of Sciences have been collaborating in reducing the available oscillator strength data to one system. Such work has already been carried out for FeI (Ref.13).

Let us now examine the basic results of studies on the chemical composition of stars. First it should be noted that most of our information on stellar atmospheres is based on an analysis of stellar spectra by the method of growth curves. A more accurate method, based on model atmospheres, was used in investigating spectra of dozens of stars, mainly those of spectral classes B and A. However, the situation is not desperate. A comparison of the relative element content determined by the method of growth curves as well as on the basis of model atmospheres shows that the relative abundance of elements with close ionization potentials (for example, metals of the iron group) is practically the same when determined by either methods (Ref.14). However, in determining the ratio H/He and H/met the differences become substantial. The reason for this lies in the simplifying assumptions of the method of growth curves, mainly in the use of the same excitation temperature for all ions. However if, in the comparison of the chemical composition of atmospheres of two stars of neigh- /226
boring spectral and luminosity classes, the method of growth curves is applied, the possible errors - even in the value of H/met - will be markedly reduced and the accuracy of analyzing the chemical composition will be satisfactory, i.e., the errors will not exceed a factor of 2.

In recent times, investigations devoted to an analysis of the chemical composition of stellar atmospheres have been carried at a stepped-up rate. At present, the chemical composition of almost 200 stars is more or less known, and this number continues to grow rapidly.

The main conclusion that can be drawn on the basis of available data is that the chemical composition of various groups of stars is dissimilar. We can already discern some regularities in the diverse characteristics of the chemical composition of different stars, if we proceed from the assumption that the original chemical composition of all cosmic bodies was the same and was characterized by a relatively high hydrogen content which, during evolution, was subsequently enriched with heavier elements produced by nuclear reactions. In this connection, let us briefly discuss various features of the chemical composition of stars. As is conventional, the chemical composition of the solar atmosphere will be considered as the norm and any deviations from it will be regarded as anomalies.

1. Characteristics of the chemical composition of stellar atmospheres associated with the general evolution of matter in the galaxy:

In the past few years, many investigations have been made on the chemical composition of normal stars making up different space-kinematic groups. Table 1 contains the values of $\left[\frac{H}{met}\right] = \log\left[\frac{H}{met}:\left(\frac{H}{met}\right)_{\odot}\right]$, showing the degree to which the relative contents of hydrogen and metals in the atmospheres of the investigated stars differ from the solar contents.

TABLE 1

Object	Hyades (15)*	Sun (12)	Stars with Small Velocities (14)	NGC 752; Stars F (16)	Stars with Large Velocities (17, 6, 18)	Halo; G Stars (19)	Globular Cluster M 29; Stars B (20)
$\left[\frac{H}{met}\right]$	−0.1	0	0	0	+0.5 to +2.00	+1.5	+1.29

*Numerals in parentheses refer to Ref.

Stars with large space velocities do not represent a homogeneous group, and for these only the limiting values of the quantity $\left[\frac{H}{met}\right]$ are given.

Table 1 indicates that, on passing from young stars (Hyades, sun) to old stars (Halo, globular clusters) the relative content of metals drops appreciably. /227 This fact is probably due to evolution of the chemical composition of prestellar matter.

TABLE 2

	H	He	C	N	O	Ne	Mg	Si
Normal	12.0	11.8	9.7	9.2	10.2	10.0	8.8	9.0
Stars								
Si	12.0	<10	<8		9.6		8.5	10.6
Eu	12.0				8.3		9.1	8.8

Recently Herbig (Ref.21) established the existence of a rather distinct relation between the lithium content in atmcspheres of stars of class G and their age. More lithium is contained in the atmospheres of young stars than in those of older stars. In stars of type T Tau lithium abundance is 100 times greater, and in stars of the Hyades, 15 times greater than in the sun.

2. Characteristics of the chemical composition of stellar atmospheres

associated with their particular state:

A rather extensive group of stars of class A exists, having a strong variable magnetic field (Ref.22). In the spectra of these stars the lines of certain elements are abnormally strong, which indicates anomalies of the chemical composition of their atmospheres (Ref.23). A strong magnetic field is apparently the reason for these anomalies, although so far it has been impossible to find an intelligent mechanism governing its influence on the chemical composition. Table 2, taken from Searl (Ref.23), presents some information on the chemical composition of the atmospheres of these stars.

The indices Si and Eu denote that the most characteristic feature of /228
the spectra of stars of these groups are strong lines of silicon and europium, respectively. The table also shows that there is a deficiency of helium and elements of the oxygen group in the atmospheres of these stars in comparison with the sun. Furthermore, various stars have a different magnitude of the anomalies.

Another example for the fact that the state of the atmosphere affects its chemical composition are close binary systems. The spectrum of a typical representative of this group of stars, β Lyr, has been studied quantitatively (Ref.24). It was found that, in the atmosphere of component B8, the ratio $\frac{H}{He}$ is almost 100 times less than in the solar atmosphere. The reason for this might lie in the influence of the companion on the regime of mixing of stellar matter, and also in the existence of vigorous ejection of matter.

3. Characteristics of the chemical composition associated with particular stages of stellar evolution:

This type of anomaly has been investigated less thoroughly than the two preceding ones. Here, mainly qualitative results have been obtained. For example, among the cool stars there is a large group of stars with intense zirconium oxide bands in the spectra. It can be assumed that the atmospheres of these stars are rich in zirconium. The same is true for "barium", "carbon", etc. stars. No quantitative determination of the spectra of these stars has been made, and in most cases the causes of the observed anomalies are completely vague.

One of the few stars of this class for which quantitative investigations of chemical composition have been carried out is R CrB (Ref.25), a supergiant of class F. It was found that the atmosphere of this star was very rich in carbon. There was ten times more carbon than hydrogen.

Some of the hot stars situated below the main sequence are another example of stars whose chemical composition has undergone a severe change during evolution. As a rule, the anomalies of their chemical composition involve mainly an appreciable deficiency of hydrogen (Ref.28). In the spectra of some stars it was altogether impossible to detect hydrogen lines.

Table 3 shows the chemical composition of stars of various classes, /229

making it possible to judge not only the anomaly in the ratio H/met. The sun, τ Sco, α Lyr are considered normal stars of plane components (population I), star + 10° 2179 has a low luminosity, and +33° 2642 belongs to the halo. This is followed by the star K from the globular cluster M92 and R CrB, a variable star of class F. Table 3 also shows that the chemical composition of the stellar

TABLE 3

Element	Sun (12)*	τ Sco, B0V (26)	α Lyr, A0V (27)	+10°2179, B3 (28)	+33°2642, B2 (20)	M 92, K (29)	R CrB, F9 (25)
H	12.00	12.00	12.00	9.7	12.00	12.00	12.00
He		11.23	11.4	12.2	10.9		
C	8.72	8.37		8.6	7.8		13.0
N	7.98	8.56	8.8	8.8	7.7		~12.0
O	8.96	9.11	9.3	7.4	8.0		
Mg	7.40	7.73	7.5	6.9	6.8		7.2
Al	6.20	6.57	5.7	6.8			
Si	7.50	7.95	8.2	7.5	7.2		
Ca	6.15		6.2	6.6		4.4	4.3
Sc	2.82		3.4			0.5	2.8
Ti	4.68		4.8			2.8	4.4
V	3.70		4.0			1.7	3.4
Cr	5.02		5.6			3.0	4.7
Mn	4.90		5.3			2.5	4.5
Fe	6.57		6.5			4.6	6.1
Co	4.64					2.2	
Ni	6.05		5.7			4.0	
Sr	2.60		2.8			0.5	
Ba	2.10					—0.7	1.6

*Numerals in parentheses refer to Ref.

atmospheres is rather diverse. A thorough account of the results of determining the chemical composition of stellar atmospheres up to 1961 was compiled by Aller (Ref.30), while the most recent information has been collected in the papers of Symposium No.26 of the International Astronomical Union, "Determination of the Chemical Composition of Stars", which will be published in the near future.

REFERENCES /230

1. Sobolev, V.V.: (Page 105 of this Volume).
2. Sobolev, V.V.: (Page 193 of this Volume).
3. Aller, L.H.: Articles in the Collection "Stellar Atmospheres". Izd. Inostr. Lit., 1963.
4. Boyarchuk, M.Ye.: Izv. Krymsk. Astrofiz. Observ., No.24, p.115, 1960.
5. Unsöld, A.: Physics of Stellar Atmospheres (Physik der Sternatmosphären). Berlin, 1955.
6. Boyarchuk, A.A.: Izv. Krymsk. Astrofiz. Observ., No.21, p.54, 1959.
7. Kopylov, I.M.: Izv. Krymsk. Astrofiz. Observ., No.26, p.232, 1961.
8. Boyarchuk, M.Ye. and Boyarchuk, A.A.: Izv. Krymsk. Astrofiz. Observ.,

No.22, p.234, 1960.
9. Bashek, B., Kegel, W.H., and Traving, G.: Z. Astrophys., Vol.56, p.282, 1963.
10. Corliss, C.H. and Bozman, W.R.: Nat. Bur. Std. (U.S.), Monograph, No.53, 1962.
11. Kohl, K.: Z. Astrophys., Vol.60, p.115, 1964.
12. Goldberg, L., Müller, E., and Aller, L.H.: Astrophys. J., Suppl. Ser., Vol.5, No.45, 1960.
13. Prokof'yev, V.K., Nikonova, Ye.I., Gruzdev, P.F., and Frish, M.S.: Izv. Krymsk. Astrofiz. Observ., No.31, p.281, 1964.
14. Boyarchuk, A.A.: In the Collection "Problems of Cosmogony" (V sb. "Voprosy kosmogonii"). Vol.VII, p.213, Izd. Akad. Nauk SSSR, 1960.
15. Parker, R., Greenstein, J.L., Helfer, H.L., and Wallerstein, G.: Astrophys. J., Vol.133, p.101, 1961.
16. Gunn, J.E. and Kraft, R.P.: Astrophys. J., Vol.137, p.301, 1963.
17. Wallerstein, G. and Huziker, W.: Astrophys. J., Vol.140, p.214, 1964.
18. Wallerstein, G.: Astrophys. J., Suppl. Ser., Vol.6, p.407, 1962.
19. Preston, G.P. and Wallerstein, G.: Astrophys. J., Vol.138, p.820, 1963.
20. Traving, G.: Astrophys. J., Vol.135, p.439, 1962.
21. Herbig, G.H.: In Press.
22. Babkock, H.W.: Astrophys. J., Suppl. Ser., Vol.3, p.141, 1958.
23. Searl, L. and Sargent, W.W.: Astrophys. J., Vol.139, p.793, 1964.
24. Boyarchuk, A.A.: Astron. Zh., Vol.36, p.766, 1959.
25. Searl, L.: Astrophys. J., Vol.133, p.531, 1961.
26. Traving, G.: Z. Astrophys., Vol.36, p.1, 1955.
27. Hunger, K.: Z. Astrophys., Vol.49, p.129, 1960.
28. Klemola, A.R.: Astrophys. J., Vol.134, p.130, 1961.
29. Helfer, H.L., Wallerstein, G., and Greenstein, J.L.: Astrophys. J., Vol.129, p.700, 1959.
30. Aller, L.: Abundance of Chemical Elements. Izd. Inostr. Lit., 1963.

PART IV. SPECTRA OF NONSTATIONARY STARS AND INTERSTELLAR MATTER

/231

SPECTRA OF NONSTATIONARY (VARIABLE) STARS

/233

V.G.Gorbatskiy

1. Introduction

The concept "nonstationary star" is not rigorously defined. Sometimes all variable stars, i.e., stars for which changes of spectrum brightness (with the exception of eclipsing variables) are observed, are called such. However, most often when referring to some star as nonstationary we use the spectroscopic criterion, i.e., the presence of bright lines in its spectrum, as basis.

There are no bright lines in the spectra of most ordinary stars. The radiation escaping from the stellar photosphere at the line frequency is weakened by the atmosphere and in the observed spectrum an absorption line is present at this place. The formation of bright lines in the photospheres of stars is impossible since they are in a state of local thermodynamic equilibrium. The presence of a bright line in the stellar spectrum shows that the radiation of the atmosphere at the corresponding wavelength is comparable with radiation of the photosphere in the continuous spectrum close to this wavelength. Therefore, bright lines appear in the spectra of stars having extensive atmospheres (shells) with a sufficiently powerful source of line emission in the stellar atmosphere. The weaker the emission of the stellar photosphere in a given spectrum region, the easier it is to note bright lines in its integrated spectrum. For example, these are observed in the spectra of many stars of class dM, and the later the spectral subclass, the greater the percentage of stars of this subclass having bright lines in the spectrum (Ref.1).

It is obvious that the division into stationary or fixed and nonstationary or variable stars based on the presence of bright lines in the spectrum is somewhat arbitrary and in a strict sense there are no stationary stars (even in the solar spectrum we can sometimes observe bright lines). Below, we will group /234 with "nonstationary stars" all stars with bright lines distinguishable against the background of the integrated spectrum, for which changes in the spectrum and brightness are generally observed.

The essence of the theory of spectra of nonstationary stars is that, on prescribing the structure of the outer layers of a star and the conditions prevailing there (radiation sources, velocity field, density distribution, electron and ion temperatures, chemical composition, magnetic field, etc.), we obtain:

1) Profiles and intensities of bright lines.
2) Profiles and intensities of absorption lines.
3) Energy distribution in the continuous spectrum of the star.

This, in principle, is the problem of modeling a spectrum. Its solution in one or another approximation is necessary for interpreting processes taking place in nonstationary stars.

Thus, the problems of the theory in the case in question are essentially the same as for stationary stars. However, the development of a theory of spectra for nonstationary stars is a more complex matter than for ordinary stars. Disturbances of the equilibrium state (radiative equilibrium, hydrostatic equilibrium), which are possible and occur in the outer layers of stationary stars but do not play a major role in the formation of their spectra, have an essential and often a determining significance here. Furthermore, one and the same star passes through a number of different states which cannot be described by one model so that different models must be investigated. The theory of the spectra of nonstationary stars of different types is also complicated by marked deviations of their shells from spherical symmetry. In view of these circumstances, the development of a general theory of spectra of nonstationary stars is a very difficult problem and is presently far from being completely solved. As regards elementary atomic processes essential for the formation of a spectrum (radiative excitation and ionization, processes of excitation and ionization of atoms upon collision with electrons, Stark effect, etc.), their theory is just as important for interpreting the spectra of nonstationary stars as for stationary stars.

There are many types of nonstationary stars. At the same time almost /235
each of such stars has its own individual characteristics and its spectrum changes with time. The relegation of a star to one or another type indicates the character of its spectrum only in most general features.

We will list the main types of nonstationary or variable stars, having combined them into groups on the basis of existing notions of the character of nonstationary phenomena:

I. Supernovae Types I and II
   Novae
   Recurrent novae
   U Geminorum and Z Camelopardalis stars
II. Wolf-Rayet stars (WR)
III. Stars of types Be and P Cygni
IV. Stars of type RR Lyrae
   Stars of type W Virginis
   Stars of type RV Tauri
   Long-period variables
V. Stars of type T Tauri
   Stars of type UV Ceti
VI. "Symbiotic" variables of type Z Andromedae.

In addition to those indicated, there is still a number of not so distinctly defined types of nonstationary stars which have not been studied at all from the theoretical point of view. Best studied are the stars of the first three groups which, therefore, can be called the "classical" nonstationary (variable) stars.

Some of the variable stars make up binary systems, which creates additional difficulties for studying their spectra. In first approximation, the duality can almost always be disregarded.

The shells of different types of nonstationary stars greatly differ in their properties, specifically in the value of the ratio of the shell mass to the stellar mass M_{sh}/M_* and in the state of motion. These differences show up mainly in the profiles of the bright lines and in their intensities (with respect to the continuous spectrum and absorption lines). Bright lines give the most extensive information on the state of the shell and the character of its motion.

High-velocity motions (tens and hundreds of km/sec) are an important characteristic of the shells of nonstationary stars. The rapid expansion of the /236 shells of novae is well demonstrated by the fact that some time after outburst the expanding shell can be seen directly on photographs. In other cases the motion of the shell is not demonstrated so clearly, but the aggregate of observations makes it certain that the shells move. As demonstrated below, the motion of a shell is one of the main factors determining the character of its spectrum (Ref.2).

2. Mechanisms and Sources of Radiation of Shells in Spectral Lines

The emission producing a bright line in the stellar spectrum arises in its shell. For a quantum to be emitted at the line frequency, some of the atoms must be excited to a higher level corresponding to this line and then undergo transition to a state with a lower energy. In this connection, when examining the bright line spectrum of stars the following questions arise: First, what are the mechanisms of atomic excitation and, second, what are the sources of energy going for excitation? When an atom is excited by emission at the line frequency, no new quanta with this frequency arise, so that this method of excitation in the given case is of no interest.

We will enumerate the possible mechanisms of atomic excitation:

1. Excitation by collisions. When an atom collides with some particle, the atom may be excited by the energy of the particle (and, at a sufficiently high energy of the particle, the atom may be ionized). As is known, collisions with electrons are most effective in this respect. The number of excitations from state A to state B occurring in unit volume per unit time is determined by the formula

$$n_A b_{AB} = n_A n_e \int_{v_0}^{\infty} \sigma_{AB}(v)\, v f(v)\, dv, \qquad (1)$$

where n_A is the number of atoms per unit volume in the lower state, n_e is the concentration of free electrons, $\sigma_{AB}(v)$ is the collision cross section for an electron moving with a velocity v, and $f(v)$ is the distribution function of /237 electron velocities. We can disregard the velocity of atoms since it is appreciably smaller than the velocity of electrons. The quantity v_0 is associated with the line frequency ν_{AB} by the relation

$$\frac{m_e v_0^2}{2} = h\nu_{AB}. \qquad (2)$$

2. Excitation by recombination. In some volume, let there be ionized atoms and free electrons. Ionization can be due either to the effect of radiation or to other factors, particularly to collisions with high-energy particles. Recombinations of atoms should occur in this same volume. As a result of the recombinations, excited atoms are produced at all levels except the ground level.

Since the number of recombinations is proportional to the concentration of ionized atoms and the number of excitations due to collisions is proportional to the number of nonionized atoms, the role of excitation by recombination with respect to excitation by collisions should be greater the higher the ionization degree of the atoms.

Frequently, both of the above methods of excitation are combined. If atoms are ionized by high-frequency radiation, the energy excess of the quantum, having caused ionization, changes into the energy of the detached electron which is able to excite atoms colliding with it. At the same time if, in some medium, the collisions cause not only excitation but also ionization of the atoms, then they should undergo recombination and recombination excitation should take place. As a rule, both mechanisms of excitation act in the star shell emitting line spectra, but their role is not the same for different lines. Emission in some lines may be excited primarily by recombination, and in others by collisions. However, cases are also possible where line emission is excited by both methods simultaneously.

3. Excitation by fluorescence. For simplicity, let us assume that the atom has three levels, 1, 2, 3, with energies $\epsilon_1 < \epsilon_2 < \epsilon_3$. Let the atom absorb a quantum with frequency ν_{13}. As a result, the atom changes to state 3, after /238 which it can change to state 2. If this transition is accomplished, an excited atom is formed in the second state. Such a method of populating the second level is called fluorescence.

In the case where the level 3 is discrete, excitation of emission in line ν_{12}, by radiation in another line of greater frequency ν_{13}, takes place. Sometimes the frequencies of individual lines of different atoms are accidentally very close and emission in line ν_{12} of one atom can occur when it absorbs emission of frequency ν_{13} coming from another atom. This mechanism was discovered by Bowen. As an example, we mention the possibility of excitation of atom O III by emission in line λ 304 belonging to He II. In this case atom O III emits a quantum of wavelength λ 374 which, in turn, can excite the atom N III.

Since the Bowen mechanism requires close agreement of the frequencies corresponding to lines of different atoms, which is comparatively rare, the applicability of this mechanism is limited. With this formulation, one can explain only excitation of emission in individual bright lines of moderate intensity.

If, for the third level, we take a state of atomic ionization, then the recombination excitation - provided ionization is induced by radiation - represents a process of the same type as fluorescence excitation. This leads to

reprocessing of radiations of higher frequencies to radiation of lower frequencies. Usually this method is called fluorescent.

The energy causing line emission of shells may be in the form of radiation or may be the kinetic energy of particles. The possible sources of this energy are as follows:

1. Emission of a hot star in the short-wave region of the spectrum.
2. Kinetic energy of moving gas masses which, upon collision, is converted into thermal energy.
3. Heating of gas when a shock wave passes through it.
4. Kinetic energy of stellar corpuscular fluxes.
5. Energy of electrical and magnetic fields.

In general, the emission lines of a gas, besides by high-frequency radiation, may be caused by any energy source raising the gas temperature. /239

The gas heating sources are not exhausted by those listed above. As an example of other sources we might mention that, under certain conditions, the temperature of an electron gas is raised by the conversion of some of the radiant energy in the lines (for example, L_α) to kinetic energy of electrons in collisions of the second kind.

Let us briefly examine the basic types of variable stars, under consideration of the above statements on the mechanisms and sources of line emission. The shells of novae, at a sufficiently late stage of development, are similar in their character of emission to small planetary nebulae. The emission of their central star in the ultraviolet spectrum region is very intense. The glow of the nebular shells of novae in allowed lines arises by recombinations while, in forbidden lines, the glow is excited by electron collision. Short-wave radiation of the newest star is the energy source.

WR-type stars, with respect to the line spectrum and ionization in their shells, correspond to the spectral class O. These stars have a sufficiently high temperature for their radiation to ionize atoms of hydrogen, helium, and other elements. Therefore, it is usually accepted that emission in the bright lines of H, He I and He II, C III, N III, etc. is excited by recombinations.

Be-type stars are very similar, in absorption spectrum and various other characteristics, to the usual stars of class B, which have a comparatively high temperature and thus radiate much energy beyond the limit of the Lyman series. Hydrogen in the shells of Be-type stars is ionized by high-frequency radiation of the star and produces recombination line emission. However, the temperature of these stars is not sufficiently high to ionize helium atoms so that bright lines of helium are usually absent from their spectra. The bright hydrogen lines in the spectra of Be stars are also weaker the later the class to which the absorption spectrum of the star belongs.

For stars of class A and later, the high-frequency radiation is insufficient to cause hydrogen line emission of the shell. Consequently, the source /240 of the emission spectrum of the stars RR Lyrae and others belonging to the IV group (see above) is different. At present the most popular explanation for the

emission spectrum of these stars is that it is caused by heating of the stellar atmosphere by shock waves periodically passing through it (Ref.3, 4, 5, 6). Atomic excitation mainly occurs by collisions, since the ionization degree of atoms in the shock wave is not very great, whereas the gas temperature is relatively high.

Excitation and ionization of atoms by collisions apparently play an essential role in the emission of shells of novae at early stages of their development (after the brightness maximum) (Ref.7). As regards stars of the type UV Ceti, T Tauri, and "symbiotic" stars, we are still uncertain as to the sources of energy emitted by their shells in lines. It is possible that we are dealing here with a highly special phenomenon - the release of intrastellar energy in the outer regions of the stars.

With known sources of energy emitted in lines and at given characteristics of the shell (density, temperature, etc.) we can find the emission and absorption coefficients at each point of the shell and on this basis construct theoretical bright line profiles and calculate their intensity. Naturally, we must first examine the effect of various elementary processes on the magnitude of these coefficients.

3. Bright Line Profiles

Let us now calculate the profiles of bright lines formed by the moving shell of a star, considering that the volume emission coefficient in the line ε_{ik} is known for each point as a function of frequency, and also that the velocity field in the shell is given. Let us first examine a shell completely transparent for line emission. We will take a rectangular coordinate system, with its origin at the center of the star and its axis Oz directed toward the observer.

As a consequence of the Doppler effect, for each point there is a central frequency at the line ν'_{ik} which is related with the velocity in the following manner: /241

$$\nu'_{ik} = \nu_{ik} + \frac{\nu_{ik}}{c} v_z(x; y; z), \tag{3}$$

where $v_z(x; y; z)$ is the projection of the velocity of motion onto the direction toward the observer and ν_{ik} is the central frequency of the line arising in a volume fixed relative to the observer.

The intensity of radiation $I_{ik}(x; y; \nu)$ coming from a point of the stellar disk with coordinates $(x; y)$ at a frequency ν within the line, is determined by the expression

$$I_{ik}(x; y; \nu) = \int_{-\infty}^{\infty} \varepsilon_{ik}(\nu - \nu'_{ik})\, dz. \tag{4}$$

The energy $\mathcal{E}_{ik}(\nu)$, emitted by the entire shell at a frequency ν within unit solid angle in a direction toward the observer, is equal to

$$\mathcal{E}_{ik}(\nu) = \iint I_{ik}(x; y; \nu)\, dx\, dy, \tag{5}$$

where integration is made over all possible values of x and y. Several authors (Ref.8, 9, 10) have calculated the bright line profiles in the spectra of Be and WR stars and of novae, in accordance with eq.(5). However, strictly speaking, eq.(4) is suitable only for calculating the profiles of forbidden lines at whose frequencies the shell can be considered transparent since the absorption coefficient at these lines is very small. As to the first two lines of the Balmer series of hydrogen, which are the most intense of all bright lines in the spectra of most variable stars, and a series of lines He I and He II, the shells of variable stars have an appreciable optical thickness here. Taking this into account, eq.(4) can be replaced by the following formula

$$I_{ik}(x; y; \nu) = \int_{-\infty}^{\infty} \varepsilon_{ik}(\nu - \nu'_{ik})\, e^{-\int_{z}^{\infty} \alpha_{ik}(\nu - \nu''_{ik})\, dz'} dz, \tag{6}$$

where α_{ik} is the absorption coefficient in the examined line. Thus, when calculating the bright line profiles the phenomenon of self-absorption must be considered, a fact first noted by V.V.Sobolev (Ref.2, 11) who derived general formulas for bright line profiles for the case in which the rate of motion of the shell is appreciably greater than the rate of thermal agitation of the atoms. In this case, the profiles of the emission and absorption coefficients can be approximately assumed as rectangular. This means that, in the range of frequency variation from $\nu'_{ik} - \frac{\Delta\nu_{ik}}{2}$ to $\nu'_{ik} + \frac{\Delta\nu_{ik}}{2}$ the quantities α_{ik} and ε_{ik} are constant and nonzero while, outside this range, they are equal to zero. Since the Doppler profile is approximated by a rectangular profile, the line width $\Delta\nu_{ik}$ is determined by the mean rate of thermal agitation of the atoms:

/242

$$\Delta\nu_{ik} = 2\nu_{ik}\frac{u}{c}. \tag{7}$$

Let us take some fixed value of ν. The equation

$$\nu = \nu_{ik} + \frac{\nu_{ik}}{c} v_z(x; y; z) \tag{8}$$

determines a certain surface called the surface of equal radial velocities. Only a narrow layer of the shell which incorporates this surface radiates at a frequency ν. The boundaries of the layer are at distances from the surfaces (along the line of sight) corresponding to a frequency variation of $\frac{\Delta\nu_{ik}}{2}$. The thickness of the layer is $\Delta z = z_2 - z_1$, where z_1 and z_2 are found from the following equations (for given x; y; ν):

$$\left.\begin{aligned} \nu \mp \frac{\Delta\nu_{ik}}{2} &= \nu_{ik} + \frac{\nu_{ik}}{c} v_z(x; y; z_1), \\ \nu \pm \frac{\Delta\nu_{ik}}{2} &= \nu_{ik} + \frac{\nu_{ik}}{c} v_z(x; y; z_2), \end{aligned}\right\} \tag{9}$$

and the signs are selected such that the condition $z_1 < z_2$ is satisfied. The remaining part of the shell does not emit radiation at a frequency ν. Therefore, eq.(6), taking our above statements into account, can be replaced by the following formula:

$$I_{ik}(x; y; \nu) = \int_{z_1}^{z_2} \varepsilon_{ik} e^{-\int_z^{z_2} \alpha_{ik}\, dz'} dz. \tag{10}$$

The value of Δz is small relative to the dimensions of the shell, which /243 makes it possible to assume ε_{ik} and α_{ik} as constant within the layer emitting at a frequency ν. Then eq.(10) yields

$$I_{ik}(x; y; \nu) = \frac{\varepsilon_{ik}}{\alpha_{ik}} [1 - e^{-\alpha_{ik}\Delta z}]. \tag{11}$$

After expanding v_z in a series and retaining terms of the first order of smallness, eqs.(9) give

$$\Delta\nu_{ik} = \frac{\nu_{ik}}{c} |v_z(x; y; z_2) - v_z(x; y; z_1)| = \frac{\nu_{ik}}{c} \left|\frac{\partial v_z}{\partial z}\right| \Delta z. \tag{12}$$

From eq.(12), taking eq.(7) into account, we obtain the expression for the thickness of the emitting layer:

$$\Delta z = \frac{2u}{\left|\frac{\partial v_z}{\partial z}\right|}. \tag{13}$$

Designating the product $\alpha_{ik}\Delta z$ by $\Delta\tau_{ik}$ and integrating eq.(11) over the entire surface (8), we find

$$\mathcal{E}_{ik}(\nu) = \iint \frac{\varepsilon_{ik}}{\alpha_{ik}} [1 - e^{-\Delta\tau_{ik}}]\, dx\, dy. \tag{14}$$

The quantities ε_{ik} and α_{ik} are expressed by the well-known formulas:

$$\varepsilon_{ik} = \frac{n_k A_{ki} h\nu_{ik}}{4\pi\Delta\nu_{ik}}; \quad \alpha_{ik} = \frac{n_i B_{ik} h\nu_{ik}}{c\Delta\nu_{ik}} \left(1 - \frac{g_i n_k}{g_k n_i}\right), \tag{15}$$

where n_i and n_k are the number of absorbing and the number of line-emitting atoms in unit volume, respectively; A_{ki} and B_{ik} are the coefficients of transition probabilities; g_i and g_k are the statistical weights of the levels. The quantity $\frac{\varepsilon_{ik}}{\alpha_{ik}}$ is obtained from eq.(15) in the following form:

$$\frac{\varepsilon_{ik}}{\alpha_{ik}} = \frac{2h\nu_{ik}^3}{c^2} \cdot \frac{1}{\frac{g_k n_i}{g_i n_k} - 1}. \qquad (16)$$

The velocity field in the shell has an influence on the shape of the line profile not only as a consequence of the relation (8) between ν and v_z, but also because of the fact that the degree of excitation of the atoms (i.e., the quantities n_k and n_i), as will be shown below, depends on the state of motion of the shell. /244

Bright line profiles are usually complex. To make them yield sufficiently complete information on the state of the shell (velocity field, distribution of atoms by states) some model of the shell should be established and the sequence of profiles be calculated for different values of the parameters. Only then can the observed profiles be compared with the theoretical ones. In view of the complexity of the profiles, it is advisable, in selecting a model shell, to work first with a low accuracy but in a large range of parameter values; this is where the first approximation comes in. Theoretical bright line profiles, in first approximation, were calculated for Be and WR stars by V.V.Sobolev (Ref.2, 12), for Be type stars by V.G.Gorbatskiy (Ref.13), and for WR stars by S.V. Rublev (Ref.14). The resultant profiles agree in general with the observed profiles and confirm the existing concepts as to the nature of the shells of these stars. However, for a thorough analysis of shells with respect to bright lines, the profiles are inadequate and more complete calculations are desirable.

In concluding this Section let us point out that, when the velocities of the shells are of the order of thermal velocities, it becomes possible to use for ε_{ik} and α_{ik} more accurate profiles than the rectangular type, for example Doppler profiles corresponding to the electron temperature of the shell. Calculations of bright line profiles with such ε_{ik} and α_{ik} coefficients have not yet been performed.

4. Intensities of Emission Lines

Calculation of line intensities for a shell transparent in lines is the simplest type. In this case, the energy emitted in a line with frequency ν_{ik} is equal to

$$E_{ik} = A_{ki} h\nu_{ik} \int n_k \, dV, \qquad (17)$$

where n_k is the number of atoms in a higher state per unit volume and integration is carried out over the entire volume of the shell. If the emission process is stationary, then the values of n_k are found from a system of algebraic equations of the type /245

$$N_k^+ - N_k^- = 0, \qquad (18)$$

which express that the number of atoms N_k^+ passing in unit time per unit volume to the k-th state is equal to the number of atoms N_k^- leaving this state during

the same time. In these equations, radiative transitions and collisional transitions should be taken into account along with spontaneous transitions and recombinations. The system of steady-state equations for the hydrogen atom was solved by Cillie (Ref.15) (for the case of 12 equations) without consideration of collisions and under assumption of transparency of the medium in lines of the subordinate series, and later was investigated in detail for a large number of levels by many authors [for example, Burgess (Ref.16)]. On the basis of the obtained solutions, the relative intensities of bright lines in the spectra of planetary nebulae were determined. The use of these results for determining the intensities of Balmer lines in the spectra of variable stars is unwarranted since, as noted above, the shells of variable stars are usually not transparent to radiation in the indicated lines.

For nonstationary emission we should replace equations of the type of eq.(18) by a system of differential equations:

$$\frac{dn_k}{dt} = N_k^+ - N_k^-. \tag{19}$$

It is natural that, in this case, the problem of determining n_k is substantially complicated, especially if it is considered that the terms corresponding to recombinations and transitions due to collisions render these equations nonlinear. The system of equations must be solved numerically. It might become necessary to solve this problem in investigations of bright lines arising in the outer layers of the atmosphere of flare stars. In most cases there is no need to solve eq.(19), and the distribution of the atoms by excited states can be considered stationary even in the absence of ionization-recombination equilibrium.

If the shell is not transparent to line emission, the basic problem /246
of determining line intensities becomes highly complex even in the stationary state since equations of the type of eq.(18) must be supplemented by transfer equations. The calculation becomes still more complex when the shell is opaque in the continuum. However, when the velocities of the macroscopic motion of the shell are large compared to the thermal velocities, the calculation of bright line intensities is greatly facilitated.

At a very great optical thickness of the shell in the lines, a quantum at the line frequency can escape from the shell only after having entered its outer boundary region. Quanta within the shell undergo only scattering (or absorption). When the layers of the shell move at different velocities, the conditions for the escape of quanta are greatly facilitated since, as a consequence of the Doppler effect, the central frequency of the line will be dissimilar at different points along the line of sight (with the exception, perhaps, of individual regions). It is obvious that, in such a case, the radiation intensity within the line in one layer depends little on the radiation in this line in another layer remote from it. The quantum which had appeared in the shell escapes from it, having undergone scattering only in a small area close to the point of its origin.

Complete independence of the atomic distribution by states in each layer on the position in other layers is possible only under the condition of trans-

parency of the shell to emission in a continuous spectrum. For example, in a planetary nebula at $\tau_{Lc} < 1$, ionization in all its parts is approximately the same. In the shells of stars, we have $\tau_{Lc} > 1$ so that a rigorous investigation necessitates a study of radiative transfer in the continuum, even if the Doppler effect in the lines is taken into account. Nevertheless, since allowance for the motion of the shell makes solving of the equation of line transfer unnecessary, the problem in question is greatly simplified.

The total energy E_{ik} emitted by a moving shell in a line with a frequency ν_{ik} can be obtained by integrating the quantity $\mathcal{E}_{ik}(\nu)$ determined by eq.(14) over the frequency and over all solid angles: /247

$$E_{ik} = \iint \mathcal{E}_{ik}(\nu)\, d\nu\, d\omega. \tag{20}$$

Replacing an integration over ν by an integration over z, with the help of the relation

$$d\nu = \frac{\Delta\nu_{ik}}{\Delta z}\, dz, \tag{21}$$

obtained from eq.(8) and introducing the designation

$$\beta_{ik} = \int (1 - e^{-\Delta\tau_{ik}})\, \frac{1}{\Delta\tau_{ik}} \frac{d\omega}{4\pi}, \tag{22}$$

eqs.(20) and (14) will yield

$$E_{ik} = 4\pi\Delta\nu_{ik} \iiint \varepsilon_{ik}\beta_{ik}\, dx\, dy\, dz. \tag{23}$$

An amount of energy $4\pi\varepsilon_{ik}\Delta\nu_{ik}$ is emitted by unit volume in the given line. Therefore, it follows from eq.(23) that β_{ik} represents the portion of energy escaping from the shell in the line out of the total energy produced in the shell at this frequency. If the shell is transparent to radiation in the line, i.e., $\Delta\tau_{ik} \ll 1$, then $\beta_{ik} = 1$ and all quanta formed in the shell escape from it unhindered. In the case in which the optical thickness of the shell in the line is very large and $\Delta\tau_{ik} \gg 1$, the quantity β_{ik} will become

$$\beta_{ik} = \frac{1}{2u\alpha_{ik}} \left| \overline{\frac{\partial v_z}{\partial z}} \right|, \tag{24}$$

where averaging of the velocity gradient is carried out over all solid angles.

Following V.V.Sobolev (Ref.2), let us now determine, from steady-state conditions, the quantities n_k for a shell opaque in lines, transparent at frequencies of the continuous spectrum, and moving with an appreciable velocity gradient. In constructing the steady-state equations we will consider the fact that, of the total number $n_k A_{ki}$ of quanta produced per sec per cm^3 of the shell, only a part equal to $n_k A_{ki}\beta_{ik}$ escapes from it while the remainder is absorbed in the same volume where it arose. These equations have the following form: /248

$$n_i\left(\sum_{k=1}^{i-1} A_{ik}\beta_{ki} + R_{ic}\right) = \sum_{k=i+1}^{\infty} n_k A_{ki}\beta_{ik} + n_e n^+ C_i(T_e) \quad (i = 1, 2, 3 \ldots), \tag{25}$$

where $n_e n^+ C_i(T_e)$ denotes the number of recombinations at the i-th level occurring in 1 cm^3 in 1 sec, while $n_i R_{ic}$ denotes the number of ionizations from the i-th level. Sobolev (Ref.2) assumed that ionization occurs by radiation of a hot star and that $R_{ic} = B_{ic} W \rho^*_{ic}$, where W is the dilution factor and ρ^*_{ic} is the density of ionizing radiation at the stellar surface.

The quantities β_{ik} may have different values in different parts of the shell. Therefore, the system (25) should be solved for each point after which, integrating over the entire shell, we can obtain the energy emitted in the line

$$E_{ik} = A_{ki} h\nu_{ik} \int n_k \beta_{ik}\, dV. \tag{26}$$

At spherical symmetry in the shell, we have

$$E_{ik} = 4\pi A_{ki} h\nu_{ik} \int_{r_*}^{\infty} n_k \beta_{ik} r^2\, dr. \tag{26'}$$

At $\beta_{ik} \ll 1$, we can use for it eq.(24) and then, by means of the second equation in the system (15) and the well-known relation between the Einstein coefficients A_{ki} and B_{ik}, obtain the relation

$$A_{ki}\beta_{ik} = \frac{\frac{g_2}{g_1} n_1 - n_2}{\frac{g_k}{g_i} n_i - n_k} \left(\frac{\nu_{ik}}{\nu_{12}}\right)^3 A_{21}\beta_{12}. \tag{27}$$

By means of eq.(27) we eliminate from the system (25) the quantities β_{ik}, which yields a system whose solution depends on the one parameter $x = \beta_{12}/W$ as well as on the stellar temperature T_* (over ρ^*_{ic}) and the electron temperature T_e (over C_i). The solution of this system for a hydrogen shell yielded the de- /249

gree of excitation $\frac{n_i}{n_1}$ and degree of ionization $\frac{n_e n^+}{W n_1}$ of the atoms therein. Here, the degree of excitation rapidly drops with increasing x and substantially differs from Boltzmannian when $x \gtrsim 0.1$.

V.V.Sobolev, having used the solution of the system (25), obtained the theoretical Balmer decrement - the relative intensities of the bright hydrogen lines - in the case $T_e = T_*$ at different values of x for a homogeneous shell, in which all quantities of the equations were independent of the position of the point. The Balmer decrement for a moving shell opaque at the line frequencies differs from that calculated by Cillie (Ref.15) for planetary nebulae. For example, if the shell is opaque only to line emission of the Lyman and Balmer series, then the ratio of intensities $\frac{H_\alpha}{H_\beta}$ at small values of x is larger in

comparison with the data of Cillie by a value close to 3, and the lines H_β, H_γ, and H_δ are close in intensities. This phenomenon was actually observed in spectra of a number of novae at a certain stage of evolution. In the spectra of stars of type Be, the relative intensities of the higher terms of the Balmer series are smaller than for planetary nebulae. The theoretical Balmer decrement, calculated at values of $0.1 \leqslant x \leqslant 1.0$, has such a character. This indicates opacity of the shells of stars of type Be in the lines.

V.V.Sobolev and V.V.Ivanov (Ref.17) calculated the Balmer decrement at an optical thickness of the shell in lines of the subordinate series less than unity, with consideration of the emission of the shell itself in a continuous spectrum. Transitions from excited states under the effect of radiation and forced recombinations were also taken into account. Although the relative populations of the levels were strongly dependent upon the quantity β_{12}, in all the examined cases the Balmer decrement proved to be approximately the same as for the nebulae. This conclusion confirms the fact noted above that, in order to explain the Balmer decrement observed for stars of type Be, we must assume /250 their shells to be opaque in lines of the subordinate series.

When comparing the theoretical Balmer decrement with the observed decrement, it must be remembered that this is an integral characteristic of the shell. The quantity x in the shell changes, and a variation in T_e is also possible. Furthermore, the parameter T_*, determining the temperature distribution in the spectrum of the ionizing radiation source need not be the Planckian temperature of the star but may have a different significance. All these facts impart a somewhat illustrative character to the results of the calculations of the Balmer decrement. Most important is the principal result of the theory - the explanation of the observed character of the Balmer decrement in the spectra of variable stars by the opacity of their shells.

When ionization of the gas is determined by radiation of the star, the effect of collisions on the magnitude of the Balmer decrement is unimportant since the free electrons produced in photoionizations have a comparatively low energy and cannot excite hydrogen atoms. If collision excitations are the main mechanism of hydrogen emission, then the Balmer decrement will be very steep. For example, the ratio of intensities $\frac{H_\alpha}{H_\beta}$ at $T = 10^4$ deg is equal to 10.8 and as $T \to \infty$ it approaches 4.2, whereas in excitation by radiation and at an electron temperature of 10^4 deg this ratio is 2.62.

Since recombinations also occur in ionization by collision, the observed Balmer decrement should have some average value between the decrement due to collisions and that caused by recombinations. Calculations of the decrement with allowance for collisions and ionization by collisions and radiation, where the role of collisions is large (for example, during passage of a shock wave over the shell of the star), are of significant interest for interpreting the observations. In such calculations we should take into account stratification of radiation associated with the unsteady state of emission behind the wave front.

5. Forbidden Lines and Unsteady State of the Radiation Field in Shells

/251

Forbidden bright lines in the spectrum arise upon transitions from the metastable state to lower energy states. In most cases of interest, the atom is brought to a metastable state by collisions since the corresponding excitation potentials are small. For a downward transition to occur, the atom excited to a metastable state should not be extracted from it either by absorption of radiation or by collisions with other particles (mainly with free electrons). Therefore, for the occurrence of forbidden lines a sufficiently small radiation density in the shell and a sufficiently small free electron density are needed. Besides in the spectra of nebulae and of the solar corona, forbidden lines are also observed in the spectra of novae at comparatively late stages, of nova-like stars, and, at times, in the spectra of long-period variables. In the spectra of Be and WR type stars there are no forbidden lines since, in their shells, the density of radiation and the density of matter are comparatively large.

The absorption coefficient at the frequency of the forbidden line is very small. Therefore, shells of stars can be considered transparent at these frequencies and the profiles of the forbidden lines are determined mainly by the velocity field in the shell. It is convenient to use the profiles of forbidden lines to investigate the structure of shells of novae at that period of the outburst when the shell is still opaque in the allowed lines.

To determine the theoretical relative intensities of forbidden lines, the Einstein coefficients A_{ki} of transition probability must be known. These have been calculated by Garstang (Ref.18) for the most important transitions of a number of atoms (O I, O III, N II, Ne III, Fe II). Furthermore, it is necessary to have the values of the effective collision cross sections for excitation and deactivation of the atoms. When Maxwellian electron velocity distribution is present, eq.(1), for the number of exciting collisions per 1 cm^3 per 1 sec, will yield the expression

/252

$$n_B b_{AB} = 8.63 \cdot 10^{-6} \frac{n_A n_e \Omega(AB)}{g_A \sqrt{T_e}} e^{-\frac{h\nu_{AB}}{kT_e}}, \tag{28}$$

and the number of collisions of the second kind in which the atom passes from state B to state A, equal to

$$n_B a_{BA} = 8.63 \cdot 10^{-6} \frac{n_B n_e \Omega(AB)}{g_B \sqrt{T_e}}, \tag{29}$$

where the quantity $\Omega(AB)$ represents a dimensionless cross section calculated by methods of quantum mechanics. Most forbidden lines in the spectra of novae in a nebular stage (just as in the spectra of nebulae) belong to ions with $2p^q$ and $3p^q$ configurations (O II, O III, N II, Ne III, etc.). The values of $\Omega(AB)$ for these configurations have been calculated by Seaton (Ref.19).

Using the available values of A_{ki} and $\Omega(AB)$ we can construct the steady-state equations for the given ion and obtain the ratio of intensities of the

forbidden lines belonging to it. This ratio depends on the quantity n_e and T_e. If we know from observations the ratios of forbidden-line intensities for two ions, then a comparison with the theoretical values will yield the electron temperature and concentration of free electrons in the shell. The complexity of the spectra of novae, caused by inhomogeneity of the shells and by smearing of the markedly broadened lines, has made it impossible for us to obtain the observational material needed for determining n_e and T_e by the indicated method.

The strong dependence of forbidden-line intensities on n_e and T_e makes these lines a convenient means for detecting phenomena of nonstationary emission in the shells. Such phenomena arise, in particular, upon an abrupt change in power of the ionization sources, which leads to disruption of the equilibrium between ionizations and recombinations. The adaptation of the medium to new emission conditions takes some time, this time being longer, the smaller the electron concentration in it. During the process of establishing equilibrium, n_e and T_e may vary substantially entraining also a change in the intensities /253 of the forbidden lines. Problems of the theory of a nonstationary radiation field will be taken up later; here, we will indicate only certain cases of variation of the forbidden lines associated with disturbances of radiative equilibrium in the stellar shell.

The appreciable increase in brightness of the Nova Herculis of 1934, after its deep minimum in April 1935, was due to an increase in high-frequency radiation of the star, thanks to which ionization of the theretofore unionized shell of the star took place (Ref.20, 21). Along with an increase in brightness there was an increase in the intensity ratio of the forbidden lines O III $\frac{E_{N_1+N_2}}{E_{4363}}$ in the stellar spectrum. The change of this ratio was explained by I.N.Minin (Ref.22). The electrons detached from the atoms, upon ionization of a given volume, have a large energy so that the electron temperature immediately after ionization is high. The electrons gradually lose energy in collisions with heavy particles and the temperature T_e drops; during this process, the quantity $\frac{E_{N_1+N_2}}{E_{4363}}$ should increase.

Another example of nonstationary emission in lines [O III] is found for certain symbiotic stars (Ref.23). After the ionization source was exhausted, the shell of the star began to fluoresce and the lines [O III] continued to be visible for a comparatively long time. This is due to the fact that atoms O III recombined, changing to atoms O II but not immediately. The relaxation time t_* in this case is determined by the formula

$$t_* = \frac{1}{n_e \sum_{i=2}^{\infty} C_i'}, \qquad (30)$$

where C_i' is the recombination coefficient of atoms O III at the i-th level and, at values of n_e characteristic for the shells of variable stars, amounts to several days. As can be demonstrated, the electron temperature during this /254 time remains high so that conditions for the excitation of emission in lines

[O III] exist in the shell.

If de-excitation (drop in the degree of ionization) of the originally highly ionized gas, consisting of hydrogen and an admixture of oxygen, takes place, conditions favorable for the occurrence of bright lines [O I] are created in this gas. The energy $E_{2\to1}$ emitted by the layer, for example, in the line corresponding to the transition of an atom O I from the ^1D level to the ^3P level (transition 2 → 1), is determined by the expression

$$E_{2\to1} \sim n_{0I} a_{21} \frac{A_{21}}{A_{21}+a_{21}} V e^{-\frac{h\nu_{12}}{kT_e}}, \qquad (31)$$

where A_{21} is the coefficient of spontaneous transition, $a_{21} = q_{21} n_e$ is the coefficient of deactivation of the atom from the ^1D state under the effect of collisions with electrons, n_{0I} is the concentration of atoms O I, and V is the gas volume. At first, when ionization is high, the oxygen is primarily in the O II state, the value of n_{0I} is small and there are no [O I] lines. After n_e diminishes by half (in time t_*) as a consequence of de-excitation, the quantity n_{0I} becomes equal in order of magnitude to the total number of oxygen atoms, i.e., increases by a multiple. The electron temperature decreases slowly and within the time t_* changes little. Therefore, $E_{2\to1}$ increases markedly and [O I] lines should appear in the spectrum of the shell. It is natural that later, as n_e diminishes, the [O I] lines should become weaker. Thus, the appearance of [O I] lines in the spectra of nonstationary stars can serve as an indication of the unsteady state of the radiation field in the shell. On this basis, the appearance of bright lines [O I] in the spectra of certain novae was explained (Ref.24).

Among the bright lines observed in the spectra of nonstationary stars, we frequently find Fe II lines and sometimes [Fe II] lines (the latter are especially intense for long-period variables shortly before minimum brightness).

The ionization potential of Fe I is less than the ionization potential of hydrogen, and for Fe II it is somewhat greater than for hydrogen. Therefore, in the layer of the shell, where almost all H atoms are ionized, the iron /255
atoms will also be primarily in the Fe III state. There should be many Fe II atoms in those layers where ionization of hydrogen is comparatively low. These have a number of low levels, some of which are metastable. Even at a comparatively low electron temperature ($T_e \approx 10{,}000^\circ$) excitation of Fe II atoms by electron collision is quite effective. These considerations permit understanding the observed changes in the intensities of Fe II and [Fe II] lines in the spectra of long-period variables (Ref.25).

As a shock wave passes over the shell of a star, the hydrogen is ionized (but not completely) and followed by de-excitation of the partially ionized gas. Some of the energy of the electron gas is spent on excitation of Fe II atoms, both the normal and metastable levels being excited. While the electron concetration n_e is sufficiently high, deactivating collisions between electrons and atoms in metastable states occur often and the forbidden lines become weak in comparison with normal lines for which collisions play no role. With de-excitation of the gas, the concentration n_e diminishes, the number of deactivating

collisions also decreases, and the intensity of [Fe II] lines increases with respect to Fe II lines (with a decrease in absolute intensity of both lines). This mode of intensity variation of the indicated lines occurs in long-period variables where, just as in the other cases examined, unique changes in the forbidden bright lines indicate disturbance of the ionization-recombination equilibrium in the stellar atmosphere.

At certain stages of evolution of some novae and in all recurrent novae, forbidden bright lines appear in the spectrum which belong to highly ionized atoms of various elements (from [Fe VI] to [Fe XIV], [Ca VII], etc.). The spectra of Z And and other symbiotic stars contain [Ne V], [Fe VI], etc. lines. Apparently special conditions of the excitation of radiation are present here. As an energy source of radiation we can suggest the action of high-energy particles (corpuscular fluxes) ejected by the star.

6. Absorption Lines in Spectra of Variable Stars /256

In the spectra of WR and P Cygni type stars the absorption lines are usually observed as an absorption component on the short-wave (violet) edge of the bright line. This fact has a simple explanation. The absorption lines arise in the expanding shell of the star or - more exactly - in the layer which is between the star and the observer. Since the indicated layer moves in a direction toward the observer, the lines produced by it shift toward short waves. Absorption lines in the spectra of novae observed at periods close to the moment of brightness maximum, have a similar character.

The absorption spectra of Be types have a different character. The bright lines of these stars are usually superposed on broad shallow absorption lines characteristic for the usual stars of class B, for which they, as is commonly considered, broaden as a consequence of the rapid rotation of the star. At the same time, the shell of a Be type star sometimes forms narrow absorption lines which are shifted comparatively little from the center (since the velocity of expansion of the shell of these stars is small). These lines can be superposed on emission lines, dividing the latter into two components. However, we cannot always consider the separation of bright line profiles into two components as being due to superimposition of absorption lines. The shells of Be type stars rotate rapidly, and calculation of the bright line profiles arising in the rotating opaque shells has shown (Ref.12) that, under certain conditions, these lines have two components even without consideration of the absorption lines. Theoretical absorption line profiles of Be stars are calculated on the basis of the theory of moving shells, which makes it necessary to take into account that the absorption lines are formed in the same region of the shell as the bright lines.

In a number of works, theoretical absorption line profiles of stars with rapidly moving shells (WR, P Cygni, novae) were obtained in the following manner: By solving the problem of transfer through a fixed shell the corresponding absorption line profile was found, after which the deformation of /257
this profile caused by motion of various portions of the shell was determined. Actually, the line profile should be calculated from the solution of the problem of radiative transfer at the line frequency through the moving shell. For this

purpose we must introduce into the transfer equations the Doppler effect caused by macroscopic motion of the gas. One attempt to consider the Doppler effect in solving the Schuster problem (of radiation scattering in the layer) was made by McCrea and Mitra as long ago as 1936 (Ref.26). It is of interest to present their transfer equations. In accordance with their procedure (Ref.26) we will first determine the frequency variation of the quanta in scattering. If a particle moving with a velocity v is struck by a quantum of frequency ν from a direction making an angle ϑ with the direction of motion, then from the point of view of the observer moving with the particle, this radiation has a frequency

$$\nu' = \nu\left(1 - \frac{v}{c}\cos\vartheta\right). \tag{32}$$

Scattering occurs at the same frequency, so that the scattering coefficient will have a value $\sigma(\nu')$. If the direction to the observer perceiving the scattered radiation ("fixed") makes an angle φ with the direction of velocity, then for him the frequency of the scattered quanta is equal to ν''

$$\nu'' = \nu'\left(1 + \frac{v}{c}\cos\varphi\right) \approx \nu\left[1 - \frac{v}{c}(\cos\vartheta - \cos\varphi)\right] \tag{33}$$

with an accuracy to within small values of the first order with respect to $\frac{v}{c}$.

It is obvious that the radiation with a frequency ν'', coming from a direction φ and scattered by the same particle in the direction ϑ, will have a frequency ν.

The transfer equation for the case of a plane-parallel purely scattering layer has the following form:

$$\cos\vartheta \frac{\partial I(\nu; x; \vartheta)}{\partial x} = -\rho\sigma(\nu')\left[I(\nu; x; \vartheta) - J(\nu; x; \vartheta)\right], \tag{34}$$

where

$$J(\nu; x; \vartheta) = \frac{1}{2}\int_0^{\pi} I(\nu''; x; \varphi)\sin\varphi\, d\varphi \tag{35}$$

and x is the distance of a point from the lower boundary of the layer. The quantity v as a function of x should be given. The Doppler effect caused by thermal agitation is disregarded in eqs.(34) and (35).

If the layer moves with a velocity gradient in a direction toward the observer, then the absorption line formed by it will shift toward short waves and broaden, with the line width being larger, the greater the velocity gradient. Whereas, in the static case, the form of the profile substantially depends on the function $\sigma(\nu)$, the profile of the line formed by a shell moving at high velocity depends mainly on the quantity v. Therefore, for the case of rapidly moving shells we can neglect all factors except the macroscopic motion of the shell when calculating the absorption line profiles. In the case of comparatively slowly moving shells, such as, for example, the atmospheres of the Cepheids, an accurate calculation of the theoretical absorption line profiles requires solving a system of the form of eqs.(34) - (35) with consideration of the

/258

thermal agitation of atoms. This problem has not yet been formulated*.

Let us examine the formation of absorption lines in a shell whose velocity of motion is sufficiently large compared to the velocity of thermal agitation of atoms. We will assume that between the shell of the star and the photosphere, i.e., the region producing the continuous spectrum, there is a distinct boundary (this corresponds to the Schuster model). Let τ_ν be the optical thickness of the shell at frequency ν for radiation escaping from a point of the stellar disk with the coordinates $(\vartheta'; \varphi')$ in the direction of the observer. A portion, $e^{-\tau_\nu}$, of the photosphere radiation coming from a point of the stellar surface with the coordinates $(\vartheta'; \varphi')$ passes through the shell. Therefore, the ratio i_ν of the radiation intensity at frequency ν escaping from the shell to the intensity in an adjacent portion of the continuous spectrum is determined by the expression

$$i_\nu = \frac{\int_0^{2\pi} d\varphi' \int_0^{\frac{\pi}{2}} \psi(\vartheta'; \varphi') e^{-\tau_\nu} \cos\vartheta' \sin\vartheta' d\vartheta'}{\int_0^{2\pi} d\varphi' \int_0^{\frac{\pi}{2}} \psi(\vartheta'; \varphi') \cos\vartheta' \sin\vartheta' d\vartheta'}, \tag{36}$$

where the function $\psi(\vartheta'; \varphi')$ expresses the brightness distribution on the surface of the photosphere. The quantity τ_ν depends on ϑ' and φ' and is determined by the known dependence of the absorption coefficient in the line on the frequency at a given velocity field in the shell. Equation (36) determines the absorption line profile. /259

Calculations by means of eq.(36) are simplest for the case of a spherically symmetric expanding shell, when τ_ν and ψ do not depend on φ'. Let us assume the width of the profile of the absorption coefficient to be so small that the shell can be considered opaque only at the frequency corresponding to the line center and transparent at all other frequencies. Then the radiation at a frequency ν coming from the photosphere is absorbed only by those atoms whose motion makes an angle ϑ with the direction toward the observer, whence

$$\cos\vartheta = \frac{\nu - \nu_0}{\nu_0} \frac{c}{v}, \tag{37}$$

where ν_0 is the frequency of the line center corresponding to a fixed volume. These atoms absorb radiation coming from the annular portion of the stellar disk included between the angles ϑ and $\frac{\pi}{2}$ (for an infinite shell). Considering that the shell is completely opaque to radiation in the line ($\tau_\nu = \infty$), we find the formula

---

* Results of the calculations of absorption line profiles formed in a plane-parallel atmosphere in the presence of a velocity gradient were published recently (Ref.33).

$$i_\nu = 1 - \frac{\int_{\delta}^{\frac{\pi}{2}} \psi(\vartheta') \cos\vartheta' \sin\vartheta' d\vartheta'}{\int_{0}^{\frac{\pi}{2}} \psi(\vartheta') \cos\vartheta' \sin\vartheta' d\vartheta'}, \tag{38}$$

which was first derived by V.V.Sobolev (Ref.2). By means of this formula and one similar to it, the profiles of lines formed by expanding shells were calculated (Ref.2) for the case of an infinite shell. Subsequently, profiles were calculated by means of eq.(36) for more general cases where the profile of the absorption coefficient was of the Doppler type.

The just described mechanism of formation of the absorption line of a moving shell is, in essence, completely different from the mechanism of formation of a line in a fixed atmosphere. In the case of Schuster's model for a fixed atmosphere, the quantity i_ν is expressed by the well-known formula /260

$$i_\nu = \frac{1}{1+\tau_\nu}, \tag{39}$$

which in no way is related, in particular, with eq.(38). According to the latter, the value of i_ν stems from a geometric effect. Therefore the dependence of the equivalent width on the number of absorbing atoms (growth curve) for a moving shell, generally speaking, should not be similar to the corresponding dependence for a fixed atmosphere. Considerable work on calculating theoretical growth curves by means of eq.(36) should precede the use of the method of growth curves for analyzing shells of nonstationary or variable stars.

7. Effect of Radiation of Stellar Shells on the Observed Continuous Spectrum

Stellar shells radiate not only at line frequencies but also in a continuous spectrum. If the optical thickness of a shell in the observed region of the spectrum is small in comparison with unity, the visible spectrum is formed simply by the combination of stellar radiation with shell radiation. Provided the shell is opaque in the indicated region and is continuous, the observed continuous spectrum belongs only to the shell.

The first of the indicated cases is quite simple for investigation and for construction of a theoretical spectrum since the shell, transparent to stellar radiation, is also transparent to its own radiation at appropriate frequencies. Stars of type Be have such shells transparent in the subordinate continua of hydrogen. For the total energy $L(\nu)$ emitted by a star in a certain frequency ν of the visible portion of the spectrum, we have the expression

$$L(\nu) = L_* (\nu) + L_{sh}(\nu). \tag{40}$$

The value of $L_*(\nu)$, the radiation of the central star, can be given approxi- /261
mately if we consider it to be Planckian, but $L_*(\nu)$ is determined more accurately by means of model atmospheres. In the luminous part of the shell of a Be type star the hydrogen is in a state of high ionization and its radiation $L_{sh}(\nu)$ is due to recombinations and free-free transitions. To calculate the recombination spectrum we must know T_e, n_e, n^+ and the volume of the ionized portion of the shell. In the case of a spherically symmetric shell we have

$$L_{sh}(\nu) = 4\pi \int_{r_*}^{\infty} n_e n^+ \varepsilon_j e^{-\frac{h\nu}{kT_e}} (1 - W) r^2 dr, \tag{41}$$

where

$$\varepsilon_j = KT_e^{-\frac{1}{2}} \left(1 + \frac{3.1 \cdot 10^5}{T_e} \sum_{i=j}^{\infty} \frac{1}{i^3} e^{\frac{h\nu_{ic}}{kT_e}}\right). \tag{42}$$

Here, ν_{ic} is the frequency of ionization of a hydrogen atom from the i-th state, W is the radiation dilution factor, and K is a known constant. If ν pertains to the Balmer series, then j = 2, while if it refers to the Paschen series, then j = 3. The dependence of T_e and n_e on r should be known for calculating $L_{sh}(\nu)$ from eqs.(41) and (42).

The energy distribution in the continuous spectrum is usually characterized by the parameter T_c, called the spectrophotometric temperature and determined by the relation

$$\frac{d}{d\nu} \log E(\nu) = \frac{3}{\nu} - \frac{h}{kT_c} \frac{1}{1 - e^{-\frac{h\nu}{kT_c}}}, \tag{43}$$

where $E(\nu)$ is the observed energy distribution in the spectrum. For the radiation of the shell, T_c is appreciably less than T_e and at the same time $T_e < T_*$. Therefore, the radiation of a star with a shell corresponds to a lower spectrophotometric temperature than the radiation of a star of the same spectral class without a shell.

Another important fact associated with the presence of a shell is the change in D, the magnitude of the jump of radiation intensity at the limit of the Balmer series which is determined by the relation

$$D = \log \frac{L(\nu_{2c} - \varepsilon)}{L(\nu_{2c} + \varepsilon)}, \tag{44}$$

where ε is a sufficiently small value. In the Balmer continuum (near the /262
series limit) less radiation escapes from the photosphere of the star than in the Paschen continuum. The shell, on the other hand, radiates in the Balmer continuum more energy than in the Paschen. When these two radiation sources are superposed, the value of D becomes smaller than for a star without a shell. In the case where the shell is sufficiently powerful, the value of D may become negative, i.e., in the spectrum of such a Be type star, emission will be observed beyond the limit of the Balmer series.

These theoretical considerations were used by the author (Ref.27) for interpreting the spectrum of the much observed star γ Cassiopeia and then for

other stars of type Be by Tsoi Tiai (Ref.28) and by R.Oganesyan (Ref.29). In these works, the characteristics of shells of Be type stars of different subclasses were obtained by comparing the theory with observations.

It is much more complicated to obtain the theoretical spectrum of an opaque shell because in this case it is first necessary to solve the problem of radiative transfer in several continua. In the general form, this problem is highly complex and has not been solved. The situation is somewhat better when dealing with very hot stars in whose shells scattering of radiation by free electrons plays a substantial role. At $T_* \gtrsim 50{,}000^\circ$, a layer caused by free electron scattering, with an optical thickness of the order of unity, has a much smaller optical thickness when caused by absorption beyond the Lyman series limit. It is obvious that in the visible spectrum region the role of electron scattering is even greater. The problem of radiative transfer is comparatively simple when only free electron scattering is taken into account.

The influence of electron scattering in the atmosphere of the hot star on its spectrum was first examined theoretically by V.A.Ambartsumyan (Ref.30). The study by S.G.Slyusarev (Ref.31) is also devoted to this problem. In his studies on radiative transfer in a plane layer with consideration of electron scattering and true absorption, he showed that electron scattering promotes reprocessing of radiation and an approach to a state of local thermodynamic equilibrium. As a result of scatterings, the path of the quanta in the layer increases, so that the probability of it being detected becomes greater and consequently the /263 effective optical thickness of the layer increases.

It was also found (Ref.31) that, with an increase in the ratio $\frac{\sigma}{\alpha_\nu}$ (where σ is the scattering coefficient and α_ν is the true absorption coefficient) the spectrophotometric temperature of radiation of the layer decreases. Thus, for $\frac{\sigma}{\alpha_\nu} \approx 10$ and at a temperature of the medium of $T \approx 60{,}000^\circ - 80{,}000^\circ$ the value of T_c in the visible spectrum region is about $15{,}000^\circ$. Furthermore, as a consequence of electron scattering the magnitude of the intensity jump at the limits of the subordinate series decreases.

The effect of electron scattering on the spectrum should be similar, in its general features, to that described when the plane layer is replaced by a spherical shell. Thus, when electron scattering is taken into account we can at least give a qualitative explanation of the observed peculiarities of the continuous spectrum of WR stars - their comparatively low spectrophotometric temperature (at a high temperature of the star, found from the bright line) and the absence of an intensity jump at the limits of the subordinate series.

Novae, after reaching maximum brightness, in addition to having a main shell which is thrown off at the moment of outburst and is transparent in the visible portion of the spectrum, also have an extended shell formed by matter continuously ejected from the star. This shell has a large optical thickness in the continuum and produces mainly an observable continuous spectrum which can be interpreted in the same manner as the spectrum of WR stars. The main shell also plays some role in the formation of the continuous spectrum, which is

apparent from the presence of a negative intensity jump (emission) at the series limit in the spectra of a number of novae (for example, the 1936 Nova Lacertae). There has still been no complete theoretical investigation of the continuous spectrum of novae.

We note that, as shown elsewhere (Ref.32), the use of the so-called theory of extended photospheres (Ref.33) for interpreting the continuous spectrum of WR stars and novae cannot yield satisfactory results. This theory, in its /264 present form, does not take into account the dependence of the absorption coefficient on the frequency and postulates the existence of a local thermodynamic equilibrium in the photosphere. These shortcomings make it applicable as a first approximation.

Molecules, and also atoms of metals and negative hydrogen ions, play the major role in the formation of the continuous spectrum of nonstationary stars of late classes (in particular, long-period variables). In their basic features, the continuous spectra of these stars should be similar to the spectra of normal stars of the corresponding class. The construction of a model atmosphere and the determination of the theoretical continuous spectrum for stars of late spectral classes encounter considerable difficulties which have not yet been overcome.

REFERENCES

1. Joy, A.: Astrophys. J., Vol.105, p.96, 1947.
2. Sobolev, V.V.: Moving Shells of Stars (Dvizhushchiyesya obolochki zvezd). Izd. Leningr. Gos. Univ., 1947.
3. Whitney, C.: Ann. Astrophys., Vol.19, p.142, 1965.
4. Abt, H.: Astron. J., Vol.130, p.824, 1959.
5. Odgers, G. and Kushwaha, R.: Publ. Dominion Astrophys. Obs., Victoria, B.C., Vol.11, No.11, 1960.
6. Gorbatskiy, V.G.: Astron. Zh., Vol.38, p.256, 1961.
7. Gorbatskiy, V.G.: Vestn. Leningr. Gos. Univ., No.13, 1960.
8. Beals, C.: Monthly Notices, Vol.90, p.202, 1929; Vol.91, p.966, 1931.
9. Wilson, O.: Astrophys. J., Vol.82, p.233, 1935.
10. Rottenberg, J.A.: Monthly Notices, Vol.112, p.125, 1952.
11. Ambartsumyan, V.A., Mustel', E.R., Severnyy, A.B., and Sobolev, V.V.: Theoretical Astrophysics (Teoreticheskaya astrofizika). Gostekhizdat, 1952.
12. Sobolev, V.V.: Astron. Zh., Vol.36, p.573, 1959,
13. Gorbatskiy, V.G.: Astron. Zh., Vol.28, p.450, 1951.
14. Rublev, S.V.: Astron. Zh., Vol.37, p.828, 1960; Vol.40, p.643, 1963.
15. Cillie, G.: Monthly Notices, Vol.92, p.830, 1932; Vol.96, p.771, 1936.
16. Burgess, A.: Monthly Notices, Vol.118, p.477, 1958.
17. Sobolev, V.V. and Ivanov, V.V.: Tr. Astron. Observ. Leningr. Gos. Univ., Vol.19 (Uch. Zap. Leningr. Gos. Univ., No.307), p.3, 1962.
18. Garstang, R.: Monthly Notices, Vol.111, p.115, 1951; Vol.124, p.321, 1962.
19. Seaton, M.: Rev. Mod. Phys., Vol.30, No.3, p.979, 1958.
20. Grotrian, W.: Z. Tech. Phys., Vol.18, p.146, 1937.
21. Sobolev, V.V.: Astron. Zh., Vol.27, p.81, 1950.

22. Minin, R.N.: Astron. Zh., Vol.29, p.154, 1952.
23. Aller, L.: Publ. Dominion Astrophys. Obs., Vol.9, No.11, 1954.
24. Gorbatskiy, V.G.: Vestn. Leningr. Gos. Univ., No.19, 1961. /265
25. Gorbatskiy, V.G.: Astron. Zh., Vol.34, p.860, 1957; Vol.35, p.748, 1958.
26. McCrea, W. and Mitra, K.: Z. Astrophys., Vol.11, p.359, 1936.
27. Gorbatskiy, V.G.: Astron. Zh., Vol.26, p.307, 1949.
28. Tsoi Tiai, O.: Astron. Zh., Vol.33, p.682, 1956.
29. Oganesyan, R.Kh.: Soobshch. Byurakansk. Observ., Vol.32, 1962.
30. Ambartsumyan, V.A.: Uch. Zap. Leningr. Gos. Univ., No.22, 1938.
31. Slyusarev, S.G.: Dokl. Akad. Nauk SSSR, Vol.95, No.4, 1954.
32. Buslavskiy, V.G.: Tr. Astron. Observ. Leningr. Gos. Univ., Vol.19 (Uch. Zap. Leningr. Gos. Univ., No.307), p.67, 1962.
33. Abhyankar, K.D.: Astrophys. J., Vol.140, p.1353, 1964; Vol.140, p.1368, 1964; Vol.141, p.1056, 1965.

ANALYSIS OF THE EMISSION SPECTRA OF NONSTATIONARY STARS /266

A.A.Boyarchuk

Many nonstationary (variable) stars have an emission spectrum that resembles the spectrum of planetary nebulae. Thus, the spectra of type Z And stars contain practically all emission lines which are observed for planetary nebulae. Therefore, methods developed for planetary nebulae are often used for analyzing conditions in the shells of nonstationary stars (Ref.1). Furthermore, it is known that the electron concentration in the shells of most nonstationary stars is by many orders larger than that of planetary nebulae. For example, it is of the order of 10^7 cm^{-3} for type Z And stars (Ref.2, 3), whereas for most planetary nebulae it does not exceed 10^4 cm^{-3}. This difference results in the role of transitions due to collisions of the second kind being greater in shells of nonstationary stars than in planetary nebulae. Therefore, the formulas for determining electron temperature and electron concentration derived for the case of planetary nebulae, i.e., low-density objects (Ref.4), must be modified before using them for analyzing the spectra of nonstationary stars. As an example let us examine the steady-state equation for low energy levels of the ion O III (Fig.1). The steady-state equation for the k-th level will have the form

$$\sum_{i=k+1}^{5} n_i (A_{ik} + n_e q_{ik}) + \sum_{l=1}^{k-1} n_e n_l q_{lk} = n_k \left[\sum_{l=1}^{k-1} (A_{kl} + n_e q_{kl} + \sum_{i=k+1}^{5} n_e q_{ki} \right], \quad (1)$$

where n_i denotes the number of atoms at the i-th level, n_e is the number of free electrons in 1 cm^3, and A_{ik} is the probability of spontaneous transition /267 between the levels i and k. The coefficient of deactivation of the i-th level by electron collision is denoted by q_{ik} $(i > k)$, whence

$$q_{ik} = \frac{8.63 \cdot 10^{-6}}{\omega_i T_e^{1/2}} \Omega_{ik},$$

where Ω_{ik} is the "effectiveness of collision" (Ref.6), ω_i is the statistical weight of the i-th level, and T_e is the electron temperature. The coefficient of excitation of the k-th level by electron collision is related with the coefficient of deactivation of this level by

$$q_{ki} = \frac{\omega_i}{\omega_k} q_{ik} e^{-\frac{h\nu_{ik}}{kT_e}}. \quad (2)$$

In constructing the steady-state equation we disregarded radiative transitions since they are all forbidden. Furthermore, we will consider this system of levels as closed and will neglect arrivals produced by direct recombinations and

successive upward transitions. As calculations have shown (Ref.5), the population of these levels due to successive transitions from upper levels and recombinations of the ion O IV for $T_e = 17{,}000^\circ$K and $n_e = 2.2 \times 10^4$ cm^{-3} amounts to less than 7% of the population produced by transitions from the ground level of the ion O III under the effect of electron collision.

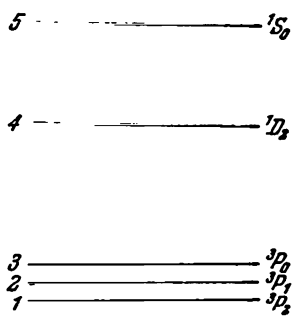

Fig.1 Diagram of Lower Energy Levels of the Ion O III.

By solving the system (1), the relative number of atoms at different levels was obtained. Similar calculations have been made for other ions having a similar configuration of the lower energy levels (Ref.6). Furthermore, knowing the populations of the levels permits determining the intensities of the lines arising upon transitions between these levels. Per unit volume we have

$$I_{ik} = \frac{1}{4\pi} n_i A_{ik} h\nu_{ik}. \qquad (3)$$

The results of the calculation are shown in Figs.2 - 5. These diagrams /268 present the curves of equal ratios $\frac{I_{54}}{I_{43} + I_{42}}$ on the plane ($\log n_e$, $\log T_e$).

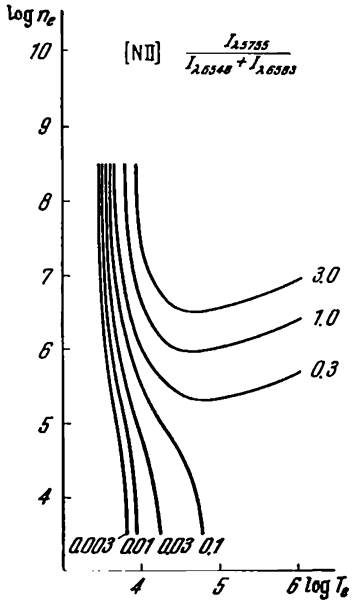

Fig.2 Curves of $\frac{I_{54}}{I_{43} + I_{42}}$ = const for Ions N II.

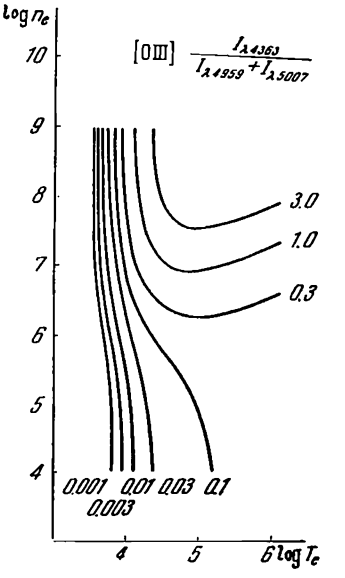

Fig.3 Curves of $\frac{I_{54}}{I_{43} + I_{42}}$ = const for Ions O III.

We see that, at low electron concentrations ($n_e \lesssim 10^4$ cm^{-3}), these intensity ratios depend only on the electron temperature. However, with an increase in n_e the ratio of the forbidden-line intensities begins to depend on both quantities, n_e and T_e. This is due to the fact that the number of transitions, under the effect of electron collisions of the second kind, becomes comparable to the number of spontaneous transitions.

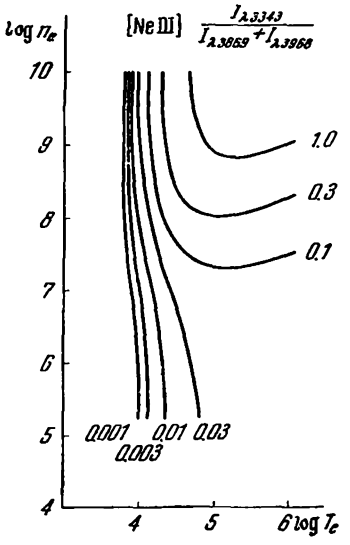

Fig.4 Curves of $\frac{I_{54}}{I_{43}+I_{42}}$ = const for Ions Ne III.

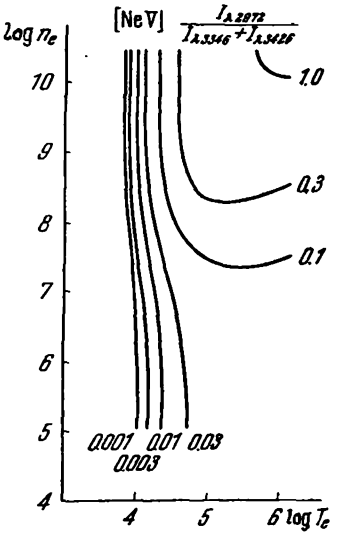

Fig.5 Curves of $\frac{I_{54}}{I_{43}+I_{42}}$ = const for Ions Ne V.

In the spectra of many nonstationary stars (novae at the beginning of the nebular stage, type Z And stars, etc.) the ratio of [O III] intensities, as /269 shown by observations, is $\frac{I_{\lambda 4363}}{I_{\lambda 4959}+I_{\lambda 5007}} \sim 0.3$ (Ref.2, 3). Hence, in this case it is impossible to determine either the electron temperature or the electron concentration from observations of only O III lines. The lower limit of the electron concentration is the only datum that can be found from the relative intensities of forbidden lines of one ion for a medium with $n_e > 10^6$, i.e., for most shells of nonstationary stars. Using the intensities of the borbidden lines of two ions, for example [N II] and [O III], we can theoretically determine simultaneously the electron temperature and electron density of the medium. Incidentally, it should be pointed out here that the lines of equal ratios $\frac{I_{54}}{I_{43}+I_{42}}$ for different ions are very similar (see Figs.2 - 5). In most /270 cases they intersect at low angles, and the accuracy of determining n_e and T_e by this method is not very great. Furthermore, the following must be taken into account: It is known that both planetary nebulae (Ref.7) and the shells of novae at a late stage (Ref.8), when photographed at the frequencies of different lines have a different appearance, i.e., there is stratification of the radiation. This indicates different conditions of excitation at different points of

the medium. This circumstance lessens the reliability of determining electron temperature and electron concentration from the relative intensities of forbidden lines of two or several ions.

Another method of determining the conditions in the medium is based on an analysis of the energy distribution in the continuous spectrum. In the range of temperatures existing in the shells of nonstationary stars, the emission in the continuous spectrum is created mainly by hydrogen and helium. The ratio of the helium and hydrogen contents in most cosmic objects does not exceed 0.20. This results in the contribution of helium to continuous radiation being small in comparison with the contribution of hydrogen. Therefore, we will henceforth limit our study to continuous radiation of a purely hydrogen medium.

The radiation intensity per 1 cm^3 at a frequency ν can then be described as

$$I_\nu = n_e n^+ \left(\sum_{i=k}^{\infty} C_i(T_e) + C_{ff}(T_e) + \frac{C_{2q}(T_e)}{1 + 0.6\cdot 10^{-4} n_e}\right)\frac{h\nu}{4\pi} = f(\nu,\ n_e,\ T_e). \tag{4}$$

Here the first term in parentheses takes into account radiation due to recombination. The value of k depends on the spectral region under study. For $\lambda\lambda$ 3646 to 8205 Å, we have k = 3. The second term corresponds to radiation due to free-free transitions of electrons in proton fields, and the third term characterizes two-photon radiation (Ref.4).

Thus, energy distribution is a function of both electron concentration and electron temperature and, in principle, permits determining the quantities n_e and T_e. For this, it is convenient to use the magnitude of the Balmer jump: /271

$$-D_B = \log\frac{I_{3647-}}{I_{3647+}} = \log\frac{\sum_{i=2}^{\infty} C_i(T_e) + C_{ff}(T_e) + \frac{C_{2q}(T_e)}{1+0.6\cdot 10^{-4} n_e}}{\sum_{i=3}^{\infty} C_i(T_e) + C_{ff}(T_e) + \frac{C_{2q}(T_e)}{1+0.6\cdot 10^{-4} n_e}}. \tag{5}$$

The results of calculations by eq.(5) are shown in Fig.6, taken from another paper (Ref.6). The diagram shows that the magnitude of the Balmer jump, at $n_e < 10^3$ cm^{-3} and $n_e > 10^6$ cm^{-3}, depends only on the electron temperature. At intermediate values of n_e, the jump D_B depends also on electron concentration. It is true that the dependence is rather weak. Thus, from the value of the Balmer jump the electron temperature can be determined if the value of the electron concentration is even approximately known.

However, the simultaneous use of the forbidden-line intensities and the magnitude of the Balmer jump for determining the values of n_e and T_e raises /272 certain objections. These are related with the possible difference of the excitation conditions in the regions of hydrogen-line and forbidden-line emission. We can present the following considerations to support the fact that such differences actually might exist. The radiation intensity of hydrogen is propor-

tional to n_e^2 which means that it arrives mainly from denser regions of the medium. The forbidden-line intensity, owing to the effect of collisions of the second kind, increases much more slowly than in proportion to n_e^2, so that these lines, on the average, will penetrate into the less dense portions of the shells. The emission in forbidden lines is excited by electron collision. Therefore, the electron temperature will be lower in those regions where the forbidden lines glow more strongly. All this results in the denser portions of the shell being hotter and the less dense being cooler, i.e., differences will exist in the conditions of excitation in the medium.

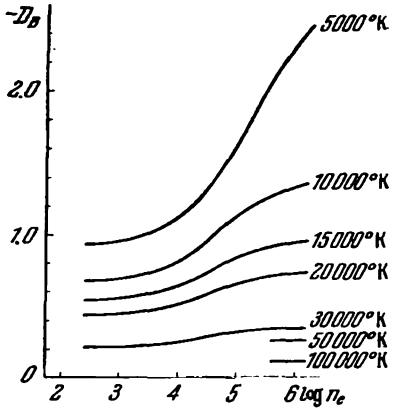

Fig.6 Balmer Jump D_B at Different Electron Concentrations and Temperatures.

In certain cases in the study of nonstationary stars, we can also use specific methods for determining conditions in their shells. The basic principle of these methods is as follows: Let us assume that the field of exciting radiation depends on time. In that case, changes in the populations of the levels and state of ionization will occur. Therefore, the character of the spectrum will also change in time. These changes should occur not immediately, but with some lag. The magnitude of this lag, i.e., the relaxation time, is determined by conditions in the medium and depends mainly on the electron concentration. The problem of the emission of a medium in a time-variant radiation field was studied in detail by V.V.Sobolev (Ref.9). Here (as an example), we will discuss a simple case - recombination emission of the medium after "disconnecting" the ionization sources. In this case, the variation in the number of ions will be determined by the equation

$$\frac{dn^+}{dt} = -n_e n^+ \sum_{i=2}^{\infty} C_i(T_e). \tag{6}$$

If, at the initial instant t = 0, the ion concentration is $n^+ = n_0^+$, then /273

$$n^+(t) = \frac{n_0^+}{1 + n_0^+ \sum_{i=2}^{\infty} C_i(T_e) \cdot t}. \tag{7}$$

In integrating eq.(6) we took into account that $n_e = n^+$. The time τ during which the ion concentration diminishes by half is known as the relaxation time:

$$t_{rel} = \frac{1}{n_e \sum_{i=2}^{\infty} C_i(T_e)}. \tag{8}$$

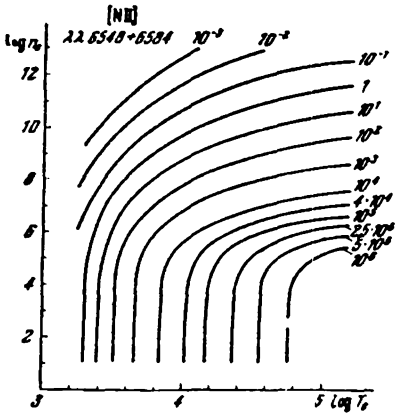

Fig.7 Curves $\theta(n_e, T_e) = \text{const}$ for Lines λλ 6548 + 6584 Å of the Ion N II.

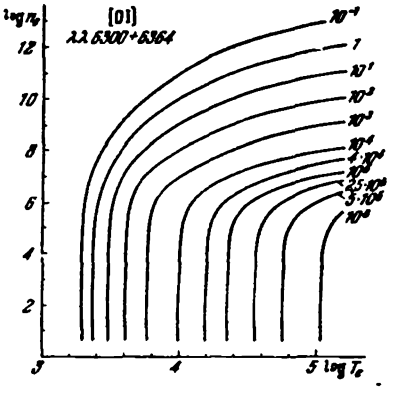

Fig.8 Curves $\theta(n_e, T_e) = \text{const}$ for Lines λλ 6300 + 6364 Å of the Atom O I.

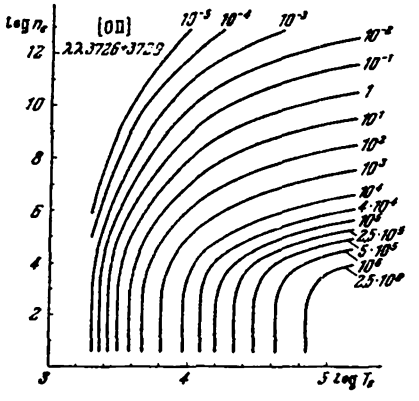

Fig.9 Curves $\theta(n_e, T_e) = \text{const}$ for Lines λλ 3727 + 3729 Å of the Ion O II.

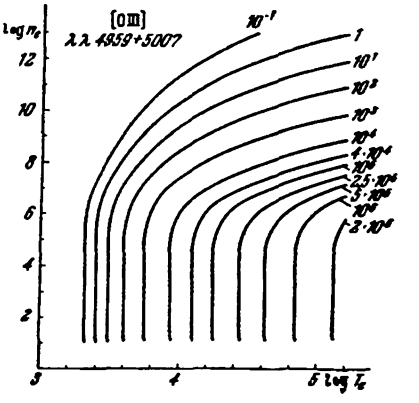

Fig.10 Curves $\theta(n_e, T_e) = \text{const}$ for Lines λλ 4959 + 5007 Å of the Ion O III.

Knowing the time of change of the line intensities in the spectrum, we can determine the electron concentration on the basis of eq.(8). The quantity $\sum_{i=2}^{\infty} C_i(T_e)$ depends only weakly on the electron temperature. However, the equality (8) permits estimating only the order of electron concentration since, in deriving and solving eq.(6), a number of assumptions were made (complete "disconnection" of the excitation sources, constancy of T_e).

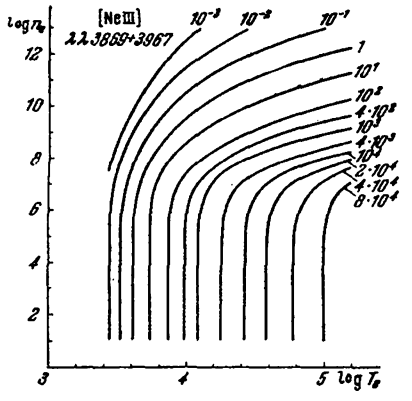

Fig.11 Curves $\theta(n_e, T_e) = \text{const}$ for Lines λλ 3869 + 3867 Å of the Ion Ne III.

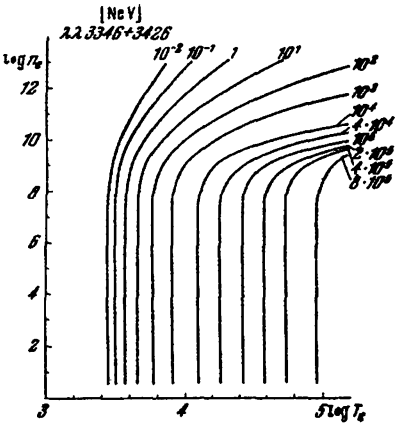

Fig.12 Curves $\theta(n_e, T_e) = \text{const}$ for Lines λλ 3346 + 3426 Å of the Ion Ne V.

Let us now define the possible influence of indeterminancy in the values of the electron temperature and electron concentration relative to the results of determining the chemical composition. The radiation intensity per 1 cm^3 in the line, corresponding to the transition i → k, is given by eq.(3). For forbidden lines, the population of the i-th level can be found from the system (1):

$$n_i = n_e n_1 \varphi(n_e, T_e), \tag{9}$$

where $\varphi(n_e, T_e)$ is some function of density and temperature, and n_1 is the number of ions at the ground level. For the line Hβ, we have

$$I_{H_\beta} = 2.24 \cdot 10^{-19} n_p n_e \frac{b_4(T_e)}{T_e^{3/2}} e^{\frac{9814}{T_e}}, \tag{10}$$

where n_p is the concentration of protons, while $b_4(T_e)$ is a coefficient indicating how many times the population of the fourth level differs from its population at thermodynamic equilibrium with $T = T_e$. From eqs.(3), (9), and (10) /275 we easily obtain

$$\frac{I_{ik}}{I_{H\beta}} = \frac{n_1}{n_p}\theta_i(n_e, T_e), \tag{11}$$

where

$$\theta_i(n_e, T_e) = \varphi(n_e, T_e)\frac{T_e^{3/2}e^{\frac{9814}{T_e}}}{2.24\cdot 10^{-19}b_4(T_e)}. \tag{12}$$

Thus, to find the relative ion concentration (n_1/n_p) from the line intensity ratios ($I_{ik}/I_{H\beta}$), the function $\theta_i(n_e, T_e)$ must be known. Figures 7 - 13 taken from another paper (Ref.6) give the curves of equal values of this function for lines of different atoms. These diagrams show that, at low concentrations ($n_e \lesssim 10^5$ cm^{-3}), the function $\theta_i(n_e, T_e)$ and thus also the quantity $\frac{n_1}{n_p}$ depend practically only on the electron temperature. As already noted above, in the shells of nonstationary stars we have $n_e \sim 10^7$ cm^{-3}. In this case, the function $\theta_i(n_e, T_e)$ substantially depends on both variables, n_e and T_e, and the accuracy of determining the ion concentration will be less than in the case of planetary nebulae. In particular, if we use the average values of n_e and T_e for the entire shell then, as a consequence of the forbidden lines arising in less dense and cooler parts, we will obtain an underestimated value of the ion concentration (Ref.10). We can obtain more reliable values of the ion concentration by investigating allowed lines. /276

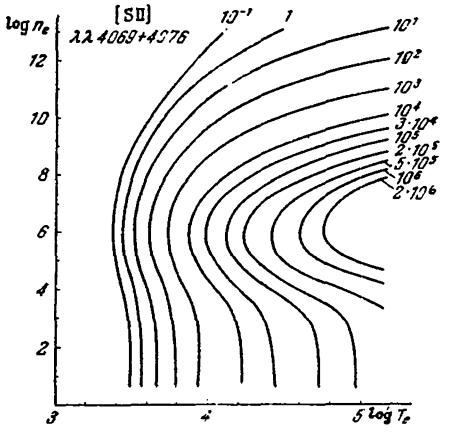

Fig.13 Curves of $\theta(n_e, T_e)$ = const for Lines λλ 4069 + + 4076 Å of the Ion S II.

As is known, the recombination coefficients depend little on the electron temperature, and this dependence is about the same for different ions. The intensity of the allowed line is given by an expression similar to eq.(10). In place of eq.(11) we then have

$$\frac{I_{ik}}{I_{H\beta}} = \frac{n_i^+}{n_p}\vartheta(T_e). \tag{13}$$

Here $\vartheta(T_e)$ is some slowly varying function of the electron temperature. Upon an increase in T_e from 10,000° to 20,000° these changes usually do not exceed a few percent (Ref.10). Thus, a determination of the ion concentration from allowed lines only requires knowledge of the approximate value of the electron temperature, making it thus more reliable than determinations based on forbidden lines. The only obstacle to the wide use of this method is the lack of calculations for the values of $b_i(T_e)$ for many ions.

REFERENCES

1. Gurzadyan, G.A.: Planetary Nebulae (Planetarnyye tumannosti). Fizmatgiz, 1962.
2. Aller, L.H.: Publ. Dominion Astrophys. Obs. Victoria, B.C., Vol.IX, p.321, 1954.
3. Boyarchuk, A.A.: Peremennyye Zvezdy, Vol.15, p.36, 1964.
4. Kaplan, S.A. and Pikel'ner, S.B.: Interstellar Matter (Mezhzvezdnaya sreda). p.118, Fizmatgiz, 1963.
5. Burgess, A. and Seaton, M.J.: Monthly Notices Roy. Astron. Soc., Vol.121, p.76, 1960.
6. Boyarchuk, A.A., Gershberg, R.Ye., and Pronik, V.I.: Izv. Krymsk. Astrofiz. Observ., Vol.29, p.291, 1963.
7. Vorontsov-Vel'yaminov, B.A.: Gaseous Nebulae and Novae (Gazovyye tumannosti i novyye zvezdy). Izd. Akad. Nauk SSSR, 1948.
8. Wyse, A.B.: Publ. Lick Observ., Vol.XIV, p.93, 1939.
9. Sobolev, V.V.: Astron. Zh., Vol.27, No.2, 1950.
10. Boyarchuk, A.A.: Izv. Krymsk. Astrofiz. Observ., Vol.33, p.186, 1965.

SPECTRA OF INTERSTELLAR MATTER /278

S.A.Kaplan

Although the present book is devoted to problems of the theory of stellar spectra, it seems of some use to discuss certain problems of the theory of spectra of interstellar matter. Despite the specific nature of conditions in the interstellar medium (extreme rarefaction of gas and dilution of radiation), we note that in many cases the theories on the formation of spectra of interstellar matter and spectra of the outer shells of stars are quite similar. For example, the mechanisms of formation of the emission spectrum of forbidden lines are identical, and the methods of the theory of growth curves are similar. On the other hand, considerable attention is devoted to the radio region - presently inaccessible to stellar observations - in the theory of the spectra of interstellar matter.

The study of the spectra of interstellar matter is intimately connected with an investigation of the physical conditions and dynamics of interstellar gas, magnetic fields, and cosmic rays in interstellar space. Even the most cursory account of all these problems within one article is impossible; therefore, for further details we refer the reader to our monograph "Interstellar Matter" (Ref.1). Here, we will devote more attention to several new problems arising in the theory of interstellar spectra, in connection with the advances in radio astronomy and extra-atmospheric astronomy.

1. Absorption Lines

Interstellar absorption lines appear in stellar spectra (optical range) or in spectra of discrete radio sources (radio range) whenever a sufficiently dense cloud of interstellar gas is between the observer and a bright star or radio source. A special feature of the interstellar absorption spectrum is that /279 all atoms and molecules are almost always in a ground state and the observed lines always arise upon absorption from this state. If the ground state is split, then often only the lowest sublevel is populated, although here a comparatively large population of the upper sublevels of the ground state is possible in view of the relatively small probability of spontaneous transition. Several lower rotational levels can be populated in the molecular spectra.

There are comparatively few lines due to absorption from the ground state and of sufficient intensity; therefore, the possibilities of interstellar spectroscopy are somewhat limited here. So far only about two dozen lines of atoms and molecules have been observed in the visible spectrum region and a few lines in the radio range. The number of observed absorption lines will increase appreciably as soon as it will become possible to observe the ultraviolet spectra of stars at high dispersion. However, as shown by an analysis of the observational conditions of interstellar absorption lines (Ref.1, Sect.7), even then it is unlikely that one will be able to investigate more than a few dozen lines.

The methods of studying interstellar absorption lines depend on whether a detailed investigation of their profiles is possible or whether determinations of equivalent widths remain the only procedure. The radio range offers better possibilities in this respect: Here, an appreciably greater resolution with respect to frequency can be obtained than in the visible spectrum region. As is well known, a comprehensive study of the hydrogen-line profiles $\lambda = 21$ cm has yielded extremely valuable data on the structure and motion of neutral hydrogen in the Galaxy. The methods and results of these investigations were described in detail by Kaplan et al. (Ref.1, Sects.4, 5) so that we will not discuss them further here.

A detailed investigation of the $\lambda = 21$ cm line is even more readily possible since this line is very intense. For most weak lines it is usually impossible to make a thorough analysis of the profile, but its width can often be determined when assuming that the line profile can be approximated by a Gaussian curve. At the appreciable rarefaction of interstellar gas, atomic collisions have no substantial effect on line broadening so that their width, at not too excessive a line intensity is determined exclusively by the thermal agitation and turbulent motion of atoms and molecules. /280

Let us assume that we can observe the lines of several atoms and molecules originating in one and the same cloud of interstellar gas. From this spectrum we can then determine: a) the velocity of the cloud as a whole, from the line shift, b) the gas temperature and the turbulent velocity, from the line broadening, c) the number of atoms and molecules along the line of sight, from the absorption in the central portions of the lines.

Let us examine more thoroughly point b). The observed half-width of the lines $\Delta\nu_D$ is made up of the Doppler half-width $\Delta\nu_D^{ther}$ describing the thermal agitation of atoms or molecules and of the Doppler half-width of turbulent motion $\Delta\nu_D^{tur}$. We have

$$\Delta\nu_D^{ther} = \frac{1}{\lambda}\sqrt{\frac{2kT}{m_a}}, \quad \Delta\nu_D^{tur} = \frac{\sqrt{\overline{V}^2_{tur}}}{\lambda}, \tag{1}$$

where λ is the wavelength of the line, T is the gas temperature in the cloud, m_a is the mass of the atom or molecule, and $\sqrt{\overline{V}^2_{tur}}$ is the mean-square turbulent velocity. The thermal velocity distribution is described by a Gaussian distribution; if we assume that a similar curve describes the turbulent velocity distribution, then the total half-width of the line is determined by the expression

$$(\Delta\nu_D)^2 = (\Delta\nu_D^{ther})^2 + (\Delta\nu_D^{tur})^2 = \frac{1}{\lambda^2}\left(\frac{2kT}{m_a} + \overline{V}^2_{tur}\right). \tag{2}$$

If two lines of half-widths $\Delta\nu_D^{(1)}$ and $\Delta\nu_D^{(2)}$, belonging to two different atoms or molecules with masses m_1 and m_2, are observed, then eqs.(2) written for each line will yield

$$\left.\begin{aligned} T &= \frac{m_1 m_2}{2k(m_2 - m_1)}\left[\left(\Delta\nu_D^{(1)}\lambda_1\right)^2 - \left(\Delta\nu_D^{(2)}\lambda_2\right)^2\right], \\ \overline{V}_{tur}^2 &= \frac{m_1}{m_1 - m_2}\left[\left(\Delta\nu_D^{(1)}\lambda_1\right)^2 - \frac{m_2}{m_1}\left(\Delta\nu_D^{(2)}\lambda_2\right)^2\right]. \end{aligned}\right\} \quad (3)$$

Using these formulas for analyzing the hydrogen lines (λ = 21.1 cm) and OH molecule lines (λ = 18.3 cm), both the temperature and the internal turbulent velocities in clouds of neutral hydrogen can be determined with high reliability. /281

Elsewhere (Ref.2), T = 90 - 120°K, $\sqrt{\overline{V_{tur}^2}} \approx 0.23 - 0.27$ km/sec were obtained in this manner. By means of this method, the hydrogen lines can be compared with the calcium and sodium lines, if one is certain that they arise in the same cloud. However, the reliability of the results thus obtained is low, since the conditions of observing absorption lines in the radio region and in the visible spectrum are quite different. Here we must take into account that, in observing the optical line, the absorption is determined within a cone resting on the cross section of the star, whereas in the radio range the absorption is observed within a cone having the cross section of the radio source; these quantities are not comparable. In other words, optical absorption occurs in a much smaller portion of the cloud than does radio-range absorption.

If the optical thickness at the line center τ_0 is not larger than unity, then from the absorption at the center

$$r_0 = 1 - e^{-\tau_0} \quad (4)$$

one can easily determine the concentration N_a of the corresponding atoms and molecules by means of the formula

$$\tau_0 = \frac{\pi e^2}{mc}\frac{fN_a}{\sqrt{\pi}\Delta\nu_D} l. \quad (5)$$

Here, m is the electron mass, f is the oscillator strength of the line, l is the length of the line of sight in the cloud, and $\Delta\nu_D$ is the total half-width of the line.

If the absorption lines are so intense that $\tau_0 \gg 1$, then the above-described method of analysis of these lines is inapplicable, and we must resort to the method of growth curves which is well known in the theory of astrophysical spectra.

Let us designate by $\tau(\nu)$ the frequency dependence of the optical thickness within the line profile. Then for the equivalent width in a wavelength scale we have

$$W_\lambda = \frac{\lambda^2}{c}\int_0^\infty (1 - e^{-\tau(\nu)})\, d\nu, \quad (6)$$

where, as usual, by λ we mean the wavelength of the line center. At a given absorption coefficient, the integral (6) can be calculated either analytically or numerically. The results of such calculations for the Doppler profile were /282

given earlier (Ref.1, Sect.7). Specifically, for the Gaussian curve, at $\tau_0 \gg 1$, we have

$$W_\lambda(\tau_0) = 2\Delta\nu_D \frac{\lambda^2}{c} \sqrt{\ln \tau_0}\left(1 + \frac{0.2886}{\ln \tau_0} - \frac{0.1335}{(\ln \tau_0)^2} + \cdots\right). \quad (7)$$

For very intense lines (for example, for the Lyman series) the optical thickness will be so great that absorption in the Lorentzian wings must be taken into consideration. Then, for $\tau(\nu)$, we have

$$\tau(\nu) = \frac{\pi e^2}{mc} \frac{f\Gamma}{4\pi^2(\nu - \nu_0)^2} N_a l, \quad (8)$$

where Γ is the damping constant ($\Gamma_n = \sum_{n' < n} A_{nn'}$), N_a (as usual) is the concentration of absorbing atoms, l is the line-of-sight length, and ν_0 is the frequency of the line center. Substituting eq.(8) into eq.(6), we obtain

$$W_\lambda = 2\frac{\lambda^2}{c}\int_0^\infty \left(1 - \exp\left\{-\frac{e^2 f \Gamma N_a l}{4\pi mc\,(\Delta\nu)^2}\right\}\right) d(\Delta\nu) =$$
$$= \sqrt{\frac{e^2\lambda^4 f\Gamma N_a l}{\pi mc^3}} \int_0^\infty (1 - e^{-x^2})\frac{dx}{x^2} = \left(1 + \frac{1}{\sqrt{\pi}}\right)\sqrt{\frac{e^2\lambda^4 f\Gamma N_a l}{mc^3}}. \quad (9)$$

If the line intensity is such that Doppler profiles are observed, then two unknown quantities enter the determination of equivalent width: the Doppler half-width $\Delta\nu_D$ and the optical thickness at the line center τ_0. In order to find, in this case, each of the quantities separately, the equivalent widths of two or more lines of the same atom or molecule arising from the ground state must be used. Then, the ratio of the optical thicknesses τ_1 and τ_2 at the line centers is equal to the ratio of the oscillator strengths of these lines, while the ratio of the Doppler widths is inversely proportional to the wavelengths. Therefore, the ratio $W_{\lambda_2}(\tau_2)/W_{\lambda_1}(\tau_1)$ is a known function of only one quantity, /283 for example τ_1, which permits determining all parameters of the lines from observations. This is the method of growth curves.

It is of interest to calculate the equivalent widths of the Lyman lines. From eq.(9), for the line L_α, we have

$$W_{L_\alpha} = 2.4\sqrt{N_a l}\,\text{Å}, \quad (10)$$

where the line-of-sight length l is expressed in parsecs. Since for the closest hot stars, in the spectra of which we could observe interstellar Lyman lines, the distances are less than 100 parsecs, it follows that the widths of these lines will be of the order of several tens of angstroms.

It is difficult, within the limits of this article, to present the results of applying these methods to observed interstellar lines. A more or less great wealth of observational material has been accumulated on the H and K lines of ionized calcium and on the doublet D of neutral sodium. Thus, two lines of one doublet from each element are observed here, for which reason the growth curve

method is often called the doublet method. In the future, one can hope to obtain valuable results from the application of this method to the ultraviolet doublet of ionized magnesium λλ 2796 - 2803.

From the interstellar radio hydrogen lines (λ = 21 cm) interstellar magnetic fields can be studied on the basis of Zeeman splitting. It is true that this is very small: $\nu_H \approx eH/2\pi mc \approx 30$ Hz, being much less than the Doppler width which, even for the narrowest absorption lines, is of the order of 10 KHz. However, here we can make use of the fact that the components shifted to different sides are circularly polarized with opposite directions of rotation. This means that, for a line formed in a magnetic field, the state of polarization of both edges of its profile is dissimilar although the line itself remains unsplit. By comparing the polarizations of the two steepest sections of the profile located on both sides from the line center, we can determine the magnitude and sign of the magnetic fields.

One of the most interesting problems of the theory of absorption lines in interstellar matter is to identify the series of observed broad diffuse lines with respect to weak intensity. The most noticeable of these lines has a /284 wavelength of λ = 4430 Å.

The intensity of these lines correlates with interstellar absorption, and there is reason to expect that the formation of these lines has to do with dust particles, but so far no explanation has been possible despite numerous different hypotheses.

2. Emission Lines

The theory of formation of the recombination spectrum of hydrogen radiation and the spectrum of forbidden lines excited by electron collision is so well known that it hardly is necessary to mention here even its basic tenets. Therefore, we will limit ourselves to certain considerations relative to the future development of this theory.

Emission in the ultraviolet region of the spectrum permits, in principle, studying the recombination spectra of other abundant elements; however, since their intensity will be approximately three orders of magnitude less than the density of hydrogen lines it is unlikely that we will obtain any essential data in this respect.

Appreciably greater interest lies in the infrared range. In the H II regions the doublet of doubly ionized sulfur λλ 9070 - 9532, in which almost half of all radiant energy produced in the H II zones is radiated, has the greatest intensity. In general, the infrared spectrum region contains many readily excitable lines of the most abundant atoms and ions. The most complete list of these lines, as well as the corresponding probabilities of spontaneous transitions, is given in Section 7 of another paper (Ref.1), where methods of calculating the intensity of these lines are described in great detail.

The infrared spectrum region also contains lines of rotational and vibrational transitions. For example, for the most abundant molecule of hydrogen H_2,

we can observe transitions under the emission of quanta with wavelengths of $\lambda = 28.2\ \mu$ (rotational transition from the second state to the ground state), $\lambda = 2.22\ \mu$ (transition accompanied by a change of the vibrational quantum number from 1 to 0), etc. The intensity of the first of these lines is equal to /285

$$I_{H_2}(28.2\,\mu) \approx \frac{2\cdot 10^{-5} e^{-\frac{515}{T}}}{1 + 3e^{-\frac{172}{T}} + 5e^{-\frac{515}{T}}} N_{H_2} l \frac{\text{erg}}{\text{cm}^2\ \text{sec}\ \text{ster}}, \qquad (11)$$

where N_{H_2} is the concentration of hydrogen molecules and l is the line-of-sight length. Observation of these lines would permit estimating the content of hydrogen molecules in interstellar space: According to many estimates, hydrogen is encountered there in a molecular form almost as frequently as in an atomic form.

In the infrared spectrum region it will be possible to observe higher series of hydrogen recombination radiation and still farther, in the radio range, transitions between adjacent levels with principal quantum numbers about 100. The theory of formation of these lines is presented elsewhere (Ref.1, Sect.5). The total radiation intensity in these lines is determined from the formula

$$I_H \approx 5.5\cdot 10^{-16} \lambda^{-2} ME \frac{\text{erg}}{\text{cm}^2\ \text{sec}\ \text{ster}}, \qquad (12)$$

where ME is the measure of emission expressed in pc/cm^6, and λ is the wavelength in centimeters. The line width is determined by the Doppler effect.

A detailed investigation of emission line profiles is difficult at present, although in a number of cases splitting of these lines into components was noted, which would indicate the presence of gas flows in the respective regions.

An exception is the hydrogen line $\lambda = 21$ cm for which, thanks to its high intensity and possibility of high frequency dispersion in the radio range, very detailed profiles were obtained. As already noted, this made it possible to construct a rather detailed picture of the distribution and motion of interstellar neutral hydrogen.

3. Continuous Emission Spectrum of Thermal Radiation

Several mechanisms of formation of the continuous emission spectrum are known. Some of these are essential for the conditions of interstellar space, while others are not.

Almost the entire scale of electromagnetic waves (from X-radiation to radio waves) is encompassed by a retardation mechanism, namely radiation of elec- /286 trons in a field of ions or, as one often says in astrophysics, radiation in the presence of free-free transitions. However, the conditions of its observation in different spectrum regions are different.

Braking radiation (bremsstrahlung) arises only in H II regions in which the temperature changes little and is approximately equal to 10^4 deg. Therefore, the intensity of this radiation per unit frequency interval is

$$I_\nu \approx 1.7 \cdot 10^{-22} g e^{-\frac{h\nu}{kT}} ME \frac{\text{erg}}{\text{cm}^2 \text{ sec ster Hz}}. \quad (13)$$

Here g is the Gaunt factor; its value in the optical range of the spectrum is somewhat less than unity (0.36 - 0.84), and in the radio range is of the order of several units (6 - 10). Hence, the intensity of bremsstrahlung increases with decreasing frequency. Consequently, continuous radiation is observed mainly in the radio range. Of course, eq.(13) holds only as long as the optical thickness of the H II zone is noticeably less than unity, which occurs at wavelengths of

$$\lambda < \frac{5 \cdot 10^4}{\sqrt{ME}} \text{ cm}. \quad (14)$$

At longer wavelengths, the radiation of the H II zone corresponds to black-body radiation:

$$I_\nu = \frac{2.76 \cdot 10^{-12}}{\lambda^2} \frac{\text{erg}}{\text{cm}^2 \text{ sec ster Hz}}. \quad (15)$$

As is known, this radiation is observed in many cases, which has made it possible to determine the distribution of interstellar ionized hydrogen in the Galaxy.

In the optical range, there are other mechanisms of continuous radiation - free-bound and two-quantum transitions. However, with the exception of several of the densest nebulae, for example Orion or the Omega Nebulae, the optical continuous thermal spectrum of interstellar matter is not observed owing to its faintness. If, moreover, we take into account that radiation of the visible spectrum region is absorbed by interstellar dust, it becomes understandable that an investigation of the continuous spectrum is limited mainly to the radio range.

In the infrared region of the spectrum rather intense thermal radiation /287 of cosmic dust particles can be expected. Actually, interstellar dust absorbs an appreciable part of the visible and ultraviolet radiations of stars, and reradiates this energy in the infrared region of the spectrum, since the temperature of the cosmic dust particles is low, probably somewhat less than 20°K.

The quantity of energy radiated by one particle per second in a unit wavelength interval is equal to

$$\frac{dW}{d\lambda} = \frac{8\sigma_a(\lambda) hc^2}{\lambda^5 \left(e^{\frac{hc}{\lambda k T_g}} - 1\right)}. \quad (16)$$

Here, T_g is the temperature of the dust grains, $\sigma_a(\lambda)$ is the effective cross section for true absorption. In deriving eq.(16) we used Kirchhoff's law

and Planck's thermal radiation function.

Since the wavelengths of infrared radiation are much greater than the size of the cosmic dust particles, we can express $\sigma_a(\lambda)$ by

$$\sigma_a(\lambda) = \frac{4\pi^2 d^3}{3\lambda} \varkappa, \tag{17}$$

where d is the diameter of the particles and $\varkappa$ is the imaginary part of the refractive index of the matter of cosmic dust particles. Below, we will take $d \approx 10^{-5}$ cm and $\varkappa = 0.05$. From eqs.(16) and (17) it follows that the energy distribution in the spectrum of the cosmic dust particles is described by the formula

$$\frac{dW}{d\lambda} = \frac{32\pi^2 hc^2 \varkappa d^3}{3\lambda^6 \left(e^{\frac{hc}{\lambda k T_g}} - 1\right)}. \tag{18}$$

The maximum spectral density of energy is accounted for by the wavelength λ_m, which is determined by the equality

$$\lambda_m T_g = \frac{hc}{5.985\, k} = 0.24 \text{ cm deg}, \tag{19}$$

representing the analog of Wien's displacement law. If $T_g \approx 20^\circ$K, then

$$\lambda_m \approx 120\ \mu. \tag{20}$$

The spectral density is one-half the maximum when $\lambda_1 \approx 0.6\ \lambda_m$ and $\lambda_2 \approx 1.6\ \lambda_m$. Thus, the bulk of thermal radiation of cosmic dust particles is concentrated /288 in the interval of $\Delta\lambda = \lambda_2 - \lambda_1 \approx \lambda_m$.

Unfortunately, the sensitivity of modern infrared radiation receivers in this range is still low, but the intensity of the thermal radiation of cosmic dust particles should be so great that we can hope to observe it with instruments carried aloft, beyond the limits of the earth's atmosphere. Integrating eq.(8) with respect to all wavelengths, we obtain for the total radiation of one particle

$$W = 24.9 \frac{32\pi^2 c\,(kT_g)^5 \varkappa d^3}{3\,(hc)^4} = 10^{-8} \frac{\text{erg}}{\text{sec}}. \tag{21}$$

Assuming that, on the average, there are 10^{-14} dust particles in one cubic centimeter, we obtain for the total radiation in a column of unit cross section along the galactic plane:

$$\frac{1}{4\pi} \cdot 10^{-8} \cdot 10^{-14} \cdot 10^{23} \approx 1 \frac{\text{erg}}{\text{cm}^2 \text{ sec ster}}. \tag{22}$$

Taking our above statements on the wavelength interval into consideration,

it is found that the intensity of this radiation, at $70 < \lambda < 200\ \mu$, is of the order of

$$I_\nu \approx 4 \cdot 10^{-13} \frac{\text{erg}}{\text{cm}^2\ \text{sec ster Hz}} \tag{23}$$

in the galactic plane in the direction of its center. The intensity of this radiation in a direction perpendicular to the galactic plane should be about 30 times less.

4. Continuous Nonthermal Emission Spectrum

The radiation discussed above has a thermal character. This should be understood in the sense that the particles (free electrons) generating this radiation have a thermodynamic equilibrium distribution with respect to the velocities. However, in interstellar space there are numerous relativistic particles whose distribution is in no way governed by conditions of thermodynamic equilibrium. Usually, their energy distribution function is written by means /289 of the power law:

$$N(\mathcal{E})\,d\mathcal{E} = \frac{K}{\mathcal{E}^\gamma}\,d\mathcal{E}, \tag{24}$$

where $\mathcal{E}$ is the total energy of the particle and K and γ are some constants. Any radiation generated by these particles, including bremsstrahlung (collisions of relativistic electrons with ions) will be nonthermal. The intensity of such radiation is low, since the concentration of the particles is small. However, there is one exception, viz., the relativistic particles moving in interstellar magnetic fields produce a rather intense magnetic bremsstrahlung which customarily is called synchrotron emission.

It should be recalled that relativistic electrons radiate in any electric and magnetic fields, for example, in a macroscopic external magnetic field (synchrotron radiation proper) and in the microscopic field of an electromagnetic wave, such as the field of the luminous thermal radiation of stars; in this case we are dealing with the inverse Compton effect.

The total quantity of energy radiated per second by a relativistic electron with energy $\mathcal{E}$ does not depend either on the geometry or on the origin of the electromagnetic field, and is equal to

$$W = \frac{2e^4 H_\perp^2}{3m^2c^3}\left(\frac{\mathcal{E}}{mc^2}\right)^2. \tag{25}$$

Here, for the sake of definitiveness, we restricted ourselves to the case of a magnetic field. Here $H_\perp$ is a component of the field perpendicular to the direction of the electron velocity. This formula follows directly from the condition that $W = 2e^2a^2/3c^3$, where a is the acceleration of a particle determined by the Lorentz force $eH/c\sqrt{1 - v^2/c^2}$. By $\mathcal{E}$ we must always mean the total energy $\mathcal{E} = mc^2/\sqrt{1 - v^2/c^2}$. In the case of radiation in an electric field, the quantity

$H_\perp$ in eq.(25) must be substituted by the electric field strength E. If the total quantity of energy being radiated is independent of the character of the fields, then its spectral distribution is closely related with the parameters of the electric and magnetic fields in which the relativistic electrons are moving.

In a magnetic field, the radiation of relativistic electrons consists /290 of individual harmonics which, however, are so closely spaced that one can consider this radiation as having a continuous spectrum extending over the entire scale of electromagnetic waves. The spectral density of the radiated energy has a comparatively sharp maximum whose position depends both on the energy of the particle and on the periodicity of its motion.

Actually, let the parameter τ characterize the periodicity of electron motion in a magnetic field. Then, in the absence of relativistic effects the frequency of the electromagnetic waves radiated by such an electron would be of the order of $1/\tau$. To allow for the relativistic effects it must be borne in mind that, first, relativistic particles radiate in the direction of their motion and, second, the Doppler effect greatly shortens the time interval. Therefore, the observed radiation frequency of a relativistic electron is approximately equal to

$$\nu_m \approx \frac{1}{\tau\left(1-\frac{v}{c}\right)} \approx \frac{2}{\tau}\left(\frac{\mathscr{E}}{mc^2}\right)^2. \tag{26}$$

Here, it was considered that $v \approx c$ and that $\mathscr{E} = mc^2/\sqrt{1 - v^2/c^2}$. More accurate calculations, for the position of the spectral density maximum, yield relations that differ from eq.(26) by factors of the order of unity. The width of the frequency interval in which the bulk of the energy is radiated is also of the order of ν_m.

Let us examine the radiation of relativistic electrons in a constant magnetic field. Here τ is of the order of the rotation period of the electron, i.e., $2\pi mc/eH$. For the position of the spectral density maximum in this case we have

$$\nu_m \approx \frac{eH_\perp}{2mc}\left(\frac{\mathscr{E}}{mc^2}\right)^2. \tag{27}$$

Now let the electron move in the field of an electromagnetic wave. Here, its state varies with a period corresponding to the frequency of the wave itself $\bar{\nu}$, provided this quantity is greater than the gyro frequency. Therefore, here the energy being radiated has a spectral density maximum at a frequency of

$$\nu_m \approx \bar{\nu}\left(\frac{\mathscr{E}}{mc^2}\right)^2. \tag{28}$$

Thus, relativistic electrons in interstellar space, moving in extended /291 and slowly varying magnetic fields, emit radio waves since the gyro frequency is only ~30 Hz, whereas moving in the rapidly varying magnetic fields of the luminous radiation of stars, they generate X-rays and even γ-rays since now $\bar{\nu} \approx 10^{15}$ Hz. Because of the fact that the energy densities of the interstellar

magnetic field and of the total stellar radiation are approximately the same, relativistic cosmic-ray electrons emit with equal success both radio waves and X-rays.

We already mentioned that the bulk of the energy produced by an electron is accounted for by the spectral interval of width $\sim\nu_m$, which is close to this same frequency. Therefore, the average radiation intensity in this frequency range is

$$p_\nu \approx \frac{W}{\nu_m} \approx \frac{e^4 H_\perp^2 \tau}{3m^2c^3}. \tag{29}$$

We note that this intensity does not depend on the energy of the particle. Hence it follows directly that the spectrum of total radiation of a system of relativistic electrons should reflect the distribution of electron energies. Actually, the emission coefficient of unit volume is

$$4\pi j_\nu \approx p_\nu N(\mathscr{E}) \frac{d\mathscr{E}}{d\nu} \approx p_\nu (mc^2)^{\gamma-1} (\tau\nu)^{-\frac{\gamma-1}{2}} \cdot K. \tag{30}$$

If a medium of length l is transparent to this radiation, then the intensity will be

$$I_\nu \approx \frac{1}{4\pi} p_\nu (mc^2)^{\gamma-1} (\tau\nu)^{-\frac{\gamma-1}{2}} Kl. \tag{31}$$

Thus, at an exponential distribution of electron energies the spectrum of non-thermal radiation also has an exponential character, with the index

$$\alpha \approx \frac{\gamma-1}{2}, \tag{32}$$

which is called the spectral index.

It is necessary to remember that eqs.(29) - (31) are valid with an accuracy to within constant factors of the order of unity, which in the case of eqs.(30) and (31) depend also on the value of the parameter γ which is the spectral /292 index of the energy distribution of relativistic electrons.

Substituting specific values of τ, we obtain explicit expressions for p_ν in the case of synchrotron emission

$$p_\nu \approx \frac{e^3 H_\perp}{mc^2} \tag{33}$$

and for the case of the inverse Compton effect (X-radiation)

$$p_\nu \approx \sigma_T c u_{\bar{\nu}}, \tag{34}$$

where $\sigma_T = \frac{8\pi}{3}\left(\frac{e^2}{mc^2}\right)^2$ is the effective Thomson scattering cross section and $u_{\bar{\nu}} \approx \frac{H^2}{4\pi\bar{\nu}}$ is the energy density of the total stellar radiation per unit fre-

quency interval. It goes without saying that eqs.(33) and (34) also hold with an accuracy to within numerical factors of the order of unity.

We note that the quantities of energy radiated in interstellar space, both in the radio range and as X-rays, are comparable; however, this means that the number of radiated X-ray quanta is less than the number of radio quanta by a factor of the order of the ratio of their frequencies. It is precisely for this reason that it is much more difficult to detect X-radiation of interstellar matter. Usually for the intensity of X-radiation a value is given that is $h\nu$-times less than eq.(31), i.e., the quantum number flux. Its spectral index thus is $(\gamma + 1)/2$.

As shown by observations, the spectrum of nonthermal radiation of interstellar matter mostly has an exponential character, but deviations are often noted. The reasons for this may differ. On the one hand, the exponential distribution of electron energies at large or small $\mathcal{E}$ may be disturbed. For example, owing to radiation the number of high-energy electrons decreases more quickly than the number of low-energy electrons. This leads to a steeper slope of the spectrum at high frequencies. Since the radiation of an electron is sensitive to its energy, transition from a less steep spectrum to a more steep one takes place rather abruptly, in a narrow frequency interval. Usually /293 this transition can be regarded as a discontinuity at which the spectral index increases by 1/2. At low energy of the electrons these are noticeably retarded owing to losses to ionization of interstellar matter. This leads to a diminution of the steepness or even to an abrupt drop of the spectrum at low frequencies.

On the other hand, the spectrum may vary due to the conditions of radiation and transmission of electromagnetic waves in the medium. Considering that relativistic electrons do not radiate in a vacuum but in interstellar plasma, it will be found that in the low-frequency range with

$$\nu < (3 \text{ to } 10)\frac{ecN_e}{H} \tag{35}$$

a steep drop should occur regardless of whether or not low-energy electrons are present there. Here, N_e is the electron concentration of the plasma. Furthermore, at low frequencies the coefficient of braking absorption (inversely proportional to the square of the frequency) increases, which often leads to an even steeper slope of the spectrum.

If the concentration of relativistic electrons or the dimensions of the system are large, allowance must be made for reabsorption, i.e., absorption - by relativistic particles - of the electromagnetic radiation generated by them. The coefficient of this absorption $\varkappa_\nu$ can be estimated on the basis of the analog of the Kirchhoff law $j_\nu/\varkappa_\nu = 2kT\nu^2/c^2$, where kT now denotes the energy of relativistic electrons

$$\frac{j_\nu}{\varkappa_\nu} \approx \frac{2\mathcal{E}}{c^2}\nu^2 \approx 2m\tau^{1/2}\nu^{5/2}. \tag{36}$$

Thus, resorption may also lead to a steep slope of the spectrum for longer waves.

For different applications of the theory of nonthermal radiation to specific problems of the physics of interstellar matter the reader is referred to other papers (Ref.1 and 2).

REFERENCES

1. Kaplan, S.A. and Pikel'ner, S.B.: Interstellar Matter (Mezhzvezdnaya sreda). Fizmatgiz, 1963.
2. Ginzburg, V.L. and Syrovatskiy, S.I.: Usp. Fiz. Nauk, Vol.84, No.2, p.201, 1964.

RADIO OBSERVATIONS OF PLANETARY NEBULAE

/294

Yu.N.Pariyskiy

Planetary nebulae are regions of ionized hydrogen and thus should be sources of thermal radiation like the numerous diffuse gas emission nebulae already recorded in the radio range.

Observations of thermal radio radiation of planetary nebulae can theoretically yield valuable information on their distance, density, mass, and kinetic temperature. A comparison with data of optical observations permits determining the absorption of light in corresponding directions and estimating the degree of inhomogeneity of the nebulae. Furthermore, data can be obtained on the ultraviolet radiation of exciting stars and (or) on the transparency of shells in the Lyman continuum. With an increase in accuracy of optical and radio observations it will become possible to estimate the composition of planetary nebulae.

There is no doubt that all these data are important for understanding processes taking place in planetary nebulae and for determining their position in the overall scheme of evolution of interstellar matter. Therefore, we will briefly discuss the methods of obtaining such data.

The absorption coefficient in the radio range is determined by free-free transitions, so that

$$\varkappa_\nu \sim \frac{N_i N_e}{T_e^{3/2}\nu^2}.$$

The solution of the transfer equation for a homogeneous layer yields the expression

$$I_\nu = B_\nu (1 - e^{-\tau_\nu}),$$

where

$$B_\nu = \frac{2kT_e\nu^2}{c^2}.$$

Therefore, for $\tau_\nu \gg 1$ (i.e., at low frequencies) the nebulae becomes opaque /295 and T_e can be determined whereas at high frequencies ($\tau_\nu \ll 1$) we can determine $\int_0^s N_1 N_e \, ds$ where s is the dimension of the nebula along the line of sight. Knowing s, we find $\sqrt{\overline{N_e^2}}$ and the mass of the nebula (more exactly, the upper limit of the mass since $\sqrt{\overline{N_e^2}} \gg \overline{N}_e$).

A further refinement of purely radio astronomy data on density and temperature of the nebula can be made after taking into account the degree of inhomogeneity of the nebula both along the line of sight and in the tangent plane.

The effect of inhomogeneities along the line of sight was estimated by Wade (Ref.1), based on convenient nomograms. It is easy to estimate the real inhomogeneities by comparing the "astronomic" density $\left(\sqrt{\overline{N_e^2}}\right)$ with the "spectrophotometric" density with respect to the relative density of the lines 3727/3729 of oxygen ($\sim N_{e\,max}$) (Ref.2). It is essential to allow for inhomogeneities in the tangent plane in determining the temperature of the nebula [see elsewhere (Ref.1, 2)].

Knowing s and N_e, we easily find the effective Strömgren parameter U:

$$sN_e^{2/3} = U \sim N_L^{1/3}.$$

Here N_L is the number of ultraviolet quanta emitted by the exciting star. It is known that the ratio N_L/N_V (N_V being the number of quanta emitted in the visible region) is an important parameter in the theory of stellar models. We note that this ratio can be found by comparing radio and optical measurements. All these parameters can be determined if the distance to the planetary nebulae is known. We will discuss here three methods of determining distances for optically thin nebulae.

1. Shklovskiy's method. This method is based on the assumption of a small dispersion of mass of the planetaries (Ref.3). As a nebula expands its brightness decreases rapidly, and it is easy to demonstrate that the distance R is determined in terms of the apparent angular dimension φ and the integral flux F_ν: /296

$$R \sim F_\nu^{-1/2}\varphi^{-3/2}.$$

2. The Sobolev-Gershberg method holds for a homogeneous nebula. Knowing N_e with respect to 3727/3729 and $N_e^2 \cdot s$ with respect to radio observations, it is easy to find s and $R = s \cdot \varphi^{-1}$ (Ref.4, 5).

3. If the flux from the nebula is known in a line of the Balmer series (for example, $H\beta$), then the distance R is determined by comparing F(radio) with $F(H\beta)$. Actually, since $F(\text{radio}) \sim F(H\beta)$ (Ref.6), any deviation of the proportionality factor can be related primarily with the absorption of optical radiation by dust. By investigating the distribution of dust in a given direction, we can estimate the distance to the nebula (Ref.6).

Finally, if we take into account that all electrons and only the ions of hydrogen participate in the radiation of Balmer lines and that all electrons and all ions are in free-free transitions, it becomes possible to estimate, with respect to the ratio $F(\text{radio})/F(H\beta)$, the contribution to the radio emission of all other elements, i.e., the chemical composition of the nebulae.

Despite the fact that the possibility of obtaining important astrophysical data by methods of radio astronomy has been known for a long time (Ref.7), radio observations of planetary nebulae are just now beginning.

The very first observations seemed to indicate the presence of an appreci-

able admixture of nonthermal (magnetic deceleration) radio emission in the nebulae NGC 7293 and 6445 (Ref.8). However, further observations showed ever smaller fluxes until radio emission was stopped completely (Ref.11). Only in 1961 did the first sufficiently reliable publications appear concerning the discovery of radio emission from the nebulae NGC 7293, 6853, 7009, 6543, 6572, and IC 418 in the range of decimeter wavelengths (Ref.9,10).

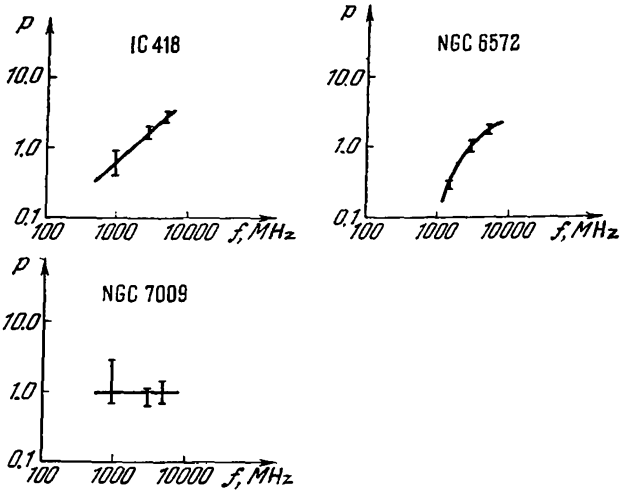

Recently, at Pulkovo, a series of observations of the nebulae IC 418, NGC 7009 and 6572 on the 6.4 cm wave was carried out by means of the large Pulkovo radio telescope*. All three /297 nebulae were actually found on this wave.

We attempted to construct the radio emission spectrum of these three objects, comparing the data of the centimeter and decimeter range (see diagram). It is obvious that all three nebulae have a purely thermal spectrum, where NGC 7009 is optically thin at all wavelengths up to 30 cm while IC 418 and NGC 6572 are already "semitransparent" on the 10-cm wave. We can assume that on the 30-cm wave these nebulae are optically thick. However, estimates of the temperatures are extremely low, being 3000 - 5000°K. This is connected with the inhomogeneous structure of the nebulae. At present, processing of the data with consideration of the inhomogeneous structure of the nebulae is being completed.

We note in conclusion that the rapid advance in radio astronomy observation methods (increase in size of antennas, greater sensitivity of receiving equipment) permits the hope that the number of planetary nebulae recorded in the radio-frequency range will rapidly increase. Even with existing equipment, /298 dozens of nebulae can be detected which number, in the next 2 - 3 years, can no doubt be increased to several hundreds. Thus, one can predict that an appreciable volume of information on planetaries will be obtained by radio astronomy.

REFERENCES

1. Wade, C.M.: Austral. J. Phys., Vol.2, p.388, 1958.

---

* The observations and their processing were carried out in collaboration with T.Pyatunina.

2. Pariyskiy, Yu.N.: Astron. Zh., Vol.38, No.5, p.798, 1961.
3. Shklovskiy, I.S.: Astron. Zh., Vol.33, p.222, 1956.
4. Sobolev, V.V.: Vopr. Kosmogonii, Vol.VI, p.112, 1958.
5. Gershberg, R.Ye.: Izv. Krym. Astrofiz. Observ., Vol.28, p.159, 1962.
6. Pariyskiy, Yu.N.: Izv. Gl. Astron. Observ. v Pulkove, Vol.21, p.54, 1960.
7. Shklovskiy, I.S.: Astron. Zh., Vol.29, p.18, 1952.
8. Bolton, J.: Austral. J. Sci. Res., Ser.A, Vol.7, p.96, 1954.
9. Lynds, C.: Publ. NRAO, Vol.1, p.5, 1961.
10. Bolton, J.: Owens Valley Radio Observatory, Cal. Tech., No.5, 1960.
11. Kuz'min, A.D. and Salomonovich, A.Ye.: Astron. Zh., Vol.38, p.2, 1961.

PART V. SPECTRA OF CELESTIAL BODIES IN THE FAR ULTRAVIOLET REGION /299

SPECTRA OF CELESTIAL BODIES IN THE FAR ULTRAVIOLET REGION /301

G.A.Gurzadyan

1. Absorption in the Earth's Atmosphere

Let us designate the region of wavelengths from 3000 Å to one angstrom the far ultraviolet. Farther on, at $\lambda < 1$ Å, there begins the region of hard X-rays, and still farther, starting at a quantum energy of $10^4 - 10^5$ ev and higher, there lies the region of γ-rays.

So far, no specific terminology exists for naming the individual regions in the interval of 3000 to 1 Å. It seems useful to divide this range into three regions with the following limits and, specifically, with the conditional designations:

1 - 200 Å, region of soft X-rays,
200 - 912 Å, region of hard ultraviolet,
912 - 3000 Å, region of vacuum ultraviolet.

All three regions are completely inaccessible to astronomic observations directly from the earth's surface; they can be seen only from the upper, rarefied layers of the atmosphere. At the same time, the limiting height of the layer reached by short-wave radiation from extraterrestrial sources, differs for different wavelengths. The dependence of the wavelength on the layer height in the earth's atmosphere where radiation arriving from without is attenuated by e times, is shown schematically in Fig.1. This curve, taken from Watanabe (Ref.1), was plotted on the basis of data obtained from numerous and diverse experiments.

The absorption of light waves of different lengths in the earth's atmosphere is caused by various molecules and atoms: in the range 3000 - 2000 Å, by ozone; in the range 2000 - 800 Å, by molecular oxygen; in the range shorter than 1000 Å, by molecular nitrogen and atomic oxygen. The curve of this dependence has a highly complex structure in the 700 - 1400 Å wavelength region where the /302 effect of absorption of molecules and ions NO^+, O^+, N_2^+, O_2^+, etc. is also felt.

As follows from Fig.1, to record celestial objects in the 3000 - 2000 Å wavelength region one must ascend to heights of at least 35 - 40 km. Beyond this region, the boundary rapidly rises so that, in order to encompass the region up to 1000 Å, it is necessary to ascend to 100 - 120 km. To record waves shorter than 1000 Å, the instrument must be carried aloft to a height of at least 140 km.

In addition to this there exist "windows" of relative transparency at individual wavelengths. For example, in favorable cases the Lyman-alpha line can be recorded at heights of 70 - 80 km. The region of soft X-rays is readily recorded beginning with a height of 100 km. However, for example the lines 304 Å of ionized helium and 584 Å of neutral helium suffer noticeable absorption even at a height of 200 km.

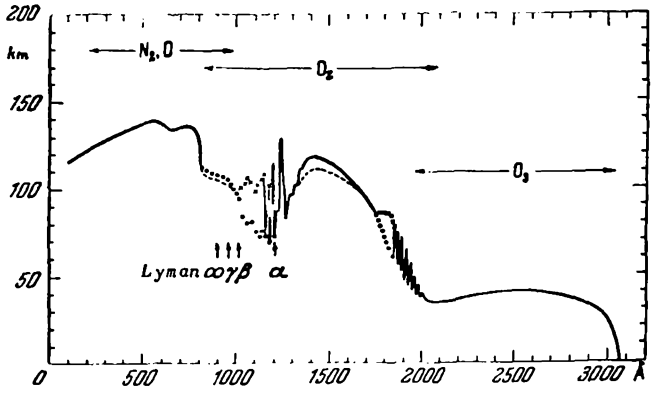

Fig.1 Penetration of Short-Wave Radiation into the Earth's Atmosphere.

2. Absorption in the Interstellar Medium /303

It is known that the absorption of radiation in the interstellar medium in various ranges - photographic, visible, and infrared - is due only to the effect of cosmic dust; interstellar hydrogen in all its states has no effect on the propagation of radiation of the mentioned ranges.

In contrast to this, both interstellar dust and interstellar neutral hydrogen play an important role in the absorption of far ultraviolet radiation.

Absorption by interstellar neutral hydrogen in this range, however, exhibits a distinctly selective character. It has no effect on radiation of the vacuum ultraviolet (912 - 3000 Å), absorbs almost completely the hard ultraviolet region (912 - 200 Å), and causes partial absorption in the soft X-radiation region (200 Å).

We know nothing on the magnitude and character of absorption caused by interstellar dust in the far ultraviolet region. At present we can extrapolate, although without sufficient justification, the law of interstellar absorption $\tau \sim \lambda^{-1}$ derived for the visible region to the vacuum and hard ultraviolet region. As a result, absorption should increase monotonically with a decrease in wavelength. However, somewhere in the region of very short waves (in the X-ray region) absorption caused by interstellar dust should begin to decrease, and then disappear altogether because in this case hard radiation can simply filter through the dust particles. In Fig.2 the dashed line represents the curve for the dependence of the optical thickness of the medium τ on λ, with τ being calculated per 1 kiloparsec and, as customary, $\tau = 1$ at $\lambda = 3000$ Å.

In speaking about absorption due to interstellar dust we must bear in mind the possibility of the existence of individual bands or areas of high (selective) absorption in the region $\lambda < 3000$ Å, caused by the presence of molecules of individual elements or molecular compounds of different elements in the interstellar medium. Incidentally, this matter is the subject of a special study.

Absorption caused by interstellar atoms of neutral hydrogen starts becoming effective from the hydrogen Lyman series limit, i.e., in the region $\lambda < 912$ Å. The law of this absorption is known: $\tau_\lambda \sim \lambda^3$, i.e., absorption rapidly drops with a decrease in wavelength. If we denote by τ_0 the optical thickness of the interstellar medium, calculated per one kiloparsec at the series limit (i.e., at $\lambda_0 = 912$ Å), then we will have

$$\tau_\lambda = \tau_0 \left(\frac{\lambda}{\lambda_0}\right)^3.$$

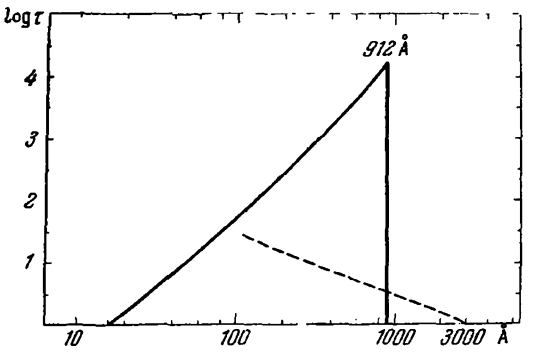

Fig.2 Dependence of Magnitude of Interstellar Absorption (Optical Thickness) on Wavelength. The solid line gives the absorption due to neutral hydrogen; the broken line represents the absorption by interstellar dust.

For a concentration of neutral interstellar hydrogen atoms of $n_1 \approx 1$ cm^{-3}, we have $\tau_0 \approx 2 \times 10^4$. Even at a distance of one parsec, the optical thickness at the Lyman series limit is very large, of the order of 20. The optical thickness becomes of the order of unity only for waves of about 50 Å (at a distance of one kiloparsec). Hence it can be concluded that interstellar space is completely opaque to radiation in the 900 - 100 Å wavelength interval. For radiation in the 100 - 50 Å wavelength region this space is partially transparent, and in the region of shorter waves ($\lambda < 10$ Å) it becomes completely transparent. /305

In Fig.2, the solid line represents the curve of the dependence of τ_λ on λ calculated per one kiloparsec distance, at $n_0 = 1$ cm^{-3}.

The question of the transparency of the interstellar medium was studied also by Aller and by Strom (Ref.2, 3). In the latter case, the effect of selective absorption caused by interstellar dust in the wavelength region $\lambda < 60$ Å was also taken into account. Table 1 gives data on τ_λ, taken from Strom (Ref.3), which were obtained on the assumption that the total number of neutral hydrogen atoms along the line of sight is equal to $N_H = 1.5 \times 10^{21}$ cm^{-2} (this value, according to radio astronomy data, corresponds to the distance from the sun to the center of the Galaxy).

Evidently, the true picture of interstellar absorption in the far ultraviolet region can be conclusively obtained by conducting special "extra-atmospheric" observations of stars.

However, regardless of the future possible advance in this direction, we can assert now already that not a single celestial body - stars, galaxies, nebulae - will be observed in the hard ultraviolet region, i.e., in the wavelength range from 912 Å to about 100 Å. The sun and planets should be an exception.

TABLE 1

DEPENDENCE OF OPTICAL THICKNESS OF THE INTERSTELLAR MEDIUM ON λ, FOR $N_H = 1.5 \times 10^{21}$ cm^{-2}

λ, Å	τ_λ	λ, Å	τ_λ
1	0.00	20	1.72
5	0.04	25	1.94
7	0.09	30	3.54
10	0.25	43.6	10.11
15	0.74	60	21.7

3. Solar Spectrum in Vacuum and Hard Ultraviolet /306

The three basic portions of the solar atmosphere whose radiation reaches the observer directly, viz., photosphere, chromosphere, and corona, exhibit greatly differing temperatures. As a consequence, there should be definite spectrum regions in which the radiation will belong completely either to the corona, or to the photosphere, or to the chromosphere. We can roughly determine these regions on the strictly conditional assumption that the radiation of these three parts of the solar atmosphere follows the black-body law. Then, for example, at an effective temperature of the photosphere of $T_{ph} = 6000^\circ$K the maximum radiation intensity will be located approximately at 5000 Å, i.e., in the visible spectrum region. The intensities of the coronal and chromospheric radiations at $\lambda \sim 5000$ Å are less by a factor of a million than the intensity of photospheric radiation. This ratio is retained in an appreciable portion of the vacuum ultraviolet (approximately to 1700 Å). Therefore, we can say that the region of the spectrum $\lambda >$ > 1700 Å belongs entirely to the photosphere.

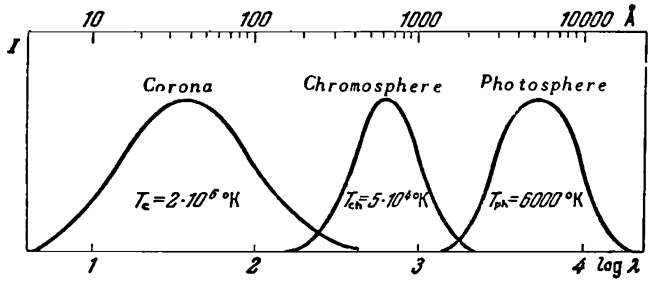

Fig.3 Diagram of the Spectral Distribution of Energy Emitted by the Photosphere, Chromosphere, and Corona. The vertical scale is arbitrary.

In contrast to this, the radiation maximum of the chromosphere should be located in the region of about 600 Å at its temperature of $T_{ch} = 5 \times 10^4$ °K. In this spectrum region, both the intensity of photospheric radiation (at $T_{ph} = 6000^\circ$K) and the intensity of coronal radiation (at $T_c = 2 \times 10^6$ °K) is many orders of magnitude less than the intensity of chromospheric radiation. In other words, the spectrum region of about 400 - 1300 Å will belong entirely to chromospheric radiation. Reasoning in this manner, it will be found that the maximum corona radiation occurs in the soft X-ray region; the intensities of chromosphere and photosphere radiations in the X-ray range should be many orders

of magnitude less than the intensity of corona radiation.

These reasonings, which are of a qualitative nature only, are schematically shown in Fig.3.

Thus, by studying the sun in X-rays we actually have the opportunity of isolating in a pure form the corona under ordinary, uneclipsed conditions; the chromosphere and photosphere will not interfere in this case. All observational data obtained in the range of hard and, particularly, of vacuum ultraviolet /307 will pertain completely to the chromosphere. Finally, the long-wave half of the vacuum ultraviolet and the entire visible region will be solar spectrum portions most amenable to studies (under ordinary conditions) of the photosphere.

The methodological advantage of such a determination of individual regions of the solar spectrum is obvious.

It follows from these statements that extra-atmospheric observations of the sun by means of high-altitude rockets and artificial satellites will permit the most complete, diverse, and systematic study of primarily the chromosphere and corona, since ordinary observations in the visible spectrum region are sufficient for studying the photosphere.

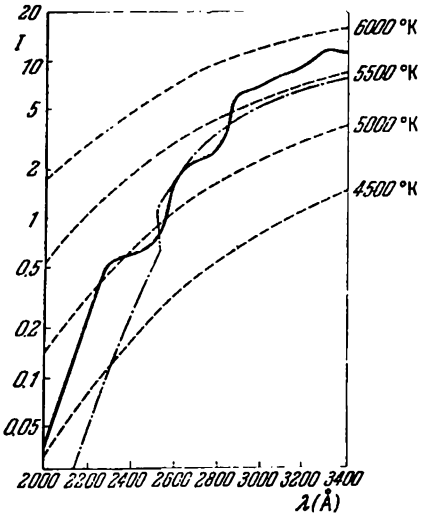

Fig.4 Energy Distribution in the Solar Spectrum in the 3000 - 2000 Å Range. Solid curve - Experiment; broken curves - Theoretical distribution at different effective temperatures.

The first spectrograms of the sun by means of high-altitude rockets were obtained as long ago as 1946 by Baum et al. (Ref.4). In this case, the wavelength region to 2100 Å was reached. Later, work in this direction advanced at a comparatively rapid rate, and within a short time the entire range of the solar spectrum from 3000 Å to several angstroms had been covered. Details of these experiments with a description of the method /308 of measurements, operating principles of the instrumentation, analysis of the obtained results, etc. are given elsewhere (Ref.5 - 18)*.

Penetration into the solar spectrum region to 2100 Å yielded no unexpected results. At this point, a drop in the level of the continuous spectrum takes place; however, this drop occurs appreciably more quickly than would be expected in the case of Planckian radiation at an effective temperature of the radiating layers of T_{ph} = 6000°K.

* Most of these papers are also contained in collections (Ref.19, 20).

This pattern is observed to 2000 Å and less; the effective radiation temperature at $\lambda \sim 2000$ Å is of the order of 4500°K. Figure 4 gives the curve of energy distribution in the 3000 - 2000 Å region (solid line) found by experiments (Ref.21) and the Planckian curves of energy distribution in the continuous spectrum for different values of the effective temperature (broken lines). The diagram also shows the theoretical curve found by DeJager (Ref.22) for some average model of the structure of the radiating layer on the assumption that radiation in the 3000 - 2000 Å region belongs mainly to the photosphere and, partially, to the transitional region from the photosphere. /309

Two depressions are noted in the 3000 - 2000 Å region of the spectrum. The first occurs in the 2800 - 2850 Å region and is caused by a broad intensive doublet belonging to ionized magnesium. The structure of this doublet (2795.5 Å and 2802.7 Å) is interesting: The centers of each of its components show narrow emission cores. The second depression is at about 2500 Å and is due to the MgI series limit.

With respect to the abundance of spectral lines, this region is in no way inferior to the visible region of the solar spectrum. Many thousands of new spectral lines were detected, some of which have already been identified. For example, V.P.Kachalov and A.V.Yakovleva (Ref.15) measured and identified on their spectrograms of the sun more than a thousand absorption lines in the 2632 - 2900 Å region. Visual estimates of the intensities of these lines are also given in the list they compiled.

The solar continuum extends almost to 1600 Å and disappears completely at 1500 Å. Among the lines identified in this portion of the spectrum, the resonance line of arsenic 1890.4 Å is of interest; this element had not previously been detected in the solar atmosphere.

The first emission lines appear in the spectrum between 1900 and 1800 Å. Farther, down to several angstroms, the solar spectrum consists of a faint continuous background with superposed emission lines. The continuous spectrum in the region $\lambda \leq 912$ Å is due mainly to the Lyman continuum of hydrogen and in the region $\lambda > 912$ Å, to the continua of various elements.

The most intense emission line in the region $\lambda < 1900$ Å is the Lyman-alpha line which has a chromospheric origin. Other lines of the Lyman series of hydrogen down to $L\eta$ are clearly discernible. The limit of the Lyman continuum (near 912 Å) is rather well defined. One of the intense lines, namely, the resonance line of ionized helium 304 Å, is no more than an order of magnitude weaker than the $L\alpha$ line. The line 585 Å of neutral helium, which is several times weaker than the 304 Å line, also appears. /310

In the 1800 - 84 Å range, several hundreds of emission lines were detected which belong to ions of helium, oxygen, nitrogen, carbon, silicon, sulfur, aluminum, magnesium, etc. Most of these lines are of chromospheric origin. However, lines in the soft X-ray region and some of the lines in the short-wave end of the hard ultraviolet should belong to the corona. At present only some of these lines have been identified and work in this direction is continuing.

The most reliable absolute and relative measurements of solar emission

lines were performed by Rense (Ref.5, 20) photometrically, using a short-wave spectrograph and by Hinteregger (Ref.18, 19, 20) electrophotometrically, using a short-wave spectrometer. The advantage of the first method lies in the high

TABLE 2

INTENSITIES OF SOLAR EMISSION LINES IN THE 1200 - 1820 Å INTERVAL

Identification	Wavelength, Å	Intensity erg/cm² sec	Identification	Wavelength Å	Intensity erg/cm² sec
SiIII	1206.5	0.23	SiII	1526.7	0.03
H(L_α)	1215.7	3.43	SiII	1533.4	0.06
HeII	1215.1	0.17	CIV	1584.2	0.55
SiII	1265.0	0.02	CIV	1550.8	0.31
OI	1302.2	0.04	CI	1560.3	0.04
OI	1304.9	0.04	CI	1561.4	0.08
OI	1306.0	0.04	HeII	1640.4	0.27
SiII	1309.3	0.04	CI	1656.3	0.28
CII	1334.5	0.31	CI	1658.1	0.20
CII	1335.7	0.33	FeII	1670.8	0.21
SiIV	1393.7	0.24	SiII	1808.0	1.05
SiIV	1402.7	0.17	SiII	1816.0	1.65

resolving power and that of the second method, in the high accuracy of measuring absolute values of the radiation fluxes. Table 2 gives the values of the absolute intensities of 24 emission lines in the 1206 - 1816 Å region based on /312 Rense's measurements. Although the accuracy of these measurements is low, it is assumed that the order of magnitude is correct. For the region of shorter wavelengths, to 84 Å, Rense gives a list of identified lines with an estimate of their intensities (Table 3).

Of particular interest here are the results of Hinteregger's unique photometric measurements which cover almost the entire far ultraviolet of the sun, from 3000 to 60 Å. He gives absolute intensity values only for individual narrow sections of the spectrum (the continuous spectrum plus weak lines) and gives the intensity of an individual line only if the latter is sufficiently strong. These data with all additional details are given elsewhere (Ref.30). Table 4 contains the latest summary data (Ref.26) for the spectral region 1216 - 283 Å, where the direct measurements of Φ (225 km) pertain to a height of 225 km /313 while Φ_0 is the intensity (number of quanta/cm² sec) extrapolated to the boundary of the earth's atmosphere; the ratio of Φ_0/Φ (225 km) obviously characterizes the magnitude of absorption at the given wavelength in the portion of the atmosphere lying above 225 km. This value is derived from the altitude gradient of the measured intensity.

In addition to these tables, it is of interest to present the results of preliminary observations of Behring et al. (Ref.27) on soft X-radiation and, partially, on hard ultraviolet radiation of the sun. These authors identified, more or less confidently, many emission lines in the spectral region 370 - 171 Å, the most noteworthy finding being that they included resonance lines of highly

ionized atoms of heavy elements. The wavelengths of some of these are given in Table 5, together with preliminary identifications.

TABLE 3

IDENTIFIED SOLAR EMISSION LINES WITH WAVELENGTHS SHORTER THAN 1216 Å, OBTAINED FROM ROCKET DATA

Observed Wavelength, Å	Estimated Intensity	Suggested Source	Observed Wavelength, Å	Estimated Intensity	Suggested Source
1215.7	1000	H (L_α)	630.3	20	O V
1206.5	75	Si III	625.1	5	O IV
1200.2	10	N I	611.4	5	O III
1195.0	10	C I	609.8	5	O III
1192.9	10	C I	—	—	O IV
1189.8	5	C I	—	—	Mg X
1176.2	5	C III	608.5	5	O IV
1169.1	10	N I	607.6	50	He II
1167.7	25	N I	599.2	5	O III
1158.1	5	C I	597.9	5	O III
1134.4	20	N I	584.7	10	He I
1085.1	10	N II	553.7	10	O IV
1040.9	5	O I	539.2	5	O II
1038.2	40	O IV	538.8	5	C III
1034.2	30	O IV	536.5	5	He I
1025.7	60	H (L_β)	525.8	15	O III
1009.8	10	C II	463.8	10	Si VI ?
990.0	15	N III	435.1	25	O III
997.0	30	C III	430.7	10	O II
979.2	10	H (L_γ)	419.4	10	C IV
964.5	10	N I	373.6	15	O III
943.7	10	S VI ?	372.2	10	C III
932.2	10	S VI ?	344.7	20	O III
916.0	10	N II	310.1	10	C III
913.0	10	S II	303.8	30	He II
911.4	100	He II	280.0	5	O IV
905.5	5	Si II ?	260.0	5	O IV
902.9	5	C II	257.1	20	He II
858.2	10	C II	243.3	10	He II
835.2	5	O III	238.5	5	O IV
834.0	5	O III	237.1	10	He II
791.2	5	O IV	234.6	5	He II
779.4	5	O IV	184.7	5	O VI
764.5	10	N III	172.7	5	O VI
703.3	20	O III	171.9	5	O V
687.3	15	C II	150.0	10	O VI
651.5	10	C II	83.9	30	Ne VIII?
644.9	20	N II			

4. Interpretation of the Short-Wave Solar Spectrum /314

The mechanism of formation of emission lines in the region of the solar spectrum $\lambda < 1800$ Å is the same as the mechanism of formation of the chromospheric emission lines in the visible spectrum region. Since the intensity of hard ultraviolet radiation in the photosphere is very low, excitation of these levels and, ultimately, excitation of the short-wave lines can occur only by

TABLE 4

EXTRAPOLATION OF MEASURED FLUXES TO BOUNDARY OF ATMOSPHERE

Wavelength Å	Φ (225 km), quanta/cm² sec	$\Phi_0 = \Phi(225\ km)\, e^{\tau}$ quanta/cm² sec
1215.7	$3.1 \cdot 10^{11}$	$3.1 \cdot 10^{11}$
1206.5	$5.1 \cdot 10^{9}$	$5.1 \cdot 10^{9}$
1025.7	$2.5 \cdot 10^{9}$	$2.5 \cdot 10^{9}$
977.0	$4.0 \cdot 10^{9}$	$4.0 \cdot 10^{9}$
972.5	$2.8 \cdot 10^{8}$	$4.7 \cdot 10^{8}$
949.7	$3.5 \cdot 10^{8}$	$3.5 \cdot 10^{8}$
885—865	$2.0 \cdot 10^{9}$ (total)	$2.3 \cdot 10^{9}$
835—833	$4.0 \cdot 10^{8}$	$4.6 \cdot 10^{8}$
790.0	$3.1 \cdot 10^{8}$	$3.7 \cdot 10^{8}$
770.4	$4.1 \cdot 10^{8}$	$4.9 \cdot 10^{8}$
629.7	$8.5 \cdot 10^{8}$	$1.4 \cdot 10^{9}$
610	$4.6 \cdot 10^{8}$	$8.0 \cdot 10^{8}$
584.3	$8.9 \cdot 10^{8}$	$1.6 \cdot 10^{9}$
554	$3.0 \cdot 10^{8}$	$5.3 \cdot 10^{8}$
500	$2.5 \cdot 10^{8}$	$4.4 \cdot 10^{8}$
465.2	$1.8 \cdot 10^{8}$	$3.0 \cdot 10^{8}$
368.1	$3.9 \cdot 10^{8}$	$6.0 \cdot 10^{8}$
335	$3.3 \cdot 10^{8}$	$4.8 \cdot 10^{8}$
303.8	$2.5 \cdot 10^{9}$	$3.8 \cdot 10^{9}$
283	$4.3 \cdot 10^{8}$	$6.2 \cdot 10^{9}$

TABLE 5

IDENTIFICATION OF SOLAR EMISSION LINES IN REGION 370 - 170 Å

Identification	Wavelength, Å	Identification	Wavelength, Å	Identification	Wavelength, Å
Fe XIV, Fe XII	370	He II	304		211
			293		204
Fe X	366	Fe XV	284		202
	365	Cu XIX	274		195
FeXVI	361		271		193
FeXII	360	S X	264		192
NiXV, FeX	347	Ar XIV	263	Ar XI	188
FeXIV	345	He II,	256	Ar XI	186
	341	Ni XVIII		Cl IX	184
Fe XVI	335	Ar XIV	250		182
Ni XV	333	He II	244	Cl IX	180
	320		243		177
Ni XV	316	He II	234		174
	315	Ca XV	227		171
	312	S IX	220		

electron collisions. However, the excitation potential of the resonance level of different ions has a different value. Hence it follows that these lines cannot be excited under identical temperature conditions; the fact that they are actually observed means that they arose in different layers of the chromosphere where the electron temperatures are different. Since the electron temperature in the chromosphere increases with an increase of height from its base, we can

expect that resonance lines corresponding to higher values of the excitation potential for transition to the next level should arise in higher layers of the chromosphere, whereas lines with a low excitation potential should arise in lower layers of the chromosphere.

Such an analysis, which is of course of a preliminary nature, was carried out by Zirin et al. (Ref.26) who showed that, for example, the lines of the ion C IV are formed in a region with a temperature of about 90,000°K, the lines O IV in a region with an average temperature of about 40,000 - 60,000°K, the lines N III in the region with a temperature of 20,000 - 30,000°K, and the lines C II in a region with a temperature of about 12,000°K. These temperatures correspond to different heights in the chromosphere, the lines C IV being generated at the greatest height in this case.

An interesting factor in this analysis is the conclusion that a distinct boundary exists between the chromosphere and the corona. This conclusion is based on the fact established by Zirin et al. that the lines of intermediate ionization stages of Ne, Mg, and Si are not observed in the solar spectrum, whereas the lines of all ionization states of C, N, and O are observed. The ionization potential of these intermediate states is within 100 - 300 ev. Comparing this with the extent of the hottest part of the chromosphere (5000 km), the authors estimated the linear extent of the transition region. This /315 proved to be of the order of 500 km, i.e., so small that one actually can speak of a sharp transition between chromosphere and corona.

In general, from an analysis both qualitative and, particularly, quantitative of the results of spectral observations in the region of soft X-rays and hard ultraviolet of the sun one could expect much help in constructing a model of the chromosphere and also in understanding the nature of the processes occurring there which lead, in particular, to the appearance of highly ionized atoms of heavy elements, to a high degree of ionization, and to a high value of the electron temperature therein.

A theoretical interpretation of the results of rocket observations of the continuous radiation of the chromosphere in the short-wave region of the spectrum was attempted by DeJager and Athay (Ref.22, 23). Comparing the empirical data of others (Ref.17, 19) with computational data under the assumption that radiation of the continuous spectrum of the chromosphere proceeds in accordance with a gray-body law, DeJager demonstrated an increase in effective temperature toward short waves from $T_{ef} \approx 5000°K$ at $\lambda \sim 1200$ Å to $T_{ef} \approx 7000°$ at $\lambda \sim 900$ Å.

Athay, in his paper, discusses the continua of H, He I, and He II and also the resonance lines of these and other ions (C IV, N V, and O IV) with emphasis on a search for energy sources or physical mechanisms leading to the formation of solar ultraviolet radiation. As such a mechanism, Athay indicates the possible role of the subphotosphere convective zone; some portion of the energy transferred by convection is changed to a form in which it passes through the photosphere without substantial losses and which then is scattered in the chromosphere and corona as radiation. Thus, Athay considers nonradiative transfer of energy from the deep layers of the photosphere to the outer layers of the sun as being the source of short-wave radiation of the chromosphere and corona.

G.S.Ivanov-Kholodnyy and G.M.Nikol'skiy (Ref.24) and Suemoto and Moriyama (Ref.25) attempted to compare hard ultraviolet radiation with the short-wave /316
radio emission of the sun. The main conclusion here is that the intensity of hard ultraviolet radiation is vastly (several hundreds of times) greater than could be expected on the basis of radio astronomy data. To explain such a great discrepancy, in one case an attempt was made to attribute this excess of energy in the hard ultraviolet to the effect of faculae fields (Ref.24), and in another case (Ref.25) a model chromosphere was proposed according to which the hard ultraviolet radiation and radio emission escape from strictly limited regions scattered over the entire disk and covering about 10% of its surface.

This problem was taken up in a paper by Allen (Ref.28) where an attempt is made to achieve satisfactory agreement between observation and theory for a homogeneous model chromosphere.

While noting the importance and the extreme need of interpreting observational data on short-wave radiation of the chromosphere, it is also necessary to note that these data are still far from sufficient for completely revealing all possible regularities and for deciphering the processes occurring in the chromosphere and in layers immediately adjacent to it above and below. Special emphasis must be placed on making experiments that will permit probing the chromosphere throughout its entire height. For this, observations are required in specially selected spectral lines generated in different layers of the chromosphere differing in physical conditions (electron concentration, electron temperature, etc.). Protracted observations from satellites are needed to reveal possible intensity variations of the emission lines. Finally, theoretical investigations are required to determine the atomic parameters of highly ionized ions (oscillator strength, coefficients of spontaneous transition probability, etc.).

5. Solar Radiation in the Lyman-Alpha Line

Of particular interest are observations of the Lyman-alpha resonance line of hydrogen (1215.67 Å). This line is emitted exclusively by the solar chromosphere. Owing to the very low level of the continuous spectrum of the photo- /317
sphere in the region around 1200 Å, the equivalent width of the L_α-absorption line of photospheric origin should be very large: according to Greenstein's calculations (Ref.36), it is of the order of 10,000 Å. From this it follows that the resulting L_α-line in the solar spectrum should be present in emission and in a completely undistorted form.

The first measurements of the intensity of the L_α-line of the sun were made in 1949-1950 by means of photon counters and with the use (in one case) of luminescent $CaSO_4$:Mn crystals. Later, the number of such measurements markedly increased, with simultaneous improvement in the measurement technique. The best results were apparently obtained by measurements that used ionization chambers and short-wave monochromators. In the first case the L_α-line was isolated from: 1) the short-wave boundary, by means of a lithium fluoride crystal with a transmittance limit of 1050 Å attached to the end window of the ionization chamber; 2) the long-wave boundary, by selecting a special filling gas for the chamber which in this case was NO that is ionized upon absorption of light quanta shorter

than 1350 Å. In the case of the grating monochromator a spectrum is first constructed in the focal plane of the chamber whose dispersive element is a diffraction grating, after which a narrow slit with a radiation receiver (a photomultiplier with a glass window coated with a special phosphor, usually sodium salicylate) automatically sweeps the spectrum.

An incomplete list of the experiments connected with a study of the intensity of the L_α-line is given in Table 6. The intensities of the L_α-line, as follows from the data of this table, proved to be different in different experiments. No doubt, this spread is to some extent caused by errors of measurement so that the results in the individual cases may differ from the actual values by a factor of 2 and more. Nevertheless, this discrepancy can be considered to be real and as being associated with solar activity: At the period of maximum activity the intensity of L_α-radiation is greater, while it is less at the period of minimum activity.

TABLE 6 /318

OBSERVED INTENSITIES OF SOLAR RADIATION IN THE L_α-LINE

Date	Intensity, erg/cm² sec	Method	Ref.
Sept. 29, 1949	1—10	Photon counter	[48]
Nov. 17, 1950	0.4	Phosphor $CaSO_4$:Mn	[49]
May 5, 1952	0.1	Photon counter	[50]
Dec. 12, 1952	0.5	Photographic	[12]
Dec. 13, 1955	3.0	»	[11]
Oct. 18, 1955	5.7	Ionization chamber	[51]
Oct. 22, 1955	4.0	» »	[51]
Nov. 14, 1955	9.2	» »	[51]
July 17, 1956	6.1	» »	[51]
July 20, 1956	6.1	» »	[51]
July 25, 1956	6.7	» »	[51]
Aug. 6, 1957	3.43	Spectrophotometric	[53]
1960	6.0	Monochromator	[54]
Jan. 19, 1960	3.3	»	[54]
Aug. 23, 1961	5.1	»	[55]

The estimate of the flux of Lyman-alpha radiation of 0.1 erg/cm² sec as obtained in one experiment (in 1952) apparently is erroneous. A maximum flux equal to 9.2 erg/cm² sec was noted only once, in one experiment in 1955. Therefore, for the limiting values of the flux of L_α-radiation we have a value of 0.5 - 5 erg/cm² sec, i.e., a discrepancy of one order of magnitude. On the average, one can take $E_\alpha \sim 3$ erg/cm² sec for the outer limit of the earth's atmosphere, which is approximately one million times less than the total intensity of the photospheric radiation of the sun.

The remaining lines of the Lyman series of hydrogen, L_β, L_γ, etc., were measured less accurately by reason of their weakness. Table 7 presents the existing data on this matter, where the intensity of the L_α-line is taken as 1000. The accuracy of these data differs; apparently Hinteregger's measure- /319
ments deserve greatest confidence. Owing to the nonuniformity and unreliability

of these data it is difficult to say at present to what extent this spread in the Lyman decrement is real and whether the variations of solar emissivity in the L_α-line (depending on the cycle of solar activity) are accompanied in general by a change in curvature of the Lyman decrement.

TABLE 7

LYMAN DECREMENT IN THE SOLAR SPECTRUM

Line	Johnson (Ref. 9)	Hinteregger (Ref. 19)	Rens (Ref. 19)	Hinteregger (Ref. 30)
1216 L_α	1000	1000	1000	1000
1026 L_β	16.7	9.1	60	9.4
972 L_γ	—	6 (?)	10	1.9
949 L_δ	—	1.8	—	1.4

The observed Lyman decrement, despite the uncertainty of the data, was somewhat steeper than would be expected - for example - in the case of recombination of protons with electrons and their subsequent successive downward transitions. Actually, this decrement should be compared with the theoretical decrement derived with consideration of the effect of atomic excitation under the influence of electron collisions. In some way or other the deviation of the observed decrement from the theoretical value can serve as an indication that the medium (chromosphere) is not completely transparent at the frequencies of the hydrogen lines of the Lyman series and that the observed intensities of these lines are distorted by the phenomenon of self-absorption. Evidently, a comparison of the observed and theoretical decrements would furnish the optical thickness of the chromosphere in lines of this series. However, owing to the unreliability of the measurement data we must presently refrain from such an attempt.

6. Profile of the Solar Lyman-Alpha Line

A special experiment was carried out to determine the profile of the solar L_α-line (Ref.37). A spectrograph with a concave grating of 1200 lines/mm with a radius of 50 cm and operating in the 15th order of the spectrum, was used. To correct astigmatism, another grating working in the first order was placed between the slit and the main grating perpendicular to the dispersion.

Figure 5 shows one of the profiles of the L_α-line of the sun obtained on July 21, 1959. The line was very broad, about 1 Å. The shape of the profile itself is noteworthy; there is wide central absorption at the line center. This is caused by absorption in the solar atmosphere. In addition to this there /320 is a deep and narrow absorption core. The appearance of this core has nothing to do with the sun and is due to absorption by the neutral hydrogen between sun and earth. Using the value of the half-width of the central core, equal to 0.025 - 0.04 Å, the temperature of this neutral hydrogen can be determined. It

is of the order of 1000 - 2000°K, which agrees satisfactorily with the previous estimate of the temperature of the outermost layers of the earth's atmosphere (geocorona). The fact that the central absorption core (telluric core) is rather symmetric relative to the line itself indicates that the neutral hydrogen (geocorona) does not move as a whole.

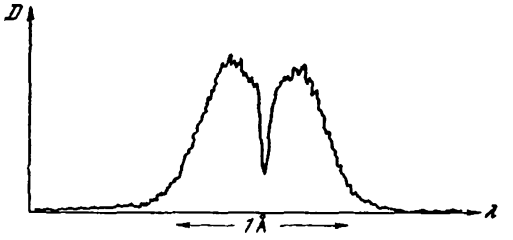

Fig.5 Microphotometer Tracing of Solar Lyman-Alpha Emission Line.

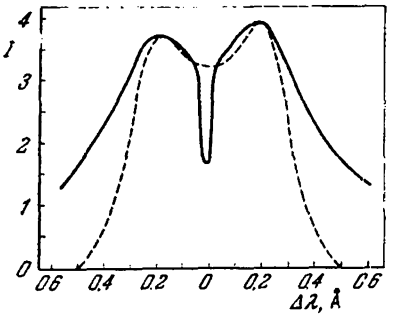

Fig.6 Profile of Solar Lyman-Alpha Line. Solid curve - experiment; Broken curve - theoretical calculation (for each peak separately).

The profile of the L_α-line was theoretically investigated by Morton and Widing (Ref.38) on the basis of the theory of Jefferies and Thomas (Ref.39) concerning the formation of chromospheric lines with consideration of incoherent scattering. The results of their calculations agree rather well with observational data; in particular, they obtained a profile with two /321 maxima and a wide, but shallow, depression at the line center. It was established that this broad core arises in the layers of the solar atmosphere with an extremely rapid temperature rise reaching 90,000°K and higher. The non-solar origin of the narrow absorption core was proved.

At the same time there are certain divergences between the calculated and observed L_α-profiles (Fig.6). First of all, the theory gives an excessively rapid drop of the profile wings within the two Doppler half-widths. However, the curvature of the wings can be reduced when assuming that the formation of the line occurs in a region with a temperature gradient lower than that used as basis in the calculations cited above. Furthermore, the theory does not explain the intensity difference of the profile peaks (the short-wave maximum is higher than the long-wave one).

Analogous profiles are exhibited by the Mg II lines (2795 and 2803 Å) and by the H and K lines of Ca II.

7. Solar Photography in the Lyman-Alpha Line

The first photograph of the solar disk in L_α-rays was obtained by Mercure et al. (Ref.40) in 1956. For this, they used a monochromatic chamber consisting of two prisms and one lens, all made of lithium fluoride. The resolving power of the camera was about 1'.5, and the diameter of the image of the solar disk

was 2.8 mm. By means of this camera several photographs of the sun in L_α at a height above 100 km were obtained. The images, however, proved to be faint and severely fogged by scattered light; even the solar disk was resolved poorly.

Better success was achieved by Purcell et al. (Ref.41, 42) who photographed the sun in the L_α-line by means of a double monochromator. Their instrument consisted of two concave diffraction gratings, the first of which was deformed so as to give it a toroidal shape. This was done to correct the astigmatism which was excessive in this case. Both gratings, with a radius of curvature /322 of 40 cm and 600 rulings/mm, worked in the first order. The first grating gave an image of the sun in L_α. The diaphragm installed in the focal plane of the first grating separated this image which, being subjected to even greater dispersions, was doubled by the second grating. Thanks to the use of double dispersion in the region near L_α, the influence of other lines superposed to the solar image in L_α was largely eliminated.

The described monochromator was used for photographing the sun in L_α only once, during launch of the high-altitude rocket on March 13, 1959. About 60 photographs with exposures from 1/50 sec to 7 sec were obtained; some of these proved to be excellent (with a resolution of the order of 1'). A comparison of these photographs with the spectroheliograms of the sun in the H_α and Ca II lines, obtained at ground observatories on the same day, led to interesting conclusions. First of all, the image in L_α resembles calcium spectroheliograms more than hydrogen ones. However, the emission zones in L_α have a larger structure than the emission zones in the K line. The faculae fields surrounding the spots have a greater extent and greater intensity in L_α than the fields in the K line. No limb brightening of the solar disk in L_α rays is observed on these photographs, but it is impossible to say anything as to limb darkening; apparently the resolving power of the photographs was insufficient here. In most cases, the details of the solar disk (in particular, filaments) are noticeable on all three photographs in L_α, H_α, and K, being unsharp only in the L_α-line. In some cases, photographs in L_α made it possible to detect fainter prominences that are absent on photographs obtained in the light of H_α.

However, for a more detailed analysis the resolving power of the instrument must be increased, specifically the pointing and guiding system. To probe the chromosphere at various altitudes it is especially valuable to obtain monochromatic images of the sun in lines excited in different layers of the chromosphere. For example, the L_β-line should be emitted mainly in the lower layers of the chromosphere where the temperature is comparatively low while, say, the line 1032 Å of the ion O VI is emitted in the transition region from the upper layers of the chromosphere to the lower corona. Correspondingly, the effect of /323 limb brightening of the solar disk should be observed at line 1032 Å and should not be observed in the L_β-line. To some extent this is confirmed by spectrograms obtained for the sun in the indicated spectrum region.

8. Effect of the Hydrogen Geocorona

In addition to L_α-radiation from the sun and from possible discrete sources of the Galaxy, there is a background of L_α-radiation of the night sky. This background is due to scattering of L_α-radiation arriving from outside, mainly

from the sun. Scattering occurs by atomic hydrogen which makes up the outer part of the earth's atmosphere (geocorona) and whose existence was first predicted by Chapman (Ref.43).

The existence of a hydrogen geocorona results in at least two effects having a direct bearing on extra-atmospheric astronomical observations:

a) The hydrogen geocorona causes absorption at the L_α-line center belonging to extraterrestrial objects, as a result of which all profiles of both emission lines and absorption lines should contain narrow telluric absorption cores. For the case of the solar emission line L_α, this has been proved by observations (see Fig.5).

b) The hydrogen geocorona, causing scattering of solar L_α-radiation, creates a background of a more or less constant brightness which limits detection of galactic L_α-sources. This must be emphasized in particular since, as will be shown in Section 14, the Galaxy - for all practical purposes - should not have a L_α-background and thus, if it is desired to record very faint L_α-sources of cosmic origin, it is necessary to carry the instrumentation far above the earth.

The first observations of L_α-radiation of the night sky were obtained by rocket soundings in 1955. Later, these experiments were repeated (Ref.44), permitting an estimate of the limiting values for the L_α-radiation intensity of the night sky. These values were within $2.7 \times 10^{-3} - 3.6 \times 10^{-3}$ erg/cm^2 sec ster at an altitude of 130 - 146 km (Ref.45). According to other measurements (January, 1960) the intensity was equal to 1.2×10^{-3} erg/cm^2 sec ster (at an altitude of 200 km) (Ref.45). It was established that the L_α-radiation intensity of the night sky decreases with altitude, which is proved by the fact that the glow is actually caused by scattering of solar L_α-radiation. /324

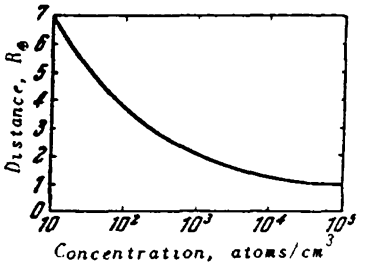

Fig.7 Distribution of Atomic Hydrogen Concentration versus Distance from the Earth's Center (Distance Expressed in Earth Radii $R_\oplus$).

Combining the results of measuring the L_α-radiation intensity at various altitudes, the vertical distribution of the hydrogen atom concentration can be derived. Such calculations were performed by Johnson and Fish (Ref.46, 47) for the most probable temperature of the geocorona $T = 1250^\circ K$, whose results are given in Fig.7 as a curve of the hydrogen atom concentration versus altitude (in earth radii). We note the comparatively rapid decrease of concentration with altitude. The number of hydrogen atoms in a column of 1 cm^2 cross section, above the 120 km level, is on the average 7×10^{12}. The concentration of neutral hydrogen at an altitude of 100 km is of the order of 10^5 cm^{-3}. This value is apparently retained up to very great heights, of the order of several thousands of kilometers. The geocorona disappears for all practical purposes at distances of 6 - 7 earth radii, where the concentration of hydrogen atoms is of the order

of 10 cm^{-3} or less.

9. Solar Radiation in the Line He II 304 Å

The helium problem is one of the unsolved problems of physics of the sun. The sparse data obtained during solar eclipses for the line 4686 Å of ionized helium and for several lines of neutral helium actually yield no information on the possible physical cause for the comparatively strong emission lines of helium or on the mode of distribution of helium in the solar chromosphere. In any case, the assumption that there is a maximum concentration of helium atoms at some height from the base of the chromosphere has not yet been confirmed. /325 There is also little known on the correlation of helium emission with active regions of the sun and with phenomena of a nonstationary character occurring in local regions of its surface.

Under such circumstances, observations of the emission lines 303.8 Å of ionized helium and 584.7 Å of neutral helium may be particularly valuable. We have in mind here both the need to determine the radiative power of the sun in these lines and the extreme desirability of obtaining monochromatic images of the sun therein.

TABLE 8

INTENSITY OF THE EMISSION LINE λ 304 He II BEYOND THE LIMITS OF THE EARTH'S ATMOSPHERE

Date	I_{304}, erg/cm² sec	Ref.
June 1958	0.83	[5, 20]
Mar. 1959	0.20	[5, 20]
	0.40	[5, 20]
Mar. 1959	0.28	[19, 29]
Dec. 1960	0.50	[31]
Aug. 1961	0.25	[30]

Various papers have been published on measuring radiation in the line λ 304 He II in vertical ascents of rockets to various heights, including measurements by A.V.Bruns and V.K.Prokof'yev (Ref.31) who used a spectrometer on board a satellite. A review of these measurements is given in Table 8. Although the data do not differ greatly, the opinions of various researchers diverge considerably as to estimating the real magnitude of the intensity of the line λ 304 He II beyond the limits of the earth's atmosphere. Estimates exist according to which the intensity reaches 1.5 erg/cm² sec, whereas according to other estimates the line λ 304 He II is even stronger than the L_α-line of hydrogen. As the other extreme, we can mention an intensity of this line equal to 0.04 erg/cm² sec.

Leaving aside these extremes and apparently unsubstantiated estimates, we can say that the intensity of the line λ 304 He II is on the average one order of magnitude less than the intensity of the L_α-line and is equal to 0.50 erg/cm² • • sec, which is in good agreement with the theoretically precalculated value (Ref.32, 33). Furthermore, the intensity of this line changes as a function of the solar activity.

The intensity of the line λ 585 He I based on, for example, Hinteregger's measurements (Ref.30) is equal to 0.055 erg/cm² sec, i.e., one order of /326 magnitude less than the intensity of the line λ 304 He II.

Of particular interest are the monochromatic images of the sun in the lines of ionized and neutral helium. Generally speaking, it is not an easy task to obtain such images when recalling the low intensities of the lines λ 304 He II and λ 585 He I and the necessity of special precautionary measures to eliminate scattered light within the monochromator. Thus, it is not surprising that so far there has been only one successful attempt (Ref.34) to obtain a monochromatic image of the sun in the line λ 304 He II. The results of this experiment have not yet been processed, but the already published photographs permit some conclusions. First of all, unlike the L_α-photographs, the photographs of λ 304 He II distinctly show the effect of limb brightening of the disk despite the fact that the disk itself has a rather uniform brightness in this line. Furthermore, a close correlation was noted between active H_α-regions on the sun and regions of increased brightnesses on the images in λ 304 He II.

A report (Ref.35) has been published on obtaining monochromatic photographs of the sun in the lines Fe XV λ 284 Å, Fe XVI λ 335 Å, and also in L_β λ 1025 Å, O VI λ 1030, λ 1036 Å, and C II λ 977 Å. However, the results of processing these photographs have not yet been published.

10. Short-Wave Stellar Spectrophotometry

So far there has been only one successful attempt at conducting spectrophotometric measurements of stars in the far ultraviolet region. We are speaking of the paper by Stecher and Milligan (Ref.56) published in 1962. For their work, they designed special spectrophotometers of an original system operating in the 1700 - 4000 Å range in one instrument and in the 1225 - 3000 Å range in the other. In both types of spectrographs, plane diffraction gratings simultaneously function as dispersive element and as objective; one parabolic and one plane mirror make up the light-gathering system; the light receiver is a photomultiplier with a glass window coated (in the instrument designed for work in the 1225 - 3000 Å region) with sodium salicylate. A honeycomb collimator installed in front of the instrument input is used to limit the working region /327 of the instrument in the necessary wavelength interval of the spectrum.

The spectrographs were mounted rigidly to the upper platform of the rocket, which was fired vertically to a height of 172 km, thus providing their normal functioning for 400 sec. The rocket was given a spin, thanks to which the light-receiving apertures of the spectrographs were able to scan the sky, getting a fix first on one and then on another star. The photocurrents arriving from the photomultipliers were transmitted to the earth after amplification and conversion by means of direct radiotelemetry. The spectral resolution of the instruments was low, about 100 Å, but the errors on the obtained results, with consideration of the errors in absolute calibration, proved to be less than 30% and probably of the order of 10%, which is not a bad accuracy for a beginning. According to calculations, the instruments should yield good spectrograms of B-stars up to 4^m. The optical system of the instrument, details of its operation, calibration, interpretation of obtained results, etc. are given in the above-mentioned paper.

Only one firing of the sounding rocket took place (on November 22, 1960) with simultaneous carrying aloft of two long-wave (1700 - 4000 Å) and two short-

wave spectrographs (1225 - 3000 Å). However, the latter for some reason did not operate; therefore, all results given below pertain to instruments operating in the long-wave range.

Signals were obtained from about 30 stars, but only for seven stars were the recordings of the spectra of good quality; for another eight stars, they contained some useful information. Mainly these were stars from the constellations Orion and Canis Major. The names, stellar magnitudes, and spectral classes of these stars are given below:

ε Canis Majoris	$1^m.43$	B1 II
β Canis Majoris	$1^m.97$	B1 II
γ Velorum	$1^m.98$	WC 7
α Leonis	$1^m.36$	B8 V
α Carinae	$-0^m.72$	F0 Ia
γ Orionis	$1^m.64$	B2 IV
ζ Orionis	$2^m.74$	09 V

TABLE 9 /328

STELLAR FLUXES OF ULTRAVIOLET RADIATION, (erg/cm^2 sec Å) • 10^9

λ, Å	Calibration Factor × 10^9	ε Canis Majoris	β Canis Majoris	γ Velorum	α Leonis	α Carinae	γ Orionis	ζ Orionis
1600	111	2.2		21			—	11
1700	21.3	1.7	2.3	7.6	0.9		2.8	11
1800	9.51	1.2	2.9	6.2	1.1		3.6	9.3
1900	6.08	1.0	3.2	5.2	1.3		3.8	8.5
2000	4.67	1.3	3.5	7.5	1.5	0.5	3.7	7.7
2100	4.15	2.9	3.9	7.4	2.0	1.0	4.5	8.5
2200	3.86	6.5	4.6	8.1	2.5	0.8	6.1	8.9
2300	3.69	8.6	5.5	9.0	2.9	1.9	6.5	9.5
2400	3.54	9.3	5.6	11.7	3.1	1.4	4.8	8.9
2500	3.57	8.5	5.3	9.1	3.1	1.4	5.5	6.6
2600	3.74	8.1	4.9	8.5	3.0	2.1	5.2	8.4
2700	3.78	7.2	4.3	7.8	2.8	1.5	4.8	7.6
2800	3.83	6.5	3.6	7.1	2.6	2.1	4.2	7.0
2900	3.74	5.8	2.8	6.4	2.4	2.3	3.6	6.2
3000	3.74	5.3	2.5	5.8	2.2	3.0	3.2	5.8
3100	3.80		2.4	5.2	2.2	3.2	3.0	
3200	3.89		2.2	4.4	2.1	2.3	2.6	
3300	4.04		2.0	4.3	2.1	2.7	2.3	
3400	3.38		1.8	4.2	2.1	2.9	2.2	
3500	4.52		1.7	3.9	2.1	2.8	1.9	
3600	4.93	3.2	1.6	3.7		3.8	1.8	
3700	5.33	3.4	1.4	3.6		5.1	1.6	
3800	6.11	3.3	1.4	3.8		11.5	1.8	
3900	7.35	3.1	1.4	3.8		13.3	2.1	
4000	8.88	2.9	1.2	3.8		18.1	1.4	
4100	11.5	2.6	0.9	3.9		14.4	0.5	

Table 9 gives the absolute values of fluxes for the aforementioned seven stars at different wavelengths. The first column of the table contains the

wavelengths; the second, the factor by which one must multiply the reading (corresponding to the signal from the star at the telemetry output) expressed in volts, in order to obtain the flux in erg/cm^2 sec Å.

Owing to the low resolving power of the spectrographs, no statements are possible on the presence or absence of short-wave spectral lines in the spectra of the investigated stars.

11. Interpretation of Short-Wave Stellar Spectra /329

As shown above, the number of stars for which the spectra are known in the wavelength interval of 1600 - 4100 Å is small at present, being only seven. Nevertheless, we can discuss these results and draw some preliminary conclusions. Here we can utilize the favorable circumstance that a large number of papers have been published on the theoretical construction of various model stellar atmospheres, making it possible to compare the results of rocket observations with the data given there. Models of high-temperature stellar atmospheres should be of particular interest. A review of these papers, with critical comments and needed explanations, is given in Munch's survey (Ref.57).

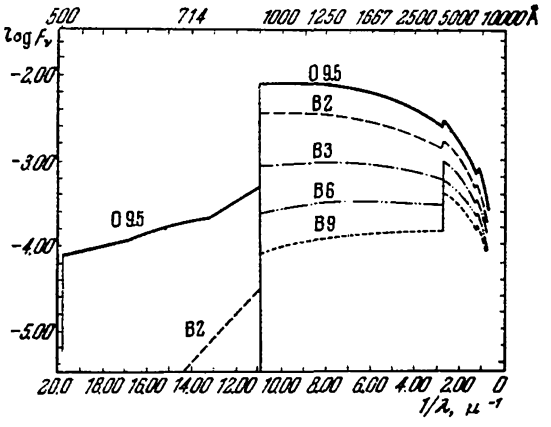

Fig.8 Continuous Spectra for Five Model Atmospheres of Stars of Early Spectral Classes.

Of the various aspects useful as basis for developing some model stellar atmosphere, main interest centers on the theoretical energy distribution in the continuous spectrum of a star of a given temperature and luminosity, with consideration of the distorting influence of the absorption lines. /330 Studies of this nature were performed by Underhill (Ref.58) for stars of classes O - B, by Saito (Ref.59) for stars of late subclasses of B, by Osawa (Ref.60) for class A stars, by Canavaggia and Pecker (Ref.61) for class F stars, and so on. The latest results on calculating (on electronic computers) theoretical continuous spectra of hot stars of classes 09.5 - B9 are given in a paper by Underhill (Ref.62). These results are represented graphically in Fig.8, plotted as the radiation flux in the continuous spectrum F_ν (in erg/cm^2 sec) versus the wavelength λ.

Let us now discuss the results obtained by Stecher and Milligan. For this, the data of Table 9 for some stars are represented graphically in Figs.9 - 12. The diagrams show the theoretical spectra (broken lines) corresponding to typical model stellar atmospheres. In each case, the theoretical spectra were arbitrarily normalized at the point λ = 2600 Å. The following theoretical spectra were

taken: for the star α Carinae, F0 Ia, from the model of Canavaggia and Pecker (Ref.61); for ε Canis Majoris, B1 III, from Underhill's model (Ref.58); for α Leonis, B8 V, from Saito's model (Ref.59); and finally, for β Canis Majoris, A3 V, from Osawa's model (Ref.60). Other details are given in the captions to the diagrams. /332

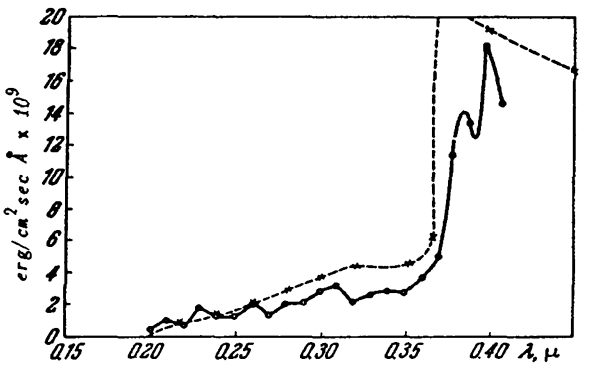

Fig.9
Solid line - observed absolute flux from α Carinae (F0 Ia); broken line - flux corresponding to the model atmosphere at θ = 0.75 and log g = = 1.80. The theoretical curve (Ref.61) was equated with the observed curve at the point 2600 Å.

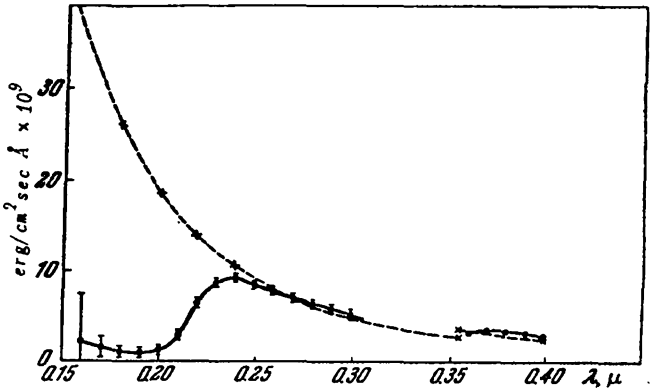

Fig.10
Solid line - observed absolute flux of ε Canis Majoris (B1 II); broken line - flux corresponding to the model atmosphere at T_e = 28,470°, log g = 3.80. The theoretical curve (Ref.58) was equated with the observed curve at the point λ = 2600 Å.

It follows from these diagrams that just in one case - for the star α Carinae which is a supergiant of a late class - was satisfactory agreement obtained between observations and theoretical continuous spectrum distribution in the entire spectral interval. For the other stars, which are objects of early classes, the observed fluxes in the spectrum region shorter than λ ~ 2400 Å are substantially smaller than the fluxes obtained from the theory of stellar atmospheres. It should be emphasized that the extent of this deviation appreciably exceeds the possible errors of measurement. On the average, for stars A IV - 05 the observed flux was smaller than the theoretically expected value by about one order of magnitude. Apparently this difference exceeds the difference between individual models, although - for example - Munch (Ref.57) mentioned a case where two authors (e.g., McDonald and Underhill), using essentially the same methods, obtained completely different results for atmospheres with almost the same parameters.

This fact, unless due to a random and unforeseen experimental oversight, /333 is exceptionally important since it poses entirely new problems. It is obvious that this flux deficit either has a direct bearing on the properties of the star which are for some reason manifested in this wavelength interval or that it is

caused by some interstellar absorbing agent.

The authors of the experiments themselves (Ref.56) do not believe in the possibility of the role of interstellar absorption and are inclined to see the

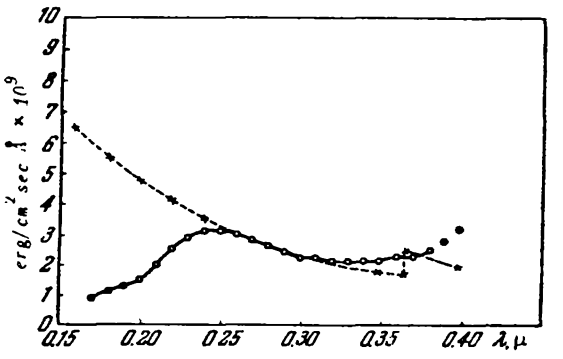

Fig.11
Solid line - observed absolute flux of α Leonis (B8 V); broken line - flux corresponding to the model atmosphere (Ref.59) at T_e = 15,500° and log g = 3.80 equated to the observed flux at the point 2600 Å. The long-wave end blends with the spectrum of μ Leonis.

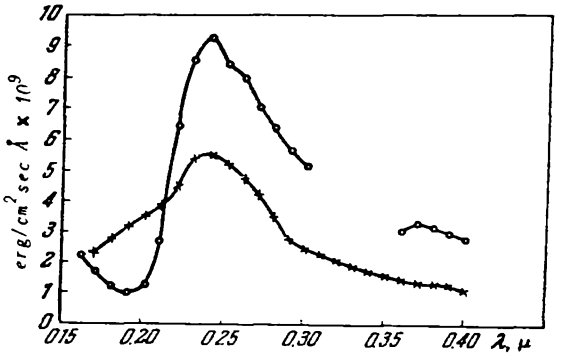

Fig.12
Curve with open circles - observed absolute flux from ε Canis Majoris (B1 II); curve with crosses - absolute flux from β Canis Majoris (B1 II).

source of the observed flux deficit in the atmosphere of the star itself. As an example, the blanketing effect caused by NO and CO molecules is indicated as a possible source of absorption of the flux near 2000 Å. Also mentioned is the possible role of quasi-molecules which represent different combinations of ions and atoms of hydrogen and helium such as H_2^+, H_3^+, HeH^+, HeH^{++}, etc. Thus, under certain conditions, as demonstrated by S.P.Yerkovich (Ref.64), absorption by the quasi-molecule H_2 near 2000 Å is 10^3 times greater than for the negative hydrogen ion. It is suggested that, in the atmospheres of hot stars, quasi-molecules are able to form in such quantities and with such effective absorption cross sections (Ref.65) that this might furnish an explanation for the flux deficit.

Meinel (Ref.66) attempted to explain the observed energy distribution in the spectra of stars of class B, for example of ε Canis Majoris, by a molecular recombination mechanism caused by hydrogen and helium molecules. In particular, the author indicated that, even at an insignificant quantity of H_2 in the atmosphere of a hot star, an exchange reaction of the type

$$H_2(X^1\Sigma_g^+) + H(2^2S) \rightarrow H_2(a^3\Sigma_g^+) + H(1^2S)$$

may play a major role at high temperatures. In this case, the difference in

reaction energies is compensated by the thermal energy of the reaction partners and by excitation of high vibrational levels of the ground state of H_2. From the excited level $a^3\Sigma_g^+$, the hydrogen molecule - by successive transitions - descends, for example, to the lowest triplet state $b^3\Sigma_g^+$. Since this level is unstable, transition to it is accompanied by emission of a continuum and by /334 direct dissociation of the temporarily formed molecule.

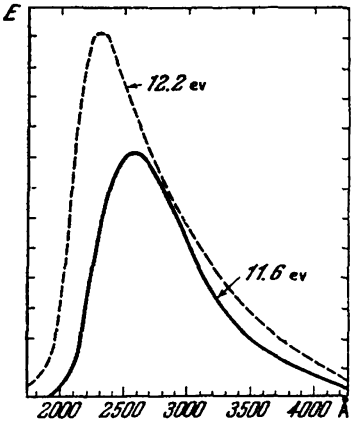

Fig.13 Theoretical Curves of the Continuous Emission Spectrum of H_2 at Different Excitation Energies.

Furthermore, Meinel found the theoretical energy distribution in the continuous emission spectrum of H_2, which proved to be in good agreement with previous experiments. The presence of a maximum near 2500 Å and a strong dip at 2000 Å is characteristic in this distribution (Fig.13). Comparing this curve with Figs.10 and 12 we see that the similarity of both distributions, observed and theoretical, is rather close - at least qualitatively. Meinel suggested that the emission zone of H_2 in the atmosphere of a star of class B is below the emission zone of H and directly adjacent to the photosphere.

In contrast to these explanations, Hoyle and Wickramansinghe (Ref.67) are inclined to attribute the cause of the flux deficit in the spectra of hot stars to interstellar absorption caused, however, by graphite particles. They demonstrated that the effective absorption cross section of light quanta $Q(\lambda)$ for graphite particles and in particular for composite particles of graphite and ice, increases with a decrease in wavelength and, already at 2000 Å, reaches a noticeable value. For example, at a sufficiently small size of such particles, the ratio $Q(1000)/Q(4000)$ may reach ten.

Thus, there are more than enough theoretical schemes and mechanisms for explaining the observational fact of the flux deficit of hot stars. We must not forget that this fact has been established only with respect to very few stars and, moreover, on the basis of only one series of observations. Therefore, /335 before we make any conclusive selection among the possible variants for explaining the above fact, new experiments must be scheduled to obtain spectrograms for a large number of stars and in the region of shorter wavelengths. This is even more necessary because of the fact that, primarily, we have no justification for assuming that, in the experiments by Stecher and Milligan, some factors leading to such paradoxical results were not overlooked. Secondly, if the indicated flux deficit is actually real and spreads even farther to the shorter wave end including the region of the Lyman continuum, then many previously established facts and theoretical conclusions will prove erroneous, including those referring to interstellar zones of ionized hydrogen, glow of diffuse and planetary nebulae, determination of star temperatures responsible for the glow of nebulae, etc.

12. Electrophotometric Observations in the Vacuum Ultraviolet Region

Various attempts have been made to measure the intensity of the ultraviolet radiation of stars and nebulae in individual spectrum regions by means of photon counters, ionization chambers, or photomultipliers carried on board high-altitude rockets into the outer layers of the earth's atmosphere (Ref.68, 69, 70).

During one of the launchings in 1957 (Ref.69), a part of the sky was scanned in the spectral interval 1225 - 1350 Å by means of an ionization chamber. In this case, several extended objects were noted which emitted rather powerful fluxes in the indicated wavelength interval. The so-called nebula in α Virginis, an object of almost circular shape and extension up to 10° from the star, was especially well-defined. On attempting to relate this nebula with Spica (α Virginis) the radiant energy of the nebula in the region 1225 - 1350 Å was found to be about 10^{37} erg/sec. On the other hand, the total radiant energy from Spica on wavelengths shorter than the Lyman series limit ($\lambda < 912$ Å) should also be about 10^{37} erg/sec, if one assumes that Spica radiates as a black body with a temperature of $32,000^{\circ}$K. Thus, we can assume, even if this means stretching a point, that the radiation of the nebula around Spica in the region 1225 - 1350 Å is no other than the energy of the star radiated in the region < 912 Å and transformed in the nebula to L_{α}-radiation. /336

However, we must then devise a mechanism (which has been done by several authors) to explain the very large (> 10 Å) Doppler shift of the maximum of L_{α}-emission toward long waves. Furthermore, it is necessary to find an explanation to the fact that no nebula in visible rays (H_{α}, N_1, etc.) has been observed around Spica. However, the commotion about the nebula of Spica quieted down as soon as it was found, during one of the repeated experiments in 1960 (Ref.69), that the radiation sources in the 1225 - 1350 Å region of the spectrum are only stars and that there is no nebula in Spica.

In 1960 there were two launchings of high-altitude sounding rockets with special photometers for measuring stellar brightnesses in two vacuum ultraviolet regions: 1350 - 1550 Å and 1290 - 1350 Å (Ref.69, 70). The photometers consisted of a series of 6" and 4" parabolic mirrors and of ionization chambers as radiation sources. The working spectral regions were separated: in the first case (effective wavelength 1427 Å) by means of 1-mm thick BaF_2 crystal and a mixture of NO and CO_2 gases; in the second case (effective wavelength 1314 Å) by means of a 1-mm thick SrF_2 crystal and a mixture of dimethylhydrazine and methane gases. The photometers operated on the free scanning principle, and the results were transmitted to the ground (without preliminary recording) over radiotelemetry channels.

A preliminary processing of the obtained data (Ref.69) confirmed the conclusion of the previous experiment that stars of early classes are the only celestial objects encountered in the 1290 - 1350 Å and 1350 - 1550 Å spectral regions. It was also established that these stars radiate as point sources in the indicated ranges and that there are no extended objects surrounding them.

Chubb and Byram compiled a list of stars of early classes, primarily of

class B, detected during these experiments. These lists are given in their /337 paper (Ref.70) and contain about 50 objects detected by means of a 1427-Å photometer and about 30 objects detected by means of a 1314-Å photometer. The faintest star was $5^m.83$ in the first case and $5^m.66$ in the second. For these stars, the absolute values of the radiation fluxes in the corresponding regions of the spectrum and the ratio of these fluxes to the flux at 5560 Å are given. The basic conclusion to be drawn from these new results is as before, viz., the measured fluxes of stars of early classes are appreciably - by one order of magnitude - less than expected from model atmospheres of stars of early classes. This follows graphically from Figs.14 and 15, where the spectral classes are laid off on the abscissa and the values of the ratios F_{1427}/F_{5560} and F_{1314}/F_{5560}, on the ordinate. The symbols in these diagrams represent observational data. Also plotted are the curves of the theoretical dependence of these values (relative fluxes) corresponding to Underhill's model atmospheres (Ref.114) and to ideal blackbody radiation. No matter /338 how paradoxical, the observation points in both cases fit more closely the curves for an ideal black body. The deviation from the Underhill model is appreciably smaller for stars of late classes and increases on passing toward stars of early classes.

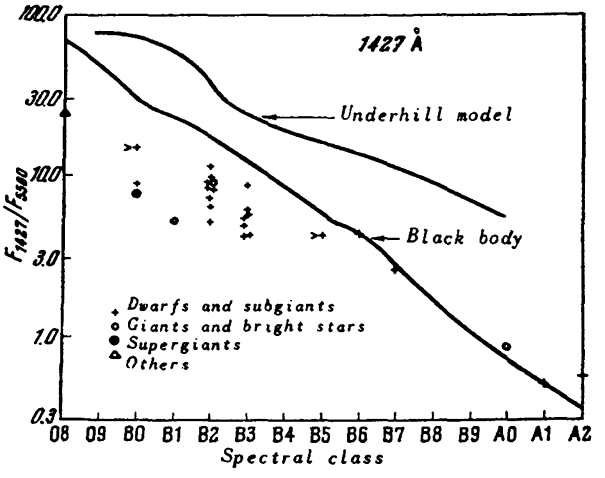

Fig.14 Ratio of Ultraviolet Luminosity of Stars at 1427 Å to Visible Luminosity at 5560 Å versus Spectral Class. The symbols represent the observations of individual stars. The solid lines denote theoretical relations for the same quantities derived from the theory of stellar atmospheres and the blackbody hypothesis.

Thus, although one cannot yet consider to have sufficient data for definite conclusions as to the character and behavior of the continuous spectra of stars in the far ultraviolet, we have to admit that two essentially different methods of observation - spectrophotometric and electrophotometric - lead to the same basic conclusion, namely that stars of early classes show an appreciable flux deficit in the far ultraviolet in comparison with that predicted by theory.

If this conclusion is substantiated by further observations, it will play a colossally important role in forming our concepts on the structure of stellar atmospheres, physical processes occurring there, composition and properties /339 of interstellar matter, etc.

This automatically shows the importance of extra-atmospheric observations, primarily of the continuous spectra of stars of different classes and luminosi-

ties. It can almost certainly be asserted that a study of the spectral absorption lines inherent to the star itself in the far ultraviolet region, although of interest and necessary, will hardly yield any fundamentally new results, with the possible exception of resonance lines. Furthermore, continuous spectra largely depend on the nature of the celestial bodies themselves and on conditions and processes within these bodies; therefore, special priority should be given their study.

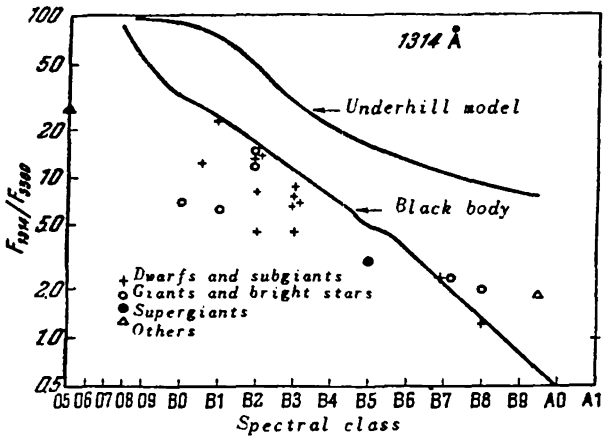

Fig.15 Ratio of Ultraviolet Luminosity of Stars at 1314 Å to Visible Luminosity at 5560 Å versus Spectral Class. The symbols represent observations of individual stars. The solid lines denote theoretical relations for the same quantities derived from the theory of stellar atmospheres and the black-body hypothesis.

This is not so for absorption lines having an interstellar origin. In fact, practically all interstellar molecular hydrogen, oxygen, nitrogen, carbon, and other elements are in the ground state. This is true also for those elements about whose existence in interstellar space practically nothing is known. We are primarily thinking here of helium. As a rule, the resonance lines of these elements are in a range inaccessible to observations from the earth's surface, in the far ultraviolet. Consequently, observations of resonance lines of interstellar atoms and molecules in the spectra of distant stars (specifically in the spectra of hot stars) will yield extremely important information on the chemical composition and physical state of interstellar matter.

Of the absorption lines of interstellar origin, the hydrogen lines of the Lyman series will most likely be the strongest. The equivalent widths of the lines of this series will obviously depend both on the distance of the star, on the galactic plane, and also on the spectral class of the star. In any case, the equivalent width will be of the order of several angstroms and for the L_α-line, of the order of tens of angstroms. Considering also that these lines will have broad wings (line broadening caused by the effect of radiation damping), we should expect an overlap of the wings of the hydrogen lines of the Lyman series. This effect will be especially pronounced at the end of the series. As a result, an excessive energy deficit in the continuous spectrum of hot stars may arise in the 1216 - 912 Å wavelength interval. In other words, it is possible that the cutoff of the continuous spectrum at 912 Å will not be sharp, as expected, but more or less smooth. /340

13. Short-Wave Spectrum of Gaseous Nebulae

Observations of gaseous nebulae, planetary and diffuse, in the vacuum ultraviolet region (3000 - 912 Å) should be of particular interest. The no less peculiar spectrum region, namely the hard ultraviolet ($\lambda < 912$ Å), will unfortunately always be inaccessible to observation because of the interstellar absorption. Such interest is due in particular to the fact that the emission lines of the short-wave region are generally emitted by highly ionized atoms concentrated in the central, hottest, regions of the nebula. Therefore, interpretation of the short-wave spectrogram of a given nebula could yield quite valuable information on the structure and physical conditions in its central portions. Furthermore, short-wave emission lines of highly ionized elements will furnish highly useful data on the energy distribution in the far short-wave spectrum region of the core which is not amenable to direct observation.

So far, no special extra-atmospheric experiments to obtain spectra or direct photographs of gaseous nebulae in the vacuum ultraviolet regions have been scheduled. Therefore, we will limit ourselves to a short review of the anticipated structure of the spectrum of gaseous nebulae in this wavelength region.

Generally speaking, if the chemical composition and temperature of the core is known it is easy to compile a list of expected emission lines in the vacuum ultraviolet region. To obtain some criterion of the possibility of observing a given emission line we also require data on the atomic parameters of various ions and transitions, of which the relative line intensities cannot be precalculated. Unfortunately, to date this requirement cannot be met for most ions and atomic transitions. Hence quantum mechanical calculations are necessary for determining atomic parameters corresponding to short-wave transitions. /341

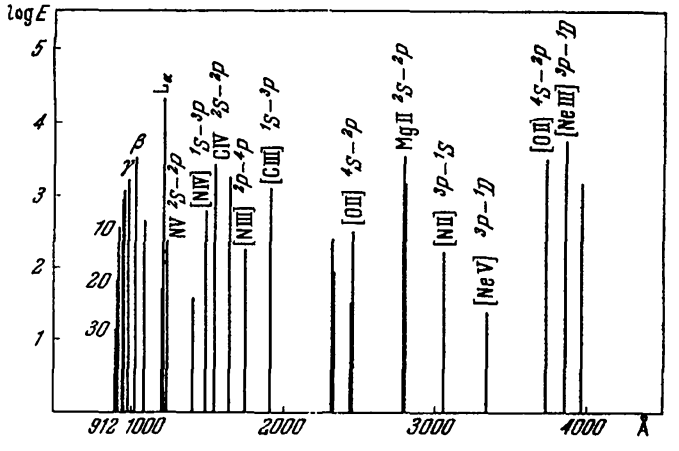

Fig.16 Expected Spectrum of Planetary Nebula in the Vacuum Ultraviolet.

Figure 16 gives a schematic view of the expected spectrum of a planetary nebula in the vacuum ultraviolet region, with an indication of wavelengths and relative intensities of emission lines. This spectrum was calculated by Deub (Ref.71) for a model nebula of the type NGC 7027 at $T_e = 10{,}000^\circ K$. However, this diagram represents a far from complete set of expected emission lines in the vacuum ultraviolet, and only lines for which the atomic parameters are known are entered. Furthermore, the plotting in this diagram of the hydrogen lines of the Lyman series, L_α, L_β, etc., has only a symbolic character since in reality they can be detected barely or not at all. As shown below, the inter-

stellar medium is opaque in the L_α-line so that the nebulae can be observed in this line only in the presence of appreciable Doppler shifts caused by high radial velocities. As for the other hydrogen lines of the Lyman series, L_β, L_γ, etc., as is known from the theory of the glow of gaseous nebulae, the quanta of these lines - under ordinary conditions - are generally unable to escape from the nebula and, specifically, are unable to reach the observer. /342

Among the lines shown in Fig.16, greatest interest centers on the forbidden line of doubly ionized carbon near 1900 Å. In fact, carbon in any stage of ionization does not give a single forbidden line which would appear in the visible range of wavelengths.

Let us now pass to lines whose intensities cannot yet be calculated because of the lack of data but which can be excited under conditions of nebulae. Here, emphasis will be placed on the forbidden lines of highly ionized atoms, since they are excited in the central, hottest, regions of nebulae (Ref.72). The lines lying in the hard ultraviolet region ($\lambda < 912$ Å) will not be included here since they cannot be observed owing to interstellar absorption. The data on the atomic energy levels are taken from Moore's catalog (Ref.73).

Nitrogen. Singly ionized nitrogen should give a doublet near the ultraviolet boundary, 3071 [N II] and 3063 [N II], in $^1S - {}^3P$ transitions. This doublet is similar to the violet doublet of singly ionized oxygen 3726 [O II] and 3729 [O II].

Doubly ionized nitrogen can give numerous close lines within 1744 - 1754 Å and 2276 - 2289 Å. The lines of triply ionized nitrogen 1488 [N IV] and 1485 [N IV] and also 1573 - 1578 [N IV] can be observed in the central parts of nebulae. Lines of quadruply ionized nitrogen 1243 [N V] and 1239 [N V], whose energy level structure is similar to the structure of O V, should be observed close to the L_α hydrogen line.

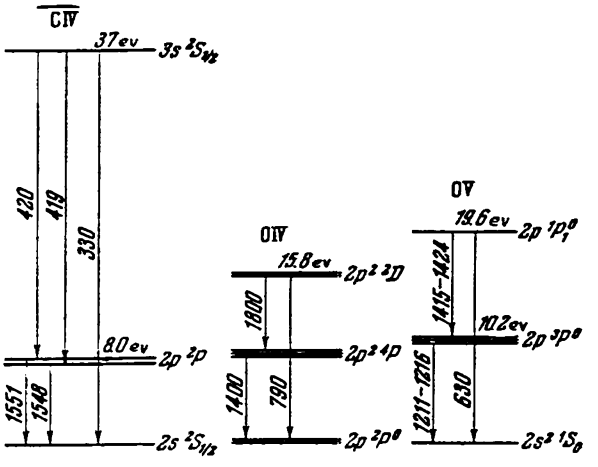

Fig.17 Diagram of Energy States C IV, O IV, and O V.

Oxygen. The line of singly ionized oxygen 2471 [O II] arising upon $^2P - {}^4S$ transitions should be observed in the near vacuum ultraviolet in the outer portions of nebulae. O^+ should give no other short-wave lines. /343

Lines of doubly ionized oxygen 2332 [O III] and 2323 [O III] ($^1S - {}^3P$) transitions should be observed in the outer portions of gaseous nebulae.

All forbidden lines belonging to O IV and O V are located in the vacuum and hard ultraviolet (Fig.17). The group of lines (1800 [O IV]) arising upon $^2D - {}^4P$ transitions may be of some interest. Another group of lines (1400-1412 [O IV]) can arise upon $^4P - {}^2P^o$ transitions, but all of these presumably are faint. Immediately adjacent to this group there is a series of forbidden lines (1415 - 1424 Å) belonging to quadruply ionized oxygen.

It is curious that in the transition $^3P_1^o - {}^1S_0$ of quadruply ionized oxygen the line 1215.7 Å, which is very close to the L_α-line of hydrogen (1215.67 Å), is radiated. Thus, the possibility of an anomalous excitation of the $^3P_1^o$ level of quadruply ionized oxygen under the effect of L_α-radiation of hydrogen is not precluded.

Neon. Figure 18 shows the diagrams of energy levels Ne III, Ne IV, and Ne V. On $^1S - {}^3P$ transitions, the doublet 1794 [Ne III] and 1815 [Ne III] is /344

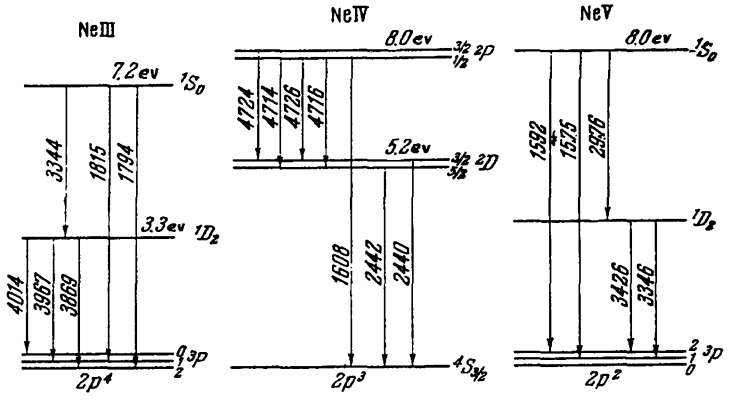

Fig.18 Diagram of Energy States of Ne III, Ne IV, and Ne V.

radiated whose intensity ratio depends on the electron concentration of the medium. The intensity ratio of the lines 1815 [Ne III] and 3344 [Ne III] (which is distinctly observed in the visible spectrum region) depends on the electron temperature T_e of the central portions of the nebula and has the following form:

$$\frac{E_{1815}}{E_{3344}} = 10.5e^{43500/T_e}.$$

Triply ionized neon with $^2P - {}^4S$ and $^2D - {}^4S$ transitions is also able to produce two short-wave doublets, namely 1608 [Ne IV] and 2441 [Ne IV]. It is interesting that the ratio of the line intensities 2440 [Ne IV] and 2442 [Ne IV] permits determining the electron concentration in the central regions of nebulae.

Quadruply ionized neon should give one short-wave line 2976 [Ne V] upon $^1S - {}^1D$ transition and a pair of lines 1573 [Ne V] and 1575 [Ne V] in $^1S - {}^3P$ transitions. The line 2976 [Ne V] should be weaker than the line 1575 [Ne V] by a factor of three.

The ratio of line intensities 3426 + 3346 [Ne V] and 1575 [Ne V] is highly sensitive to the electron temperature and has the form /345

$$\frac{E_{3426+3346}}{E_{1575}} = 3.80e^{50\,000/T_e}.$$

This relation can be used for determining the electron temperature in the central regions of nebulae.

Carbon. A group of forbidden lines of singly ionized carbon near 2328 Å can be observed in the outer portions of nebulae. On $^3P - {}^1S$ transitions doubly ionized carbon should emit very closely spaced lines 1911 [C III] and 1908 [C III] (see Fig.17). Triply ionized carbon can give only two lines in the vacuum ultraviolet region, 1551 [C IV] and 1548 [C IV], on $^2P - {}^2S$ transitions (see Fig.17).

Sulfur. All forbidden lines up to doubly ionized sulfur inclusive are located in the visible and infrared regions of the spectrum. Triply ionized sulfur can give emission lines near 1410 Å on $^4P - {}^2P^o$ transitions.

TABLE 10

EXPECTED FORBIDDEN LINES OF PLANETARY NEBULAE IN THE VACUUM ULTRAVIOLET, OF UNKNOWN THEORETICAL INTENSITIES

Line, Å	Ion	Line, Å	Ion
1215.7	O V	1794	Ne III
1239	N V	1800	O IV
1243	N V	1815	Ne III
1400—1412	O IV	1908	C III
1410	S IV	1911	C III
1415—1424	O V	2276—2289	N III
1485	N IV	2323	O III
1488	N IV	2328	C II
1548	C IV	2332	O III
1551	C IV	2440	Ne IV
1573	Ne V	2442	Ne IV
1573—1578	N IV	2471	O II
1575	Ne V	2976	Ne V
1608	Ne IV	3063	N II
1744—1754	N III	3071	N II

The short-wave lines of other elements, such as fluorine, iron, etc., owing to their low abundance in nebulae, cannot be of particular interest. A review of the aforementioned emission lines, which can be observed in short-wave spectra of planetary nebulae and for which relative intensities cannot be calculated at present, is given in Table 10. This table can be considered a supplement to Fig.16, which gives a view over those short-wave emission lines for which calculated relative intensities are known.

It is especially important to discuss in more detail the continuous spectrum

of gaseous nebulae in the vacuum ultraviolet region. In fact, the maximum intensity of two-photon radiation is far from the visible wavelength range (at 1400 Å) and rapidly drops toward long waves (Fig.19). For example, at 4000 Å the intensity of two-photon radiation amounts to about 5%, whereas at 6000 Å /346 it is about 1% of the maximum intensity at 1400 Å. Incidentally, at one time this caused appreciable difficulties in interpreting the continuous spectra of planetary nebulae. The occurrence of a maximum near 1400 Å on the short-wave spectrogram of some nebula, which can be obtained under extra-atmospheric /347 conditions, will be convincing proof of the nebulae conditions. Furthermore, the occurrence of a rather sharp discontinuity in the distribution of the continuous spectrum near 1216 Å already serves the purpose since, according to the theory of two-photon radiation, its intensity in the region $\lambda < 1216$ Å should be equal to zero. The continuous spectrum in the region $\lambda < 1216$ Å, if detected at all, will be due mainly to two-photon radiation of neutral and ionized helium.

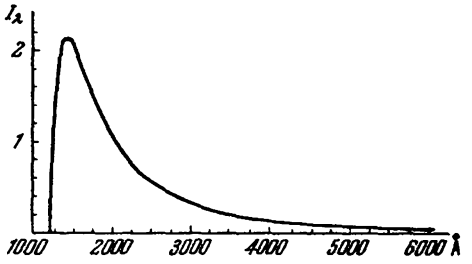

Fig.19 Spectrum of Two-Photon Radiation of Hydrogen.

14. Possibility of Observing Gaseous Nebulae in the Lyman-Alpha Line

The interstellar medium in our Galaxy is practically opaque in the L_α-line. Actually, according to observational data on monochromatic radio emission on the 21-cm wavelength, the average concentration of neutral interstellar hydrogen is of the order of 1 cm^{-3}. Taking, for the coefficient of selective absorption in the L_α-line calculated per one neutral hydrogen atom, the value $s_\alpha \approx 10^{-14}$ cm^2, which corresponds to a temperature of interstellar hydrogen of 100°K, it will be found that at a distance of one parsec from the sun the optical thickness of the interstellar medium t_o (without consideration of the dust component) at the frequency of L_α-radiation will be of the order of 10,000!

Let us examine first the problem having to do with absorbed L_α-quanta in the Galaxy (Ref.74).

Under conditions of the interstellar medium, L_α-quanta cannot be transformed into quanta of other discrete frequencies. However, owing to the large optical thickness t_o of this medium at the frequency of the L_α-line center (of the order of $10^6 - 10^7$ at a distance of the nebulae of 100 - 1000 parsec from earth), the probability of fractionation of L_α-quanta (two-photon radiation) increases appreciably. Of all the existing mechanisms of L_α-quanta fractionation, the most effective one is apparently the cycle $1s \rightarrow 2s \rightarrow 1s$, which was discussed in detail elsewhere (Ref.75, 76). The probability of fractionation of L_α-quantum into two quanta in this mechanism is virtually independent of /348 the environmental conditions and is equal to $p = 0.44 \times 10^{-8}$ per scattering event. Hence, if the quantum, on the average, undergoes 2×10^8 scattering and

absorption events it will perish, having been transformed into two quanta of arbitrary frequencies.

TABLE 11

r, parsec	t_α	N	T, years	L, parsec
10	$3 \cdot 10^5$	$3.8 \cdot 10^6$	400	130
100	$3 \cdot 10^6$	$3.1 \cdot 10^7$	4700	1400
500	$1.5 \cdot 10^7$	$2.1 \cdot 10^8$	23000	7000
1000	$3 \cdot 10^7$	$4.4 \cdot 10^8$	46000	15000

In this respect what are the real conditions prevailing in the Galaxy? The answer is given in Table 11 which contains, in relation to the distance r of the nebula from earth, the total number of scattering events N suffered by a L_α-quantum on traversing the distance r, the total path L, and the time T for the L_α-quantum to traverse this path as a result of multiple scattering. Calculations were carried out for $n_1 = 1$ cm^{-3} with consideration of the effect of the radiation frequency redistribution by means of the following relations (Ref.78, 76):

$$t_\alpha = n_1 s_\alpha r, \tag{1}$$

$$N = 2t_\alpha \sqrt{\pi \ln t_\alpha}, \tag{2}$$

$$T = \frac{N}{n_1 s_\alpha c}, \tag{3}$$

$$L = Tc. \tag{4}$$

It follows from the data of this table that, first, for all practical purposes not a single nebula can be observed in direct L_α-rays ($t_\alpha \gg 1$). Second, if the nebula is at a distance of the order of several hundred parsecs, then at best only the diffuse component of L_α-radiation ($N < 10^8$) will reach the observer. However, already at $r \sim 1000$ parsec the time T necessary for the L_α-quantum to reach the observer is several tens of thousands of years, which /349 is commensurable with the lifetime of the nebulae themselves, although the risk of L_α-quanta fractionation is not so acute here. Furthermore, in this case the path covered by the quantum is substantially lengthened, being of the order of several thousand parsecs. Thus, even a negligible quantity of interstellar dust in the investigated volume of the Galaxy is sufficient for complete absorption of L_α-quanta by dust.

Finally, interstellar dust may also cause scattering of L_α-quanta. However, it is known that, for small particles, the absorption coefficient considerably exceeds the scattering coefficient (Ref.77). Only in one case, when the dust medium consists exclusively of ferromagnetic particles (i.e., particles with a very high dielectric constant) can diffusion of L_α-quanta from the medium occur without absorption of the quanta. However, apparently the Galaxy does not contain more or less extensive dust regions consisting of ferromagnetic particles.

Nevertheless, it is not impossible that the Galaxy contains individual hydrogen clouds with a diameter of several ten parsecs that are "not contaminated" by dust. In such clouds, diffusion of L_α-quanta may actually terminate in splitting of such quanta into two, causing the cloud to become a source of continuous radiation whose total energy should be equal to the energy of the initial flux of L_α-quanta. The result would be a sort of bright nebula, but without emission lines, whose glow is not directly connected with the presence of an exciting star.

Thus, any prolonged stay of L_α-quanta in the interstellar medium of the Galaxy should inevitably cause their annihilation. This leads us to the important conclusion: The diffuse component of L_α-radiation (L_α-background) should be virtually absent from the Galaxy.

However, although the possibility of observing the diffuse component of L_α-radiation from some nebula is virtually precluded (when $r > 500$ parsec), /350 there exists the probability of observing nebulae in direct L_α-rays. This is possible if the radial velocity of these objects is sufficiently large.

The half-width of the L_α-line emitted by a nebula is determined by the Doppler effect associated with thermal agitation of absorbing and radiating atoms in nebulae at $T_e = 10{,}000^\circ K$, and is of the order of 0.05 Å. The half-width of the absorption line caused by interstellar neutral hydrogen is determined by the natural damping effect and by the total number of hydrogen atoms in a column of unit cross section and of a height equal to the distance of the nebula from earth.

At $r = 100$ pc and $n_1 = 1\ cm^{-3}$, the half-width of the absorption line at $\lambda = 1216$ Å is equal to about 1 Å - exceeding by many times the half-width of the L_α-emission line - and the optical thickness at the center of the L_α-line is of the order of 10^6. Therefore, the L_α-line emitted by a nebula will be completely absorbed by interstellar hydrogen.

Nevertheless, at sufficiently large radial velocities of nebulae, a smaller portion of the L_α-energy radiated by these will reach the observer. The calculation performed for one particular case showed that, at a radial velocity of the nebula of the order of 50 km/sec and a distance of $r = 100$ pc, about 1% of the L_α-energy radiated by the nebula reaches the observer.

Even such a seemingly negligible quantity of L_α-energy is sufficient for the nebula to become visible (in the L_α-line) on photographs because of the fact that, first, the brightness of the nebula will here be only 3.5 stellar magnitudes (rather than 5) fainter than the brightness of a nebula in photographic rays, considering that the bulk (75%) of the L_α-energy radiated by the central star is changed to L_α-energy. Secondly, the L_α-background, as shown above, is virtually absent from the Galaxy, which greatly reduces the limiting brightness of celestial objects that can still be observed on photographs in L_α-rays (without consideration of the effect of the hydrogen geocorona).

More than 35% of the total number of planetary nebulae for which the /351 radial velocities are known, have a velocity greater than 50 km/sec. Furthermore, a considerable percentage of the planetary nebulae are high above the

plane of the galactic equator, i.e., outside the layer of interstellar neutral hydrogen. Thus, the possibility of observing some planetary nebulae in the light of the L_α-line does not seem completely hopeless.

As for the classical diffuse nebulae, Orion, M20, M8, and others, they should be completely invisible in the L_α-line.

The gas shells ejected during outbursts of novae and supernovae (Crab nebula, N Persci 1901, N Aquilae 1918, N Herculis 1934, etc.) should be clearly observed in the L_α-line: the Doppler shift caused by their expansion in this case will be almost twice as great as in the case of planetary nebulae.

The other hydrogen lines of the Lymann series (L_β, L_γ, etc.) can be observed for nebulae that are virtually transparent at the line frequencies of this series, i.e., for which $T_c \lesssim 10^{-4}$. For most planetary and diffuse nebulae, this requirement is apparently met so that their Lyman series is represented as the single line L_α.

In concluding this Section, we should make the following comment which is of basic significance: Depending on the nature of scattering, different portions of the emission line behave differently. For example, scattering in the central parts of the line (Doppler core) is incoherent, whereas in the Lorentzian wings it is coherent (we owe this observation to V.V.Ivanov). Furthermore, the above calculations were performed on the assumption of completely incoherent scattering and, moreover, are based on eq.(3) which, even for this case, is not entirely correct. Therefore, the data in Table 11 should be regarded as rather rough estimates of the order of magnitude of the parameters of interest here.

15. Observations of Galaxies in the Lyman-Alpha Line /352

Both direct photographs and measurements of fluxes in the Lyman-alpha line for individual galaxies may yield highly important information on their structure and composition. The results might differ substantially depending on the type and structure of the galaxy.

The lifetime of a L_α-quantum in a given galaxy, as we saw above, is determined by two factors: the finite probability of splitting of the L_α-quantum into two quanta and the absorption of the L_α-quantum by an interstellar dust particle. The probability of escape of L_α-quanta beyond the limits of a given galaxy depends in the first case on the concentration of interstellar hydrogen and in the second case on the density of the interstellar dust matter. Furthermore, in both cases this probability decreases with an increase of the linear dimensions of the galaxy.

Let us analyze this question in somewhat greater detail. Let the examined galaxy be completely invisible in L_α-rays. This means that either there are no sources of L_α-radiation in it (hot stars), or the actual conditions in the interstellar space of this galaxy are such that the L_α-quanta perish long before escaping beyond this galaxy. But if the galaxy belongs to the spiral type (especially to late spirals) rich in hot giants, then the first objection is no longer valid. Furthermore, spiral galaxies should be the most powerful genera-

tors of L_α-radiation. At the same time, they are rich in interstellar hydrogen and interstellar dust, which leads to the annihilation of L_α-quanta long before they reach the outer limits of the galaxy.

Table 12 gives data on the total optical thickness t_α in the L_α-line, the total number of scattering events of L_α-quanta N, and the overall path L which the L_α-quantum traverses before leaving a galaxy of dimension D, depending upon the concentration of neutral hydrogen atoms therein. Calculations were carried out by means of eqs.(1) - (4). For the coefficient of absorption of L_α-quanta, we usually take $s_\alpha \approx 10^{-14}$ cm^2.

TABLE 12

/353

OPTICAL THICKNESS (t_α), TOTAL NUMBER OF SCATTERING EVENTS (N), AND TOTAL PATH TRAVERSED BY THE L_α-QUANTUM (L) NECESSARY FOR ESCAPE OF QUANTA FROM A GALAXY OF DIMENSION D

n_1, cm^{-3}	1			0.1			0.01		
D, pc	t_α	$N \cdot 10^{-8}$	L	t_α	$N \cdot 10^{-8}$	L	t_α	$N \cdot 10^{-8}$	L
1 000	$3 \cdot 10^7$	4.4	15 000	$3 \cdot 10^6$	0.41	1 400	$3 \cdot 10^5$	0.04	130
5 000	$1.5 \cdot 10^8$	23	77 000	$1.5 \cdot 10^7$	2.2	7 300	$1.5 \cdot 10^6$	0.2	700
10 000	$3 \cdot 10^8$	47	157 000	$3 \cdot 10^7$	4.4	14 700	$3 \cdot 10^6$	0.41	1370
20 000	$6 \cdot 10^8$	96	320 000	$6 \cdot 10^7$	4.6	15 300	$6 \cdot 10^6$	0.42	1400

As mentioned in the preceding Section, after approximately 2×10^8 scattering events the L_α-quantum will perish, having been split into two quanta that subsequently will not be absorbed by hydrogen. A comparison of this value with that given in Table 12 shows that, even in the absence of interstellar dust in a galaxy such as our Galaxy ($n_1 \sim 1$ cm^{-3}), the L_α-quanta cannot survive until escape beyond its limits. In a galaxy where $n_1 \sim 0.1$ cm^{-3} and smaller, the probability of fractionation of L_α-quanta is slight; however, the probability of escape of the quanta from the galaxy will depend on the concentration of interstellar dust. If this concentration is the same as in our Galaxy, then the L_α-quantum, having traversed a path of the order of 10,000 pc under multiple absorption and scattering, will no doubt be absorbed by interstellar dust particles. Only when $n_1 < 0.1$ cm^{-3} does the possibility of escape of L_α-quanta beyond the limits of the galaxy become real.

We note that the indeterminancy of the data given in Table 12 has the same character as in the case of Table 11 (see the statements at the end of the preceding Section).

However, there might exist a case in which the galaxy is low in interstellar dust while hydrogen is present in such a quantity that the condition $N > 10^8$ will be satisfied. Apparently, such conditions are present in elliptical galaxies where diffuse (absorbing) nebulae are absent while a negligible quantity of

interstellar hydrogen is definitely present. In this case, all L_α-quanta /354
will be split into two quanta while they still are within the galaxy. The continuous spectrum of two-quantum radiation has an abrupt boundary on the short-wave end, at $\lambda = 1216$ Å. Thanks to this, the continuous spectrum of two-photon origin, being superposed to the general continuous spectrum of stellar origin of the galaxy itself, should exhibit some discontinuity at $\lambda = 1216$ Å. Evidently, the magnitude of this jump will depend primarily on the energy of the L_α-sources in the given galaxy. Since there are no hot giants in elliptical galaxies, high-temperature subdwarfs may constitute the probable source of L_α-radiation. Owing to their low absolute luminosity ($M \sim +1 - 4$) the total contribution of hot subdwarfs to the brightness and observed color of the galaxy will be negligible, but in return 75% of the energy radiated by them beyond the limit of the Lyman series will be converted, under the conditions of a given galaxy, at first to Lyman-alpha and then to two-quantum radiation.

Apparently the suggestion of the existence of hot subdwarfs with a composition of elliptical galaxies is not far from the truth; this is substantiated by the fact that emission lines of hydrogen and of ionized oxygen are observed in the spectra of some elliptical galaxies.

Thus, observations of elliptical galaxies in the L_α-line permit solving the following problems:

1. Verification of the possibility of the existence of hot subdwarfs of an early class (O, B) but of a low luminosity in the composition of elliptical galaxies.

2. Estimates on the upper limit of concentration of interstellar hydrogen in these galaxies. In particular, if a given elliptical galaxy is detected in the L_α-line, this means definitely that $n_H < 0.01$ cm^{-3} there. If, on the other hand, no such galaxy can be demonstrated in the L_α-line but a discontinuity, although insignificant, is present in its spectrum at $\lambda \sim 1216$ Å, this means that $n_1 > 0.1$ cm^{-3}. Other cases mean that there are simply no sources of L_α-radiation, i.e., hot subdwarfs, in the given galaxy (or else that the concentration of interstellar dust in it is high, which is unlikely).

In principle, the method of photographing elliptical galaxies in the L_α-line will permit determining the concentration of interstellar hydrogen in /355
these galaxies, even as low as 10^{-6} cm^{-3}.

Let us now return to the case where some galaxy will be detected on photographs in the L_α-line.

First, let us recall that, on such a photograph, it is quite useless to search for structural features; the image of the galaxy in the L_α-line should have the form of a disk of more or less uniform brightness. The outer boundary of this image will obviously be defined from the condition that the optical thickness in the L_α-line in the line of sight be of the order of unity.

It is customary to assume that the boundaries of a given galaxy in optical rays have their limit where the stars end. Judging from radio astronomy observations, interstellar hydrogen in a given galaxy may extend even farther.

Therefore, with respect to size the monochromatic image of a given galaxy in the L_α-line is quite discernible and, in some cases, might even appreciably exceed the "optical" size of this galaxy. Thus, it is possible to determine the real (physical) size of a given galaxy when it can be detected in the L_α-line.

The possibility of existence of differences of the external form of galaxies in L_α-rays from their form in visible rays is also not precluded.

If a galaxy is detected in the L_α-line at dimensions considerably exceeding the "optical" dimensions of the given galaxy, a new problem arises, namely, whether the interstellar hydrogen at the outer limits of the galaxy is in a static state or whether escape or removal by suction of the gaseous matter from its outer boundaries is taking place. In the first case, the distribution of interstellar hydrogen is determined by its kinetic temperature and acceleration of the gravitational field at the outer limits of the galaxy. In any case, the light pressure on atoms of interstellar neutral hydrogen caused by L_α-radiation should exceed the gravitational force of the galaxy. The cosmogonic significance of both possibilities is obvious.

Thus, observations of galaxies of different types in the L_α-line will make it possible to solve a number of interesting problems relating to their structure, composition of stellar population, density of interstellar hydrogen /356
and interstellar dust, determination of true dimensions, possibility of escape of interstellar matter from a given galaxy, etc.

16. Detection of Star Associations

As is known, O associations are usually detected by analysis of the distribution of hot giants among the enormous number of stars of late classes. The method of photographing the sky in certain regions of the far ultraviolet permit recording only the O association, so to speak, filtering out and separating it from the star field surrounding it.

The continuous spectrum of stars of the sun type and later, as demonstrated above, ends at 1600 Å, and in the region $\lambda < 912$ Å the interstellar medium is completely opaque. Therefore, in the spectrum region from 912 to 1500 Å the images of medium-temperature and cool stars should be extremely faint on photographs. Conversely, hot stars of classes O - B in the above wavelength range should appear very bright. Therefore, photographing the sky in the 912 - 1500 Å wavelength region will yield a simple and reliable method of detecting clusters of hot stars and O associations both in our Galaxy and in other galaxies. In particular, this will furnish information on the spiral structure of regions of our Galaxy remote from the sun and also some idea as to the number and distribution of O associations.

17. X-Radiation of the Sun

The first extra-atmospheric experiments on measuring the flux of X-radiation of the sun in the 2 - 8 Å wavelength range by means of rocket-borne instrumentation were started in 1948-1949, first by Behring and later by Friedman and

coworkers. The radiation intensity in the indicated wavelength interval proved to be of the order of 10^{-4} erg/cm^2 sec. Later, such measurements were repeated at many occasions, and it soon became obvious that the level of X-radiation of the sun was not constant and fluctuated rather extensively depending on solar activity or conditions on the sun. Table 13 presents a review of our observations (Ref.79 - 84, 45, 51) pertaining to the wavelength ranges of 2 - 8 Å and 8 - 20 Å. In addition, one or two measurements in the 44 - 60 Å and 44 - 100 Å ranges were performed in 1953. As these data indicate, the X-radiation flux during one cycle of solar activity varies by 2 - 3 orders of magnitude, whereas the general short-wave radiation of the sun (vacuum and hard ultraviolet) stays at a relatively constant level. Furthermore, a detailed analysis of individual observations and a comparison of the obtained results with the structure of the sun show that variations and, in general, any anomalies in X-radiation have a direct bearing on local active formations in the solar atmosphere. One gains the impression that X-radiation does not completely originate from the "quiet" corona and that the emissivity of individual active regions is comparable to, and sometimes substantially exceeds, that of the "quiet" corona. /357

TABLE 13

Launching	Counter Readings, 10^4 counts/cm^{2}sec		Conditions on Sun
	2–8 Å	8–20 Å	
Sept. 29, 1949	1.0		160 min after flare of degree 1
May 1, 1952	495		Quiet sun, minimum
May 5, 1952	$\leq$125		
Nov. 15, 1953	$\leq$40		
Nov. 23, 1953	332		
Dec. 1, 1953		4.5	
Oct. 18, 1953		14	
July 20, 1956	12		End of flare of deg. 1
Aug. 14, 1959	1.3	200	Quiet sun, minimum
Aug. 31, 1959	>70	>1000	Flare of degree 2+

In the experiments presented in Table 13, the radiation receivers used were photon counters with end windows of beryllium and aluminum foil and also of organic films (mylar, cryptal) which acted as filters and separated the individual regions of the X-ray spectrum. It is thus obvious that, to determine the total energy emitted by the sun in the X-ray range from the measurement data in individual spectral regions, a law of energy distribution and radiation temperature must be established. /358

Such an attempt was made by Byram (Ref.83) who stipulated a Planckian distribution and estimated the total flux on the basis of measurements in the 44 - 60 Å interval. The value obtained for the total flux of solar radiation in the X-ray range (1 - 100 Å) was about 0.13 erg/cm^2 sec at $T_e = 10^6$ °K (during minimum solar activity in 1953) and 0.35 erg/cm^2 sec at $T_e = 2 \times 10^6$ °K. At the period of maximum solar activity the total flux reached 1 erg/cm^2 sec, which

corresponds to a coronal temperature of more than 2×10^6 °K. In the shortest wave region of the spectrum (shorter than 8 Å) the variations were much greater. Radiation in the 2 - 8 Å interval disappears almost completely near minimum solar activity.

Available data indicate that the sources of high-temperature radiation (shorter than 8 Å) are individual local regions on the surface of the sun, with a total area less than 1% of the disk, rather than the corona itself.

Of interest also are the results of long observations of solar X-radiation by instruments on board of satellites and spacecraft. Such observations were carried out by S.L.Mandel'shtam and his associates during August-December 1960 (Ref.86) and by A.Ye.Yefremov et al. during the same period (Ref.87).

In the second case, an open-end photomultiplier was used as radiation receiver, equipped with a specially selected photocathode which, in combination with various filters, separated out different wavelength ranges.

The basic results of these measurements were as follows:

1. The X-radiation flux in the region 2 - 10 Å during the entire course /359 of measurements remained constant and equal to 2.4×10^{-4} erg/cm^2 sec. During a brief increase in solar activity the flux in this region increased by one order of magnitude.

2. The radiation flux in the 8 - 21 Å region, on the average, was constant and equal to 6.2×10^4 counts/cm^2 sec except for individual, very short intervals when it increased in one case by about a factor of 1.5, and in another case more than tripled.

3. The radiation flux in the 44 - 110 Å region was constant (with an accuracy to within ±8%) and equal to 1.5×10^7 counts/cm^2 sec.

4. In the 1.4 - 3 Å region the instruments recorded only the radiation background of nonsolar origin.

Observations by means of a special X-ray spectrometer operating in the 10 - 400 Å range and installed on an orbiting solar observatory were conducted in March 1962 by Behring et al. (Ref.88). Specifically, the recording and identification of emission lines in the soft X-ray region and the beginning of the hard ultraviolet, the list of which was given in Table 5, were the result of these observations. However, the enormous amount of data obtained during this launch (about 3500 solar spectra in the 10 - 400 Å interval) has not yet been processed; we can expect that the final work-up will yield highly interesting information on the intensities of these lines, their variations in connection with solar activity, etc.

The very first observations already show the possibility of the existence of at least two components of solar X-radiation: quiet radiation (background) and radiation associated with the appearance of a solar flare; in the second case it is more proper to speak of an "X-ray flare".

Special experiments were carried out to detect an X-ray flare (Ref.51). In this case it was established that the powerful X-radiation appears simultaneously with the eruption of a visible flare and may last from several minutes to half an hour. An energy of the order of 10^{31} erg can be released during one X-ray flare, which is at least two orders of magnitude greater than the energy dissipated in giant ejections of solar gas. Although the data are still insufficient for establishing the character of the dependence of the power of an /360 X-ray eruption on the degree of a visible flare, it can be stated that the higher the degree of the visible flare, the greater the power of the X-ray eruption. Table 14 compares two measurements of solar X-radiation (Ref.85), of which one pertains to the "quiet" corona (background) and the second to the instant of appearance of a flare of degree 2+. As the data of this table indicate, the relative increase in the flux at the instant of appearance of a visible flare differs for all wavelengths and increases markedly toward short waves. For example, this increase in the 20 - 100 Å region amounts to almost one order of magnitude, whereas in the 2 - 8 Å region it is already two orders of magnitude. From this there follows still another property of X-ray eruptions; these are characterized not only by the power of the energy released but also by a broadening of the spectral radiation region on the short wavelength end.

TABLE 14

FLUX OF X-RAYS DURING AND AFTER APPEARANCE OF A FLARE
(erg/cm^2 sec)

Wavelength Interval, Å	Background, Aug. 14, 1959	Flare of Deg. 2+ Aug. 31, 1959
20—100	0.6	4.0
8—20	0.002	0.09
2—8	0.00055	0.03
0.6	—	0.000023

If the increase in X-radiation, in particular broadening of its spectrum on the short wave end up to 1 - 2 Å is due to thermal excitation, then the effective temperature in coronal condensations should reach 10^7 °K and even more. It is suspected that, in very rare cases, the coronal condensations are able to emit hard X-rays with a wavelength shorter than one angstrom. Therefore, it might well be that the effective temperature in these reaches 10^8 °K. Apparently something like this took place during the X-ray eruption of August 31, 1959 which was recorded by Chubb et al. (Ref.91). In such cases we have to do with possible and very brief thermonuclear reactions which may occur in coronal /361 condensations.

Observations during solar eclipses can yield valuable information on the distribution of X-radiation sources over the solar disk. Such observations were carried out, for example, during the total solar eclipse of October 12, 1958 by Chubb et al. (Ref.89). For this, four launchings were made before the eclipse and at various phases during the eclipse, including totality. A comparison of

the results obtained in these launchings permits the following conclusions: During the total phase of the optical eclipse, X-radiation does not completely disappear - the residual flux amounts to 10 - 13% of the total flux of the uneclipsed disk. In other words, an annular eclipse took place with respect to X-radiation. This, evidently, is possible only if the corona constitutes the radiation source. It is characteristic that the residual flux of L_α-radiation originating in the chromosphere amounted to only 0.05% at the total phase of the eclipse. Furthermore, asymmetry of the "X-ray" disk of the sun was established from the viewpoint of brightness distribution; the radiation flux in the disk half where there were more than active formations (faculae, sunspots) was also more intense.

During another solar eclipse (February 15, 1961) the residual intensity was measured at the moment of totality in the 2 - 10 Å region (Ref.14) and was found to be equal to 8×10^{-5} erg/cm^2 sec. However, because of the absence of measurements for the total radiation flux in the indicated spectral region before the eclipse, it is impossible to determine the relative magnitude of the residual intensity.

18. Solar Photography in X-Rays

Measurements of X-rays by means of electrophotometric radiation receivers whose angular aperture appreciably exceeds the apparent size of the sun, are able to give an idea only on the integrated flux over the entire solar disk. /362 As shown above, some data on the distribution of the X-radiation sources over the solar disk can be obtained from comparisons of the onset of X-ray and visible eruptions and from observations during solar eclipses. Under such conditions, X-ray photographs of the sun can be of invaluable help.

The first photograph of the sun in the soft X-ray region (20 - 60 Å) was obtained on April 19, 1960 by Friedman and his team (Ref.89). They used a camera obscura in a vertical ascent of a rocket to an altitude of 195 km. The pinhole diameter of the camera obscura was 0.13 mm, length 160 mm, and angular resolution of about 0.1 solar diameter. In front of the aperture, a filter (cellulose nitrate coated with an aluminum layer of 2500 Å thickness) was attached which transmitted the 20 - 60 Å region. The effective exposure was 282 sec.

This X-ray photograph of the sun was not too successful: The image of discrete X-radiation sources was blurred over an arc of about 170°, due to precession of the rocket about the earth-sun axis. Nevertheless, even such a photograph permitted interesting conclusions.

A comparison of the X-ray photograph with a spectroheliogram in ionized calcium lines shows that bright flocculi constitute local regions of intense X-radiation. Furthermore, as established by photometric measurements, the brightest flocculi in X-rays were at least 70 times more intense than the undisturbed regions of the solar disk.

Despite the blurring of the photograph, it was possible to establish that the intensity of the X-radiation background near the center was approximately

half that on the limbs, i.e., the phenomenon of limb brightening proceeds analogously to that observed in radio emission of the sun at wavelengths of 10 and 21 cm. The increase in brightness toward the limb does not take place too abruptly, which points toward (see next Section) a line rather than a continuous type of X-radiation spectrum in the $\lambda > 10$ Å region.

New interesting facts were discovered on further processing of the photograph (Ref.92). In particular it was established that the regions on the solar disk active in X-radiation have appreciably smaller dimensions than the same regions in ionized calcium lines. At the same time, these regions produce 75% of the X-radiation of the entire sun in the 20 - 60 Å region. Furthermore, a strict correlation was established between distribution of the X-radiation sources and the radiofrequency sources in the decimeter range. Finally, the curve of limb brightening in these rays, shown in Fig.20, was plotted. /363

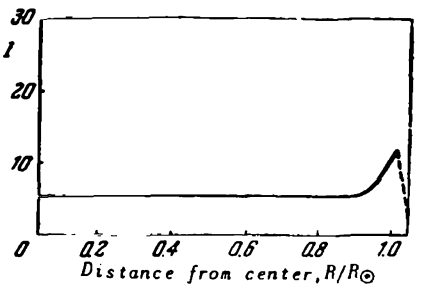

Fig.20 Distribution of X-Radiation Intensity over Solar Disk.

On June 21, 1961 Friedman's group (Ref.92) was able to obtain a second series of X-ray photographs, this time in different ranges (12 - 25 Å, 23 - 40 Å, and 44 - 90 Å) and with different resolving powers. Preliminary analysis of these photographs generally confirms the conclusion made on the basis of the first photograph.

19. Formation of Solar X-Radiation

Generation of X-radiation in celestial objects, generally speaking, can be the consequence of the following processes:

1. Bremsstrahlung of nonrelativistic, but sufficiently fast neutrons in the field of a proton or atomic nuclei; this is otherwise called "free-free" transition of electrons. The spectrum of X-radiation occurring in this case is continuous. /364

2. Recombination of electrons with highly ionized atoms ("free-bound" transitions); the spectrum of the X-radiation is continuous also in this case.

3. Excitation of highly ionized atoms by electron collisions and by successive downward transitions ("bound-bound" transitions). Here, radiation in X-ray lines occurs.

4. Bremsstrahlung of relativistic electrons in magnetic fields of the medium. This is otherwise called X-radiation of synchrotron origin. The emission spectrum is continuous.

5. Radiation in the presence of nuclear transformations.

6. Thermal (Planckian) radiation at high temperatures.

As shown in investigations (Ref.93 - 103), under the conditions of the solar atmosphere the principal role is played by the first mechanism, i.e., the generation of continuous X-radiation, and by the third mechanism, the generation of monochromatic (line) X-radiation. In principle, these mechanisms should be effective in planetary and diffuse nebulae and also in the gas shells of novae and supernovae.

The fourth or synchrotron mechanism may be involved in radio galaxies, in nebulae, and in the remnants of supernovae explosions whose radiation is of the synchrotron type.

The fifth mechanism, nuclear transformations, apparently is not amenable to direct detection. In special cases, nuclear reactions may occur in strictly localized regions or in formations in the solar atmosphere. In that case, X-radiation - as a secondary result of these reactions - can be detected. This mechanism may become effective under conditions of interstellar and intergalactic space, as a secondary product of collisions and transformations of cosmic relativistic particles.

As regards the last, sixth (thermal) mechanism of X-ray radiation, it can be stated that it is essentially composed of the first three mechanisms, except that thermodynamic equilibrium conditions are assumed for the radiating medium. By virtue of this, it becomes possible to use Planck's formulas for calculating the intensity of X-radiation at a given temperature of the medium. This ap- /365 proach is convenient in determining the emissivity of, for instance, atmospheres of neutron, hyperon, and - in general - superdense (baryon) configurations of stars in the X-ray range.

Some of these mechanisms have not been developed at all (especially for the X-ray range), or have been developed insufficiently. The theory of solar X-radiation, based on the action of the first three mechanisms, has been developed most fully. Main credit in this respect must be given to Elwert.

For a quantitative evolution of the theory of solar X-radiation at least the following data are required:

a) Distribution of electron concentration in the solar atmosphere (upper chromosphere and corona).
b) Electron temperature of the corona and limits of its possible variations (during a quiet sun and during eruptions).
c) Absolute chemical composition of the solar atmosphere.
d) Effective ionization and photorecombination cross sections for highly ionized atoms.

At present, these data are more or less reliably known.

Let us now examine the continuous spectrum of X-radiation of the undisturbed corona. It originates during free-free transitions (bremsstrahlung of an electron in the field of a proton) and recombinations of electrons with ions. In both cases it is necessary that the energy of the electrons be sufficiently

high (although not relativistic), of the order of $10^3 - 10^4$ ev, which corresponds to an electron temperature of the medium of the order of 10^6 °K.

The effective cross section dq for the emission of a photon in the energy range dhν during deceleration of a nonrelativistic electron in the field of a proton (free-free transitions) in the Sommerfeld approximation and for short waves is given in the following form (Ref.100):

$$dq = \frac{32}{3} \Phi \frac{1 - e^{-2\pi\alpha Z/\beta}}{\beta^2} \frac{d\nu}{\nu}, \tag{5}$$

where $\Phi = r_0^2\alpha = 5 \times 7 \times 15^{-28}$ cm^2; r_0 is the classical electron radius; /366
$\alpha = 1/137$ is the Sommerfeld fine structure constant; $\beta = v/c$.

The energy radiated by unit volume of the corona in the continuous spectrum per unit time is equal to

$$E_f(\nu) = n_e n^+ \int h\nu \, dq \, vf(v) \, dv, \tag{6}$$

where f(v) is the Maxwell distribution function of electron velocities. Substituting eq.(5) into eq.(6) and integrating, we find

$$E_f(\nu) = n_e n^+ 7 \cdot 10^{-41} \left(\frac{10^6}{T_e}\right)^{1/2} e^{-h\nu/kT_e} \bar{g} \, d\nu \quad \text{erg/cm}^2 \text{ sec}, \tag{7}$$

where $\bar{g}$ is the Gaunt factor (of the order of unity).

Equation (7) is none other than the spectrum of continuous X-radiation at the given electron temperature of the corona, in view of the fact that, because of the total transparency of the corona at frequencies of continuous X-radiation, the spectral distribution of the escaping radiation is not distorted by absorption in the corona. In Fig.21, the broken lines show the spectrum of continuous radiation of the solar corona due to free-free transitions of electrons at two values of the electron temperature, 1.5×10^6 °K and 1×10^6 °K. Mean values of electron concentrations were used here. The magnitude of the flux is divided by the uncertainty factor Q which takes into account fluctuations in the electron concentration.

The radiation emitted by unit volume of the corona per second, in recombinations of electrons with protons, is again determined by means of eq.(6) except that the effective cross section for bremsstrahlung dq must be substituted by the effective recombination cross section dq_r (Ref.93). The resultant $E_r(\nu)$ must be added to $E_f(\nu)$. Curves of the function $E_r(\nu)$, plotted under the same assumptions, are given in Fig.21 as a smooth solid line.

It is known that the energy of each photon emitted as a result of recombination is composed of the kinetic energy of the electron and of the ionization energy. Therefore, additional recombination radiation arises in the region of wavelengths shorter than the ionization limit. Thus, discontinuities might /367

occur in the continuous spectrum. It was found that the ionization limits of a number of ions (He III, Fe VI, VII, C XIV, etc.) are in the interval of wavelengths of about 20 - 230 Å. The curves of the total continuous radiation flux, with consideration of free-free transitions of hydrogen and helium and free-bound transitions for other most important elements present in the solar atmosphere, are represented by the upper curves in Fig.21.

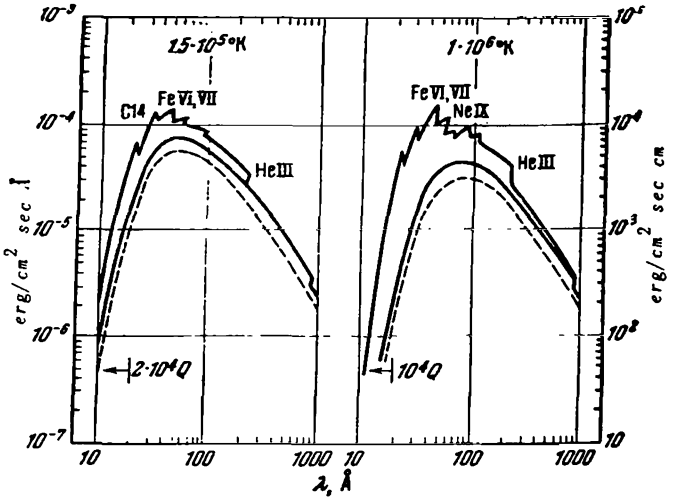

Fig.21 Spectrum of Continuous Radiation of the Solar Corona for Temperatures 10^6 °K and 1.5×10^6 °K. The curves give the intensity at the distance of the earth, divided by the uncertainty factor Q. The broken lines denote free-free transitions; the thin lines denote free-free transitions for H and He and free-bound transitions for H; the heavy lines denote total intensity, with consideration of the radiation of individual elements.

As follows from these curves, the theoretical maximum of the continuous spectrum of X-radiation of the sun is located in the 50 - 70 Å region. For comparison, the spectrum of X-radiation of the sun found by the described method for $T_e \sim 10^6$ °K is given in Fig.22 along with the spectrum of black-body radiation at the same temperature. Despite the substantial difference in the /368 mechanisms of radiation, both spectra are rather similar so that, in first approximation, the spectral distribution of the solar corona radiation in the X-ray range can be represented by Planck's law.

Let us now examine the line spectrum of the undisturbed corona. The X-ray emission line rises upon spontaneous transition of an ion from an upper excited level to a lower excited or normal level. Excitation at discrete levels may take place as a consequence of electron recombination to higher levels. However, under coronal conditions (high electron temperature), excitations caused by collisions of electrons with ions are more effective. Numerous investigations are in existence on calculating the effective cross sections in such collisions.

Elwert (Ref.103), having critically checked all pertaining data, carried out detailed calculations to determine the intensities of the most important X-ray lines in the spectrum of the solar corona. The basic result of these investigations is as follows: In the $\lambda > 10$ Å region the X-ray spectrum of the sun is primarily a line spectrum, and in the $\lambda < 10$ Å region a continuous spectrum.

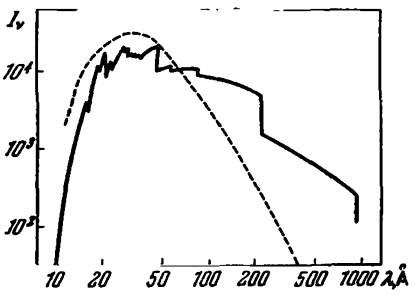

Fig.22
Solid line - theoretical distribution of coronal X-radiation; broken line - black-body radiation at $T = 10^6$ °K.

Knowing the volume emission coefficient of the solar corona in X-rays (both in the continuous spectrum and in lines) it is possible to find the relative intensity distribution of X-radiation over the solar disk. Here, we must prescribe a model spatial structure of the corona. Such calculations were performed by Elwert (Ref.103) for a "flattened" corona (Waldmeyer's model). In a formal respect, this problem is solved just as in the determination of radio brightness distribution over the solar disk in the 10 - 21 cm wave range. /369

As could be expected, limb brightening of the solar disk occurs in X-rays, with the intensity at the limbs being approximately double that at the center of the disk. This theoretical conclusion, as shown in the preceding Section, is confirmed by observational data (see Fig.20).

Having the brightness distribution over the solar disk, it is finally possible to find the total residual intensity of X-radiation during the total phase of the solar eclipse as a function of the ratio η of the apparent radii of moon and sun. This residual intensity, for example at $\eta = 1.06$, amounts to about 10%, whereas at $\eta = 1.00$, it is about 23% of the total intensity of the solar disk.

20. X-Radiation of Galactic Origin

The first proof of the existence of X-radiation of nonsolar, i.e., galactic, origin was obtained by Giacconi and his associates (Ref.104) during the night launch of a high-altitude rocket on June 18, 1962. Strictly speaking, their experiment was intended for studying the X-ray fluorescence of the lunar surface caused by X-radiation of the sun and for investigating the night sky to elicit other possible sources. Instead, they discovered X-radiation of galactic origin, thus repeating what had occured more than 30 years previously when Jansky, while studying radio waves of atmospheric origin, discovered radiofrequency radiations of galactic origin. /370

The range of sensitivity of X-ray detectors in this experiment was within 2 - 8 Å; the sensitivity itself was of the order of 0.1 photon/cm^2 sec. The detectors operated on the principle of free scanning of the region of the sky accessible to observation. As a result, one extended source of X-radiation was

recorded near the center of the Galaxy, in Scorpius, with the rather approximate coordinates $\alpha \sim 16^h40^m$ and $\delta \sim -40^\circ$. The angular size of this source was equal to about 10°, and the measured value of the flux was 5.0 photon/cm^2 sec. The author suggests that the radiation originates in a source which in no case is a member of the solar system.

Furthermore, a high intensity of the X-radiation background was recorded approximately in a direction where there are two peculiar objects: Cassiopeiae A and Cygni A. The authors call attention to the fact that the region near the center of the Galaxy where the main maximum of X-radiation is located and the region of Cassiopeiae A and Cygni A where a secondary source of X-radiation is observed, are simultaneously regions of strong RF radiation. This recalls a synchrotron nature of the detected X-radiation. The flux from the general isotropic background, recorded during this experiment, was equal to 1.7 quanta/cm^2 sec ($\sim 10^{-8}$ erg/cm^2 sec).

This was followed by the work of Fisher and Meyerott (Ref.105) devoted to the same problem, namely the search for X-radiation sources of cosmic origin. Their report generalized the results of observations in two rocket launchings, on September 30, 1962 and on March 15, 1963. The sensitivity of their X-radiation detectors was within 1 - 20 Kev (1 - 20 Å). The basic results of these observations are as follows: 1) X-radiation sources are not very rare in the sky (in the 1 - 20 Kev region); 2) X-radiation sources do not show a tendency to be related with stars; 3) the Crab Nebula is not especially intense in the sky in X-rays; 4) Cassiopeiae A and Cygni A can be included in the category /371 of sources of X-ray emission secondary in intensity.

Of particular interest are the results of observations of X-radiation of cosmic origin obtained by Friedman's group (Ref.106). During the launch of a high-altitude rocket on April 29, 1963, it was possible to clearly distinguish at least two X-ray sources, the Crab Nebula and a source in Scorpius. The observations were carried out in three spectral regions: 1 - 1.5 Å, 1.5 - 2.5 Å, and 2.5 - 8 Å. The sensitivity of the detectors in this case was by one order of magnitude higher than in Fisher's case (Ref.105).

The proposed center of the source in Scorpius was found by interpolation of the measurement results obtained with different intersections of the radiation detectors. The coordinates of the center of this source are as follows: $\alpha = 16^h15^m$, $\delta = -15^\circ$, i.e., substantially different from the estimate given elsewhere (Ref.104). The Friedman group (Ref.106) assumes that the source in Scorpius is a star or a starlike object. However, it could not be identified either with a visible object or with a radio source. The absolute radiation flux in the 1.5 - 8 Å region, on the assumption that the radiation of the source proceeds according to the black-body law at a temperature of 2×10^7 °K, was equal to 1.4×10^{-8} erg/cm^2 sec Å.

The location of the other source of X-radiation coincides, with an accuracy to 1 - 2°, with the position of the Crab Nebula. Its intensity in the 2.5 - 8 Å region is approximately 1/7 that of the source in Scorpius. The absolute radiation flux in the 1.5 - 8 Å region, under the same assumptions, was equal to 2.0×10^{-9} erg/cm^2 sec Å.

The limit of detecting discrete cosmic X-ray sources is determined by the background of the radiation detectors. Within the limits of their sensitivity, Cygni A and Cassiopeiae A were not detected in X-rays although each of these objects was intersected three times. It was also established that the background of X-radiation, when the detectors were pointed skyward, is greater (approximately by 25%) than when they are directed earthward.

According to the authors (Ref.106), the intensity of X-radiation of the Crab Nebula in the 1.5 - 8 Å spectral region is sufficiently high to have /372
been caused by relativistic electrons during their retardation in the magnetic fields of the nebula. In their opinion, the X-ray sources in Scorpius and the Crab Nebula are neutron stars. We will go into this more thoroughly in the next Section.

In concluding this Section, let us mention certain investigations of a general character in which attempts were made to estimate the expected X-radiation fluxes from various objects.

The X-radiation flux from bright stars in the 20 - 100 Å region, according to calculations by G.M.Nikol'skiy, may be - on the average - 10^{-3} quantum/cm^2 sec (Ref.107). The total X-radiation caused by all stars in the Galaxy, on the assumption that all stars on the average radiate like the sun, according to the calculations by Clark, is of the order of 10^{-12} to 10^{-10} erg/cm^2 sec in the 8 - 20 Å region (Ref.108), or 5×10^{-4} to 5×10^{-2} quantum/cm^2 sec. According to another author (Ref.107), this flux in the $\lambda < 8$ Å region may be of the order of 0.1 quantum/cm^2 sec.

Gold and Burbidge (Ref.109) studied the possible nature of X-radiation from the center of the Galaxy. They showed that bremsstrahlung of nonrelativistic electrons in a proton field is the explanation for the flux in the direction of the Galaxy center, provided that the total energy density of these electrons is not less than 1% of the energy density of all thermal electrons at the center of the Galaxy. Furthermore, if the Galaxy center emits a flux of elementary particles (electrons and protons) of high energy, one should simultaneously observe monochromatic X-radiation caused by transitions in ionized K-shells. Thus, it is suggested that detailed observations of X-radiation will yield some information both on particles ejected from the center of the Galaxy and on the relative content of elements emitting the K-series of X-rays. It was shown, finally, that the observed intensity of the isotropic background of X-radiation is incompatible with the model of a "hot universe" studied by Hoyle within the scope of the static cosmological theory (Ref.110).

21. Neutron Stars as X-Ray Source /373

It is believed that, along with white dwarfs, neutron stars may be one of the final phases of stellar evolution. The mass of neutron stars is of the same order as the mass of white dwarfs, slightly more than the solar mass. However, the density of matter in these stars is extremely great, being of the order of 10^{15} gm/cm^3, while the dimensions are extremely small, of the order of tens of kilometers. At such densities of matter and at a sufficiently high temperature, the atomic nuclei begin to absorb electrons and thus change into neutrons, which

furthermore are in a degenerate state. This process is known as neutronization of nuclei.

The first theoretical investigations of neutron configurations of stars were performed as early as in the 1930s by L.D.Landau (Ref.111) and by Oppenheimer and associates (Ref.112, 113). In recent years, interest in neutron and, in general, superdense (baryon) configurations has been renewed, as evidenced by the publication of numerous papers, e.g., by Cameron, by Hamada and Salpeter, by V.A.Ambartsumyan and G.S.Saakyan (Ref.114, 115, 116), and by other authors. This resulted in a more or less definite concept on the structure and development of neutron stars, on their basic physical parameters, and on processes occurring within these bodies. At present, the most probable parameters of a typical neutron star are assumed to be: mass $1.3\odot$, radius $R \sim 10$ km, density of matter $\rho \sim 1.5 \times 10^{15}$ gm/cm^3, surface temperature $10^6 - 10^7$ °K, acceleration due to gravity at the surface of the star $g = 2 \times 10^{14}$ cm/sec^2.

Less clear is the mechanism of the origin of neutron stars. The notion exists that a neutron star is formed as a result of the collapse of the outer layers of the star in a supernova explosion. The shock wave arising in the explosion, as shown by calculations, at sufficiently high temperatures may compress the stellar matter to nuclear densities. However, the internal temperature of such a star cannot be higher than 10^9 °K. Otherwise, as shown by Chiu (Ref.117), it will cool rapidly as a result of processes associated with the liberation and ejection of a neutrino which entrains an appreciable portion /374 of the energy reserve of the star.

At the same time, the concept exists that a neutron star can be formed from a red giant whose reserves of nuclear energy have been exhausted. In this case, it would be necessary that the mass of the red giant be greater than $1.4\odot$ (limit of the mass of white dwarfs) but less than $1.7\odot$ (limit of the mass of a neutron star). Contraction of a star can continue until its temperature reaches the limit at which the neutrino process begins.

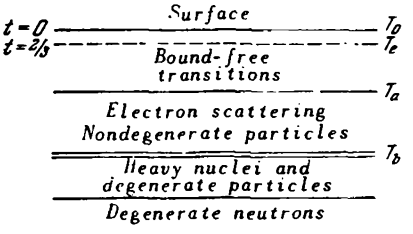

Fig.23 Schematic Representation of the Atmosphere of a Neutron Star.

What is the structure of the outer layers of a neutron star? At present, it is difficult to give a confident answer to this question; however, for instance, Hamada and Salpeter (Ref.115) propose that the neutron "stuffing" or core of such a star is surrounded by a thin layer of ordinary, nondegenerate nuclei and degenerate electrons, with the density of the matter of this layer being of the order of the density of white dwarfs. This layer is adjoined by an atmospheric layer consisting of nondegenerate electrons and nuclei of heavy atoms. The opacity of this layer in the optical region is due mainly to electron scattering and bound-free transitions. The described structure of the outer layers of a neutron star is depicted schematically in Fig.23 (Ref.118). Proceeding from this model atmosphere of a neutron star and using the conditions of static equilibrium at the interfaces of the individual layers, Morton (Ref.118) derived

simple relations between the effective temperature T_e, surface temperature T_0, density ρ_b, and temperature of the transitional layer T_b. In addition, he derived another quantity T_a, representing the temperature of the intermediate layer where electron scattering predominates over Kramer's absorption (bound-free transitions). The transitional layer where both these mechanisms play an identical role corresponds to a temperature of 1.19×10^8 °K. /375

TABLE 15

PHYSICAL CHARACTERISTICS OF THE ATMOSPHERE OF A NEUTRON STAR

T_b, °K	gm/cm^3	T_e, °K	λ_{max}, Å	πF_λ ($\lambda = 5$ Å), erg/cm^{2}sec Å
2×10^9	4.3×10^3	1.6×10^7	1.8	2.3×10^{31}
10^9	1.5×10^6	1.2×10^7	2.4	1.3×10^{31}
5×10^8	5.4×10^5	9.4×10^6	3.1	6.0×10^{30}
2×10^8	1.4×10^5	6.7×10^6	4.3	1.6×10^{30}
10^8	4.8×10^4	4.3×10^6	6.8	1.4×10^{29}
5×10^7	1.7×10^4	2.0×10^6	14	8.6×10^{25}
2×10^7	4.3×10^3	7.7×10^6	38	6.6×10^{15}

The wavelength λ_{max} corresponding to maximum radiation and the emissivity of unit surface of a neutron star πF_λ are calculated by means of Planck's formula for a given effective temperature T_e. The results of these calculations are given in Table 15, where πF_λ pertains to the wavelength 5 Å. It turns out that, with the exception of the coolest configurations ($T_e < 2 \times 10^6$ °K), the precalculated luminosity in X-rays is sufficiently high to explain the observed flux from the source in Scorpius as emanating from a neutron star at a distance from 1200 to 100 parsecs.

After analyzing the cooling process of a neutron star, Morton estimated its lifetime. This proved to be very small, of the order of several thousand years.

The suggestion of the existence of neutron stars as probable X-radiation sources is, generally speaking, rather attractive. The best verification of this assumption would lie in obtaining, by observation, proof of the stellar dimensions of such sources. For this, one would have to work with X-ray source detectors of sufficiently high angular resolution. Such detectors (X-ray telescopes) are not yet in existence. In addition, larger areas of the celestial vault will have to be investigated.

However, in individual cases when the X-radiation source is located in /376 the belt of the ecliptic, success can be achieved by using the method of lunar eclipse of the source. This pertains specifically to the Crab Nebula whose occultation by the moon was expected on July 5, 1964*. By installing an ordinary wide-angle X-ray detector on a rocket and launching it near the time of occulta-

* The next occultation is expected in 1972.

tion of the source, it is possible to trace the changes in X-radiation intensity as a function of the phase of the eclipse. If the X-radiation intensity diminishes slowly, in proportion to the part of the Crab Nebula covered by the moon, this will be an indication that X-radiation emanates in no case from a point or discrete object and, in all probability, is generated by the nebula itself. Only in the case of a rapid, practically instantaneous disappearance of the source at some phase of occultation will it be possible to assert that a neutron star is a source of X-radiation.

Such an experiment was successfully performed by Friedman and coworkers on July 5, 1964 (Ref.119). They found that the source of X-radiation in the Crab Nebula has rather large dimensions - about 1 minute of arc, i.e., 1/5 the size of the entire nebula. Therefore, at least for the Crab Nebula, the observed X-radiation cannot be reconciliated with the suggested existence of a neutron star in it. At the same time the proposed synchrotron origin of the X-radiation of the Crab Nebula becomes even more probable (see next Section).

The method of lunar occultation of an X-ray source is of only limited and infrequent usefulness for the detection of neutron sources. It is also impossible to hope for detection of neutron stars by ordinary optical observations: Despite the fact that the radiation intensity of neutron stars in the visible spectrum region is several orders of magnitude greater than the radiation intensity of ordinary stars in the same region, their absolute luminosity, /377 owing to the extremely small dimensions of the star, is very low being of the order of $+17^m$ at $T_e = 10^7$ °K and of $+19^m$ at $T_e = 10^6$ °K.

Under such conditions, it is more promising to use the method of comparing the spectra of X-ray sources obtained from observations with theoretical spectra derived for various mechanisms of X-ray generation. In particular, in the case of neutron stars, as shown above, the X-radiation spectrum, in first approximation, should have the form of a Planckian distribution at a given effective temperature of the surface layers of the neutron star. For instance, if the spectrum of some discrete X-ray source obtained from observations is similar to a Planckian distribution, with a characteristic maximum in the X-ray range, it is certain that one has to do with a neutron star in this case.

22. Possibility of X-Radiation of Cosmic Radio Sources

The generation of X-rays in the 1 - 100 Å range in the case of bremsstrahlung by relativistic electrons in magnetic fields of the medium is caused by electrons with energies of the order of $E_0 \sim 10^{14} - 10^{13}$ ev at a magnetic field strength of $H \sim 10^{-5}$ gauss. However, the lifetime of such electrons determined from the relation (Ref.120)

$$t_0 = \frac{3m^4c^7}{2e^4H^2E_0}, \qquad (7)$$

is short, being only several years.

Let us now assume that there are such forces of synchrotron radiation in which the energy spectrum of relativistic electrons, responsible for the appear-

ance of synchrotron radiation in the optical range, is not cut off in the investigated object at a given instant, at least to an energy of 10^{13} to 10^{14} ev, meaning that there is a continuous formation or injection of the mentioned types of relativistic electrons. Based on this assumption, let us determine the spectrum and power of the X-radiation being generated (calling it radiation /378 of "synchrotron origin") (Ref.121).

As the volume emission coefficient ε_ν in X-rays of synchrotron origin, we can use the following expression (Ref.126):

$$\varepsilon_\nu = C(\gamma) K H^{(\gamma+1)/2} \nu^{(1-\gamma)/2} \quad \text{erg/cm}^2 \text{ sec}, \tag{8}$$

where K and γ are parameters of the energy spectrum of relativistic electrons: $N(E) = KE^{-\gamma}$, while the numerical values of the function $C(\gamma)$ are tabulated elsewhere (Ref.126).

Let τ_ν be the total optical thickness of the examined object (for example, a radio galaxy) at a frequency ν of the X-ray range. Assuming that the matter (atoms of interstellar hydrogen and helium and also dust particles), absorbing X-rays and relativistic electrons, is distributed uniformly over the entire object, we can write the intensity of the X-radiation, issuing from the object I_ν in the form

$$I_\nu = \frac{\varepsilon_\nu}{\alpha_\nu}(1 - e^{-\tau_\nu}) \text{ erg/cm}^2 \text{ sec}, \tag{9}$$

where α_ν is the volume absorption coefficient at a frequency ν of the X-ray range: $\tau_\nu = \alpha_\nu 2s$ with 2s being the linear dimension of the object. For the total energy E_ν, radiated by the object of volume V in all directions in one second, we have

$$E_\nu \approx 4\pi s^2 I_\nu \approx 4\pi V \frac{\varepsilon_\nu}{\tau_\nu}(1 - e^{-\tau_\nu}) \quad \text{erg/sec}. \tag{10}$$

Denoting by R the distance of the studied object from the earth, the observed flux of X-rays F_ν in the frequency interval $\Delta\nu$, substituting also the value ε_ν from eq.(8), will read

$$F_\nu = \frac{V}{R^2} \frac{1 - e^{-\tau_\nu}}{\tau_\nu} C(\gamma) K H^{(\gamma+1)/2} \nu^{(1-\gamma)/2} \Delta\nu \quad \text{erg/cm}^2 \text{ sec}. \tag{11}$$

If the object is completely transparent to X-rays ($\tau_\nu = 0$), the spectrum of pure emission will become

$$F_\nu = \frac{V}{R^2} C(\gamma) K H^{(\gamma+1)/2} \nu^{(1-\gamma)/2} \Delta\nu, \tag{12}$$

For discrete sources of cosmic RF radiation (radio galaxies and remnants of supernovae), we usually have $\gamma \approx 3$. Equation (12) will then yield /379

$$F_\nu = \frac{V}{R^2} 9.5 \cdot 10^{-5} K H^2 \frac{\Delta\nu}{\nu} \quad \text{erg/cm}^2 \text{ sec}. \tag{13}$$

Changing from the energy flux to the number of X-ray quanta N_ν per 1 cm^2 per 1 sec, we will obtain

$$N_\nu = \frac{F_\nu}{h\nu} = 9.5 \cdot 10^{-5} \frac{V}{R^2} KH^2 \frac{\Delta\nu}{\nu^3} = \\ = 9.5 \cdot 10^{-5} \frac{V}{R^2} KH^2 \frac{\Delta\lambda}{ch} \quad \text{quanta/cm}^2 \text{ sec.} \qquad (14)$$

It follows from eqs.(13) and (14) that, in the absence of absorption within the object emitting the X-rays, the observed radiation intensity is inversely proportional to the frequency, and the observed quantity of X-ray photons per unit wavelength interval is constant and independent of the wavelength (Fig.24).

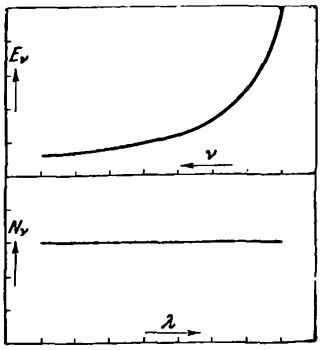

Fig.24 Theoretical Spectrum of X-Radiation of Synchrotron Origin.

A characteristic feature of objects such as our own Galaxy (from the viewpoint of structure of the interstellar medium), as shown in Section 2, is its virtual transparency in the region of short X-rays (1 - 100 Å). With an increase in wavelength, the optical thickness rapidly increases reaching a value of 100 at $\lambda \sim 100$ Å (see Table 1).

The pattern shown in Fig.24 markedly changes as soon as absorption in the object itself and during travel of the X-rays through our Galaxy is taken into consideration.

As a typical example, let us determine the expected quantity of X-ray quanta arriving at the earth in 1 sec per 1 cm^2 from the well-known irregular galaxy M82. Since we have no data as to the distribution and quantity of absorbing matter in this galaxy, let us use the same /380 values of τ_ν as those in our Galaxy. No less difficult is the determination of the effective volume where generation of the X-rays takes place. Let us take for this a volume smaller by one order of magnitude, in which - in accordance with the data by Lynds and Sandage (Ref.123), the remnants of the matter ejected from the center of this galaxy are distributed. This will yield $V \approx 10^{66}$ cm^3. Furthermore, at a modulus of distance $m - M \approx 27.5$ (Ref.123) we find $R \approx 10^{25}$ cm. Finally, substituting the value of $KH^2 = 1.7 \times 10^{-19}$ (Ref.124), the use of eq.(11) will yield

$$N_\nu = 10.2 \frac{1 - e^{-\tau_\nu}}{\tau_\nu} \Delta\lambda \quad \text{quanta/cm}^2 \text{ sec.} \qquad (15)$$

where $\Delta\lambda$ is expressed in angstroms. The third column of Table 16 shows the values of N_ν calculated by this formula for $\Delta\lambda = 1$ Å. Actually, eq.(15) gives the observed spectrum of X-radiation for M82 (without consideration of interstellar absorption in our Galaxy).

Similar calculations were also performed for the Crab Nebula (see Table 16). In this case, absorption of X-rays in our Galaxy was taken into account while /381 absorption within the nebula itself was neglected. The total number of neutral

TABLE 16

CALCULATED NUMBER OF X-RAY QUANTA N_ν (quanta/cm^2 sec Å) ARRIVING FROM M82 AND FROM THE CRAB NEBULA

λ, Å	M82		Crab Nebula	
	τ_ν	N_ν	τ_ν	N_ν
1	0	10.2	0	1.93
5	0	10.2	0	1.93
10	0.25	9.0	0.017	1.93
20	1.72	4.85	0.115	1.90
30	3.54	2.80	0.236	1.53
60	21.7	0.47	1.45	0.453
80	53	0.19	3.13	0.084
100	110	0.093	6.33	0.004
120	230	0.045	16.7	—

hydrogen atoms in the direction of this nebula is estimated as $N_H \approx 10^{20}$ cm^{-2} (Ref.125). Accordingly, the values of τ_ν should be reduced by a factor of 15 in comparison with those given in the second column of Table 16. Furthermore, assuming $V = 5 \times 10^{55}$ cm^3, $R = 3.7 \times 10^{21}$ cm and $KH^2 = 1.08 \times 10^{-16}$ (Ref.125), we obtain for the observed spectrum of X-radiation of the Crab Nebula

$$N_\nu = 1.93 e^{-\tau_\nu} \Delta\lambda \quad \text{quanta/cm}^2\text{sec.} \qquad (16)$$

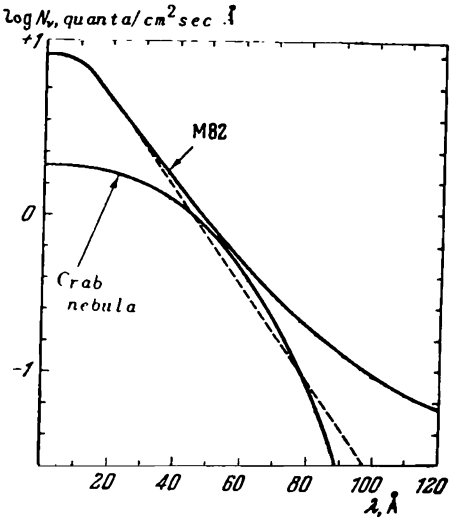

Fig.25 Theoretical Spectra of X-Radiation of Synchrotron Origin Arriving at the Observer's Position from the Crab Nebula and M82.

Figure 25 gives curves for the theoretical X-ray spectra of the M82 galaxy and the Crab Nebula. The broken line depicts the X-ray spectrum of M82, with consideration of absorption in our Galaxy ($N_H \approx 0.25 \times 10^{20}$ cm^{-2}). A slower drop in the number of X-ray quanta in the 1 - 60 Å range, with an increase in wavelength is noted in the case of the Crab Nebula. Apparently, both the M82 galaxy and the Crab Nebula will be easier to detect in short-wave than in long-wave X-rays. This follows, in particular, from the data of Table 17 which gives the total number of X-ray quanta reaching the observer from M82 and from the Crab Nebula at individual wavelength intervals. /382

Thus, the expected emissivity of M82 and of the Crab Nebula in X-rays of synchrotron origin is quite low (in comparison with the sun, being only several

tens of quanta per second per cm^2). Nevertheless, this is within the limits of sensitivity of the best modern X-ray detectors.

The Crab Nebula is one of the strong sources of cosmic RF radiation, whereas M82 is weaker by two orders of magnitude. At the same time, both these objects, according to the above calculations (which are, of course, approximate), are similarly accessible to the ground observer in the X-ray range. This fact suggests that certain sources of cosmic RF radiation may simultaneously be sources of X-radiation and of synchrotron emission. Depending on the internal structure of these objects and on their content of relativistic electrons with an energy of $\sim 10^{14}$ ev, the X-ray fluxes reaching the observer may undergo very appreciable variations (the concentration of relativistic electrons, with an energy of $\sim 10^{14}$ ev based on calculations, is about 6×10^{-13} cm^{-3} in the case of the M82 galaxy and 4×10^{-13} cm^{-3} in the case of the Crab Nebula). /383

TABLE 17

CALCULATED QUANTITY OF X-RAY QUANTA N ARRIVING FROM M82 AND THE CRAB NEBULA IN SEPARATE WAVELENGTH INTERVALS

Wavelength Interval, Å	N, quanta/cm^2 sec	
	M82	Crab Nebula
1—10	100	20
10—20	70	20
20—40	60	30
40—100	25	20

The other mechanism of X-ray generation - bremsstrahlung of nonrelativistic (but fast) electrons in a proton field - is most effective at electron energies of 10^4 - 10^2 ev. Such electrons, as shown above, exist in the solar atmosphere (owing to the high temperature of the corona) so that this mechanism is basic for the generation of solar X-rays. The possibility of action of this mechanism for galaxies and nebulae depends primarily on their content of electrons with energies of 10^4 - 10^2 ev. Let us estimate the order of magnitude of this concentration:

Designating by $q\left(\frac{v}{c}\right)$ the coefficient of probability (effective cross section) that an X-ray quantum of frequency ν is emitted in the interval $\Delta\nu$ when a fast electron with a relative velocity v/c travels past the nucleus of an atom, the radiation power (number of quanta) in 1 cm^3 per 1 sec can be expressed by

$$F_\nu = n_p n_e q\left(\frac{v}{c}\right), \tag{17}$$

where n_p is the concentration of thermal protons (atomic nuclei) in the medium and n_e is the concentration of fast electrons (with an energy of 10^4 - 10^2 ev). At a volume V of the galaxy (or nebula) and a distance R from earth, the observed radiation power, without consideration of absorption, will be

$$N_\nu = \frac{V}{4\pi R^2} n_p n_e q\left(\frac{v}{c}\right) \quad \text{quanta/cm}^2 \text{ sec.} \tag{18}$$

For the function $q\left(\frac{v}{c}\right)$ eq.(5) yields

$$q\left(\frac{v}{c}\right) = 0.608 \cdot 10^{-26} \frac{1 - e^{-2\pi\alpha Z/\beta}}{\beta^2} \frac{\Delta\nu}{\nu}, \qquad (19)$$

where $\beta = v/c$. Using eqs.(18) and (19) for the galaxy M82 with $n_p \approx 1$ cm^{-3}, the concentration of fast electrons would have the improbably large value of $n_e \approx$ $\approx 10^6$ cm^{-3} in order to record even 4 - 5 quanta at $\lambda \sim 100$ Å per sec per cm^2 /384 and in the $\Delta\lambda = 10$ Å interval. For $\lambda \sim 1$ Å, n_e is even larger being of the order of 10^{11} cm^{-3}. Approximately the same figures are obtained for the Crab Nebula.

Thus, it is unlikely that the mechanism of retardation of fast electrons in the proton field plays a noticeable role in the generation of X-rays in radio galaxies, ordinary galaxies, and remnants of supernovae. In individual cases, this mechanism may play some role in dense planetary and diffuse nebulae.

REFERENCES

1. Watanabe, K.: Advan. Geophys., Vol.5, p.153, 1958.
2. Aller, L.H.: Publ. Astron. Soc. Pacific, Vol.71, p.324, 1959.
3. Strom, S.E. and Strom, K.M.: Publ. Astron. Soc. Pacific, Vol.73, p.43, 1961.
4. Baum, W.A., Johnson, F.S., Oberley, J.J., Strain, C.V., and Tousey, R.: Phys. Rev., Vol.70, p.781, 1946.
5. Aboud, A., Behring, W.E., and Rense, W.A.: Astrophys. J., Vol.130, p.381, 1959.
6. Behring, W.E., McAllison, H., and Rense, W.A.: Astrophys. J., Vol.127, p.676, 1958.
7. Durand, E., Oberley, J.J., and Tousey, R.: Astrophys. J., Vol.109, p.1, 1949.
8. Johnson, F.S., Purcell, J.D., and Tousey, R.: Phys. Rev., Vol.95, p.621, 1954.
9. Johnson, F.S., Malitson, H.H., Purcell, J.D., and Tousey, R.: Astrophys. J., Vol.127, p.80, 1958.
10. Jursa, A.S., LeBlance, F.J., and Tanaka, Y.: J. Opt. Soc. Am., Vol.45, p.1085, 1955.
11. Miller, S.C., Mercure, R., and Rense, W.A.: Astrophys. J., Vol.124, p.580, 1956.
12. Rense, W.A.: Phys. Rev., Vol.91, p.299, 1953.
13. Tousey, R., Purcell, J.D., Packer, D.M., and Hunter, W.R.: Astron. J., Vol.64, p.133, 1959.
14. Viollet, T. and Rense, W.A.: Astrophys. J., Vol.130, p.954, 1959.
15. Kachalov, V.P. and Yakovleva, A.V.: Izv. Krymsk. Astrofiz. Observ., Vol.27, p.5, 1962.
16. Kachalov, V.P., Khokhlov, M.Z., Khokhlova, V.L., and Yakovleva, A.V.: Izv. Krymsk. Astrofiz. Observ., Vol.27, p.44, 1962.
17. Johnson, F.S., Purcell, J.D., Tousey, R., and Wilson, N.: Astrophys. J., Vol.117, p.238, 1953.
18. Hinteregger, H.E.: Astrophys. J., Vol.132, p.801, 1960.
19. Ultraviolet Radiation of the Sun and Interplanetary Medium. Izd. Inostr. Lit., 1962.

20. Cosmic Astrophysics. Ed. Liller, Izd. Inostr. Lit., 1962. /385
21. Johnson, F.S., Purcell, J.D., and Tousey, R.: Bull. Am. Chem. Soc., Vol.29, No.4, 1954.
22. DeJager, C.: Ann. Geophys., Vol.11, p.1, 1955.
23. Athay, R.G.: J. Geophys. Res., Vol.66, p.385, 1961.
24. Ivanov-Kholodnyy, G.S. and Nikol'skiy, G.M.: Astron. Zh., Vol.88, p.45, 1961.
25. Suemoto, Z. and Moriyama, F.: See Collection, Short-Wave Radiation of Celestial Bodies. p.90, Izd. Inostr. Lit., 1963.
26. Zirin, H., Hall, L.A., and Hinteregger, H.E.: See Collection, Short-Wave Radiation of Celestial Bodies. p.101, Izd. Inostr. Lit., 1963.
27. Behring, W.E., Noypert, W.M., and Lindsey, J.: See Collection, Short-Wave Radiation of Celestial Bodies. p.78, Izd. Inostr. Lit., 1963.
28. Allen, C.W.: Eighth Symposium, Liege, 1960.
29. Hinteregger, H.E., Damon, K.R., Heroux, L., and Hall, L.A.: Space Research. Vol.I, p.615, Amsterdam, 1960.
30. Short-Wave Radiation of Celestial Bodies. Izd. Inostr. Lit., 1963.
31. Bruns, A.V. and Prokof'yev, V.K.: Iskusstv. Sputniki Zemli, No.11, p.15, 1961.
32. Severnyy, A.B.; Izv. Krymsk. Astrofiz. Observ., Vol.23, p.311, 1960.
33. Athay, R.G.: Astrophys. J., Vol.128, p.447, 1958.
34. Tousey, R., Austin, W.E., Garrett, D.L., Purcell, J.D., and Widing, K.G.: Sky and Telescope, Vol.27, p.213, 1964.
35. U.S. Naval Research Laboratory, Astron. J., Vol.68, No.9, 1963.
36. Greenstein, J.L.: See "Atmospheres of the Earth and Planets". Izd. Inostr. Lit., 1950.
37. Purcell, J.D. and Tousey, R.: J. Geophys. Res., Vol.65, p.370, 1960.
38. Morton, D.C. and Widing, K.: Astron. J., Vol.65, p.58, 1960.
39. Jefferies, J.T. and Thomas, R.N.: Astrophys. J., Vol.129, p.401, 1959.
40. Mercure, R., Miller, S., Rense, W., and Stuart, F.: J. Geophys. Res., Vol.61, p.571, 1956.
41. Purcell, J.D., Packer, D.M., and Tousey, R.: Nature, Vol.184, p.8, 1959.
42. Purcell, J.D.: J. Opt. Soc. Am., Vol.47, p.1057, 1957.
43. Chapman, S.: See Collection, On the Threshold of Space. Izd. Inostr. Lit., 1960.
44. Kupperian, J.E., Byram, E.T., Chubb, T.A., and Friedman, H.: Planetary Space Sci., Vol.1, p.3, 1959.
45. Chubb, T.A., Friedman, H., Kreplin, R.W., and Mendge, P.: See Collection, Ultraviolet Radiation of the Sun and Interplanetary Medium. p.210, Izd. Inostr. Lit., 1962.
46. Johnson, F.S.: See Collection, Ultraviolet Radiation of the Sun and Interplanetary Medium. p.345, Izd. Inostr. Lit., 1962.
47. Johnson, F.S. and Fish, R.A.: Astrophys. J., Vol.131, p.502, 1960.
48. Friedman, H., Lichtman, S.W., and Byram, E.T.: Phys. Rev., Vol.83, p.1025, 1951.
49. Tousey, R., Watanabe, K., and Purcell, J.D.: Phys. Rev., Vol.83, p.792, 1951.
50. Byram, E.T., Chubb, T.A., Friedman, H., and Gailer, N.: Phys. Rev., Vol.91, p.1278, 1953.
51. Chubb, T.A., Friedman, H., Kreplin, R.W., and Kupperian, J.E.: J. Geophys. Res., Vol.62, p.389, 1957. /386
52. Byram, E.T., Chubb, T.A., Friedman, H., and Kupperian, J.E.: Astrophys. J.,

Vol.124, p.480, 1956.
53. Rense, W.A.: See Collection, Cosmic Astrophysics. p.26, Izd. Inostr. Lit., 1962.
54. Hinteregger, H.E.: See Collection, Cosmic Astrophysics. p.116, Izd. Inostr. Lit., 1962.
55. Hinteregger, H.E.: See Collection, Ultraviolet Radiation of the Sun and Interplanetary Medium. Izd. Inostr. Lit., 1962.
56. Stecher, T.P. and Milligan, J.E.: Astrophys. J., Vol.136, p.1, 1962.
57. Munch, G.: See Collection, Stellar Atmospheres. p.21, Izd. Inostr. Lit., 1963.
58. Underhill, A.B.: Publ. Dominion Astrophys. Obs., Victoria, B.C., Vol.10, p.357, 1957.
59. Saito, S.: Contr. Inst. Astrophys. Univ. Kyoto, No.69, 1956.
60. Osawa, K.: Astrophys. J., Vol.123, p.513, 1956.
61. Canavaggia, R. and Pecker, J.C.: Ann. Astrophys., Vol.16, p.47, 1953.
62. Underhill, A.B.: See Collection, Short-Wave Radiation of Celestial Bodies. p.47, Izd. Inostr. Lit., 1963.
63. Goldberg, L. and Pierce, A.K.: Handbook of Physics (Handbuch der Physik). Vol.52, p.38, 1959.
64. Yerkovich, S.P.: Optika i Spektroskopiya, Vol.8, p.307, 1960.
65. Fallon, R.J., Mason, E.A., and Vanderslice, J.T.: Astrophys. J., Vol.131, p.12, 1960.
66. Meinel, A.B.: Astrophys. J., Vol.137, p.321, 1963.
67. Hoyle, F. and Wickramansinghe, N.C.: Monthly Notices, Vol.126, p.401, 1963.
68. Bogges, L.: See Collection, Cosmic Astrophysics. p.153, Izd. Inostr. Lit., 1962.
69. Byram, E.T., Chubb, T.A., and Friedman, H.: See Collection, Ultraviolet Radiation of the Sun and Interplanetary Medium. p.199, Izd. Inostr. Lit., 1962.
70. Chubb, T.A. and Byram, E.T.: Astrophys. J., Vol.138, p.617, 1963.
71. Code, A.D.: Astron. J., Vol.65, p.278, 1960.
72. Gurzadyan, G.A.: In Press, Journal "Astrofizika".
73. Moore, C.E.: Atomic Energy Levels. Washington, 1949.
74. Gurzadyan, G.A.: Dokl. Akad. Nauk SSSR, Vol.136, p.1055, 1960.
75. Gurzadyan, G.A.: Dokl. Akad. Nauk SSSR, Vol.141, p.1061, 1961.
76. Gurzadyan, G.A.: Planetary Nebulae (Planetarnyye tumannosti). Fizmatgiz, 1962.
77. Shifrin, K.S.: Scattering of Light in a Turbid Medium (Rasseyaniye sveta v mutnoy srede). Gostekhizdat, 1951.
78. Sobolev, V.V.: Astron. Zh., Vol.34, p.694, 1957.
79. Burnight, T.R.: Phys. Rev., Vol.76, p.165, 1949.
80. Tousey, R., Watanabe, K., and Purcell, J.D.: Phys. Rev., Vol.83, p.792, 1951.
81. Friedman, H., Lichtman, S.W., and Byram, E.T.: Phys. Rev., Vol.83, p.1025, 1951.
82. Byram, E.T., Chubb, T.A., and Friedman, H.: Phys. Rev., Vol.92, p.1066, 1953.
83. Byram, E.T., Chubb, T.A., and Friedman, H.: J. Geophys. Res., Vol.61, p.251, 1956.
84. Friedman, H.: Ann. Geophys., Vol.11, p.174, 1955. /387
85. Friedman, H.: See Collection, Cosmic Astrophysics. p.136, Izd. Inostr. Lit., 1963.

86. Mandel'shtam, S.L., Tindo, I.P., Voron'ko, Yu.K., Shurygin, A.I., and Vasil'yev, B.N.: Iskusstv. Sputniki Zemli, Vol.10, p.12, 1961; Vol.11, p.3, 1961; Dokl. Akad. Nauk SSSR, Vol.140, p.1058, 1961.
87. Yefrenov, A.Ye., Podmoshenskiy, A.L., Ivanov, M.A., Nikiforov, V.N., and Yefimov, O.N.: Iskusstv. Sputniki Zemli, Vol.10, p.48, 1961; Vol.10, p.3, 1961.
88. Behring, W.E., Noypert, W.M., and Lindsey, J.K.: See Collection, Short-Wave Radiation of Celestial Bodies. p.78, Izd. Inostr. Lit., 1963.
89. Blake, R.L. and Unzicker, A.E.: See Collection, Ultraviolet Radiation of the Sun and Interplanetary Medium. p.129, Izd. Inostr. Lit., 1963.
90. Mandel'shtam, S.L., Voron'ko, Yu.K., Tindo, I.P., Shurygin, A.I., and Vasil'yev, B.N.: Dokl. Akad. Nauk SSSR, Vol.142, p.77, 1962.
91. Chubb, T.A., Friedman, H., and Kreplin, R.W.: J. Geophys. Res., Vol.65, p.1831, 1960.
92. Blake, R.L., Chubb, T.A., Friedman, H., and Unzicker, A.E.: Astrophys. J., Vol.137, p.3, 1963.
93. Elwert, G.Z.: Z. Naturforsch., Vol.9a, p.637, 1954.
94. Elwert, G.Z.: Astrophys. J., Vol.41, p.67, 1956.
95. Peterson, L.E. and Winckler, J.R.: J. Geophys. Res., Vol.64, p.697, 1959.
96. Elwert, G.Z.: J. Geophys. Res., Vol.66, p.391, 1961.
97. DeJager, C.: Ann. Geophys., Vol.11, p.330, 1955.
98. Wooley, R. and Allen, C.W.: Monthly Notices, Vol.108, p.292, 1948.
99. Ivanov-Kholodnyy, G.S. and Nikol'skiy, G.M.: Astron. Zh., Vol.88, p.45, 1961.
100. Elwert, G.: See Collection, Ultraviolet Radiation of the Sun and Interplanetary Medium. p.151, Izd. Inostr. Lit., 1962.
101. DeJager, C.: See Collection, Ultraviolet Radiation of the Sun and Interplanetary Medium. p.141, Izd. Inostr. Lit., 1962.
102. Elwert, G.Z.: Ann. Phys., Vol.34, p.178, 1939.
103. Elwert, G.Z.: J. Atmospheric Terrest. Phys., Vol.12, p.187, 1957.
104. Giacconi, R., Gurskiy, G., Paolini, F., and Rossi, B.: Phys. Rev. Letters, Vol. 9, p.439, 1962; Vol.11, p.530, 1963; See also Collection, Ultraviolet Radiation of Celestial Bodies. p.56, Izd. Inostr. Lit., 1963.
105. Fisher, P.C. and Meyerott, A.J.: Astrophys. J., Vol.139, p.123, 1964.
106. Bowyer, S., Byram, E.T., Chubb, T.A., and Friedman, H.: Nature, Vol.201, p.1307, 1964.
107. Nikol'skiy, G.M.: Dokl. Akad. Nauk SSSR, Vol.151, p.536, 1963.
108. Clark, G.: The Relation between Cosmic X-Rays and Gamma-Rays. Preprint, 1962.
109. Gold, R.J. and Burbidge, G.R.: Astrophys. J., Vol.138, p.969, 1963.
110. Hoyle, F.: Astrophys. J., Vol.137, p.993, 1963.
111. Landau, L.: Nature, Vol.141, p.333, 1938.
112. Oppenheimer, J.R. and Volkoff, G.M.: Phys. Rev., Vol.55, p.374, 1939. /388
113. Oppenheimer, J.R. and Snyder, H.: Phys. Rev., Vol.56, p.455, 1939.
114. Cameron, A.G.: Astrophys. J., Vol.130, p.884, 1959.
115. Hamada, T. and Salpeter, E.E.: Astrophys. J., Vol.134, p.683, 1961.
116. Qmbartsumyan, V.A. and Saakyan, G.S.: Astron. Zh., Vol.38, p.785, 1961.
117. Chiu, H.Y.: Ann. Phys., Vol.26, p.364, 1964.
118. Morton, D.C.: Nature, Vol.201, p.1308, 1964.
119. Sky and Telescope, Vol.28, p.139, 1964.
120. Landau, L.D. and Lifshits, Ye.: Field Theory (Teoriya polya). p.230, Gostekhizdat, 1948.

121. Gurzadyan, G.A.: Dokl. Akad. Nauk SSSR, Vol.158, No.6, p.1291, 1964.
122. Underhill, A.B.: Space Science Rev., Vol.1, p.749, 1963.
123. Lynds, C.R. and Sandage, A.R.: Astrophys. J., Vol.137, p.1005, 1963.
124. Gurzadyan, G.A.: Dokl. Akad. Nauk SSSR, Vol.152, No.6, p.1331, 1963; Soobshch. Byurakansk. Observ., Vol.34, p.59, 1963.
125. Shklovskiy, I.S.: Cosmic Radiofrequency Radiation (Kosmicheskoye radioizlucheniye). Gostekhizdat, 1956.
126. Gurzadyan, G.A.: Soobshch. Byurakansk. Observ., Vol.27, p.73, 1954.

Translated for the National Aeronautics and Space Administration by the O.W.Leibiger Research Laboratories, Inc.